Czech Technical University in Prague

Faculty of Electrical Engineering

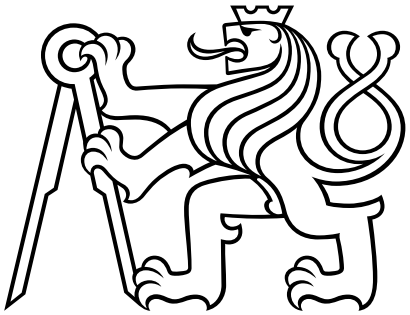

Doctoral Thesis

March 2023

Milan Němý

Czech Technical University in Prague

Faculty of Electrical Engineering
Department of Cybernetics

BASAL FOREBRAIN, CHOLINERGIC WHITE MATTER PATHWAYS, AND COGNITION IN NORMAL AGING AND ALZHEIMER'S DISEASE

Doctoral Thesis

Milan Němý

Prague, March 2023

Ph.D. Programme: Electrical Engineering and Information Technology
Branch of study: Artificial Intelligence and Biocybernetics

Supervisor: prof. RNDr. Olga Štěpánková, CSc.
Supervisor-Specialist: Ing. Lenka Vysloužilová, Ph.D.

DECLARATION

This doctoral thesis is submitted in fulfillment of the requirements for the degree of Doctor of Philosophy (Ph.D.). The work submitted in this thesis is the result of my own investigation, except where otherwise stated. I declare that I have written this thesis independently and quoted all used sources of information in accordance with Methodical instructions on ethical principles for writing an academic thesis. Moreover, I state that this thesis has neither been submitted nor accepted for any other degree.

In Prague, 22. 3. 2023

ABSTRACT

Cholinergic neurons in the central nervous system play a critical role in controlling brain circuitry responsible for cognitive functions, such as memory and attention. The cholinergic hypothesis of cognitive aging suggests that age-related disruptions in cholinergic activity occur in the brains of healthy older adults and those with dementia, leading to memory loss and other cognitive impairments. This theory has gained renewed attention due to the development of advanced imaging techniques that enable the visualization of the cholinergic system *in vivo*.

In this thesis, we created a promising method for modelling cholinergic pathways and assessing their integrity *in vivo*. **In Study I**, we applied a probabilistic fibre-tracking procedure using the ball-and-sticks model and prior anatomical knowledge to identify the main cholinergic pathways. For this task, a large cohort of cognitively normal individuals was used. We designed a complex pipeline of image processing steps that pre-processes the diffusion-weighted imaging data and tracks pathways rising from the cholinergic basal forebrain and its subregions originally from stereotaxic cytoarchitectonic maps. The modelled human white matter tracts closely resembled cholinergic pathways depicted in previous post-mortem findings.

Additionally, we investigated the contribution of basal forebrain volume, cholinergic white matter pathways, markers of cerebrovascular disease, and age to cognitive performance using a multivariate model. We found that lower integrity of these cholinergic pathways along with age were strong contributors to performance in tests of attention and memory in our cohort of cognitively normal middle-aged and older individuals. In another cohort **(Study II)**, we used a similar approach to determine which pathological processes might contribute to the degeneration of the cholinergic system in aging. Underlying cerebrovascular disease was shown to play a central role in the degeneration of cholinergic white matter projections over amyloid and tau pathology in cognitively unimpaired elderly.

Finally, we evaluated our model in individuals along the Alzheimer's disease continuum **(Study III)**. We found progressive loss in the white matter cholinergic projections with the advancement of the disease and that the integrity of the pathways reveals alterations as early as the stage of subjective cognitive decline. We were also able to locate spatial patterns of substantial disruptions along these tracts between groups. These disruptions were more focal in the initial stages of the continuum and became more widespread in its advanced stages.

To conclude, we created and investigated a method of modelling cholinergic pathways *in vivo* in two independent cohorts of cognitively normal individuals and a third cohort of individuals along the Alzheimer's disease continuum. Accurately measuring the cholinergic pathways may be relevant for diagnostic and prognostic purposes, as well as to advance the knowledge of pathological mechanisms involved in dementia and normal aging.

Keywords: cholinergic system, basal forebrain, normal aging, Alzheimer's disease, magnetic resonance imaging

ABSTRAKT

Cholinergní neurony v centrální nervové soustavě hrají klíčovou roli v řízení mozkových obvodů zodpovědných za kognitivní funkce, jako je paměť či pozornost. Cholinergní hypotéza kognitivního stárnutí předpokládá, že v mozku zdravých starších osob a osob s demencí dochází k narušení cholinergní aktivity v souvislosti se stárnutím, což vede ke ztrátě paměti a dalším kognitivním poruchám. Tato teorie si získala novou pozornost díky rozvoji pokročilých zobrazovacích technik, které umožňují vizualizaci cholinergního systému *in vivo*.

V této práci jsme vytvořili slibnou metodu pro modelování cholinergních drah a hodnocení jejich integrity *in vivo*. **Ve Studii I** jsme k identifikaci hlavních cholinergních drah použili pravděpodobnostní přístup sledování vláken pomocí modelu "ball-and-sticks" a předchozích anatomických znalostí. Pro tento úkol byla využita početná kohorta kognitivně normálních jedinců. Navrhli jsme netriviální sled kroků pro zpracování obrazu, který předzpracovává difuzně vážené obrazy magnetické rezonance a sleduje dráhy vycházející z cholinergního bazálního předního mozku a jeho podoblastí přejatých ze stereotaxických cytoarchitektonických map. Modelované dráhy bílé hmoty se velmi podobaly cholinergním drahám zobrazeným v předchozích posmrtných nálezech.

Kromě toho jsme pomocí multivariačního modelování zkoumali podíl objemu bazálního předního mozku, cholinergních drah bílé hmoty, markerů cerebrovaskulárního onemocnění a věku na kognitivním výkonu. Zjistili jsme, že nižší integrita cholinergních drah spolu s věkem silně přispívá k výkonu v testech pozornosti a paměti v naší kohortě kognitivně normálních jedinců středního a staršího věku. V obdobné kohortě **(Studie II)** jsme použili podobný přístup k určení, které patologické procesy mohou přispívat k degeneraci cholinergního systému při stárnutí. Ukázalo se, že cerebrovaskulární onemocnění hraje důležitější roli v degeneraci cholinergních projekcí bílé hmoty než amyloidová a tau patologie u kognitivně nenarušených starších osob.

Nakonec jsme náš model vyhodnotili u jedinců v kontinuu Alzheimerovy choroby **(Studie III)**. Zjistili jsme, že s progresí onemocnění dochází k postupnému úbytku kvality cholinergních drah v bílé hmotě a že integrita těchto drah vykazuje změny již ve fázi subjektivního kognitivního poklesu. Dále se nám podařilo lokalizovat prostorové uspořádání podstatných narušení v těchto drahách mezi diagnostickými skupinami. Tato narušení byla v počátečních stádiích kontinua soustředěna v oddělených ložiscích. V pokročilejších fázích se poté rozšířila i do ostatních oblastí uvažovaných drah.

V rámci této práci jsme vytvořili a zkoumali metodu modelování cholinergních drah *in vivo* ve dvou nezávislých kohortách kognitivně normálních jedinců a třetí kohortě jedinců v kontinuu Alzheimerovy choroby. Přesné měření cholinergních drah může mít význam pro diagnostické a prognostické účely a také pro prohloubení znalostí o patologických mechanismech podílejících se na demenci a normálním stárnutí.

Klíčová slova: cholinergní systém, bazální přední mozek, normální stárnutí, Alzheimerova choroba, zobrazování pomocí magnetické rezonance

LIST OF AUTHOR'S PUBLICATIONS

This thesis is based on the following original articles (publications in journals with impact factor):

I. **Nemy, M.**, Cedres, N., Grothe, M.J., Muehlboeck, J.S., Lindberg, O., Nedelska, Z., Stepankova, O., Vyslouzilova, L., Eriksdotter, M., Barroso, J., Teipel, S., Westman, E., Ferreira, D., 2020. Cholinergic white matter pathways make a stronger contribution to attention and memory in normal aging than cerebrovascular health and nucleus basalis of Meynert. *Neuroimage* 211, 116607. https://doi.org/10.1016/j.neuroimage.2020.116607
Authorship share: 88%, cited by: 34 (WoS, 24 without self-citations), 48 (Google Scholar), 37 (V3S, 24 without self-citations) IF=7.4.

II. Cedres, N., Ferreira, D., **Nemy, M.**, Machado, A., Pereira, J.B., Shams, S., Wahlund, L.O., Zettergren, A., Stepankova, O., Vyslouzilova, L., Eriksdotter, M., Teipel, S., Grothe, M.J., Blennow, K., Zetterberg, H., Schöll, M., Kern, S., Skoog, I., Westman, E., 2022. Association of Cerebrovascular and Alzheimer Disease Biomarkers With Cholinergic White Matter Degeneration in Cognitively Unimpaired Individuals. *Neurology* 99, e1619–e1629. https://doi.org/10.1212/WNL.0000000000200930
Authorship share: 5.26%, cited by: 1 (WoS, 0 without self-citations), 2 (Google Scholar), 1 (V3S, 0 without self-citations), IF=9.901.

III. **Nemy, M.**, Dyrba, M., Brosseron, F., Buerger, K., Dechent, P., Dobisch, L., Ewers, M., Fliessbach, K., Glanz, W., Goerss, D., Heneka, M.T., Hetzer, S., Incesoy, E.I., Janowitz, D., Kilimann, I., Laske, C., Maier, F., Munk, M.H., Perneczky, R., Peters, O., Preis, L., Priller, J., Rauchmann, B.-S., Röske, S., Roy, N., Scheffler, K., Schneider, A., Schott, B.H., Spottke, A., Spruth, E.J., Wagner, M., Wiltfang, J., Yakupov, R., Eriksdotter, M., Westman, E., Stepankova, O., Vyslouzilova, L., Düzel, E., Jessen, F., Teipel, S.J., Ferreira, D., 2022. Cholinergic white matter pathways along the Alzheimer's disease continuum. *Brain*. https://doi.org/10.1093/brain/awac385
Authorship share: 61.5%, cited by: 1 (WoS, 1 without self-citations), 2 (Google Scholar), 1 (V3S, 1 without self-citation), IF=15.255.

The (interim) results were presented at the following international conferences:

I. **Nemy, M.**, Westman, E., Barroso, J., Ferreira, F., 2018. Probabilistic Fiber-tracking of the Human Cholinergic System. *World Congress on Medical Physics and Biomedical Engineering*, Prague, Czech Republic.

II. **Nemy, M.**, Westman, E., Barroso, J., Ferreira, D., 2019. Cholinergic White Matter Pathways, Cerebrovascular Disease, and Cognition in Normal Aging. *14th International Conference on Alzheimer's & Parkinson's Disease*, Lisbon, Portugal.

III. **Nemy, M.**, Westman, E., Barroso, J., Ferreira, D., 2020. Novel multimodal imaging methods for in vivo investigation of the human cholinergic system. *Advances in Alzheimer's and Parkinson's Therapies An AAT-AD/PD Focus Meeting*, virtual conference.

IV. **Nemy, M.**, Grothe, M., Westman, E., Barroso, J., Ferreira, D., 2020. Multimodal imaging reveals human cholinergic system functional and structural integrity in vivo. *Alzheimer's Association International Conference*, virtual conference.

V. **Nemy, M.**, Dyrba, M., Buerger, K., Düzel, E., Laske, C., Perneczky, R., Peters, O., Priller, J., Schneider, A., Spottke, A., Wiltfang, J., Westman, E., Stepankova, O., Jessen, F., Ferreira, D., Teipel, S., 2021. Cholinergic white matter pathways, cerebrovascular disease, and cognition along the spectrum of Alzheimer's disease. *15th International Conference on Alzheimer's & Parkinson's Disease*, virtual conference.

VI. Cedres, N., Ferreira, D., **Nemy, M.**, Machado, A., Pereira, J.B., Wahlund, L.O., Zettergren, A., Teipel, S., Grothe, M.J., Eriksdotter, M., Stepankova, O., Vyslouzilova, L., Blennow, K., Zetterberg, H., Kern, S., Skoog, I., Westman, E., 2021. The association of Alzheimer's disease and cerebrovascular disease biomarkers towards the neurodegeneration of the cholinergic pathways. *Alzheimer's Association International Conference*, virtual conference.

VII. Hernandez-Rodriguez, M.A., Alemany, I., Diaz-Galvan, P., **Nemy, M.**, Westman, E., Barroso, J., Ferreira, D., Cedres., N., 2022. Degeneration of the cholinergic system in subjective cognitive decline: a systematic review. *Alzheimer's Association International Conference*, virtual conference.

VIII. Alemany, I., Cedres, N., Diaz-Galvan, P., **Nemy, M.**, Rodriguez-Hernandez, M.A., Barroso, J., Westman, E., Ferreira, D., 2022. The neurodegeneration of the cholinergic pathways in subtypes of subjective cognitive decline. *Alzheimer's Association International Conference*, virtual conference.

IX. **Nemy M.**, Stepankova, O., Vyslouzilova, L., Düzel, E., Jessen, F., Teipel, S., Ferreira, D., 2023. Cholinergic white matter pathways in early stages of Alzheimer's disease. *International Conference on Alzheimer's and Parkinson's Diseases and related neurological disorders*, Gothenburg, Sweden.

The following publications were (co-)authored by the PhD candidate but are not part of this dissertation thesis:

I. **Nemy, M.**, Vyslouzilova, L., 2018. Measurement of Basal Forebrain Atrophy in Alzheimer's Disease using Tensor-Based Morphometry: Preliminary Study, in: Georgi, H., Slamberova, R. (Eds.), *Ageing 2018: Proceedings of the 4th Gerontological Interdisciplinary Conference*. Charles University, Third Faculty of Medicine, Prague, pp. 184–193.

II. Vysloužilová, L., Zvoníček, V., Duška, F., Jirman, J., Kubr, J., Lhotská, L., Macík, M., **Němý, M.**, Niebauerová, E., Povišer, L., Samek, M., Vaněk, J., 2021. Nová technologie v intenzivní péči pomáhá vzdáleně sledovat pacienty nejen s COVID-19. *Medsoft* 33, 84–87. https://doi.org/10.35191/medsoft_2021_1_33_84_87

CONTENTS

TABLE OF FIGURES

LIST OF ABBREVIATIONS

AChE	Acetylcholinesterase
AD	Alzheimer's disease
ADAS-Cog	Alzheimer’s Disease Assessment Scale – Cognitive subscale
APOE	Apolipoprotein E (gene)
APP	Amyloid precursor protein
ASL	Arterial spin labelling
Aβ	Amyloid beta
BDRS	Blessed Dementia Rating Scale
BOLD	Blood oxygenation level-dependent
CDR	Clinical Dementia Rating
ChAT	Choline acetyltransferase
CNS	Central nervous system
CSF	Cerebrospinal fluid
DTI	Diffusion tensor imaging
DWI	Diffusion-weighted imaging
FA	Fractional anisotropy
FAQ	Functional Activity Questionnaire
FDG	Fluorodeoxyglucose
FLAIR	Fluid-attenuated inversion recovery
fMRI	Functional MRI
FSL	FMRIB Software Library
GM	Grey matter
HC	Healthy control
mAchR	Muscarinic acetylcholine receptor
MCI	Mild cognitive impairment
MD	Mean diffusivity
MMSE	Mini-Mental State Examination
MRI	Magnetic resonance imaging
nAhR	Nicotinic acetylcholine receptor
NBM	Nucleus basalis of Meynert

NFT	Neurofibrillary tangle
NIA-AA	National Institute on Aging and Alzheimer's Association
p-tau	Phosphorylated tau
PET	Positron emission tomography
RF	Radio frequency
ROI	Region of interest
SCD	Subjective cognitive decline
SVD	Small vessel disease
t-tau	Total tau
TAVEC	Test de Aprendizaje Verbal España-Complutense
TE	Echo time
TI	Inversion time
TIV	Total intracranial volume
TR	Repetition time
VAchT	Vesicular acetylcholine transport protein
WM	White matter
WM-hypo	White matter hypointensities

1 INTRODUCTION

Alzheimer's disease (AD) is a devastating condition that significantly impacts the lives of millions of people worldwide (Guerchet et al., 2020). AD is a complex neurodegenerative disorder characterized by progressive cognitive decline and the eventual loss of memory, executive functions, and other cognitive abilities. The disease can severely impact a person's quality of life and ultimately lead to fatality. As such, it is a major public health concern that affects individuals, families, and entire communities.

One of the challenges associated with AD is that it often goes undetected until the later stages of the condition. The onset of AD pathology can begin decades before observable clinical symptoms, with patients often experiencing memory impairment and eventually a decline in executive and language functions as well as physical abilities. The early detection of AD is critical to developing effective interventions and treatments that can slow or even halt its progression.

The basal forebrain is a critical brain region that is believed to play a significant role in the onset and progression of AD. The cholinergic system of the human brain consists of several subsystems originating from the basal forebrain, in particular from the nucleus basalis of Meynert, and from the brainstem. As the widespread projections from the basal forebrain to the cortex play an important role in learning, declarative and procedural memory and many other cognitive processes that are significantly impaired in senile disorders such as AD and Dementia with Lewy Bodies, it is favourable to assess the affected pathways and cortical regions *in vivo*.

To evaluate AD, Magnetic Resonance Imaging (MRI) scans are commonly utilized as they can non-invasively measure brain tissue atrophy, brain function or the integrity of grey (GM) and white matter (WM), providing insights into neuronal loss and molecular changes. Recent studies have highlighted the potential of imaging biomarkers for the early diagnosis of AD. These biomarkers can be used to identify changes in the brain associated with AD pathology before the onset of clinical symptoms. Some of the most promising imaging biomarkers include beta-amyloid PET imaging, tau PET imaging, and MRI, which can provide insights into brain structure, function, and metabolism changes. This thesis primarily focuses on imaging the human cholinergic system using images used in research and clinics.

1.1 AIMS OF THE THESIS

The overall aim of this thesis is to model the human cholinergic system *in vivo* using diffusion-weighted MRI and to identify and investigate the properties of cholinergic pathways in healthy individuals and in the AD spectrum. This is a particularly unique challenge as there are no tools or methodology for extracting the respective brain pathways from brain imaging data (state in 2018). We aim to design and implement an image-processing pipeline to resolve this task. To approach this problem, we will select and improve

the existing methods of fibre-tracking and propose a suitable algorithm for the evaluation of the pathways. To achieve this plan, the following tasks have to be accomplished:

T1. Review of limits of existing fibre-tracking pipelines.
T2. Means to overcome these limits in the context of cholinergic pathways.
T3. Design of an original novel algorithm for tracking the cholinergic pathway in *in vivo* images.
T4. Implementation of the pipeline.
T5. Evaluation and validation of the novel approach.

The created pipeline will be applied to answer the research questions identified in the three studies included in the thesis as specified below.

In **study I**, we create an *in vivo* model of the human cholinergic system using diffusion-weighted MRI based on a cohort of cognitively normal individuals. Further, we investigate the association of cerebrovascular disease with the integrity of the cholinergic system and cognitive functions known to be mediated by cholinergic circuitry.

In **study II**, we evaluate the contribution of amyloid and tau pathology in combination with cerebrovascular disease toward the degeneration of cholinergic white matter projections in cognitively normal individuals. To do this, we use the model derived in Study I.

In **study III**, we extend our investigation of the cholinergic system to the study of neurodegeneration of the cholinergic system across the stages of the AD continuum. We compare cholinergic WM pathways between individual stages and healthy controls and evaluate their predictive power towards diagnosis. Then, we demonstrate the association of cholinergic WM pathways and basal forebrain volumetric changes with cognitive performance across stages of the AD continuum.

In order to successfully achieve the described aims, we identified and attained several research objectives. The main one was undoubtedly the development of the cholinergic pathways segmentation pipeline, which unlocked a novel way of researching the cholinergic system *in vivo*. A detailed description of our proposed multimodal pipeline with a justification of several critical technical aspects can be found in **Section 5.3.5**. Our next objective was the identification and use of a suitable method for the evaluation of the cholinergic pathways in a highly multicollinear setup. In **Section 5.3.6**, we present selected procedures which allowed the investigation of the associations of the integrity of the cholinergic system in the presence of typically correlated variables.

2 BASAL FOREBRAIN CHOLINERGIC CIRCUITS

Cholinergic neurons in the central nervous system provide vital control over brain circuitry responsible for cognitive processing. Since its discovery, the cholinergic circuitry of the basal forebrain (BF) has been scrutinized for possible responsibility for the cognitive impairments associated with neurodegeneration (Bartus et al., 1982; Drachman and Leavitt, 1974) and changes in cholinergic signalling in disorders of cognitive control and attention functions (Higley and Picciotto, 2014; Wallace et al., 2011).

Most of the cholinergic neurons can be located in the brainstem pedunculo-pontine and lateral dorsal tegmental nuclei (Ch5-6), a subset of thalamic nuclei, the striatum and the basal forebrain nuclei (Ch1-4). Together they serve as the major sources of cholinergic projection neurons[1] to the neocortex, amygdala, and hippocampus (Mesulam et al., 1983; Woolf, 1991).

This thesis deals in particular with the cholinergic neurons of the basal forebrain, which provide the principal source of cholinergic projections involved in cognitive processing in mammals (Ballinger et al., 2016).

2.1 CHOLINERGIC NEURONS AND PROJECTIONS

Most of the cholinergic inputs to the cortical and subcortical areas engaged in the cognitive processes consist of the projections of the neurons whose bodies are located in the basal forebrain.

The particular localization of the cholinergic cell bodies that innervate the cerebral cortex was made possible by the combined visualization of the hydrolytic enzyme acetylcholinesterase (AChE) with retrogradely transported horseradish peroxidase (HRP). Experiments in the macaque monkey showed that cortically injected HRP led to the retrograde labelling of AChE-rich basal forebrain neurons (Mesulam and Van Hoesen, 1976). Later, AChE histochemistry was replaced by immunolabeling with the synthetic enzyme of acetylcholine (ACh), choline acetyltransferase (ChAT), for the more definitive identification of cholinergic neurons (Mesulam et al., 1986).

In the early research on the topological organization of the basal forebrain, the cholinergic system was considered both spatially and functionally diffuse (Woolf, 1991). However, more recent approaches based on the aforementioned immunological and histochemical labelling that enabled enhanced mapping of cell bodies and their projections identified a functionally based topographical organization of the basal forebrain (Zaborszky et al., 2015).

The cell bodies of the cholinergic neurons of the basal forebrain are intermingled with a heterogeneous population of non-cholinergic neurons (Geula et al., 1993) and located in several nuclei: the medial septal (MS) nucleus, the diagonal band (DB) nuclei (the horizontal

[1] Projection neurons are neurons whose axons extend from the neuronal cell body within the central nervous system (CNS) to one or more distant regions of the CNS (Nusbaum, 2008).

and vertical limb), the nucleus basalis of Meynert (NBM), and the substantia innominata (SI) (Woolf, 1991).

Another nomenclature – Ch1-4 – was introduced to designate cholinergic neurons within these four overlapping cell groups of the basal forebrain (Mesulam and Geula, 1988):

- Ch1 = cholinergic cells in medial septal nucleus
- Ch2 = vertical limb of the diagonal band
- Ch3 = horizontal limb of the diagonal band
- Ch4 = nucleus basalis of Meynert and substantia innominata

The nuclei of MS and DB send their cholinergic projections to the hippocampus, parahippocampus, olfactory bulb, and midline cortical structures (Knox and Keller, 2016). NBM and SI provide most of the cholinergic inputs to the neocortex and amygdala (Mesulam et al., 1986, 1983). However, a precise topography of the basal forebrain cholinergic neurons projections to the cerebral cortex is unknown. Nevertheless, the white matter connections of cholinergic axons can be traced as these fibers contain AChE, ChAT and NGFr (nerve growth factor receptor). The examination of the whole-hemisphere sections labelled with these cholinergic markers helped to identify the NGFr-positive cholinergic pathway passing from the basal forebrain to the cortex. The medial pathway joins the white matter of the gyrus rectus; curves around the rostrum to the corpus callosum; enters the cingulum bundle; and supplies the parolfactory, cingulate, and retrosplenial cortices. The lateral pathway subdivides into a capsular division travelling in the external capsule and uncinate fasciculus and a perisylvian division travelling within the claustrum. The perisylvian division supplies the frontoparietal operculum, insula, and superior temporal gyrus. Branches of the capsular division supply the remaining parts of the frontal, parietal, and temporal neocortex (Selden et al., 1998).

Modern MRI scanners allow visualization of these pathways *in vivo* using diffusion tensor imaging (DTI). These techniques are discussed in more detail in the following chapter.

2.2 CHOLINERGIC SIGNALING IN ATTENTION AND MEMORY

Acetylcholine signalling takes part in various aspects of cognitive processing, such as memory or attention. The prefrontal cortex (PFC) represents a major node for attention processes performing top-down control for cortical sensory centres. It is also an essential target of the cholinergic projections of the basal forebrain. Previous studies (Howe et al., 2013; Parikh et al., 2007) showed that the basal forebrain engages in PFC and sensory cortex in attentional processing, and they propose that ACh mediates cue detection.

Next, memory is one of the most complex cognitive functions, taking place in many brain regions and consisting of various mechanisms for initial acquisition, short-term and long-term storage, recall and forgetting. The most consistent finding states that the endogenous release of ACh plays an essential role in the induction of long-term potentiation – synaptic substrate of memory (Hasselmo and Stern, 2014). For example, cholinergic signalling from the basal

forebrain to the hippocampus is vital for the formation of spatial memories. Another example is the consolidation of emotionally salient memories, which is mediated predominantly by the amygdala, a limbic structure that receives a dense cholinergic projection (Woolf, 1991).

3 ALZHEIMER'S DISEASE

Alzheimer's disease (AD) is one of the most common forms of dementia, affecting more than 50 million people worldwide (Guerchet et al., 2020). AD pathogenesis begins several decades before detectable clinical symptoms such as memory impairment. Later, patients suffer from progressive loss of executive, language, and other cognitive functions, as well as physical abilities.

Extracellular deposition of amyloid-beta (Aβ) plaques and the intracellular formation of neurofibrillary tangles (NFT) represent the two critical markers of Alzheimer's pathology. Their presence uniquely characterizes AD among several diseases that can lead to dementia. The time course of these neuropathological components of AD is rather complex. Initially, in an asymptomatic period, amyloid plaques and a few NFTs emerge without any detectable clinical consequences. Afterwards, the pathology intensifies in an intermediate stage characterized by mild cognitive impairment (MCI). The final stage is described by widespread plaque and tangle accumulation and major behavioural and cognitive impairments.

3.1 ALZHEIMER'S DISEASE CONTINUUM

Current research in the field of AD suggests that pathological changes in the human brain can be observed decades before the onset of clinically detectable dementia (Albert et al., 2018; Buchhave et al., 2012; Villemagne et al., 2013). This was made possible predominantly with the development of AD pathologic biomarkers (described more in detail in Section 3.2). Most importantly, we could observe cognitively normal individuals with these biomarkers already present – a concept known as preclinical AD (Dubois et al., 2016). The fact that the disease starts many years before the symptoms are developed enabled the emergence of new strategies for risk factor assessment, early detection and early intervention through screening, and later diagnosis and treatment.

For these reasons, a conceptual shift occurred considering the disease as a continuum, ranging from preclinical AD (e.g., subjective cognitive decline, SCD) to mild cognitive impairment (MCI) and fully developed dementia. In the later stages of the continuum, major pathological and clinical changes are prominent, e.g., extracellular Aβ plaques and intracellular NFT pathology, memory loss, and other cognitive alterations.

Individuals that experience a self-reported worsening of cognitive performance but with cognition still not considered abnormal based on formal neuropsychological evaluation are said to have *subjective cognitive decline (SCD)*. In 2014, the SCD Initiative Working Group proposed a research framework which includes criteria for SCD subjects (Jessen et al., 2014). The definition of SCD according to these criteria is quite broad and only includes a self-perceived decline in cognitive ability (not caused by an acute event) while still performing normally (adjusted for age and education) on cognitive tests. This framework also lists SCD as one of the risk factors for MCI and AD dementia. It has to be noted that the SCD

population is highly heterogenous as self-reported cognitive decline is perceived very differently among individuals. It has been shown that SCD increases the risk of future cognitive impairment and dementia (Mitchell et al., 2014; Slot et al., 2019). Other findings demonstrated that individuals with subjective memory complaints have, on average, reduced volumes of the entorhinal cortex (Jessen et al., 2006), reduced cortical thickness in brain regions usually affected in AD (Schultz et al., 2015), as well as an increased amyloid burden (Perrotin et al., 2012) compared to controls.

Patients whose worsening cognition is already detectable, but its severity is not sufficient to be identified as dementia are clinically diagnosed as having a *mild cognitive impairment (MCI)*. Petersen (2004) proposed diagnostic and research criteria for MCI and subdivided MCI into two clinical subtypes: amnestic (with impaired memory function) and non-amnestic (with no memory impairment) MCI. Later, the National Institute on Aging and Alzheimer's Association (NIA-AA) formalized a refined version of diagnostic guidelines for *MCI due to AD* to characterize the predementia symptomatic phase of AD (Albert et al., 2011). The proposed evaluation algorithm establishes the clinical and cognitive criteria, the aetiology examination, and the biomarker evaluation. The use of biomarkers is not required by these criteria and serves only to increase the likelihood of a correct diagnosis of MCI due to AD.

Diagnostic criteria for *AD dementia* were proposed by McKhann et al. (1984), and it is called the NINCDS-ADRDA[2] criteria. In 2011, NIA-AA revised and updated these to reflect current research (McKhann et al., 2011). These diagnostic guidelines describe the AD pathophysiological process as having three phases: pre-clinical AD, MCI due to AD, and probable AD. A European version of AD diagnostic guidelines – IWG-2 – was proposed by The International Working Group (IWG) by Dubois et al. (2007) and revised in 2014 (Dubois et al., 2014). Both NIA-AA and IWG criteria are suggested mainly for use in research and not for clinical diagnosis of AD. In the Czech Republic, the MKN-10 criteria[3] – an adaptation of ICD-10 criteria (World Health Organization, 1993) – are used for diagnosing AD.

3.2 BIOMARKERS IN ALZHEIMER'S DISEASE

A biomarker is usually defined as "a characteristic that is objectively measured and evaluated as an indicator of normal biological processes, pathogenic processes, or pharmacologic responses to a therapeutic intervention" (Atkinson et al., 2001). In contrast to a clinical symptom, a biomarker is an objective measure of the medical state observed from outside the patient. One of its main properties is that it can be measured accurately and reproducibly.

Historically, multidomain amnestic dementia was used to define probably AD. However, this approach could not "rule in" AD pathological changes at autopsy. The absence of the syndrome could also not "rule out" AD pathologic changes (Nelson et al., 2011; Serrano-

[2] National Institute of Neurological and Communicative Disorders and Stroke (NINCDS) - Alzheimer's Disease and Related Disorders Association (ADRDA)
[3] *Mezinárodní klasifikace nemocí a souvisejících zdravotních problémů*

Pozo et al., 2014). A more recent approach suggested by the core clinical NIA-AA criteria from 2011 (described above) would recommend using biomarkers in research and clinical trials to support a diagnosis of AD in symptomatic individuals. The main reason was the lack of biomarker standardization and the belief that the core criteria were good enough for the diagnosis in most cases (McKhann et al., 2011). European IWG-2 criteria support the role of biomarkers in increasing the probability of a correct AD diagnosis but not being sufficient to diagnose AD pathology alone.

In order to understand and diagnose the disease better, a biological rather than symptomal definition was introduced. This was also supported by the requirements for treatment strategies which must engage biologically defined targets. NIA-AA has recently suggested a research framework in which neuropathological changes detected by biomarkers define the disease (Jack et al., 2018). This framework uses biomarkers as proxies for AD neuropathological changes: Aβ deposition, pathological tau, and neurodegeneration. The framework introduces a descriptive classification scheme for biomarkers used in AD and brain aging research. This scheme - labelled as AT(N) – recognizes three groups of biomarkers based on the kind of pathological processes that they measure:

- A – biomarkers of Aβ plaques
    - Cortical amyloid PET ligand binding
    - Low concentration of CSF $A\beta_{42}$
- T – fibrillar tau
    - Cortical tau PET ligand binding
    - Elevated concentration of CSF phosphorylated tau (p-tau)
- N – neurodegeneration or neuronal injury
    - CSF total tau (t-tau)
    - Fluorodeoxyglucose (FDG) PET
    - Atrophy on MRI

Note that each group of biomarkers include both CSF and imaging biomarkers. It is, therefore, possible to complete AT(N) characterization using imaging or CSF biomarkers alone or their mixture. The ‘N’ in the AT(N) scheme was put in parenthesis to denote that neurodegeneration is not AD-specific, whereas Aβ (A) and tau (T) uniquely define AD pathology.

3.2.1 Neuropsychological assessment

Neuropsychological testing is commonly used to aid in the diagnosis and treatment monitoring of dementia. Its main advantages include widespread use, standardisation and relatively low costs. The main disadvantage is low reproducibility and the inability to capture underlying biological mechanisms.

From a clinical point of view, the onset of AD is considered to begin with the deterioration of cognitive abilities. Although cognition is a rather complex abstract, its quantification and

evaluation are usually done through a battery of tests assessing impairment in several specific cognitive domains, such as episodic memory, attention, language and visuo-spatial processing.

Traditionally, the assessment is done by relating the patient's score on each individual test to criteria based on the reference group. It is essential to understand how each of the tested cognitive domains is influenced by an individual's environment and compare their performance to a reference group sampled from a population with similar demographic and social background.

3.2.2 Cerebrospinal fluid and blood biomarkers

Cerebrospinal fluid (CSF) acts as a cushion, protecting the brain and spinal cord from impact or injury. The fluid also helps the central nervous system work properly by removing waste products from the brain. CSF is primarily synthesised in the choroid plexus and is resorbed in arachnoid granulations.

As brain metabolism and pathology are reflected in CSF, its analysis is often used for diagnosis, treatment, and prevention strategies in neurodegenerative diseases. CSF is easily collected with a lumbar puncture (spinal tap). Commonly used CSF biomarkers are related to major pathological changes in AD brains: Aβ deposition into extracellular Aβ plaques, intracellular neurofibrillary tangles (NFT) formation, and neuronal loss.

Extracellular Aβ deposits in AD brains are formed by highly insoluble β-amyloid peptide composed of 42 amino acids ($A\beta_{42}$). $A\beta_{42}$ is the result of the cleavage of transmembrane amyloid precursor protein (APP), and it is detected as decreased CSF $A\beta_{42}$ concentration in AD.

Tau proteins are predominantly found in the cytosol of neurons, where they stabilize microtubules. In AD, an imbalance in enzyme kinetics causes tau hyperphosphorylation (p-tau), which leads to tau detachment from microtubules and accumulation in NFT. This can be detected as increased CSF p-tau.

In the neurodegenerative process, tau and phosphorylated tau proteins are released into the extracellular space, detected as increased CSF total tau (t-tau) concentration in AD. Plaques and NFT further stimulate neuronal injury. Neuronal and synaptic degeneration follows.

As the first Aβ plaques occur 10-30 years before the onset of the first symptoms (Jansen et al., 2015), analysis of CSF serves as an excellent biomarker for early diagnosis. Changes in CSF tau biomarkers can be observed later in the pathophysiological process (Buchhave et al., 2012; Jack and Holtzman, 2013).

Recent advances made it possible to measure Aβ and tau in blood plasma (Blennow and Zetterberg, 2018; Janelidze et al., 2020).

3.2.3 Brain imaging

Brain imaging in AD serves predominantly to show (1) spatial distribution of pathophysiological hallmarks of AD - Aβ, tau and glucose metabolism, and (2) neurodegeneration and function. Amyloid and tau accumulation can be quantified using positron emission tomography (PET). Visualization of cellular glucose uptake is facilitated by FDG PET. Magnetic resonance imaging (MRI) is often used to measure brain neurodegeneration and function.

PET imaging is a common nuclear imaging modality that detects and measures the concentration of target molecules in body tissue. This is achieved through radiotracers which are intravenously injected prior to the scan and which have a specific affinity to target structures. Afterwards, a ring of detectors is utilized to detect pairs of photons originating from the radiotracer's positron annihilation in the tissue. In contrast to amyloid CSF or tau CSF biomarkers, PET imaging is capable of providing *in vivo* spatial distribution of Aβ and tau. FDG PET is commonly used to measure cerebral metabolic rates of glucose, an indicator of neuronal activity (Marcus et al., 2014). It has been shown that cerebral metabolic alterations precede the clinical manifestation of AD symptoms (Mosconi, 2013). In AD, the retention of amyloid and tau PET tracers is increased, whereas FDG PET shows a decrease in glucose metabolism (Nordberg et al., 2010; Schilling et al., 2016).

MRI is capable of capturing the third important biomarker in dementia and AD – neurodegeneration, both on macroscopic and microscopic levels. Data in MRI are collected by turning certain magnetic fields on and off in a pre-defined sequence, referred to as a 'pulse sequence', in the presence of a strong magnetic field. Pulse sequences include spin echo sequences, inversion recovery sequences, and gradient echo sequences. A pulse sequence is generally defined by multiple parameters, including echo time (TE), repetition time (TR), inversion time (TI), flip angle, and field of view. Different combinations of these parameters affect tissue contrast and spatial resolution. The specific parameters for any given study differ from one manufacturer to another as well as from one imaging centre to another.

The analysis described in this thesis predominantly uses T1-weighted, fluid-attenuated inversion recovery (FLAIR) and diffusion-weighted imaging (DWI) sequences. Images originating from each of them show different contrast influencing the appearance of brain tissues.

The **T1-weighted** image reflects differences in the T1 relaxation times (also known as spin-lattice relaxation times) of tissues, making the water appear dark and fat bright, resulting in a good contrast between grey and white matter. This sequence is predominantly used for the study of brain atrophy, including volumetry of subcortical structures and measurement of cortical thickness.

FLAIR sequence exhibits no net transverse magnetization of fluid, resulting in images without a signal from CSF. In FLAIR images, grey matter appears brighter than white matter, but CSF is dark instead of bright. This sequence is helpful for the evaluation of many diseases

of the central nervous system, such as infarction, multiple sclerosis, head injuries, subarachnoid haemorrhage, and others. The Neuroimaging standards for research into small vessel disease (STRIVE criteria[4]) suggests consistently using FLAIR sequences for research and clinical diagnosis of cortical and subcortical infarcts (Wardlaw et al., 2013).

The contrast in the **DWI sequence** is sensitive to diffusion, which reflects the mobility (i.e., Brownian motion) of water within the tissue. In a homogeneous medium, diffusion is random and isotropic. However, the body's water volume is divided into cells and extracellular space, making the diffusion variably restricted. As different human tissues contain different cell types and shapes, they also show different diffusion properties. This is also true for the human brain. In white matter, the displacement of water molecules is bounded in long axons, whereas in cell bodies of grey matter, water molecules can move more freely in all directions. Brain tissue pathologies usually alter the diffusion properties of the tissue as well.

The basics of modern diffusion measurement were introduced by Stejskal and Tanner (1965). Their pulsed gradient spin echo (PGSE) sequence is based on a spin echo sequence (Hahn, 1950). In short, the scan starts with the excitation of the nuclei with a 90° radiofrequency (RF) pulse that tilts the magnetization vector into the plane whose normal is along the main magnetic field. The spins start to precess around the magnetic field (Larmor precession) with an angular frequency given by

$$\omega = \gamma B, \tag{1}$$

where B is the strength of the static magnetic field and γ is the gyromagnetic ratio – a constant specific to the nucleus under examination. In water, the hydrogen nucleus has a gyromagnetic ratio of approximately $2\pi \cdot 42.58 \cdot 10^6$ rad·s^{-1}·T^{-1}. Ensembles of spins which are initially coherent dephase from each other due to magnetic field inhomogeneities and dipolar interactions (Abragam and Hebel, 1961), leading to a decay of the signal induced in the receiver, often called T2* ('T2 star') signal loss. The dephasing due to magnetic field inhomogeneities can be reversed through a subsequent application of a 180° RF pulse, and the signal is reproduced as illustrated in Figure 1. This moment of spin coherence is usually referred to as a 'spin echo'. The time between the first RF pulse and the formation of the echo is called TE (echo time), and it is twice the time between the two RF pulses, which is denoted by τ. To achieve diffusion sensing (weighting), a pair of symmetric, strong magnetic field gradients G are applied on either side of the 180° RF pulse (pulse duration, δ). A stationary spin remains unaffected, but particles diffusing in the measured direction (given by the gradient orientation) during the allowed time (separation of the two pulses, Δ) fall out of phase and lose signal.

[4] STandards for ReportIng Vascular changes on nEuroimaging

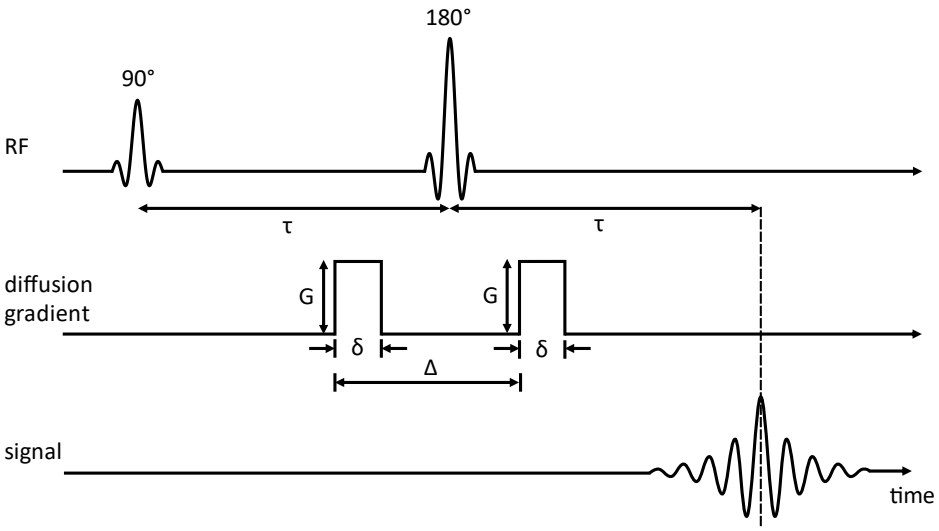

Figure 1. A schematic of the pulsed gradient spin echo (PGSE) MRI technique. Translational motion is encoded using a pair of gradient pulses with duration δ and magnitude G during the diffusion time Δ.

Figure 2 illustrates that the pair of gradient pulses has no net effect on spins which do not move. They are entirely in phase after its application. As shown in Figure 3, if there is a particle diffusing, the final signal is attenuated exponentially by the product of the diffusion coefficient D and the factor b, which is a function of the diffusion-weighting gradients.

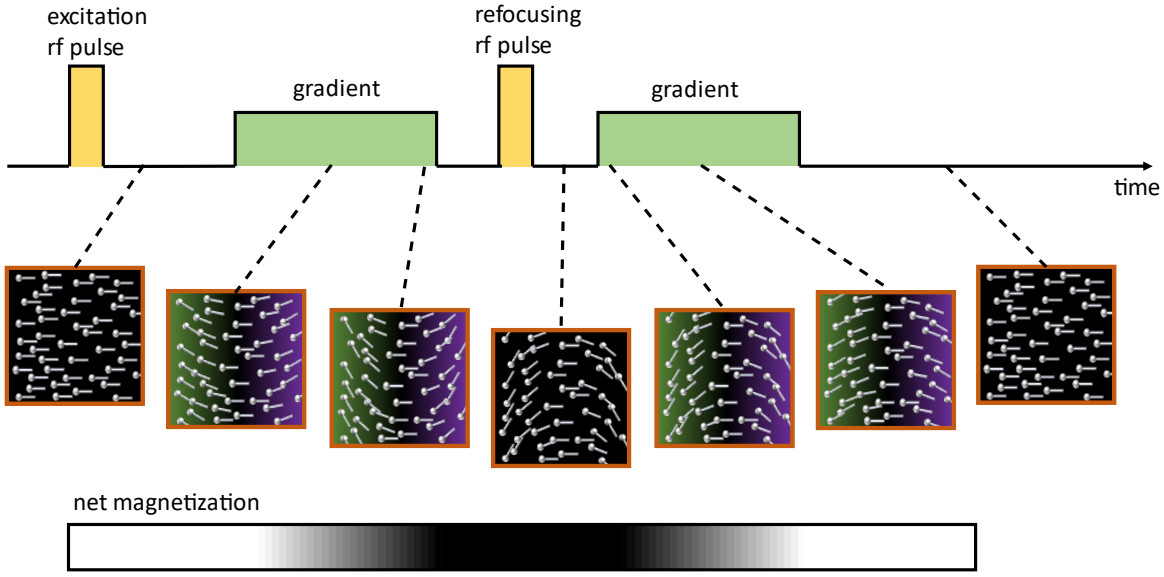

Figure 2. Explanation of how a pair of gradient pulses affects the phase of spins (no motion). Initially, after being excited, all spins are in phase. Then, when a positive gradient pulse is applied, the spins to the right are exposed to a stronger magnetic field (indicated by a magenta background), while those to the left experience a weaker magnetic field (indicated by a green background). As a result, the precessional frequencies of the right spins increase compared to those of the left spins. When the gradient pulse is turned off, all spins precess at the same frequency, but their relative phases remain the same. Because of the phase incoherence of the spins, the net magnetization is negligible at this point. To refocus the spins, an RF pulse is used to flip them in the plane perpendicular to the main magnetic field, with the faster precessing spins ending up behind the slower precessing ones. If the same gradient parameters are used again without any displacement between the first and second gradient, there will be no net effect on spin phase, net magnetization, or pixel brightness.

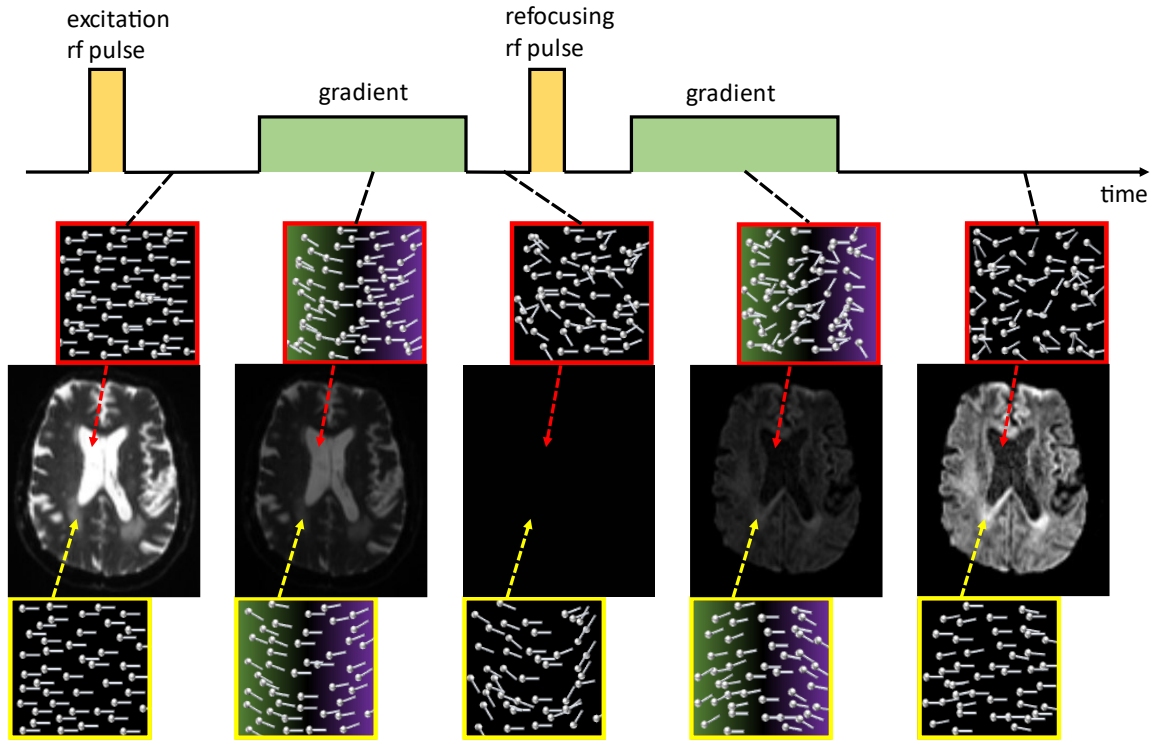

Figure 3. Explanation of how a pair of gradient pulses affects the phase of spins (presence of diffusive motion). Initially, after excitation, all spins are in phase. When a positive gradient pulse is applied, the spins lose their phase coherence and the net magnetization decreases in all pixels. A second gradient pulse is applied to remove most of the dephasing, but the magnetization does not fully recover due to motion caused by diffusion during the application of the gradient pulses. Consequently, spins in regions with high diffusion (such as CSF, indicated by a red pixel) exhibit greater phase incoherence and signal loss compared to those in regions with low diffusion (such as the area of stroke, indicated by a yellow pixel).

A variety of techniques for generating diffusion maps have been developed. By far, the most commonly used technique relies on a spin-echo echo-planar sequence (SE-EPI). Instead of repeated 180° RF pulses following the 90° RF pulse, echo planar imaging refers to sequences in which data for an entire 2D plane is collected following a single RF-excitation pulse. However, the necessarily long duration of the sampling trajectory makes this method prone to image artefacts.

Usually, diffusion protocol starts with the diffusion gradient turned off, i.e., $G = 0$. The resulting images are usually called *B0 images*. In the next steps, the diffusion contrast can be modulated in two different ways:

1. Diffusion weighting is achieved by choice of *gradient strength* G and *diffusion time* Δ. It is customary to denote different weighting by a b-value: $b \propto G^2 \cdot \Delta$. Generally, the higher the b-value, the better the diffusion contrast, but less signal is left due to exponential decay.
2. Sensing the diffusion signal along different spatial directions is determined by choice of *gradient directions*.

Usually, a few B0 images are acquired along with shells at higher b. A shell is a set of volumes acquired with the same b-value and various gradient directions. As the diffusion

may not be uniform in all directions, such as in WM, it is desirable to model the diffusion at all possible orientations in the three-dimensional space.

The simplest approach to model diffusion orientation distribution is by fitting a diffusion-tensor model in each voxel, a technique called *diffusion tensor imaging (DTI)*. This model can be described by the Stejskal-Tenner equation (Eq. 2).

$$S_j = S_0 \mathrm{e}^{-b_j \boldsymbol{x}_j^T \boldsymbol{D} \boldsymbol{x}_j}, \tag{2}$$

where S_j is a signal (image intensity at a voxel) measured after applying a gradient j with a (unit) direction $\boldsymbol{x}_j$ and a b-value b_j, S_0 is a signal measured with no diffusion gradient applied, and $\boldsymbol{D}$ is a diffusion tensor. As the entire set of diffusion-weighted images is used (rendering many values for S_j and $\boldsymbol{x}_j$), this is actually a system of equations that is solved for $\boldsymbol{D}$, the diffusion tensor. In an effort to calculate the six independent elements in the 3×3 symmetric matrix $\boldsymbol{D}$, at least seven images are required: a baseline image (giving S_0) and six diffusion-weighted images from 6 noncollinear gradient directions (giving six values for S_j). This system of equations can be solved with the least squares method or its variant at each voxel. For a more robust estimation of $\boldsymbol{D}$, a higher number of images, i.e., diffusion directions, is almost always used.

DTI models can be displayed in various forms: condensing the tensor into one scalar (single number), into four numbers (which are coded as red, green and blue colour components and brightness values) or using glyphs (3D representations of the tensor or its major eigenvector). The simplest scalar is the average of the diffusion tensor's eigenvalues – mean diffusivity (MD), or the sum of eigenvectors – the trace of the tensor. Both measures relate to the total amount of diffusion in a voxel, which is related to the amount of water in the extracellular space. Therefore they are sensitive to conditions that affect the barriers that restrict the movement of water, such as cell membranes (Zhang et al., 2014). Another widely used diffusion index is a normalized variance of the eigenvalues (Eq. 3) - fractional anisotropy (FA).

$$FA = \sqrt{\frac{3}{2}} \frac{\sqrt{\left(\lambda_1 - \bar{\lambda}\right)^2 + \left(\lambda_2 - \bar{\lambda}\right)^2 + \left(\lambda_3 - \bar{\lambda}\right)^2}}{\sqrt{\lambda_1^2 + \lambda_2^2 + \lambda_3^2}}, \tag{3}$$

where $\lambda_1, \lambda_2, \lambda_3$ are eigenvalues of the diffusion matrix $\boldsymbol{D}$, and $\bar{\lambda}$ is the mean diffusivity. FA ranges from 0 to 1. It describes the degree of anisotropy of a diffusion process. In extreme cases, FA = 1 only when diffusion occurs in one axis and is restricted in the other two, FA = 0, when the diffusion is isotropic. The FA index is clinically useful as the decrease in FA has been linked to the loss of myelin and axons in the white matter (Winklewski et al., 2018).

A negative aspect of the DTI model is that it can only describe Gaussian diffusion processes, which has been shown to be insufficient in representing the true diffusion process in the

human brain. A key limitation is that it can recover only a single fibre orientation in each voxel and fails at fibre crossings. For this reason, various alternative models and algorithms have been developed that aim to recover more detailed information about the orientations of fibres from diffusion MRI measurements and, in particular, to resolve the orientations of crossing fibres. The most direct extension is a multi-tensor model that is a simple generalization of DTI, which replaces the Gaussian model with a mixture of *n* Gaussian densities. Such a model assumes the voxel contains *n* distinct populations of fibres, and each population is modelled by a separate diffusion tensor. The multi-tensor model assumes that the number, *n*, of distinct fibre populations is known. A particular model with this form is a "ball-and-stick(s)" model (Behrens et al., 2003), which is used in the studies described in this thesis. This model assumes two water molecules populations: a restricted population around fibres (modelled with a Gaussian model in which the diffusion tensor has only one non-zero eigenvalue) and a free population that does not interact with fibres (modelled with an isotropic Gaussian model). The ball-and-stick model is implemented in the tractography toolbox of the FSL software package (University of Oxford) and TRACULA (FreeSurfer) software (Massachusetts General Hospital and Harvard Medical School). Another example of beyond-DTI methods involves non-parametric algorithms such as diffusion spectrum imaging (Tuch, 2002; Wedeen et al., 2005), Q-ball imaging (Hess et al., 2006), and spherical deconvolution (Tournier et al., 2004), which attempt to estimate the fibre orientation distribution function directly from data with minimal constraints.

DTI and other diffusion models are also often used for estimating the course of white matter pathways in a process called **tractography**. These pathways create the framework for information transfer between brain regions, and therefore it is of utmost importance to understand their function in the normal and diseased brain. Currently, tractography is the only available technique for identifying and measuring these pathways *in vivo* and non-invasively. It is important to note that compared to invasive tools, the tractography measurements are indirect, difficult to interpret and prone to error. Nevertheless, due to its non-invasiveness and ease of measurement, it is often a preferred method for addressing scientific and clinical questions that cannot be answered by any other means (Passingham, 2013). The basic principle lies in the fact that the diffusion of water molecules is more prominent along the direction of axon bundles than across them. For this reason, when diffusion is measured in several different directions, the preferred direction will be along the axon bundle. Therefore, to reconstruct the fibre bundles, the tractography algorithms try to find paths through the diffusion field along the directions which are least hindered. The basic principle is to integrate voxel-wise fibre orientation into a pathway that connects anatomical brain areas. This can be done in several ways. *Deterministic fibre tracking* finds fibre tracts using streamline fibre tracking with methods for solving ordinary differential equations, such as the Euler method, Runge–Kutta methods or FACT approach (Mori et al., 1999). It gave rise to structural connectomics and network-based analysis. The tracts can be used for sampling FA or MD and proceed with tract-specific analysis. *Probabilistic fibre tracking* methods model propagation directions as a distribution. The direction of propagation in each tracking step is

a sample drawn from the distribution. Thus, every time a track is generated from the same seed point, the algorithm may give a different result. This method proceeds in a high number of iterations, and it outputs a probabilistic map of possible fibre pathways. A popular probabilistic fibre tracking tool is *probrackx* from the FSL software package. More detailed use of diffusion-weighted MRI and tractography in cholinergic system imaging is presented in the next chapter.

Whereas diffusion and structural MRI describe anatomical features, **functional MRI (fMRI)** measures dynamic changes in the brain. In fact, this technique is sensitive to changes in blood and blood flow (hemodynamics) due to neuronal firing. More precisely, it is sensitive to hemoglobin and its property of distinct interaction of its oxygenated and deoxygenated forms with the magnetic field. This induces variation, which in the local magnetic field depends on the concentration of deoxygenated hemoglobin and creates small but detectable changes in the MRI signal. The relationship between neuronal activation and MRI signal changes is known as the blood oxygenation level-dependent (BOLD) effect, and this technique of functional MRI is often referred to as BOLD imaging or BOLD MRI. The main alternative style of sensing dynamic brain changes is the arterial spin labelling (ASL) technique. There are two main research objectives in fMRI: analyzing task-related activity using task fMRI and functional connectivity using resting state fMRI. For task fMRI, the participant performs a specific task within the scanner, and the aim is to locate and analyze the brain activity in response to it. Such studies are helpful in the context of understanding the working of the healthy brain but also for studying changes due to diseases. Resting-state fMRI is captured using the same type of MRI acquisition as task fMRI but in the absence of a stimulus or a task. Here, the participants are asked just to "relax" and "not think about anything in particular" (often with their eyes open to help stop them from falling asleep). The measured signal reflects spontaneous brain activity, and correlations between activation patterns of different brain areas provide information about their functional connectivity (Biswal et al., 1995). In AD, resting state fMRI has mainly been used for studying AD-related neurodegenerative changes in the hippocampus and the default mode network (Wang et al., 2016; Zhang et al., 2009; Zhou et al., 2008).

The chronology of the AD biomarker changes has been proposed by Jack et al. (2013), see Figure 4. This model describes the temporal evolution of AD biomarkers in relation to each other and to the onset and progression of clinical symptoms. In this model, Aβ abnormality in the CSF represents the first detectable phase, followed by abnormal tau levels in the CSF. Only then the brain atrophy is detectable before the onset of clinical symptoms. This model also suggests various cognitive impairment curve shifts depending on genetic, lifestyle, and environmental factors.

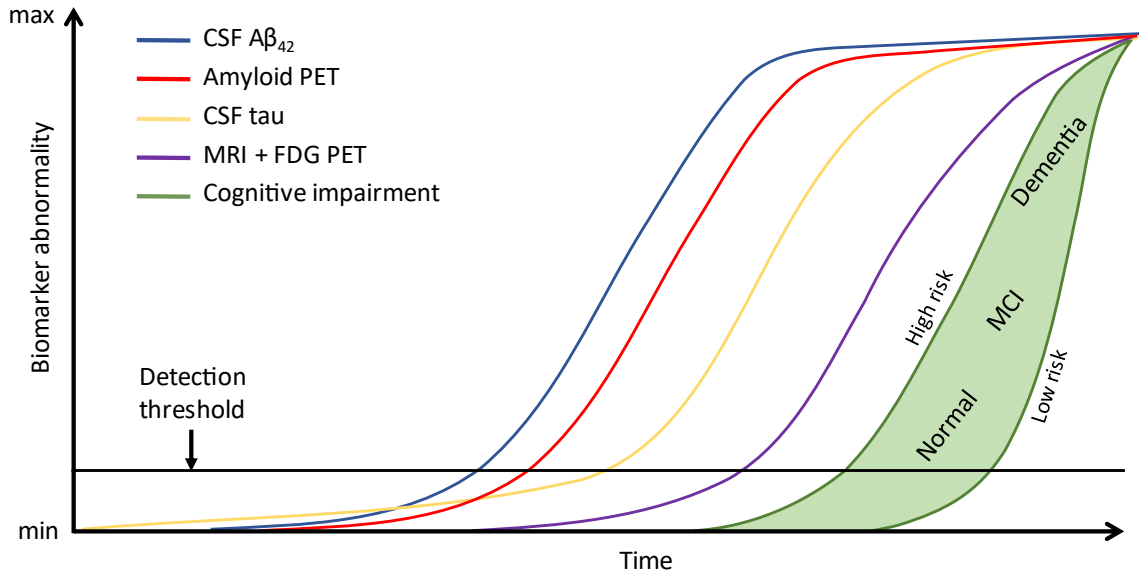

Figure 4. A model of dynamic biomarkers of the Alzheimer's disease pathological cascade. The area below the detection threshold denotes the zone in which abnormal pathophysiological changes cannot be detected by currently used Alzheimer's disease biomarkers. The figure is redrawn from the model presented in Jack et al. (2013).

3.3 CHOLINERGIC CIRCUITS ALTERATIONS IN THE PATHOPHYSIOLOGY OF ALZHEIMER'S DISEASE

The central role of the cholinergic system in relationship to normal cognition and age-related cognitive decline, including dementias such as AD, is described by the cholinergic hypothesis of cognitive ageing. This hypothesis postulates that functional disturbances in cholinergic activity occur in the brains of healthy older adults and demented patients and that these disturbances play a role in memory loss and related cognitive problems (Dumas and Newhouse, 2011). It is based on three milestones: the discovery of depleted presynaptic cholinergic markers in the cerebral cortex (Bowen et al., 1976; Davies and Maloney, 1976); the discovery that NBM in the basal forebrain is the source of cortical cholinergic innervation that undergoes severe neurodegeneration in AD (Mesulam, 1976; Whitehouse et al., 1981); and the demonstration that cholinergic antagonists impair memory whereas agonists have the opposite effect (Drachman and Leavitt, 1974). The hypothesis was further supported when cholinesterase inhibitor therapies were shown to lead to significant symptomatic improvement in patients with AD (Summers et al., 1986). Since the 1970s, other relevant hypotheses have received significant research attention, but the treatment based on the restoration of cholinergic function remains the prevailing therapeutic strategy in the management of AD.

As mentioned above, neurodegeneration of NBM cholinergic neurons plays an important part in the AD cascade. Studies (Mesulam, 1976; Whitehouse et al., 1981) showed that the cholinergic disruptions, emerging as early as the asymptomatic or prodromal stage of the disease, are predominantly presynaptic rather than postsynaptic. That is, the cholinergic loss in NBM cholinergic neurons and their axons projecting to the cerebral cortex precede degeneration of cortical cholinergic endings. Hence, a progressive loss of cholinergic basal

forebrain neurons represents a pivotal event followed by a disruption in cortical connections in the cerebral cortex, hippocampus and amygdala (Sassin et al., 2000).

The significance of the cholinergic system in the pathophysiology of AD is further underlined by the effects of anticholinergic agents and cholinergic therapies. There are several studies which demonstrated the adverse pharmacological effects of anticholinergic medications on human memory and learning (Drachman and Leavitt, 1974; Mewaldt and Ghoneim, 1979; Petersen, 1977), reaction times (Sittironnarit et al., 2011), and activities of daily living (Salahudeen et al., 2015). In addition, recent data suggest that these negative cognitive effects may not be transient (Risacher et al., 2016). It was also shown that greater cumulative use of anticholinergic drugs is linked to an increased risk of progression of cognitively normal adults to MCI or AD dementia (Gray et al., 2015; Risacher et al., 2016). On the other hand, a treatment that promotes cholinergic function in individuals with (or at risk for) AD may have substantial brain structural protective effects than a short-term boost of cognitive function. Studies (Cavedo et al., 2017, 2016) found that the use of donepezil (cholinesterase inhibitor) in suspected prodromal AD was associated with substantially less regional cortical thinning and basal forebrain atrophy over time and a significant reduction in the rate of hippocampal atrophy after one year of treatment (Dubois et al., 2015).

It has been established that cholinergic deficit plays a key role in the neuropathology of AD, not only in late disease but also in preclinical and early stages. It has been shown that specifically the cholinergic neurons of the basal forebrain are affected by the accumulation of abnormally phosphorylated tau, in the form of neurofibrillary tangles and pretangles, in cognitively normal elderly subjects and patients with MCI and significant correlation with performance in memory tasks was found (Mesulam et al., 2004). Cholinergic axon abnormalities demonstrated in middle-aged adults have been shown to increase with age. This suggests that cholinergic loss in established AD is preceded by cholinergic pathology (Geula et al., 2008). Interestingly, cholinergic function outside of the NBM, namely in the caudate, putamen, and thalamus – appears relatively spared in this process. This infers a preferential vulnerability of the NBM. The principal cause may be the anatomical location of NBM in a continuous band of basolimbic structures, including the amygdala, hippocampus, and entorhinal cortex, which are collectively at the highest risk of neurofibrillary degeneration and neurofibrillary tangle formation in the ageing-MCI-AD continuum (Mesulam, 2013). This is also in line with a study (Schmitz and Nathan Spreng, 2016), which has shown using longitudinal MRI and amyloid biomarkers that volume loss in the NBM precedes and predicts both entorhinal pathology and memory impairment. This observation further reinforces the conclusion that the loss of NBM neurons is an early and clinically relevant event on the AD continuum.

It is important to note that pronounced disturbances in the cholinergic system have also been implied in other neurodegenerative diseases, such as dementia with Lewy bodies, traumatic brain injury, and Parkinson's disease (Pepeu and Grazia Giovannini, 2017).

4 CHOLINERGIC SYSTEM IMAGING

As outlined in the previous chapters, the cholinergic system has a dominant role in the pathophysiology of AD, especially notable in its preclinical and early phases. It is also a prime target in the currently available methods of treatment. For these reasons, the ability of *in vivo* visualizing and examining the properties of the cholinergic system is of major interest in the study of AD pathophysiology. It would also possibly facilitate early diagnostics and disease progression monitoring during treatment and drug development. There are several currently used techniques for cholinergic system imaging. They range from post-mortem histological methods using histochemical labelling to minimally invasive PET imaging of radiotracers with a high specific affinity to different components of the cholinergic transmission chain to fast and noninvasive MRI imaging.

4.1 PET IMAGING

Currently, possibly the most direct possibility of obtaining *in vivo* information about the integrity of cholinergic transmission is by means of PET imaging. Many PET tracers targeting different compartments of cholinergic transmission are available. These include radioligands for the neuronal vesicular acetylcholine transport protein (VAChT), radioligands for muscarinic (mAChRs) and nicotinic (nAChRs) receptors, and radiolabelled acetylcholinesterase (AChE) inhibitors and substrates. Some of these imaging agents have been used to study the underlying mechanisms of human dementia. Most notable examples include: [^{18}F]FEOBV (Petrou et al., 2014), a presynaptic cholinergic PET radioligand with good sensitivity and specificity for VAChT, has recently been developed and tested in humans and showed a promise to be a valuable tool to assess dysregulation of the cholinergic system in AD and parkinsonian (Petrou et al., 2014); [^{18}F]AZAN (Kuwabara et al., 2011), [^{18}F]XTRA (Coughlin et al., 2018), [^{18}F]nifene (Lao et al., 2017), [^{18}F]flubatine (Sabri et al., 2015), second-generation imaging agents of nAChR α4β2 subtype, showed high potential for PET imaging in monitoring disease progression and the respective therapies (Coughlin et al., 2018; Sabri et al., 2018; Wong et al., 2013); [^{17}F]ASEM (Wong et al., 2014), a second-generation imaging agent of nAChR α7 subtype, is seen as the most promising for disease staging, progression estimation and drug testing in neurodegenerative diseases (Coughlin et al., 2020); [^{11}C]PMP (Kuhl et al., 1999) and [^{11}C]MP4A (Iyo et al., 1997), radioligands of AchE, have showed distinctive patterns of cortical activity in AD than in healthy controls (Iyo et al., 1997; Kuhl et al., 1999) and have been successfully employed to assess the efficacy of donepezil (AChE inhibitor) treatment (Bohnen et al., 2005; Kuhl et al., 2000; Richter et al., 2018).

It has to be noted that acetylcholine synthesis in the human brain cannot be quantified with PET imaging since a successful tracer for the enzyme choline acetyltransferase (ChAT) has not yet been developed. Instead, the assessment of AChE activity is regarded as a reliable biomarker of the cholinergic system in the CNS (Bohnen and Frey, 2007; Shinotoh et al., 2021). A comprehensive overview of PET agents in imaging of cholinergic neurotransmission in neurodegenerative disorders can be found in (Tiepolt et al., 2022).

Although the molecular imaging of the cholinergic system may bring certain benefits for disease diagnostics and treatment, especially with the emergence of second-generation radioligands, its high costs so far hinder its routine use in a clinical environment. Moreover, due to the invasive nature of the PET imaging, its use might not always be appropriate for investigation of certain clinical and research conditions.

4.2 CHOLINERGIC BASAL FOREBRAIN

Direct visualization of neurons of NBM is possible with histological techniques. As described in Section 2.1, Mesulam and collaborators (Mesulam and Geula, 1988) identified various populations of cholinergic neurons in the human basal forebrain using histochemical and immunohistochemical labelling for choline acetyltransferase and acetylcholinesterase. Histological methods have also been used for the assessment of the volume of NBM (Grinberg and Heinsen, 2007; Halliday et al., 1993). The resulting volumes are considered to fairly estimate the true volume of the structure.

Imaging using MRI offers a noninvasive *in vivo* alternative. The study of NBM with MRI is, however, challenging. This is because the NBM does not have restricted boundaries surrounded by fibre bundles or by distinct cellular groups. Together with a limited resolution of MRI, this can lead to an inclusion of surrounding non-NBM structures resulting in an overestimation of the NBM region of interest (ROI). There are several methods of the localization of NBM and estimating its volume.

The first method (Kilimann et al., 2014; S. J. Teipel et al., 2014; Teipel et al., 2005; Wolf et al., 2014) identifies the basal forebrain nuclei from the histological sections of the dehydrated brain and then transfers these sections to a single T1-weighted post-mortem MRI scan and finally into the MNI space. Using this approach, a grey-matter ROI was made which is used to automatically extract modulated grey-matter voxels within the ROI for individual participants to report a volume. This NBM segmentation template was used by several later studies (Grothe et al., 2013, 2012; Teipel et al., 2011) to report a volume loss in AD patients.

Another method of defining the NBM using MRI is based on the application of probabilistic atlases. Zaborszky et al. (2008) introduced a probability atlas of the basal forebrain based on the post-mortem brains of 10 participants. They used silver-stained serial brain sections for cytoarchitectonic mapping. The position and extent of cell groups were traced in high-resolution digitalized histological sections, 3D reconstructed and warped to the reference MNI space. Due to the low interindividual variability of subcortical structures, the resulting probability maps showed to be efficient tools for precise topological analysis of structural changes in the basal forebrain in aging and AD (Zaborszky et al., 2008). This segmentation map is ready to use to estimate the position and size of NBM in studies without access to the post-mortem brain in SPM Anatomy Toolbox.

Lastly, NBM can also be localized using a manual segmentation protocol directly in the MRI brain scans. The exact procedure can be found in (George et al., 2011). This method was

previously used in several studies (Choi et al., 2012; Lin et al., 2022) to estimate NBM volume.

4.3 CHOLINERGIC PROJECTIONS

The most direct mapping of the efferent cholinergic projections from the NBM was made possible by an immunohistochemistry study in post-mortem brain tissue from healthy subjects (Selden et al., 1998). The study revealed that the projections leave the nucleus in two highly discrete organized fibre bundles forming the medial and lateral cholinergic pathways. The medial pathway leaves the NBM anteriorly and joins the white matter of the gyrus rectus. It curves around the rostrum of the corpus callosum to enter the cingulum, travels posteriorly to the splenium and enters the retrosplenial white matter to merge with fibres of the lateral pathway in the occipital lobe (Selden et al., 1998). The lateral pathway subdivides into a capsular division, travelling within the external capsule, and a perisylvian division, travelling within the claustrum.

Except for the post-mortem brain studies, it is currently possible to evaluate NBM and its cholinergic pathways using diffusion-weighted imaging. Authors in (Hong and Jang, 2010) claim to be the first ones to investigate cholinergic pathways *in vivo*. They tracked neuronal pathways from NBM passing through the cingulum in the brains of cognitively healthy individuals using probabilistic diffusion tensor tractography. The tracts found were not only described and identified, but also their volume and integrity (via FA and MD indices) were measured. A study (Liu et al., 2017) tracked cholinergic pathways from the cholinergic basal forebrain through the external capsule, cingulum and claustrum in a cohort of patients with vascular cognitive impairment, no dementia. DTI tractography was used as well. These studies relied on a precise definition of NBM ROI in the MRI image space from which the tractography was initiated.

MRI techniques based on resting-state functional MRI could provide further information on the NBM cholinergic pathways *in vivo*. This technique was recently used to investigate coordinated signal fluctuations between the basal forebrain and the cortex, revealing distinct functional connectivity patterns of the basal forebrain (Fritz et al., 2019; Herdick et al., 2020; Markello et al., 2018). Interestingly, the derived networks, which were based on functional connectivity, closely overlapped with known anatomical basal forebrain connections.

5 PARTICIPANTS AND METHODS

The following chapter is dedicated to the description of the cohorts used in the studies of this thesis, inclusion criteria for the participants, a detailed presentation of the pipeline for the segmentation of the cholinergic pathways, and an overview of statistical methods used in the study designs of the three studies.

5.1 ETHICAL CONSIDERATIONS

All included studies were conducted in accordance with the Helsinki Declaration of 1975 and its later amendments. Participation in the GENIC study was completely voluntary, and all the participants gave written informed consent. The protocol was approved by the local ethics committee of the University of La Laguna (Spain). The H70 study was approved by the Regional Ethical Review Board in Gothenburg (Sweden) and by the Radiation Protection Committee. The DELCODE study was conducted in multiple centres. All participants or their legal representatives provided written informed consent. The study protocol was approved by the local institutional review boards and ethics committees of the participating centres.

5.2 PARTICIPANTS

5.2.1 Cohorts

GENIC

The participants in the GENIC cohort come from the population sample of the Canarian Neuropsychological Study Group (Grupo de Estudios Neuropsicológicos de las Islas Canarias, GENIC), which currently consists of data from over 600 baseline participants. The collection of GENIC sample data began in 2004 and is still on-going today, mainly the part corresponding to the follow-up phase (Ferreira et al., 2017). The main goal of the study is to provide a cognitive and neuroanatomical characterization of aging in the general population, from early middle age to older adults.

These participants come from different municipalities on the island of Tenerife. The vast majority are native to these same municipalities, although there are also some from other islands in the Canary archipelago, as well as from other regions of Spain and a few from abroad. Contact with volunteers is established through different channels: primary care health centres in the respective municipalities, cognitive stimulation workshops, relatives and acquaintances of students from the Psychology Faculty at the University of La Laguna, people known by the research staff, etc. All participants were invited to take a comprehensive semi-structured interview and neuropsychological evaluation. Participation was voluntary and disinterested, evidenced by signing an informed consent. At the end of each study, a personal report of the results is provided upon request.

For each participant, a semi-structured interview is conducted that includes personal and sociodemographic data (age, sex, marital status, education level, occupation, and hobbies), general health status (appetite, sleep, control of sphincters, vision, hearing, presence of motor

problems, delusions and/or hallucinations, and changes in character); family and personal medical history (cardiovascular, psychiatric, dementia or other diseases). Subsequently, the subjective cognitive complaints questionnaire is administered, which includes the following cognitive domains: temporal and spatial orientation, attention and concentration, memory, and language (reading, writing, naming, comprehension, speech).

Next, a general cognitive state exploration, functional autonomy, and depressive symptoms are evaluated using different scales depending on the participant's age. Additionally, to determine participants' hand preference, the Edinburgh Handedness Inventory (EHI) questionnaire is administered. Finally, different instruments are used to evaluate cognitive reserve, including the Information and Vocabulary subtests of the WAIS-III and the Cognitive Reserve Questionnaire.

Once the interview phase is complete, a comprehensive neuropsychological evaluation protocol is administered to all GENIC sample participants, which covers the different cognitive functions and different cognitive components within each function in an exhaustive manner.

Finally, for each GENIC participant, an MRI study is performed using a 3.0 T Signa Excite HD General Electric machine, which takes place in the facilities of the Canarian University Hospital, managed by the Magnetic Resonance Service for Biomedical Research. The MRI protocol includes T1-weighted, FLAIR, DWI, and resting state fMRI sequences.

H70

The Gothenburg H70 Birth Cohort Studies (H70 studies) are multidisciplinary epidemiological studies examining representative birth cohorts of older populations in Gothenburg, Sweden. The first study started in 1971. So far, six birth cohorts with baseline examination at age 70 have been followed longitudinally (Rydberg Sterner et al., 2019). The overarching aim of the H70 studies is to examine the impact of mental, somatic and social health on the functional ability and well-being of individuals aged 70 years and above, taking into account the complex interactions with age, sex, gender, socioeconomic gradients, environmental exposures, psychosocial, neurobiological, and genetic factors.

In the study described in this thesis, the baseline examination of the Birth cohort 1944, conducted in 2014–16, was used. Every 70-year-old listed in the Swedish Population Registry as a resident in Gothenburg (Sweden) was invited to a comprehensive examination on aging and age-related factors. A total of 1,203 individuals born in 1944 (response rate 72.2%; mean age 70.5 years) agreed to participate, of whom 430 consented to a lumbar puncture (response rate 35.8%). The study comprised a one-day general examination at the Neuropsychiatric Clinic at Sahlgrenska University Hospital, as well as a number of additional examinations. Examination procedures included blood and cerebrospinal fluid sampling, examination of genetics and family history, psychiatric examination, clinical cognitive examination, general health interview, medication reporting, physical examination, body composition, lung

function, audiological and ophthalmic examinations, assessment of functional abilities and disabilities, physical fitness and physical activity examination, interview regarding social factors, self-rating questionnaires, an overall quantitative rating of medical burden. Participants also underwent both computed tomography (CT) and magnetic resonance imaging. The CT data were acquired on a 64-slice Philips Ingenuity CT system (Philips Medical Systems, Best, Netherlands). The MRI data were acquired on a 3.0T Philips Achieva system (Philips Medical Systems). The MRI protocol consisted of T1-weighted acquisition, FLAIR, T2-weighted images, DWI, and a resting-state fMRI sequence. More information can be found in (Rydberg Sterner et al., 2019).

DELCODE

DELCODE (DZNE-Longitudinal Cognitive Impairment and Dementia Study) is a longitudinal memory clinic-based observational study focusing on SCD in the context of AD. The DZNE (Deutsches Zentrum für neurodegenerative Erkrankungen, German Center for Neurodegenerative Diseases) is a national research institution dedicated to molecular, clinical, epidemiological, healthcare, and nursing research on neurodegenerative diseases. It has nine operational sites in Germany, of which seven collaborate with respective local university memory centres. In total, this provides a network of 10 memory clinics. The clinical research branch of the DZNE created methodological cores for clinical assessment/neuropsychology, MRI, PET, and biomaterial. Next to SCD, the DELCODE study also includes individuals with MCI and mild AD as well as control subjects without subjective or objective cognitive impairment. In addition, first-degree relatives of patients with AD dementia are enrolled as an exploratory at-risk group. The main aims of DELCODE are: the development of a refined understanding of SCD in the context of AD; the establishment of prediction models and estimates of cognitive decline in SCD; the investigation of the effects of risk and protective factors on the cognitive decline; and development of new disease markers (Jessen et al., 2018).

All participants underwent an MRI acquisition on a Siemens 3.0 T scanner (Erlangen, Germany) in one of the ten recruitment sites using identical acquisition parameters and harmonized procedures. Scanners comprised 3 Magnetom Trio TIM systems, 2 Magnetom Verio systems, 1 Magnetom Prisma system, and 4 Magnetom Skyra systems. The acquisition protocol included T1-weighted and T2-weighted imaging, FLAIR scans, a task fMRI, and DWI. To ensure high image quality throughout the acquisition phase, all scans had to pass a semiautomated quality check during the study conduction so that protocol deviations could be reported to the study sites and the acquisition at the respective site could be adjusted. More information can be found in (Jessen et al., 2018).

5.2.2 Study I participants (GENIC)

A sample of the baseline data from the GENIC cohort was used to address the goals of Study I (Table 1). The whole subset was split into low and high WM hypointensity (WM-hypo) load groups (as specified in section 5.3.6) for the purpose of the analysis.

Table 1. Demographic and clinical variables of a subset of GENIC in Study I.

	Whole sample	Low WM-hypo group	High WM-hypo group
N	262	226	36
Sex (male/female)	122/140	97/129	25/11
Age	55.6 (10.4)	53.9 (9.5)	65.2 (8.9)
WAIS-III Information	16.6 (5.9)	16.6 (5.9)	16.5 (5.9)
BDRS	0.9 (1.5)	0.8 (1.3)	1.4 (2.2)
FAQ	0.4 (0.8)	0.4 (0.8)	0.4 (0.6)
BDI-GDS composite	0.0 (1.0)	-0.04 (0.92)	0.15 (1.32)
MMSE	28.8 (1.3)	28.8 (1.2)	28.5 (1.4)
PCV – reaction time	476 (82.1)	471.0 (74.8)	511.0 (111.0)
STROOP – words	99.5 (18.9)	99.9 (18.6)	97.5 (21.2)
TAVEC learning	55.3 (9.1)	56.0 (9.2)	51.8 (7.4)
TAVEC delayed recall (5 min)	11.6 (2.8)	11.8 (2.7)	10.4 (2.6)
TAVEC delayed recall (30 min)	13.6 (2.5)	13.8 (2.5)	12.7 (2.3)
TAVEC recognition	15.6 (0.6)	15.7 (0.6)	15.4 (0.9)

Values represent mean value (SD) or count. WAIS-III, Wechsler Adult Intelligence Scale – Third revision; BDRS, Blessed Dementia Rating Scale; FAQ, Functional Activity Questionnaire; GDS, Geriatric Depression Scale; BDI, Beck Depression Inventory; MMSE, Mini-Mental State Examination; PCV – reaction time, PC-Vienna cognitive reactive time; TAVEC, the Spanish version of the California Verbal Learning Test (CVLT); WM-hypo, WM hypointensities on T1-weighted images appearing as WM hyperintensities on T2/FLAIR sequences.

5.2.3 Study II participants (H70)

For Study II, a data sample from the Gothenburg H70 Birth Cohort 1944 was used (Table 2). All participants were aged 70 years.

Table 2. Demographic and clinical variables of a subset of H70 in Study II.

	Whole sample
N	203
Sex (male/female)	100/103
APOE status (% ε4 carriers)	35
MMSE	29.23 (0.98)
Education (y)	13.22 (3.95)
$A\beta_{38}$ (pg/ml)	2498 (679.15)
p-tau (pg/ml)	49.45 (17.56)
Hypertension (%)	73.8
Diabetes (%)	11.3
Smoking (%)	61.7
Ischemia (%)	6.0
Cerebral microbleeds (%)	16.7
Lacunes (%)	8.4
Superficial siderosis (%)	1.5

Values represent mean (SD) unless another parameter is specified. MMSE, Mini-Mental State Examination; Aβ, β-amyloid; p-tau = phosphorylated tau 181.

5.2.4 Study III participants (DELCODE)

In Study III, a subset of baseline data from the DELCODE cohort was used (Table 3). The data were stratified according to the primary diagnosis into four groups: healthy controls (HC), SCD, MCI, and AD dementia. In a subsample, APOE4 genotype and/or CSF biomarkers were available.

Table 3. Demographic and clinical variables of baseline DELCODE data from Study III.

	HC	SCD	MCI	AD dementia
N	112	172	66	52
Age	69.1 (5.6)	71.6 (6.3)	72.6 (6.4)	75.2 (6.8)
Sex (male/female)	48/64	96/76	43/23	23/29
Education (y)	14.8 (2.7)	14.5 (3.0)	14.1 (3.1)	12.6 (3.0)
MMSE	29.4 (0.9)	29.2 (0.9)	27.8 (1.8)	21.9 (3.1)
ADAS word list learning (immediate recall)	23.2 (3.5)	21.6 (3.7)	16.4 (3.9)	10.7 (4.0)
ADAS word list recall (delayed recall)	8.09 (1.62)	7.23 (1.78)	4.03 (2.44)	1.24 (1.61)
ADAS figure learning (recall)	9.99 (1.60)	9.78 (1.79)	6.64 (3.22)	1.98 (2.18)
Trail making test A	43.9 (17.3)	41.0 (14.7)	57.0 (27.1)	94.2 (52.2)
Trail making test B	90.5 (25.8)	101.0 (38.4)	133.0 (60.7)	244.0 (84.0)
Symbol digit modalities test	49.6 (9.2)	45.7 (9.8)	37.3 (9.8)	21.2 (12.0)
APOE genotype available (n)	109	166	63	50
APOE4 genotype (n, %)	24 (22.0)	51 (30.7)	30 (47.6)	27 (54.0)
CSF biomarkers (n)	40	73	47	25
Aβ42/Aβ40	0.079 (0.023)	0.088 (0.027)	0.066 (0.028)	0.052 (0.017)
total tau (pg/ml)	368 (143)	378 (188)	544 (257)	883 (438)
p-tau181 (pg/ml)	51.3 (17.3)	52.5 (24.7)	70.1 (31.8)	107.0 (58.4)
Amyloid positive (n)	11	28	35	23

Values reflect mean value (SD) or count unless another parameter is specified.

5.3 METHODS

5.3.1 Diagnostic criteria

Subsamples and diagnostic groups of each cohort used in the studies of this thesis were selected with regard to the following diagnostic criteria.

GENIC subset

Inclusion diagnostic criteria for the Study I were: (1) Normal cognitive performance in comprehensive neuropsychological assessment using pertinent clinical normative data and excluding individuals with performance below 2 SD using own sample descriptive values (i.e., individuals did not fulfil cognitive criteria for MCI or dementia); (2) preserved activities of daily living and global cognition operationalized as a Functional Activity Questionnaire (FAQ) score ≤ 5, a Blessed Dementia Rating Scale (BDRS) score ≤ 4, and a Mini-Mental State Examination (MMSE) score ≥ 24 (the MMSE cut-point of ≥ 24 is used for screening according to the demographic characteristics of the cohort, but cognitive impairment is ruled out using comprehensive neuropsychological assessment as described in criterion #1 above);

(3) Availability of MRI data; (4) No abnormal findings such as stroke, tumors, hippocampal sclerosis, etc., in MRI according to an experienced neuroradiologist; (5) no medical history of neurological or psychiatric disorders (including a diagnosis of major depression), systemic diseases or head trauma; and (6) no history of substance abuse.

H70 subset

For the current study, inclusion criteria were (1) a Clinical Dementia Rating (CDR) score of 0; (2) a Mini-Mental State Examination (MMSE) score > 24; (3) availability of CSF biomarkers; and (4) availability of MRI data.

DELCODE subset

The participants underwent a clinical assessment of their cognitive status, including the Mini-Mental State Examination (MMSE) and an extensive neuropsychological testing battery (Consortium to Establish a Registry for Alzheimer's Disease neuropsychological test battery). Depressive symptoms were assessed with the Geriatric Depression Scale. The DELCODE exclusion criteria are current major depressive episodes, past or present major psychiatric disorders, neurological diseases other than AD or MCI, or unstable medical conditions.

SCD was defined as a persistent self-perceived cognitive impairment in the absence of objective cognitive impairment, lasting at least six months and being unrelated to an acute event (Jessen et al., 2014). The MCI patients met the core clinical criteria for MCI according to National Institute on Aging-Alzheimer's Association (NIA-AA) workgroup guidelines (Albert et al., 2011). The AD patients had a clinical diagnosis of probable AD dementia according to the NIA-AA workgroup guidelines (McKhann et al., 2011). The HC participants had no objective cognitive impairment in cognitive tests, no history of neurological or psychiatric disease, and did not report a self-perceived cognitive decline.

5.3.2 Cognitive assessment

In Study I, according to the aims of the study, a set of tests of memory and attention was selected:

- TAVEC (Benedet MJ, 1998), the Spanish version of the California Verbal Learning Test (CVLT), was used to measure verbal episodic memory. Total learning score after five learning trials, delayed recall after 5 minutes, delayed recall after 30 minutes, and recognition were included. Higher values reflect better performance.
- The first sheet (words) of the Stroop test (Stroop, 1935), a verbal task with higher demands on focussed attention. Participants were given 45 seconds to complete the task, and the score obtained was the total number of words correctly read (higher values reflect better performance). Stroop is also a common test for processing speed and executive functioning.
- Choice Reaction Times task of the PC-Vienna System (PCV – reaction time) (Schuhfried, 1992), a visual task with higher demands on vigilance. Participants

underwent a 15-min computerised vigilance task in which a response is required when a specific stimulus is displayed. Time is recorded, with higher time values and errors denoting worse performance. PCV is also a traditional test for processing speed, and it includes a component of motor inhibition.

A slightly different set of similar tests of memory and attention was available in the DELCODE dataset (Study III):

- Selected tasks of the Alzheimer's Disease Assessment Scale–Cognitive 13-item subscale (ADAS-Cog 13) (Mohs et al., 1997): ADAS word list learning (immediate recall), ADAS word list recall (delayed recall), and ADAS figure learning, to assess verbal and spatial episodic memory.
- An oral form of the Symbol Digit Modalities Test (Smith, 1982) to measure attention.
- Train Making Test A and B (Reitan, 1958) forms to measure attention.

5.3.3 Neuroimaging data

A comprehensive overview of neuroimaging data, including the specification of MRI sequences used in the studies of this thesis, is listed in Table 4.

Each of the three studies presented in this thesis used MR images acquired with T1-weighted (T1w) MRI sequences. As the T1w scans show excellent contrast of tissues with a high-fat content (such as white matter), they are suitable for imaging brain anatomy. In our studies, these structural scans were predominantly used for a precise definition of structural landmarks of the brain. First, high-resolution T1w scans were used for the segmentation of NBM, hippocampus and other brain structures. Consequently, the segmented regions of interest served as seed points and midpoints in the diffusion tracking process. For this, segmentation masks of respective brain structures defined in T1-based atlases were transferred into the patient's T1-based space using nonlinear registration. Only after that could the mask have been transferred again into the patient's DWI-based space in which the tracking was performed. The reason behind this rather complicated procedure is a far better resolution (and anatomical detail) of T1w images as compared to DWI images minimizing localization and quantification errors. Second, the ROI definition in T1w images can also be used for volumetric purposes, e.g., the estimate of NBM volume was calculated as a volume of GM voxels within the NBM ROI in the patient's T1w space. The GM segmentation was obtained using the T1w as well (Zhang et al., 2001). The total intracranial volume (TIV), which can also be estimated from T1w images, was used to normalize raw volumetric values to account for between-subject variability in head size.

Study II investigates WM lesions using images acquired with a FLAIR sequence due to its increased conspicuity of WM lesions after the suppression of signal from CSF. The number and volume of these lesions serve as a marker of cerebral small vessel disease (SVD) (Wardlaw et al., 2013). In FLAIR scans, they appear as WM hyperintensities. Interestingly, WM lesions can also be segmented in T1w images as they appear as WM hypointensities. It

was previously shown that there is a strong correlation between FLAIR-based WM hyperintensities and T1-based WM hypointensities (Cedres et al., 2020). On the ground of the availability of T1w images in all data sources used for our analyses, we performed T1-based WM lesions segmentation and quantification to investigate the association of SVD with the cholinergic system and cognitive functions in aging and AD continuum. In all three studies, the segmentation of WM hypointensities and corresponding volumetrics was performed on T1w images using the probabilistic procedure implemented in FreeSurfer (Brands et al., 2006; Fischl et al., 2002).

Table 4. Imaging modalities used in the three studies.

	T1w			DWI			FLAIR
	GENIC	H70	DELCODE	GENIC	H70	DELCODE	H70
Sequence	FSPGR	TFE	MPRAGE	SS-EPI	SS-EPI	Multi shell SS-EPI	FLAIR
TR	8.73 ms	7.2 ms	2500 ms	15000 ms	7340 ms	12100 ms	4800 ms
TE	1.74 ms	3.2 ms	4.37 ms	72 ms	83 ms	88 ms	280 ms
FoV (mm)	250×250	256×256	256×256	256×256	224×224	240×240	250×250
Matrix size	250×250	250×250	256×256	128×128	112×112	120×120	250×237
Flip angle	12°	9°	7°	90°	90°	90°	90°
Slice thickness	1 mm	1 mm	1 mm	2.4 mm	3.0 mm	2.0 mm	2.0 mm
Orientation	Sagittal	Sagittal	Sagittal	Axial	Axial	Axial	Sagittal
Diff. directions (n, b-value)	-	-	-	31 (1000 s/mm^2), 1 (b=0)	32 (800 s/mm^2), 1 (b=0)	30 (700 s/mm^2), 30 (1000 s/mm^2), 10 (b=0)	-
Other parameters	-	-	-	-	-	-	TI=1650 ms

FSPGR, fast spoiled gradient echo sequence; TFE, turbo field echo sequence; MPRAGE, magnetization prepared rapid gradient echo sequence; SS-EPI, single-shot echo-planar imaging sequence; TR, repetition time; TE, echo time; FoV, field of view; TI, inversion time.

In our analysis, DWI data found two different applications. First, they were used to find and identify cholinergic WM pathways. More specifically, the DWI data were used to build a diffusion orientation distribution model, which in turn facilitated the tracking of pathways stemming from NBM. This modelling was conducted separately in Study I and Study III. Another application of the DWI data is the generation of fractional anisotropy (FA) and mean diffusivity (MD) maps. These maps contain information about the integrity of the brain tissue in all its parts. After applying the cholinergic pathway masks, it is then possible to compute summary information about the integrity along these pathways. This information can then be compared between individuals and diagnostic groups. Another approach we used in Study III is to compare segmented FA or MD maps between diagnostic groups directly voxel-wise in order to preserve spatial information. The DWI data in Study III were accompanied by a B0 field map which was used for unwarping EPI distortions due to magnetic field inhomogeneity.

5.3.4 Other markers

CSF biomarkers

In Study II, one of the selected age-related pathologies whose impact on the degeneration of the cholinergic system was investigated was amyloid and tau pathology. For this reason, a lumbar puncture for CSF sampling was conducted, and CSF biomarker levels were determined. We used CSF phosphorylated tau181 (p-tau181) to assess tau neurofibrillary tangle pathology. CSF $A\beta_{42}/A\beta_{40}$ ratio was used as a marker of amyloidosis. CSF Aβ38 was included to determine its association with AD biomarkers and cerebrovascular disease in the general population. Its role in aging is, however, still poorly understood. It was previously reported that it could be a marker of AD (Wiltfang et al., 2002), it was predominantly found within the vascular vessels in patients with AD (Reinert et al., 2014), and it was also present in other non-AD dementias (Heywood et al., 2018; Mulugeta et al., 2011) and patients with chronic neuroinflammation (Wiltfang et al., 2002).

In Study III, the diagnostic groups of SCD, MCI and AD dementia in the whole sample were determined clinically. In order to confirm our results in individuals with Alzheimer's pathologic change as defined currently by a positive Aβ biomarker (Jack et al., 2018), we used available CSF biomarkers to repeat all our analyses in a biomarker-supported AD continuum subsample. We used the CSF $A\beta_{42}/A\beta_{40}$ ratio as a biomarker for amyloid-β pathology, CSF phosphorylated tau181 levels as a biomarker for tau neurofibrillary tangles and total CSF tau levels as a biomarker for unspecific neurodegeneration, according to the most recent NIA-AA guidelines AT(N) system (Jack et al., 2018). The cut-off value for the $A\beta_{42}/A\beta_{40}$ ratio was < 0.09, based on a previous study (Janelidze et al., 2016): cases below the cut-off of 0.09 were designated amyloid positive and cases above the cut-off as amyloid negative.

APOE genotyping

APOE ε4 carriership was included in Study II as a variable of interest to test the degree of importance of the APOE status towards the integrity of NBM projections. In Study III, APOE ε4 carriership was used as an auxiliary variable for descriptive analysis. In both studies, participants were classified as APOE ε4 carriers if they were ε3/ε4 or ε4/ε4 carriers.

5.3.5 Cholinergic pathways segmentation pipeline

The main aim of all three studies lies in finding, identifying, and evaluating the human cholinergic WM projection *in vivo*. In Study I and Study III, these cholinergic WM projections were searched by means of diffusion-based fibre tracking. The following paragraphs describe the processing pipeline and explain its individual parts. In Study II, due to the limited quality of the DWI data, instead of performing fibre tracking, the diffusion properties of the cholinergic pathways were evaluated using a segmentation mask of two cholinergic pathways (cingulum and external capsule pathway) derived in Study I.

In all three studies, the DWI data were preprocessed using *FSL* (FMRIB Software Library, www.fmrib.ox.ac.uk/fsl). First, non-brain tissue was removed with *BET* (Jenkinson et al., 2005) (Figure 5A). In Study III, the EPI distortion (susceptibility-induced off-resonance field) was additionally corrected using EPI-based field mapping (Reber et al., 1998) (Figure 5B). Then, eddy currents and head motion were corrected (Andersson and Sotiropoulos, 2016) (Figure 5C). Before further analysis, all T1w images were also skull-stripped and corrected for bias field (Zhang et al., 2001).

Study I and III

Next, we created a standard ball-and-sticks diffusion orientation model for each voxel with the *bedpostX* toolbox (Hernández et al., 2013), considering three fibres modelled per voxel (Figure 5E). As this modelling proved to be computationally and time expensive, a graphic processing unit accelerated version of the modelling software was used, shortening processing time from ~15 hours to ~30 minutes per case.

The fibre tracking was guided by six ROI masks. As the tracking was performed in the subject's individual (native) diffusion space, the ROIs needed to be delineated there as well. A detailed description of each ROI follows:

- An ROI mask of NBM served as the initiating seed region for probabilistic tracking. It was based on a cytoarchitectonic map of basal forebrain cholinergic nuclei in T1 MNI space, derived from combined histology and *in cranio* MRI of a post-mortem brain (Kilimann et al., 2014). For the purpose of fibre tracking in individual (native) diffusion space, the (nonlinear) registration parameters from individual T1 space to standard T1 MNI space (Figure 5F) were inversely applied to the NBM ROI, following (linear or nonlinear) registration to native diffusion space (Figure 5G). This is a preferred way of transferring an ROI mask from a T1 template space to a non-T1 native space. Direct image registration of the T1 MNI template to a native diffusion space can lead to unsatisfactory results. By a native diffusion space, we mean a preprocessed B0 image. Both registration steps (T1→T1 MNI and B0→T1), as well as all the registration and warping procedures in case of other segmentation ROIs, were carried out using the non-linear SyN registration algorithm (Avants et al., 2008) in Advanced Normalization Tools (ANTs, http://stnava.github.io/ANTs/).
- The cingulum and external capsule masks were used to constrain the fibre-tracking process. Only those streamlines initiated from the NBM ROI that reach a voxel in midway cingulum or external capsule ROI masks were retained. The purpose of these restricted models was to reconstruct two well-known major WM pathways of the cholinergic system projecting through the cingulum and the external capsule (Liu et al., 2017; Selden et al., 1998). The cingulum and external capsule segmentation masks were based on the Johns Hopkins University (JHU) WM atlas, available as part of the FSL package (Mori et al., 2005). As these masks were defined in a standard B0 MNI space, the registration procedure had only one step, inversely applying the

(nonlinear) registration parameters of a native B0 image to the standard B0 MNI template (Figure 5H) to warp the ROI masks from standard space to native space.

- In order to avoid contamination from non-cholinergic pathways going through the anterior commissure and connecting to the cerebellum and medulla, we also restricted the fibre-tracking process with 2 ROIs used as exclusion masks. Fibres that reached a voxel in these two regions were discarded. The brainstem ROI mask was extracted using FSL's FIRST segmentation routine (Patenaude et al., 2011). The anterior commissure ROI mask was delineated in the MNI template by a trained expert. These ROI masks were brought from the T1 MNI space to a native diffusion space using the same procedure as in the case of the NBM ROI (Figure 5F and Figure 5G).
- The specificity of the cholinergic pathways in our analysis was tested with the help of a negative control mask of remaining WM. The remaining WM mask was created by excluding the cholinergic tracts described below (i.e., a union of external capsule and cingulum pathways) from the whole WM mask. The whole WM mask was obtained from the FSL's Automated Segmentation Tool (FAST) (Zhang et al., 2001).

Note that the choice of registration algorithms and their parameters is crucial here. When aligning brain images from the same subject but acquired using different MRI sequences, often called inter-modality registration, such as in the case of a T1 - B0 pair, it is sufficient to employ a linear registration procedure. In the case of Study III, it was a rigid registration followed by an affine one. A rigid registration does not deform or scale the brain; it only rotates and moves it. An affine registration allows not only rotation and motion but also shearing and scaling. As it is assumed that the brain does not structurally change between individual scans, it would even be inadvisable to use a registration algorithm with a higher-order transformation as it could induce undesirable warps. In the case of Study I, the diffusion sequence could not, however, be corrected for the distortion due to susceptibility-induced off-resonance field due to missing corrective measures (such as EPI-based field mapping or two acquisitions with opposing polarities of the phase-encode blips). This caused a geometric mismatch between the diffusion image and the structural images which are typically unaffected by distortions. For this reason, it was preferable to apply non-linear registration even between these two scans of the same subject. Another parameter to tune for the registration algorithm is a similarity metric, a measure that evaluates how similar two images appear. For inter-modality registration, there is no linear relationship between the intensities of the two images and simple metrics such as mean squared intensity difference (Friston et al., 1995) or cross-correlation (Gee, 1999) cannot be simply used. Instead, we optimized the registration process with mutual information (Viola and Wells, 1997), a metric based on information theory.

Co-registration of a native scan to a template, often called normalization, was implemented with a nonlinear registration with a mutual information similarity metric. Both images, one from a study subject and a template, are generally based on the same modality (MRI sequence) and depict the same sets of rough features. The goal of the normalization is to align the subject's scan onto the template image so that the anatomy in both images matches.

Because of the local differences in the placement of sulci, gyri and other brain anatomical features, it is impossible to achieve this by merely rotating, moving or scaling the whole image. Instead, non-linear registration techniques are used. This applies to T1→T1 MNI and B0→B0 MNI registration steps.

Next, probabilistic tracking was performed by repeating 5000 random samples from each of the NBM ROI voxels and propagated through the local probability density functions of the estimated diffusion parameters (Figure 5J). The tracking was performed with the *probtractx* program of FSL (Behrens et al., 2007). In Study I and III, only fibres traversing through the cingulum or external capsule ROI and not through the anterior commissure or brainstem were kept. In Study I, we created an additional explorative model, with streamlines initiating in the NBM and propagating across the brain with no midway constraints other than excluding anterior commissure and brainstem ROI masks. The aim of conducting this unconstrained model was to explore potential cholinergic projections not covered by the constrained model.

In order to compare the tracked pathways across individuals, we needed to bring them to a common space. For this purpose, an average group template was created based on B0 preprocessed images using the *buildtemplate* module in ANTs (Figure 5K). In Study I, this template was based on 100 randomly selected cases (out of 262) from the whole cohort of cognitively healthy individuals. In Study III, it was based on all HC cases (N = 112). Briefly, to construct the group template, an initial affine average template is created by taking a voxel-wise average of globally aligned scans after intensity normalization. Next, a non-linear average template is built after warping individual brain scans to the affine template. These steps are repeated several times until a full-resolution group template (Figure 5L) is achieved.

After that, the individual tracking results of all HC cases were nonlinearly warped into the space of this group template (Figure 5M). Finally, pathway-specific binary masks were created by considering all the individual warped tracts and retaining only the voxels that were present (i.e., met by at least one fibre) in at least 70% (Study I) or 60% (Study III) of the cases (Figure 5N). A study (de Reus and van den Heuvel, 2013) suggested a broad threshold of 30-90%, with a group threshold of 60% representing an optimal balance between false positives and false negatives. We chose a group threshold closer to the higher limit to be more restrictive with false positives and to be specific to the cholinergic pathways. This threshold was chosen as a trade-off between false positive and false negative rates visually regarded as tracts with clear fibre-like structure as opposed to difficult-to-identify 'swelled' tracts with probably a lot of false positive voxels or 'gappy' tracts with a risk of losing true positive voxels. Furthermore, the different values of the group threshold between Study I and Study III might be explained by a better alignment of diffusion and structural images in Study III due to the availability of EPI correction maps. These pathway masks were based on healthy controls as they should represent intact cholinergic tracts.

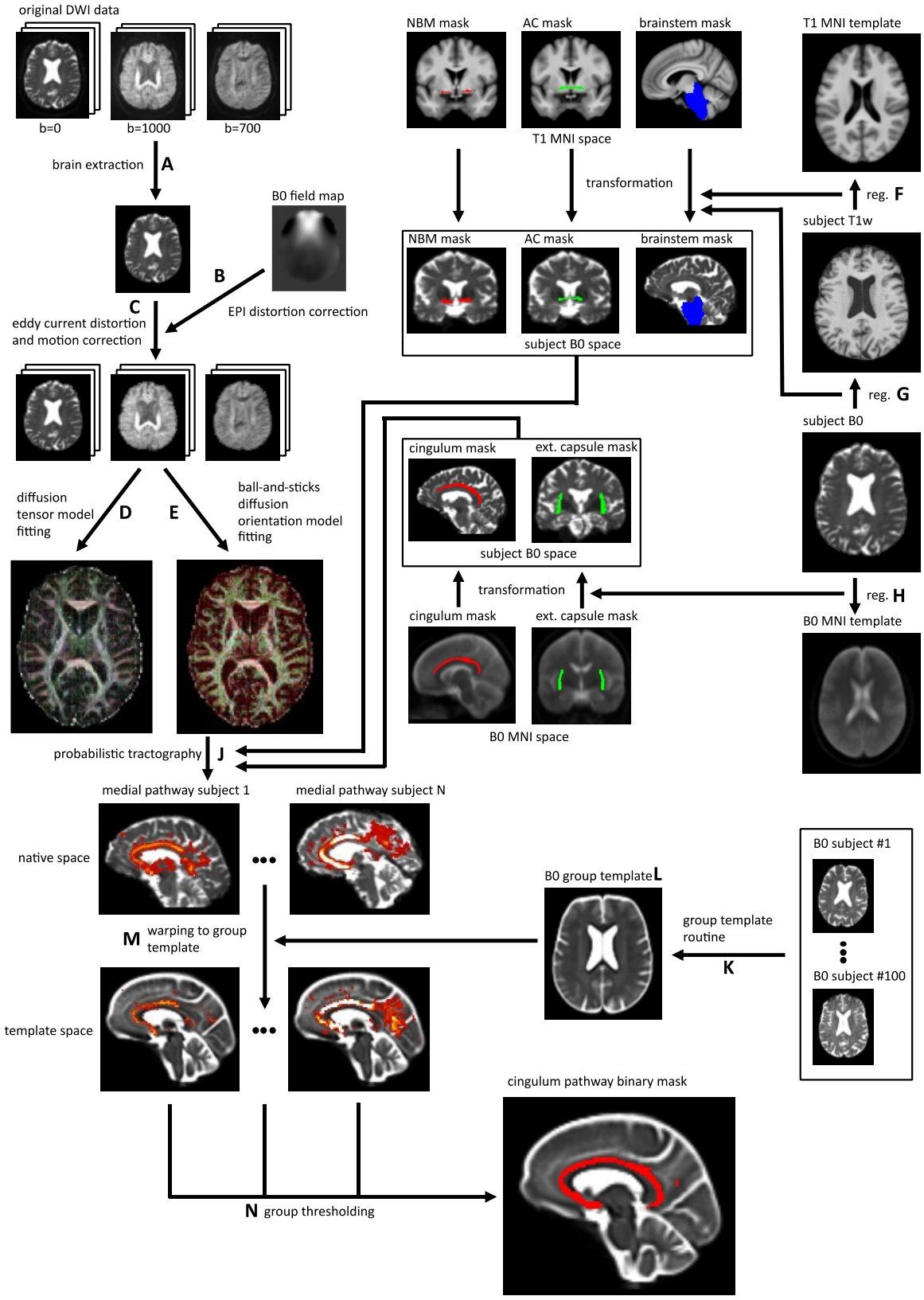

Figure 5. Cholinergic pathways segmentation pipeline. DWI, diffusion-weighted imaging; EPI, echo-planar imaging; NBM, nucleus basalis of Meynert; AC, anterior commissure; MNI, Montreal Neurological Institute; B0 image, DWI image with b = 0 s/mm^2. Units of presented b-values are s/mm^2. The I letter was intentionally omitted to improve readability.

To describe the microstructure properties of the tracked cholinergic pathways in individuals, we created a DTI model from the preprocessed diffusion data (Figure 5D), and then we extracted the mean diffusivity (MD) map. Next, we calculated the average value of the MD index for each participant and pathway, i.e., an average value of the diffusion index map within the cingulum, external capsule, or unconstrained pathway binary mask. The same procedure was applied to the negative control remaining WM mask. In all our studies, the MD index was used to assess WM microstructural integrity. The MD index was chosen over other DTI metrics for several reasons: (1) MD is sensitive to conditions that affect the barriers that restrict the movement of water, such as cell membranes (Zhang et al., 2014), (2) MD precedes changes in other DTI indexes, such as fractional anisotropy (FA), grey matter volume in pre-symptomatic individuals with familial AD (Li et al., 2015), preclinical individuals with sporadic AD (Li et al., 2014), and individuals with AD (Acosta-Cabronero et al., 2010), (3) increase in MD in the cingulum and inferior front-occipital fasciculus was linked with lower performance in several visual abilities in the GENIC cohort, (4) MD is less susceptible than FA to alterations due to different fibre populations in individual voxels, i.e., the crossing fibres problem. In Study III, the MD-based analysis is additionally accompanied by FA-based comparisons for reference.

Our approach of using probabilistic tractography to create masks and then extract DTI metrics was used to address the problem of crossing fibres which hinders deterministic tracking from NBM. Another method we considered was an analysis of probabilistic measures based on the number of streamlines. While the number of streamlines is an interesting measure in whole brain tractography, in probabilistic tractography with seeds (the method used in our studies), the number of streamlines has the added problem to reflect the distance from the seed area: locations close to the seed area have many streamlines, while distant locations have only a few streamlines, which does not necessarily mean that the integrity in distant locations is impaired. In order to avoid that and to capture pathways common to most of the subjects, we decided to apply the method described above. With the current method, we were able to capture very distant tracts that were not met by many streamlines in individual cases, but that were consistent across all subjects. Thus, we might be able to uncover difficult-to-find yet important tracts.

Study II

In this study, a separate fibre-tracking analysis was not performed. Instead, microstructural properties of the cholinergic pathways were examined with the above-described procedure for the extraction of diffusion indices using cingulum and external capsule pathway binary masks derived in Study I. For this purpose, the preprocessed B0 images were nonlinearly registered to the B0 group template (from Study I) and the registration parameters were used to warp the binary pathway masks back to the image space of the native B0 images. After that, the tract-specific diffusion indices were extracted in the same manner as in Study I or III.

5.3.6 Statistical analysis

The processed imaging data and other demographic and clinical variables were further processed with methods of statistical analysis to infer answers to our research questions. The most important statistical methods are described in the following paragraphs.

Study I

In this study, next to the identification of the NBM WM projections using diffusion tractography, we aimed to investigate the association of small vessel disease (SVD) with the integrity of the cholinergic system and cognitive functions.

First, we split the study cohort into two groups, high WM-hypo and low WM-hypo groups, with respect to the WM hypointensity load using the Gaussian mixture model estimated by the expectation-maximization algorithm. This group division was used in the subsequent analysis to investigate the role of SVD in cognitive aging.

Next, cognitive measures and the extracted NBM volume were compared between groups using the one-way analysis of variance with covariates (ANCOVA), controlling for age, sex, and WAIS-III Information (a measure of crystallised intelligence). For a better understanding of the role of the control variables, we report the outcome of these analyses in a stepwise manner: without correction, with a correction for the effect of sex and WAIS-III Information, and with an additional correction for the effect of age.

For the assessment of the SVD influence on tract integrity, we applied ANCOVA to test for differences in tract-specific MD measures between high and low WM-hypo groups. In this way, we compared the MD values in the cingulum and external pathway, and in the remaining WM mask, as a negative control.

To evaluate the degree of contribution of the integrity of the cholinergic system and SVD with domain-specific cognitive performance, we conducted a random forest analysis. We included age, sex, WAIS-III Information, MD in the cingulum, external capsule tracts and in the remaining WM, NBM volume, WM hypointensity load, and MMSE score as predictors, and scores of tests of cognitive performance as outcome variables. We used random forest regression with a conditional inference tree for unbiased variable selection. Random forest is an ensemble method in machine learning that involves growing multiple decision trees via bootstrap aggregation (bagging). Each tree predicts a classification independently and votes for the corresponding class. The majority of the votes decides the overall prediction (Breiman, 2001). Random forest has important advantages over other regression techniques in terms of the ability to handle highly non-linear biological data, robustness to noise and tuning simplicity (Lebedev et al., 2014). Conditional feature importance scores for random forest were computed by measuring the increase in prediction error if the values of a variable under question were permuted within a grid defined by the covariates that were associated with the variable of interest. This score was computed for each constituent tree and averaged across the entire ensemble. The conditional feature importance scores were designed to

diminish an undesirable effect of preference of correlated predictor variables. Variables receiving higher importance scores are more likely to be closely linked to the output variable (cognitive scores). The random forest was composed of 2000 conditional inference trees. The *party* package (Strobl et al., 2007) in R statistical software was used for this analysis.

Study II

Here, we studied pathological processes which might contribute to the degeneration of the cholinergic system in aging. Namely, we assessed the contribution of amyloid (CSF levels of $A\beta_{38}$ and $A\beta_{42/40}$), tau (CSF levels of p-tau), and cerebrovascular pathology (through automatic segmentation of WM lesions in MRI scans) towards the degeneration of cholinergic WM projections (using cholinergic pathway model derived in Study I).

To assess the differential contributions of these pathology-specific biomarkers towards the integrity of the NBM projections, we ran random forest regression models in a similar way as in Study I. WM lesion load (T1-based WM hypointensity and FLAIR-based WM hyperintensity), CSF $A\beta_{42/40}$ ratio, $A\beta_{38}$, p-tau, sex, and APOE status were included as predictors, and an average MD value in the cingulum and the external capsule pathway as outcome variables. The random forest comprised 5,000 conditional inference trees. Conditional feature importance scores were computed to assess the degree of contribution of each predictor (biomarker) towards the integrity of the respective cholinergic pathway.

Study III

In order to address the aims of this study, we performed several statistical analyses on the input data. Our diagnostic groups of SCD, MCI and AD dementia were clinically in the AD continuum, but since they rely on a clinical diagnosis, it is likely that some individuals do not have AD pathologic changes as defined by a positive Aβ biomarker (Jack et al., 2018). Therefore, all our analysis was conducted in the whole cohort and to confirm the results in a biomarker-supported AD continuum subsample, also repeated in a subsample of amyloid-positive SCD, MCI and AD dementia groups, as well as amyloid-negative HC.

First, to gain insight into the data, we investigated differences in demographic and clinical variables between HC and other diagnostic groups using standard statistical testing. Age and years of education were group-wise compared with independent *t*-tests, sex and APOE genotype with chi-square tests. Differences in cognitive measures, CSF biomarkers, NBM and hippocampal volumes (corrected for TIV), and WM hypointensity load between diagnostic groups were evaluated using ANCOVA with age and sex as covariates. Then, paired *post hoc t*-tests adjusting for multiple comparisons with the Tukey method followed. We reported comparisons of our interest: SCD vs HC, MCI vs HC, and AD dementia vs HC.

Our primary research interest lies in the differences in the cholinergic pathways between stages of the AD continuum. To investigate this, we performed two types of comparative analysis: global and local analysis. First, the global analysis was conducted in a similar way as in Study I, i.e., we statistically compared average FA and MD values in cholinergic

pathways between diagnostic groups. We investigated the differences in the cingulum, external capsule, and remaining WM control mask using ANCOVA with age and sex as covariates. ANCOVA was followed by paired *post hoc* *t*-tests adjusting for multiple comparisons with the Tukey method. Second, to obtain more detailed spatial information about changes in the cholinergic pathways across stages of the AD continuum, we performed a voxel-wise generalized linear model using permutation-based non-parametric testing (*randomize* program in FSL) (Winkler et al., 2014) and correcting for multiple comparisons across space (threshold-free cluster enhancement, TFCE), with age and sex as covariates. Significance maps were corrected for multiple comparisons using a familywise error rate of $P < 0.05$. For the reasons stated above, in this analysis, we favoured the MD index over the FA index for its reduced susceptibility to the crossing-fibre problem.

Another question was how well each of the suggested MRI-based biomarkers (MD values in the cholinergic pathway) distinguishes between HC and other diagnostic groups and how their predictive power differs between each other and compares to the standard volumetric measures of AD pathology (NBM and hippocampal volume). In order to evaluate this question, the receiver operating characteristic (ROC) curve analysis was carried out. We performed this analysis for each pair of an HC group and one clinical group, resulting in three models (SCD versus HC, MCI versus HC, AD dementia versus HC). Next, a cumulative statistic of the overall discriminative power of the biomarkers was computed by means of the area under the ROC curve (AUC) for each curve. AUCs were then pairs-wise compared using the bootstrap method (2000 replications) from the *pROC* package (Robin et al., 2011).

Our final aim of Study III was to assess the association of MRI markers of the cholinergic system (NBM volume and integrity of cholinergic pathways) with cognitive performance. Inspired by Study I and II and considering the inherent non-linearity of the examined relationships, we selected a random forest analysis to elucidate this research question. We conducted several random forest analyses with cognitive performance as outcome variables and MD in cingulum pathways, external capsule pathway and in remaining WM (negative control mask) as predictors. In addition, we included WM hypointensity load as a predictor as an important factor in the progress of aging. Finally, we also included age, sex and years of education to consider the contribution of these variables, as they usually influence cognitive performance. Here, to assess the differential role of the integrity of the cholinergic pathways and the NBM volume along the AD continuum, we created two separate sets of random forest models: one for HC and SCD combined and one for MCI and AD combined. This data pooling allowed the normal cognition groups (HC and SCD) and impaired cognition groups (MCI and AD dementia) to be evaluated separately while providing sufficient statistical power. The actual implementation of the random forest models followed the same approach as in Study I.

Study I (GENIC)

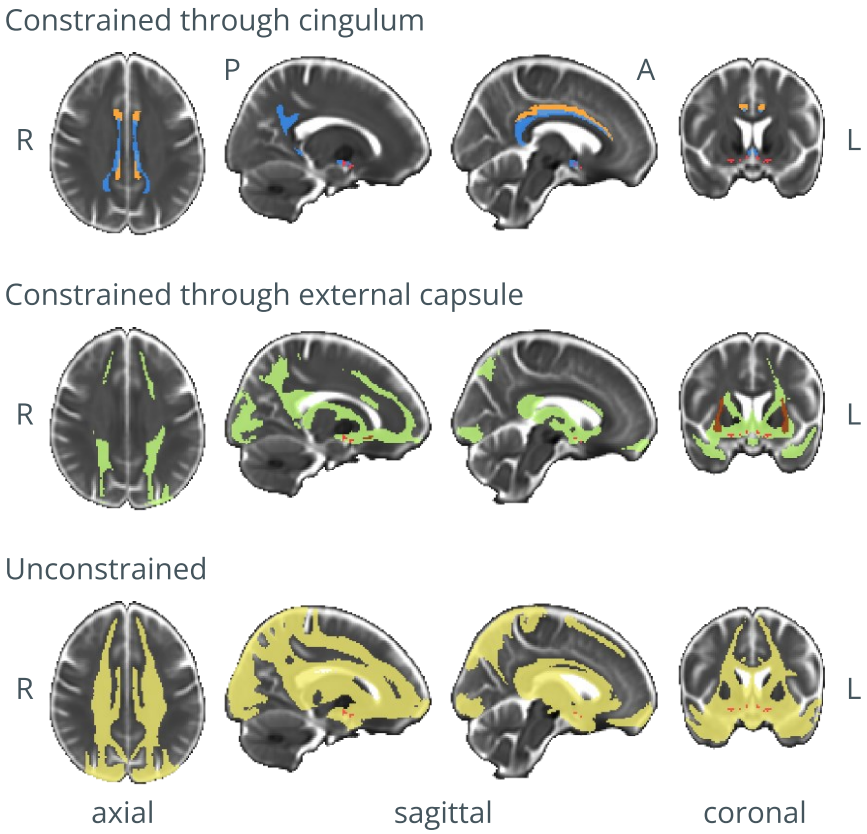

Figure 6. Cholinergic WM pathways (Study I, GENIC cohort). From (Nemy et al., 2020), used under Creative Commons BY-NC-ND license.

Study III (DELCODE)

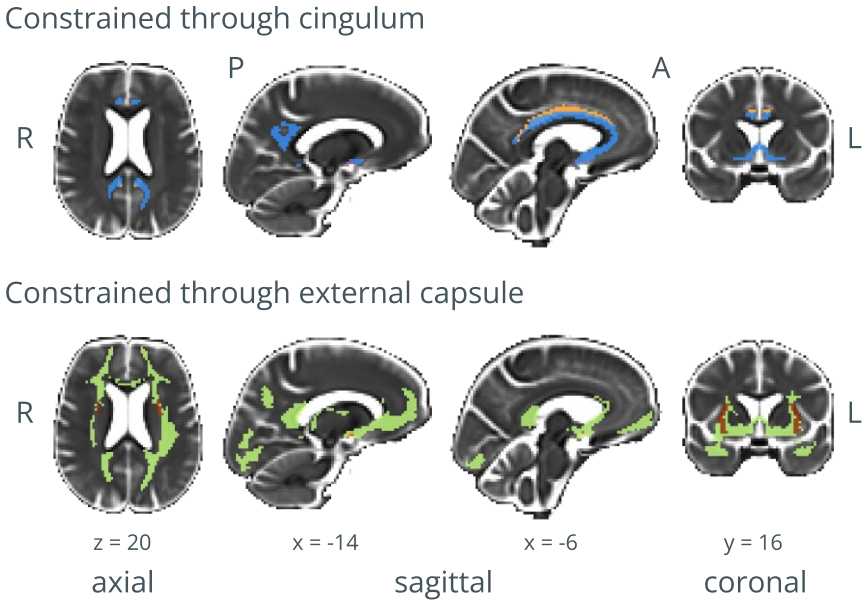

Figure 7. Cholinergic WM pathways (Study III, DELCODE cohort). Red for NBM ROI mask. (First row) Orange for the cingulum mask, blue for the pathway passing through the cingulum. (Second row) Brown for the external capsule mask, green for the pathway passing through the external capsule. (Third row, GENIC only) Yellow for the pathway without restrictions (no explicit midpoint masks). R, right; L, left; A, anterior; P, posterior.

6 RESULTS

The following chapter summarizes the most significant results of each presented study.

6.1 IN VIVO MODELLING OF THE CHOLINERGIC PATHWAYS

Probabilistic tractography analysis was conducted in order to reveal *in vivo* white matter pathways arising from the NBM. Our image processing protocol was designed to minimize the influence of the crossing-fibres problem, which is particularly prominent in tracking WM pathways from brain structures located in the vicinity of several other pathways, and so that it could be easily employed in the clinical setup even with lower quality input data. We used our pipeline to process imaging data in two independent cohorts (GENIC and DELCODE). Figure 6 and Figure 7 show respective tracked cholinergic pathways. Even when the source data had different origins (different MRI scanners and study population) and came with different degrees of quality (single-shell DWI without EPI distortion correction versus multi-shell DWI with EPI distortion correction), it is apparent that the resulting spatial layout of the pathways is very similar in both cases and it also closely resembles cholinergic pathways depicted in post-mortem findings (Selden et al., 1998).

More specifically, the models showed that the medial pathway (in blue) projects from the NBM through the gyrus rectus and continues to the cingulate cortex and retrosplenial cortex. For the lateral pathway (in green), the external capsule division was tracked to the inferior frontal cortex (frontal pole) through the uncinate fasciculus, as well as to the parietal and temporal cortex via posterior thalamic radiation and internal capsule. Even though no specific guidance (via midway mask) was chosen for the perisylvian division of the lateral pathway, this division was also successfully tracked throughout the insula, superior temporal gyrus, and frontoparietal operculum.

The unconstrained model (in yellow) included the areas described for the medial and lateral pathways but was more widespread, including other brain areas such as the posterior cingulate and superior medial areas of the parietal and frontal lobes.

Even though the main tracking results are comparable in both studies, it can still be clearly seen that our technique greatly benefits from using multi-shell diffusion MRI data. Even though used in the probabilistic tracking technique, high-angular multi-shell data help to clean the estimated fibre probability

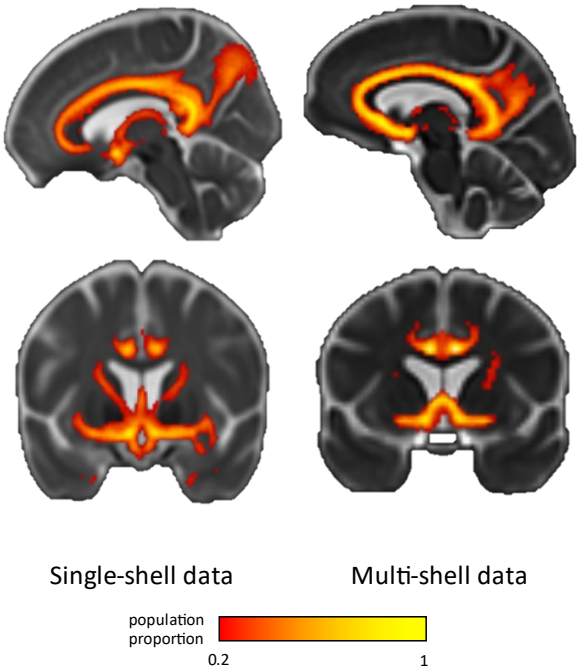

Figure 8. Comparison of a single-shell and a multi-shell-based cholinergic WM model.

distribution from spurious lobes, preserving simultaneously less prominent but still essential branches of the scrutinized pathways. Figure 8 demonstrates the resulting pathways derived from single-shell data (b = 1000 s/mm^2, N = 262, GENIC dataset) and multi-shell data (b = 700 s/mm^2, b = 1000 s/mm^2, N = 112, DELCODE dataset). Even with a smaller number of participants, the pathways based on the multi-shell data are distinctly more precisely defined, with a greater inter-subject agreement and fewer non-anatomical connections.

6.2 CHOLINERGIC PATHWAYS IN NORMAL AGING

In study I, we investigated SVD as an important age-related factor in relation to the deterioration of the cholinergic system in a cohort of aging cognitively intact individuals.

First, we divided the whole cohort into two subsets based on WM hypointensity load, a low WM-hypo and a high WM-hypo group. The threshold (WM-hypo = 3400 mm^3) was defined by the intersection of two Gaussian probability density functions (Gaussian mixture model fit), which were fitted to the distribution of the data (Figure 9).

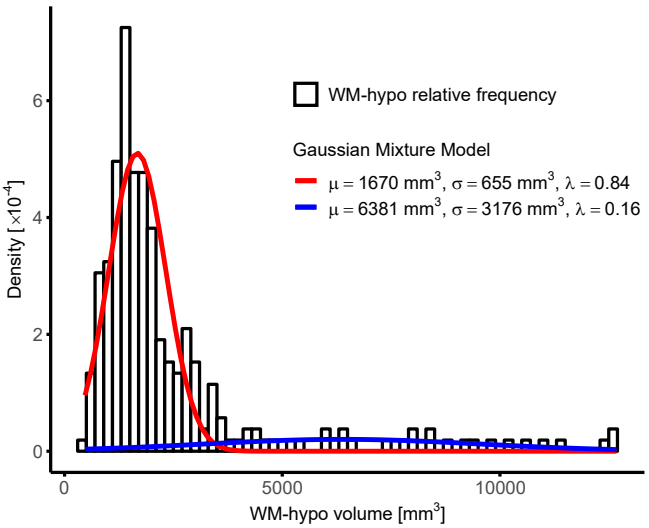

Figure 9. Gaussian mixture model fit to separate the cohort into two groups of high and low WM-hypo load. Mixture components are characterized by Gaussian distribution with a mean value μ and a standard deviation σ; λ is a mixture weight. From (Nemy et al., 2020), used under Creative Commons BY-NC-ND license.

Next, we compared NBM volume and tract integrity between these two groups. The NBM volume was significantly smaller in the high WM-hypo load group (Table 5), both without and with controlling for sex, WAIS-III Information, and age. The high WM-hypo load group showed significantly higher MD values in the tracked cingulum and external capsule pathways as compared with the low WM-hypo load group after controlling for sex, WAIS-III Information, and age (Table 5). In contrast, WM-hypo load did not have any significant effect on the negative control remaining WM after controlling for sex, WAIS-III Information, and age (Table 5).

Then, we examined the degree of contribution of MD in the cingulum and external capsule pathways, MD in remaining WM, WM-hypo load, and NBM volume towards cognitive measures with a random forest analysis. The unconstrained pathways were not considered for this analysis as the main interest was in specific pathway-cognition associations. The analysis results showed that MD in the external capsule pathway had a higher importance score in the prediction of both TAVEC delayed recall tests (Figure 10). MD in the cingulum pathway was more important in the prediction of PCV – reaction time and TAVEC delayed recall (30 minutes). Performance in Stroop and TAVEC learning was driven mainly by factors other

than MD in the cholinergic pathways. WM-hypo, NBM volume, and remaining WM received low importance scores in all the random forest models (Figure 10).

Table 5. Association between WM-hypo, mean diffusivity in the cholinergic NBM pathways, and NBM volume [mean value (SD)] in high and low WM-hypo load groups.

	Low WM-hypo load group	High WM-hypo load group	$F_{1,260}$ (no correction)	$F_{1,258}$ (corrected for sex and WAIS-III Information)	$F_{1,257}$ (corrected for sex, WAIS-III Information, and age)
MD in cingulum pathway	0.00083 (0.00003)	0.00089 (0.00006)	72.1***	62.6***	23.2***
MD in external capsule pathway	0.00090 (0.00005)	0.00102 (0.00009)	141.7***	127.3***	69.0***
MD in remaining WM	0.00079 (0.00003)	0.00080 (0.00003)	5.9*	6.6*	0.5
NBM volume (TIV corrected)	0.00025 (0.00003)	0.00023 (0.00004)	9.10**	7.87**	8.47**

MD, mean diffusivity; WM-hypo, WM hypointensities on T1-weighted images.

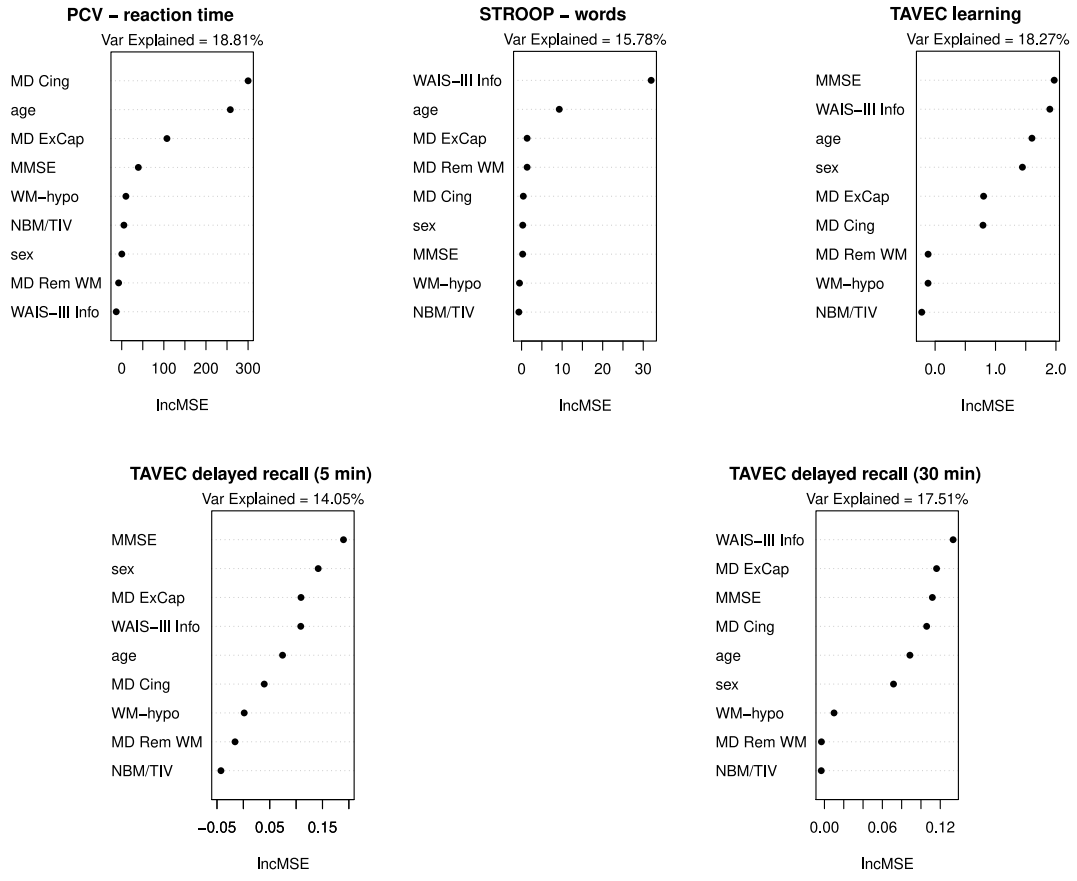

Figure 10. Contribution of MD in cholinergic pathways, WM-hypo load, and NBM volume towards cognitive scores. MMSE, Mini-Mental State Examination; MD, mean diffusivity; ExCap, external capsule tract; Cing, cingulum tract; Rem WM, WM excluding cholinergic tracts; WAIS-III Info, Wechsler Adult Intelligence Scale – Third revision Information subtest; WM-hypo, WM hypointensities on T1-weighted images; NBM/TIV, volume of nucleus basalis of Meynert scaled by total intracranial volume. IncMSE, conditional variable importance score. From (Nemy et al., 2020), used under Creative Commons BY-NC-ND license.

Having investigated the contribution of MD in the cholinergic pathway towards cognition, in Study II, we went one step back and analyzed age-related pathological factors and the degree of their contribution towards degenerations of the pathways in question. Our random forest models revealed that WM lesion load was by far the most important predictor of degeneration of both cingulum and external capsule pathways (Figure 11). In addition, p-tau, $A\beta_{38}$, and APOE ε4 carriership were also important towards MD in the cingulum pathway, and $A\beta_{38}$, p-tau and sex were important towards MD in the external capsule pathway.

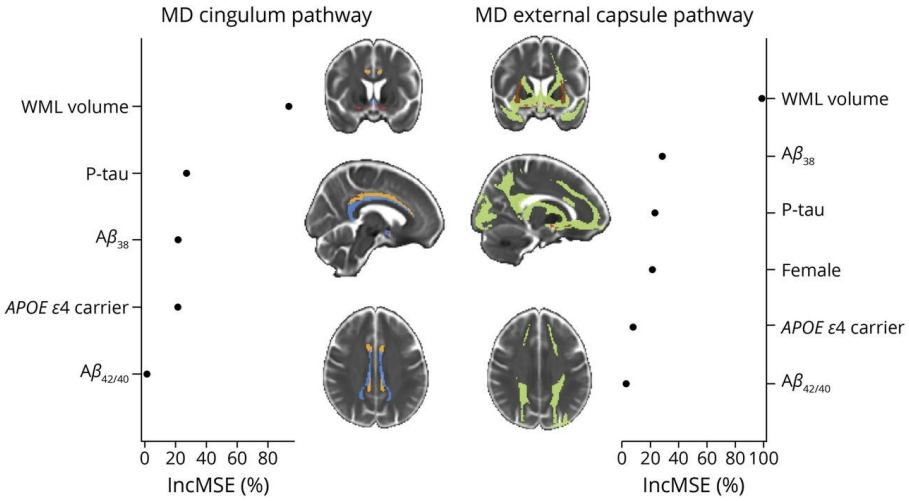

Figure 11. Contribution of amyloid, tau, and cerebrovascular biomarkers toward the integrity of cholinergic WM pathways. From (Cedres et al., 2022), used under Creative Commons CC BY 4.0 license.

6.3 CHOLINERGIC PATHWAY IN AD CONTINUUM

Similar to healthy aging analysis, in Study III, we investigated the cholinergic WM pathways by means of their integrity. In this case, we based all steps of our analysis on comparisons between HC groups and all other diagnostic groups (SCD, MCI, AD dementia).

First, we evaluated global measures (average FA and MD values) of WM integrity. As shown in Figure 12, the most remarkable finding was a significant decrease in FA and an increase in MD in SCD individuals as compared with the HC group (all comparisons, in both pathways), revealing early alterations of cholinergic pathways in the AD continuum. Similar results were found in the MCI and AD dementia groups compared to the HC group (all comparisons, in both pathways). In the remaining control WM, it was only FA in MCI and AD dementia, and MD in SCD and AD dementia which showed significant differences when compared to the HC group. Importantly, in the amyloid-positive individuals, we observed a similar pattern of findings in both cholinergic pathways. As opposed to the whole sample, differences in the remaining WM in SCD and MCI groups compared to the HC groups were non-significant (Nemy et al., 2022).

Statistical maps of voxel-wise differences in MD between groups further revealed the spatial layout of changes in the WM integrity of the cholinergic pathways. The cingulate pathway (Figure 13) showed significantly higher MD values in the retrosplenial and posterior

cingulate in the SCD group compared to the HC group. This suggests an early regional vulnerability of the posterior cholinergic WM in the AD continuum.

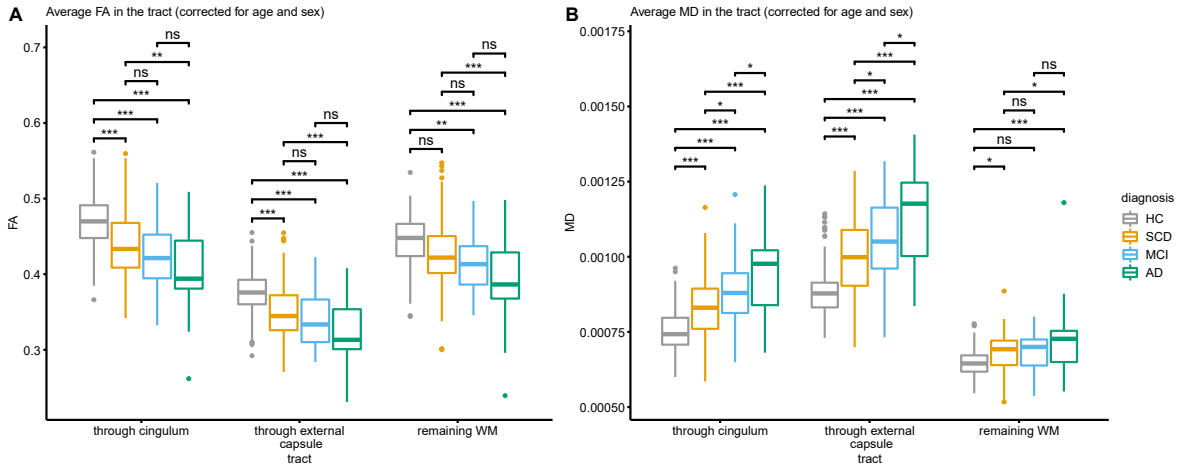

Figure 12. Parameters of diffusivity in cholinergic pathways and remaining WM. All clinical groups differed in FA and MD compared to the HC groups in all observed pathways. (A) Average FA. (B) Average MD. ns = not statistically significant ($P > 0.05$), *$P < 0.05$, **$P < 0.01$, ***$P < 0.001$ (assessed using a two tailed alpha). AD = Alzheimer's disease dementia. From (Nemy et al., 2022), used under Creative Commons CC-BY-NC license.

These differences were more spatially pronounced in the MCI group and were complemented by significant differences in a small area of the rostral anterior cingulate. All of the differences seen in the MCI group were present in the AD dementia group, but they were spatially extended and statistically more pronounced, with additional significant differences in the dorsal anterior cingulate. When compared to the HC group, differences in MD values in the WM beneath NBM emerged only in the MCI and AD dementia groups but not in the SCD group. This could suggest that it is the distal cholinergic WM that shows the earliest alterations in the AD continuum.

In the case of the external capsule pathway (Figure 14), we observed a similar pattern of differences in MD values in the SCD and MCI groups: in the external capsule, retrosplenial and posterior cingulate, and part of the uncinate fasciculus. In the AD dementia group, additional differences were apparent in temporal and prefrontal WM areas compared to the HC group. These findings, therefore, further indicate early regional vulnerability of posterior cholinergic WM in the AD continuum.

Notably, a resembling overall pattern of results was found when we repeated the regional analysis in the amyloid stratified subsample (Nemy et al., 2022). Although the subsample included a considerably smaller number of subjects rendering reduced statistical power, we could observe significant differences already in the SCD group (both cholinergic pathways). Again, the differences became more pronounced in the MCI and AD dementia groups.

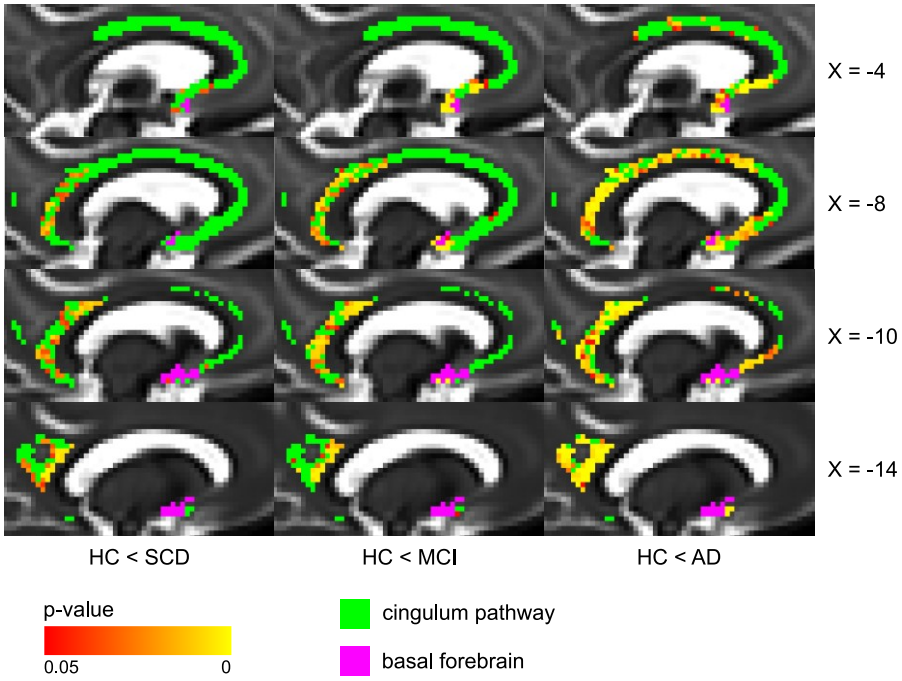

Figure 13. Voxel-wise differences in MD between diagnostic groups and controls (cingulum pathway), controlling for age and sex. BF mask (in purple) was inflated for illustrative purposes. From (Nemy et al., 2022), used under Creative Commons CC-BY-NC license.

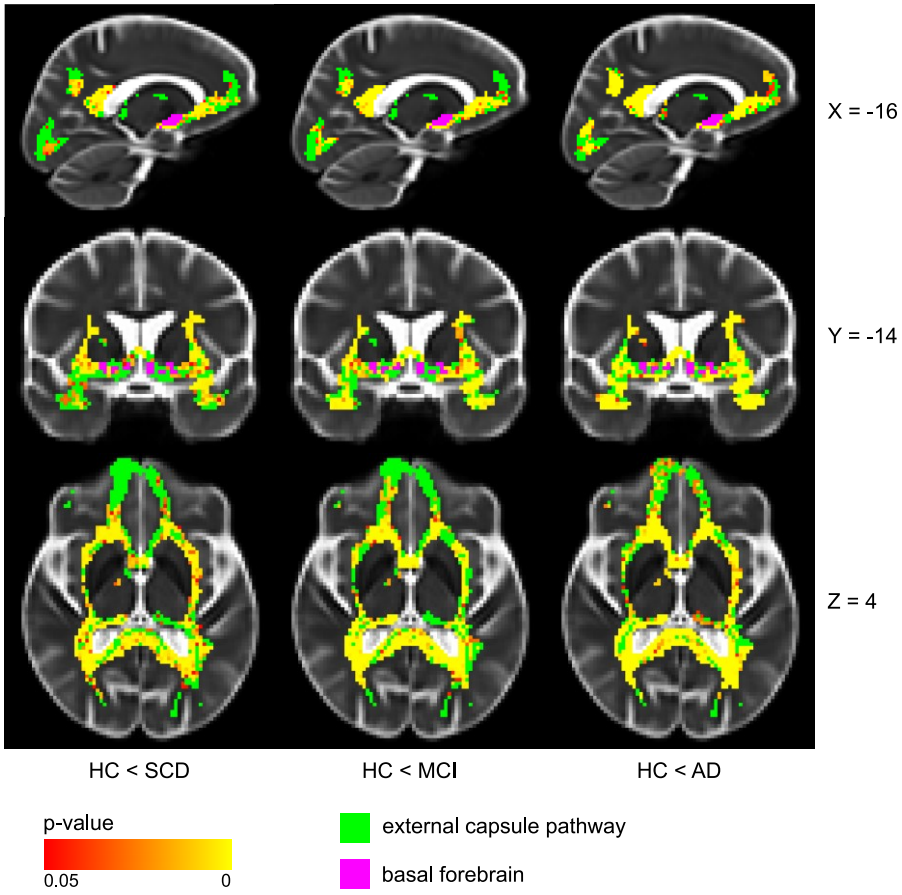

Figure 14. Voxel-wise differences in MD between diagnostic groups and controls (external capsule pathway), controlling for age and sex. BF mask (in purple) was inflated for illustrative purposes. From (Nemy et al., 2022), used under Creative Commons CC-BY-NC license.

Knowing that the suggested measures of the integrity of considered WM pathways showed significant alterations in all stages of the AD continuum, including its very early stages, we might ask how these proposed biomarkers compare to more conventional measures, such as hippocampal and NBM volumes. To answer this question, we conducted a ROC analysis, each time between HC groups and one of the clinical groups (SCD, MCI, and AD dementia). Figure 15 shows that it was MD in the external capsule pathway, followed by MD in the cingulum pathway, which performed the best in distinguishing SCD from HC. In the case of MCI, all considered biomarkers, except for MD in the remaining WM, reached statistically comparable AUC values. MD in the remaining WM performed significantly worse. For the AD dementia group, the best discriminative performance was shown by hippocampal volume, NBM volume and MD in the external capsule pathway. To summarize, the findings of the ROC analysis were stage-specific. Differentiation between SCD and HC was performed significantly better by the cholinergic WM pathways than by any of the other biomarkers. Further, all considered biomarkers performed better with the advancement of the disease in the AD continuum. Similar findings were observed in the amyloid stratified subsample (Nemy et al., 2022).

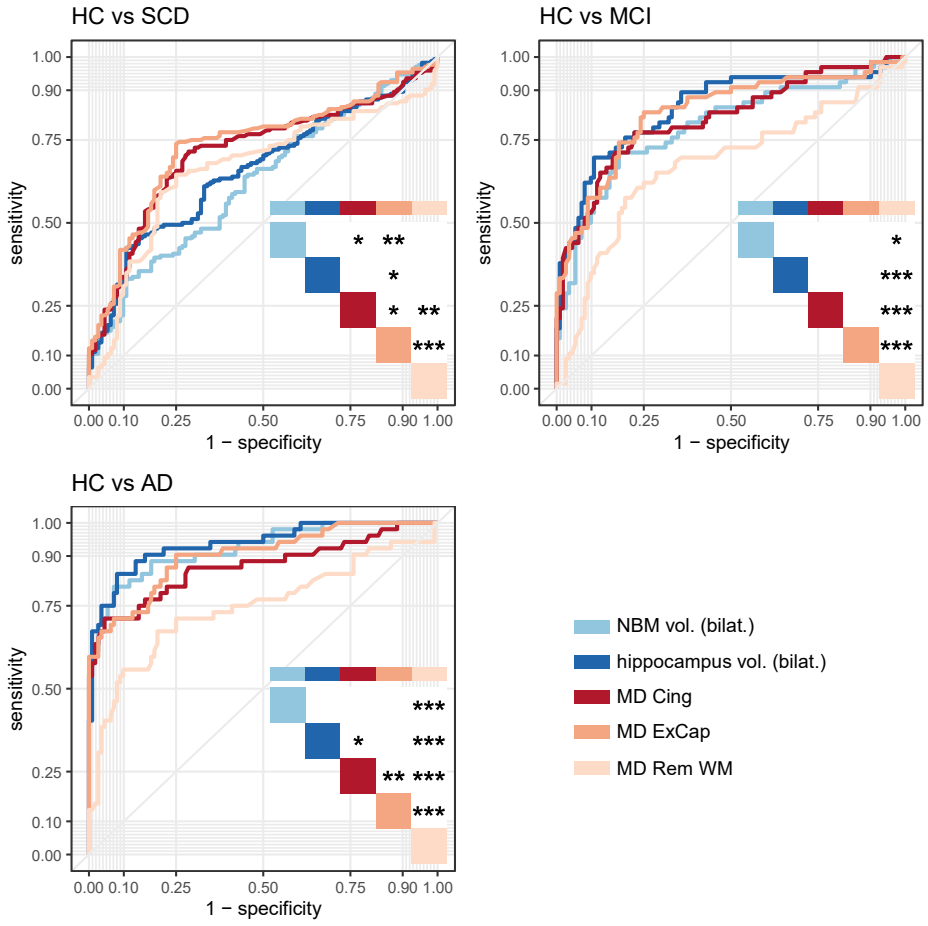

Figure 15. ROC curves for diffusion and conventional MRI biomarkers. *$P < 0.05$, **$P < 0.01$, ***$P < 0.001$ (assessed using a two-tailed alpha). AD, Alzheimer's disease dementia; ExCap, external capsule pathway; Cing, cingulum pathway; Rem WM, WM excluding cholinergic pathways; NBM vol., volume of NBM scaled by TIV; hippocampus vol., volume of hippocampus scaled by TIV. From (Nemy et al., 2022), used under Creative Commons CC-BY-NC license.

To address our last aim in the study of cholinergic pathways in the AD continuum, we demonstrated the association of WM pathways and NBM volumetric changes with cognitive performance across the stages of the continuum. More specifically, we conducted two separate random forest models for the groups with normal cognition (HC and SCD) and the groups with impaired cognition (MCI and AD dementia) (Figure 16). In the normal cognition group, all the ADAS memory tests were dependent only on sex, age, and years of education. MD in the external capsule pathway had a stronger importance in attention tests (Symbol digit modalities test and Trail making test B). In the impaired cognition group, NBM volume was an important predictor towards ADAS word list learning and recall tests, Symbol digit modalities test, and Trail making test B. MD in the external capsule pathway was important towards ADAS memory tests and Trail making test A. MD in the cingulum pathway was a notable predictor only of Trail making test A. Moreover, in both sets of random forest models, WM hypointensity load received low importance scores. In sum, performance in attention tests in HC and SCD individuals was particularly driven by the integrity of the external capsule pathway. The contribution of cholinergic pathways (and NBM volume) to cognitive performance, however, became stronger in the groups with impaired cognition, both for memory and attention tests.

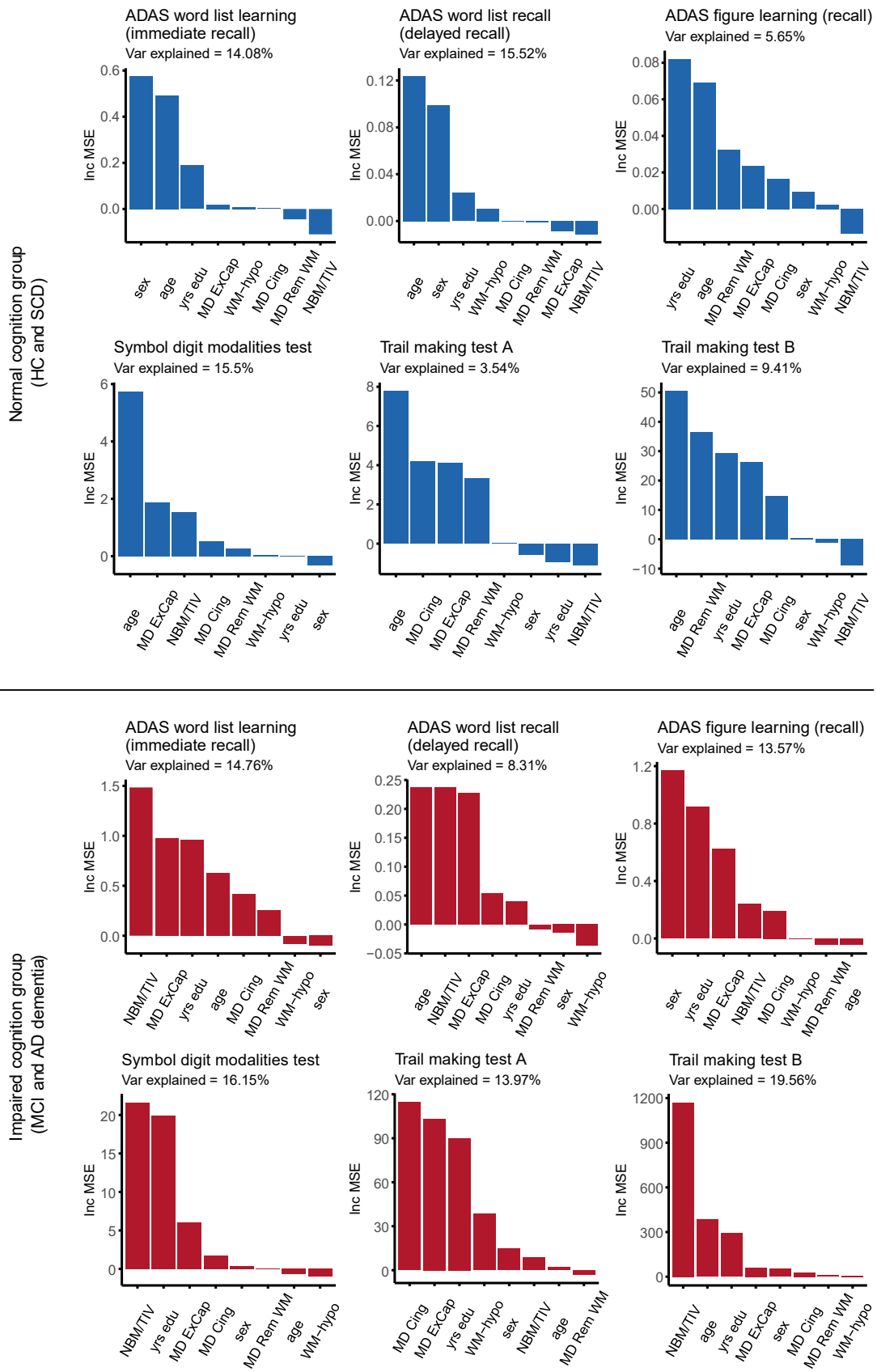

Figure 16. Random forest models (increase in prediction error). ExCap = external capsule pathway; Cing = cingulum pathway; RemWM=WMexcluding cholinergic pathways; NBM/TIV = volume of NBM scaled by TIV; Var = variance; yrs = years. IncMSE = conditional variable importance computed by increase in the mean square error of prediction. This IncMSE is the result of a corresponding variable being permuted within a grid defined by the covariates that are associated to the variable of interest. From (Nemy et al., 2022), used under Creative Commons CC-BY-NC license.

7 DISCUSSION

In a series of studies, we aimed to elucidate the role of cholinergic white matter pathways in cognitive function and neurodegenerative diseases. Specifically, we investigated the contribution of cholinergic white matter pathways to attention and memory performance in healthy older adults, as well as their relationship to cerebrovascular and AD biomarkers in cognitively unimpaired individuals. Finally, we examined changes in cholinergic white matter pathways at different stages of AD and their association with cognitive decline.

In order to assess the integrity of white matter pathways originating from the NBM *in vivo*, a probabilistic tractography analysis was performed. The results of our studies showed that our constrained models were able to successfully identify tracts in both medial and lateral pathways, consistent with previous AChE histochemical and ChAT and NGFr immunohistochemical analyses (Selden et al., 1998) as well as a prior DTI tractography study (Liu et al., 2017). The unconstrained model also identified tracts in areas such as the posterior cingulate and superior medial areas of parietal and frontal lobes, which have been previously labelled as cholinergic projections in histochemical and immunohistochemical studies (Selden et al., 1998) and were depicted in a recent rs-fMRI study (Fritz et al., 2019). Our pipeline for NBM segmentation and diffusion-based tracking of NBM WM projections was used by Schumacher et al. (2022) to replicate the tracking results in an independent patient cohort. The authors reported medial and lateral NBM group tracts with comparable WM regions to those found in our studies.

Next, we investigated the role of SVD in cognitive aging. As the evidence suggests a central role of cholinergic deficiency in vascular impairment (Liu et al., 2017), we aimed to explore the connection between SVD (evaluated with WM-hypo load), cholinergic dysfunction, and age-related cognitive decline. Study I found that older individuals and males had a higher load of WM-hypo. This result is consistent with previous studies (Habes et al., 2016; Raz et al., 2012). We also observed that lower performance in attention and memory in the high WM-hypo load group was largely accounted for by older age (and, to some extent, male sex and WAIS-III Information). This finding is in agreement with a previous study by Gustavsson et al. (2015). It is currently unclear whether WM-hypo in cognitively normal older individuals indicate preclinical stages of vascular cognitive impairment or are a feature of normal aging that does not reach the clinical threshold. Our data suggest that WM-hypo are strongly associated with age, but they do not directly impact attention or memory. Instead, their effect on cognitive function is indirect and occurs through the aging process.

More specifically, Study I discovered that high WM-hypo load is linked to a decrease in integrity within the two cholinergic pathways and the unconstrained model, even after considering the influence of age. In a study by Liu et al. (2017), it was also observed that vascular cognitive impairment leads to a decrease in integrity within the medial and lateral cholinergic pathways. Therefore, it appears that WM-hypo have an effect on the cholinergic system in both cognitively normal individuals and patients with vascular cognitive

impairment. Moreover, the impact of WM-hypo on the cholinergic pathways was specific and did not extend to the remaining WM when adjusting for age.

These conclusions were further supported by the results of Study II, which investigated the contribution of several age-related pathologies towards the disruption of cholinergic pathways. In this study of elderly individuals without cognitive impairment, we showed that WM-hypo were the most significant factor contributing to the degeneration of the studied cholinergic pathways, followed by levels of CSF Aβ38 and p-tau.

In Study I and Study III, we also demonstrated that the WM integrity of cholinergic projections but not WM lesion load was closely linked to attention and memory performance in cognitively unimpaired individuals. The burden of WM lesions on cortical disconnection in the cholinergic system may be associated with subclinical cognitive impairments in the elderly. Longitudinal studies have demonstrated that a high WML burden increases the risk of future cognitive impairment (Benedictus et al., 2015). Therefore, future studies should investigate the disruptive role of WM lesion load in the association between cholinergic projections and cognitive performance in normal aging and the continuum of AD.

Our next point of interest was NBM and its volume. In Study I, the higher WM-hypo load was associated with the lower NBM volume above and beyond the effect of age. However, a prior study found no significant connection between NBM volume and vascular cognitive impairment (Liu et al., 2017). A possible reason for the discrepancy could be the smaller sample size in the study, which may have made it difficult to identify an association between SVD and NBM volume. Another explanation could be methodological differences: SVD, one of the criteria used to define vascular cognitive impairment in the study by Liu et al. (2017), was assessed using the Fazekas rating scale, which provides four rough scores from 0 to 3 based on 2D images of a limited set of brain sections. In contrast, our study used an automated estimation of WM-hypo volume in 3D images across the entire white matter to assess SVD. Additionally, it is possible that the link between NBM degeneration and SVD is stronger in normal aging, while this association may be weaker or non-existent in patients diagnosed with vascular cognitive impairment.

Despite the fact that NBM volume is important in AD (Grothe et al., 2012, 2010) and cognitive function in general (Ballinger et al., 2016), it consistently ranked very low among the other predictors in our random forest models predicting scores of attention and memory in cognitively unimpaired individuals (Study I). Previous studies have not reported any connection between BF or NBM volume and measures of memory and attention in cognitively normal individuals (Grothe et al., 2016; Lammers et al., 2016; Wolf et al., 2014). This is in line with the results of an analogous random forest analysis in cognitively unimpaired individuals in Study III. Another study (Schumacher et al., 2022) also showed that attentional performance was only associated with cholinergic pathway integrity but not with NBM volume. On the contrary, Study III also demonstrated that NBM volume played a significant role in the performance of memory and attention tests among individuals with MCI and AD dementia. This is consistent with previous research on AD (Fernández-Cabello

et al., 2020) and Parkinson's disease (Schulz et al., 2018), which has shown that NBM volume is a crucial predictor of disease progression.

Next, we investigated cholinergic WM pathways and their relationship to cognition and other biomarkers. Based on the findings obtained from the random forest models in cognitively healthy aging population, it has been revealed that the integrity of cholinergic pathways is crucial for various cognitive measures. Specifically, the external capsule pathway, which contains several memory-related regions such as the frontal cortex and hippocampal structures (Preston and Eichenbaum, 2013), was essential for delayed recall in an episodic memory test (TAVEC delayed recall, at both 5 and 30 minutes). In contrast, cognitive measures that demand effortful attention, such as TAVEC delayed recall at 30 min and PCV - reaction times, relied on the integrity of the cingulum, which involves the posterior cingulate cortex, known to be related to attention and memory (Klaassens et al., 2017; Pearson et al., 2011). A noteworthy observation is that the remaining WM did not exhibit any contribution to performance in any of the cognitive tests. This observation highlights the specificity of the cholinergic pathways to performance in the tests of attention and memory. Moreover, older age significantly impacted all cognitive variables. However, the contribution of age was less than that of the integrity of the cholinergic pathway in TAVEC delayed recall (both 5 and 30 minutes). These findings suggest that the contribution of the cholinergic system to cognitive measures is more pronounced in cognitively normal individuals and extends beyond the contribution of age in memory tasks that require effortful attention, such as delayed recall. Our results support a revised interpretation of the cholinergic hypothesis of cognitive aging (Dumas and Newhouse, 2011), which suggests that the cholinergic system plays a greater role in effortful attention processes than memory in cognitively normal individuals. Thus, the cholinergic system is especially engaged in attention and memory tasks that are challenging and require effortful attention to achieve high performance (i.e., PCV - reaction time and TAVEC delayed recall, in our study). Our study (Study I) further corroborates this interpretation, showing that none of the variable combinations could predict the TAVEC recognition task, indicating that the cholinergic system is not involved in this relatively easy memory task with minimal attention process involvement.

In the AD continuum, we discovered that the integrity of cholinergic WM pathways was decreased in all its stages. Our findings for the MCI and AD dementia groups, therefore, align with a recent study that indicated NBM degeneration accompanies changes in cholinergic WM pathways in MCI and AD dementia (Schumacher et al., 2022). Furthermore, a recent post-mortem study that employed post-mortem MRI and histopathology found no significant differences between AD and healthy controls in cholinergic WM pathways. Still, it demonstrated that decreased cholinergic cell density in NBM correlated with decreased integrity of cholinergic WM pathways towards the temporal lobe (Lin et al., 2022). Our current research broadens these previous studies by demonstrating that cholinergic pathway integrity is already impaired at the stage of SCD.

Study III found that the integrity of the cholinergic pathways was reduced in all stages of the AD continuum, which was consistent with a recent study demonstrating the alterations of cholinergic WM pathways in MCI and AD dementia (Schumacher et al., 2022). The amyloid stratified subsample replicated these findings, indicating that cholinergic pathways are particularly sensitive to Alzheimer's pathologic change. In addition, we found that the remaining WM also showed reduced integrity in all stages of the disease (whole sample), a finding that has been reported by others (Sun et al., 2014). However, this integrity reduction was not clearly observed in the amyloid stratified subsample. Although this could be due to the small sample size, the integrity of both cholinergic pathways remained significantly different between clinical groups and healthy controls in the amyloid stratified subsample, indicating that these pathways are particularly sensitive to AD pathologic changes (Aβ positivity), whereas the remaining WM changes in integrity may rather provide information about global degeneration. This was supported by our statistically significant correlation between CSF Aβ levels and the integrity of cingulum and external capsule pathways, as well as the correlation between CSF tau biomarkers and the integrity of these pathways. Although there are no studies investigating *in vivo* cholinergic projections in AD other than a recent study by Schumacher et al. (2022), studies focusing on NBM volume have similarly reported that NBM volume is more closely associated with AD-related pathology than other grey matter areas (Schmitz and Nathan Spreng, 2016; S. Teipel et al., 2014). This finding is also supported by our ROC analysis, in which the integrity of remaining WM consistently performed worse in all cases.

Study III further provided another finding regarding the spatial distribution of differences in WM integrity of the cholinergic pathways along the AD continuum. The study demonstrated that reduced integrity in the retrosplenial and posterior cingulate cortex, as well as in the external capsule, was already apparent in the SCD group. These regions were previously identified as having the earliest neuronal and metabolic changes and reduced connectivity and are emerging as vulnerable AD-associated epicentres (Lee et al., 2020). Additionally, these regions have been associated with early accumulation of amyloid in PET studies (Palmqvist et al., 2017). The MCI group had differences in the same areas as the SCD group and additionally involved the rostral anterior cingulate. In AD dementia, WM integrity alterations extended to the dorsal anterior cingulate and temporal and prefrontal areas. These areas are usually associated with increased neuronal loss in MCI and AD dementia (Coughlan et al., 2018). Although the analysis was cross-sectional, the replication of regional damage as the disease progresses and the stepwise addition of cholinergic WM areas following a posterior-anterior pattern of degeneration is a robust finding. If confirmed in longitudinal designs, these findings could help understand the progression of cholinergic system changes *in vivo* along the development of AD.

Another set of results (Study III) concerned the association between the integrity of the cholinergic pathways and cognitive scoring. The results of the respective random forest analysis indicated that different predictors contributed to cognitive scores in cognitively unimpaired and impaired groups. The combined analysis of healthy controls and SCD groups

showed that age, sex, and education were the main predictors of cognitive performance, and the integrity of the external capsule pathway also played a moderate role in tests of attention. The external capsule pathway projects to cortical regions involved in attention, such as the frontal lobe and posterior cortex. In contrast, the analysis of cognitively impaired groups (MCI and AD dementia) revealed that the integrity of the external capsule and cingulum pathways were important predictors of most tests of memory and attention. In addition to frontal and posterior cortical areas, the external capsule pathway also projected to cortical regions related to memory, such as medial temporal structures. The cingulum pathway also projected to memory-related cortical regions such as hippocampal structures and the posterior cingulate cortex. These results demonstrate the importance of the cholinergic system in cognitive processes related to effortful attention and memory. Similar results have been reported in recent studies of healthy aging and AD and dementia with Lewy bodies (Schumacher et al., 2022). Importantly, in the cognitively unimpaired groups (HC and SCD), we were able to replicate the findings of Study I that age and sex were important predictors of most cognitive tests, while the integrity of the cholinergic pathways was highly important only for tests involving effortful attention. In summary, the combined results of our studies suggest that the cholinergic system may deteriorate earlier in the WM, followed by a decline in NBM volume in more advanced stages of AD. The observed posterior-anterior pattern of WM cholinergic disruption may indicate that NBM starts deteriorating after enough cholinergic WM damage has occurred, consistent with the "dying-back pattern" of degeneration seen in AD (‘Wallerian-like degeneration’). This pattern of degeneration has been demonstrated in previous experimental and pathological studies (Kanaan et al., 2013; Nishioka et al., 2019). Overall, these findings indicate the early involvement of cholinergic pathways in the AD continuum and support the use of diffusion-based tracking as a promising emerging biomarker for microstructural changes in the earliest stages of the disease.

The results of our ROC analysis further support our findings. Firstly, all biomarkers, both conventional volumetric and new measures of WM integrity showed higher predictive importance with disease progression, validating the conventional biomarkers and suggesting that the proposed measures of WM integrity are sensitive to neurodegeneration. Moreover, the ROC analysis consistently showed low predictive power of the remaining WM integrity, indicating that the measures of the cholinergic system pathways are both sensitive and specific. Secondly, the ROC data revealed that cholinergic WM pathways were more effective in predicting AD at an early stage compared to the conventional volumetric measures. Lastly, in the amyloid-positive subsample, cholinergic WM pathways were more accurate in detecting SCD and MCI than the NBM volume. Thus, the findings suggest that alterations in cholinergic WM projections occur earlier than neurodegeneration in NBM in the context of an Alzheimer's pathologic change.

Our studies come with several limitations. Here, we present the most noteworthy ones. (1) All studies have limitations related to the accurate tracking of WM pathways that traverse crossing-fibre regions. Various techniques, including multi-tensor fitting, Q-ball imaging,

spherical deconvolution, and ball-and-sticks, have been proposed to overcome this problem. In this study, we used a ball-and-sticks model, which balances model capacity and data quality (Wilkins et al., 2015), to predict multiple fibre directions in a voxel. False positives and false negatives are common errors when tracking WM pathways through crossing-fibre regions (Dauguet et al., 2007; de Reus and van den Heuvel, 2013). To address this, we performed a combined reconstruction across the entire cohort and set a robust group threshold. A high group threshold eliminates false positives by requiring the connection to be present in a high number of individuals, while a low group threshold allows for unique tracks and ensures a low false-negative rate. We adapted the methods from previous studies (de Reus and van den Heuvel, 2013; Liu et al., 2017) and constrained fibre tracking by using hypothesis-driven *a priori* information to reduce the number of false positives in our cingulum and external capsule models. We also performed an unconstrained tractography model to include areas not considered in *a priori* knowledge. We used the MD index over other diffusion indices to reduce susceptibility to the crossing-fibre problem. (2) While investigating the NBM, which provides the major cholinergic input to cortical and subcortical areas, we suggest that future studies investigate the fornix, which contains cholinergic projections from the septal nuclei to the hippocampus, due to its involvement in episodic verbal memory. (3) Other cognitive functions related to the cholinergic system, such as cognitive control, also warrant investigation in future studies. (4) The associations between amyloid/tau biomarkers, WM lesion and NBM volumes, age, and MD (globally or in specific tracts) might lead to collinearity problems. Random forest regression with conditional inference trees handles multicollinearity to some extent. It may, however, underestimate the contribution of multicollinear variables. For this reason, we also included a correlation matrix between all variables for the reader to be able to judge this. (5) In contrast to the data of Study I and III, all included individuals were 70 years old in Study II. Hence, the generalizability of the findings to other age groups might be limited. (6) We have established a link between the degeneration of the cholinergic system and the levels of CSF Aβ38. However, given the limited literature on the role of Aβ38 in neurodegenerative processes, it would be too speculative to draw any conclusions, and additional research is required. (7) Our primary aim was to examine cross-sectional differences along the AD continuum and draw inferences about cholinergic WM pathways and clinical progression based on different groups. Although this approach provided a preliminary demonstration of early differences in cholinergic WM pathways in the SCD group, which extended to other WM areas in the MCI and AD dementia groups, we need to expand our current approach to include longitudinal analyses in the future. Longitudinal analyses will help to validate our initial interpretation of cholinergic alterations preceding AD pathology, with positivity in both Aβ and tau biomarkers. (8) Not all subjects in the DELCODE cohort (Study III) had CSF biomarker data, and while the CSF biomarker subsample was adequate to replicate the main findings, the analysis could benefit from an even larger CSF sample. However, our comparison of participants with and without CSF data available revealed no difference in crucial demographic variables and MMSE scores, suggesting a low risk of selection bias concerning the subsample with CSF data available. (9) Data in Study III were pooled from multi-centre MRI for a larger sample size. The related

inter-scanner variance may have influenced some of our results. To mitigate this limitation, the scanners were carefully harmonized at front, and the scanning protocol was the same across all centres in the DELCODE cohort. One could additionally use methods *post hoc* that may be able to further reduce variability across centres in the data. While there are some high-quality procedures that improve the harmonization of T1-weighted images (Chen et al., 2014), the field for harmonizing diffusion MRI data *post hoc* has not advanced that much.

8 CONCLUSIONS AND FUTURE DIRECTIONS

This thesis presents a summary of three original studies with a common goal and theme of finding, identifying and evaluating human cholinergic pathways *in vivo* using diffusion MRI. We started by developing a method to reveal the position of these pathways using retrospective MRI data (i.e., data were acquired before the requirements for the more advanced models have been characterized). Although working with such data comes with a number of limitations such as relative high signal-to-noise ratio or inapplicability of higher-order diffusion models, we present a robust algorithm based on a combined reconstruction across the cohort. The spatial layout of the recovered pathways strongly resembled the anatomy of the cholinergic pathways as we know them from post-mortem studies. We regard having a method to identify cholinergic pathways *in vivo* as an important step towards more detailed research of these pathways and, most importantly, diseases affecting this brain system, such as AD or Lewy body dementia. The only other *in vivo* method is PET imaging of cholinergic neurotransmission, which is, however, still very limited and much more demanding for the patient.

Having this model in our hands, we discovered several interesting implications in the population of healthy individuals. First, in healthy aging it is the macroscopic quality of cholinergic WM pathways but not the cellular bodies of NBM that correlates with the cognitive performance. In turn, we learnt that among several common age-related pathologies, it is predominantly the cerebrovascular factors that contribute to the variability of the integrity of the pathways in cognitively unimpaired individuals. Altogether, this indicates that prevention programs for neurodegeneration and cognitive decline should consider the management of cholinergic white matter lesions and vascular risk factors. These findings could inform clinical decisions related to biomarkers for AD and related dementias, cholinergic dysfunction, and cognitive impairment.

Then we investigated the properties of our model of the cholinergic pathways in the context of the AD continuum. Not only did we observe the overall effect in the AD dementia group, but we were able to detect significant changes in a very early stage of the disease (particularly in amyloid-positive SCD individuals). In discriminating between the groups of individuals with SCD and HC, the cholinergic WM pathways even demonstrated superior performance compared to non-cholinergic WM integrity and conventional assessments of hippocampal and NBM volumes. In conclusion, we demonstrated that the integrity of cholinergic WM pathways is a sensitive and specific biomarker for detecting early stages of neurodegeneration in individuals who display Alzheimer's pathological changes.

In summary, this thesis presents a novel technical solution for the identification and evaluation of the white matter cholinergic pathways *in vivo* using diffusion MRI, its validation and use in three independent cohorts. Thus, we can declare that the objectives of the thesis were met. A point-by-point overview of completed tasks follows:

T1. Existing fibre-tracking pipelines were identified and evaluated (Section 4.3, and Section 5.3.5, p. 38).
T2. Uncovering difficult-to-find yet important cholinergic tracts was addressed with a group analysis with a robust group threshold and selection of the MD index among other DTI-based measures of integrity (Section 5.3.5, p. 36-38).
T3. We designed a complex image processing pipeline for tracking the cholinergic pathways *in vivo* (Figure 5). We proposed a set of tracking seeds and targets, and a series of rules for their optimal use (e.g., registration parameters) in the pipeline.
T4. The pipeline was successfully implemented using state-of-the-art subroutines (Section 5.3.5, p. 34-36).
T5. The proposed image processing pipeline was employed in two independent patient cohorts (Section 6.1). The spatial layout of both resulting pathways was consistent and resembled findings from post-mortem studies. The integrity of the pathways correlated with the cognitive functions related to the cholinergic system (Section 6.2, and Section 6.3).

More detailed technical considerations and aspects of the proposed image processing pipeline with a general recommendation for fibre-tracking strategies from difficult-to-reach seeds are currently being compiled into a research article which will be published by the PhD candidate in the foreseeable future.

Future research of WM cholinergic pathways can be expanded in several ways. First, our preliminary demonstration of early differences in the cholinergic WM pathways in the SCD group should be confirmed using longitudinal analyses. Second, the model of cholinergic WM pathways could be possibly used in the context of other brain pathologies known to affect the cholinergic system (Lewy body dementia, multiple sclerosis, and others). Finally, the cholinergic model itself could be upgraded to utilize highest-quality data or provide a more accurate definition of the pathways.

9 ACKNOWLEDGEMENTS

I would like to express my gratitude to many people who have contributed to making my PhD studies a delightful and memorable experience:

Above all, **Olga Stěpánková**, my main supervisor, for her unwavering support, guidance, and countless thought-provoking discussions throughout my years of study. For consistently encouraging me to pursue my own research interests while offering invaluable direction and assistance whenever I encountered challenges. I feel incredibly fortunate to have had such an exceptional supervisor.

Lenka Vysloužilová, my co-supervisor, for her feedback, perspective, scientific guidance and support during my PhD studies. For introducing me to machine learning. For offering me the PhD position and encouraging me to apply.

Daniel Ferreira, my mentor, for taking me under his wings and introducing me to the world of science. For countless inspiring discussions and passing on enthusiasm for science. For considering me as a part of his research group. Dani, this thesis would not have been possible if it were not for your help and kindness. Thank you.

Eric Westman, for receiving me at Karolinska Institute and making my KI experience possible.

Zuzana Nedelská, for passing on enthusiasm for neuroimaging and years-long collaboration. For introducing me to Dani and Eric. For suggesting applying for the Alzheimer's Foundation internship and giving me courage even though I did not believe in myself that much. For all the pro bono consultations.

Lenka Lhotská, for management of the department and continuous support.

Eva Snášelová, Petra, **and Anette**, for taking care of me and patiently helping with all my questions.

IT guys at CIIRC and Sebastian at KI, for being a great source of help with all things related to computers over the years.

To my collaborators over the years: **Stefan, Michel, and Martin** for an excellent and highly efficient collaboration, **Vojta**, for inspiring collaboration and supply of new imaging techniques, **Nira, Lissett, and Patri**, for all your knowledge and kindness. To my friends and collaborators from the VentConnect project: **Míra, Jan K., Kuba, Jan J., Jan D., Lukáš, Eliška, Jaroslav, Petr, Václav, and František**, for inspiring collaboration.

To my friends from CTU: **Marek, Kamila, Jarda, Arnošt, Vašek, Michal**, for all the help and discussions along the way. **Petr**, for sharing the office with you.

Tomáš and Michal, for co-teaching the PRG course. It was a fun experience, even when it did not look like it at times. It certainly made me a better teacher.

To the people I had the honour to meet and collaborate with at Karolinska Institute: **Emilia, Juraj, Konstantinos, Mona-Lisa, Amit, Laetitia, Nenad, Gustav, Olga, Una, Joana, Alejandra, Olof, Urban, Annegret, Cene, Russell, Tobias, Rosaleena, Anna R., Anna C., Anna I., Blanca, Carmen, Caroline, Stephanie, Federico**. For making my KI experience smooth and enjoyable. It's been a pleasure working with you.

To my friends to **Jana**, **Lenka**, and **Lukáš**, for being the pragmatic and cool ones, for listening to me whenever I needed it.

Šárka Kovandová, for believing in me and my ideas, thus making the journey much easier.

To my family, especially my parents, siblings, and partner. Thank you for your support, encouragement, and everyday inspiration not only during my PhD studies.

This research was supported by the Grant Agency of the Czech Technical University in Prague, grant no. SGS19/111/OHK4/2T/13 "Measurement of basal forebrain atrophy and integrity of cholinergic pathways using MRI".

10 REFERENCES

Abragam, A., Hebel, L.C., 1961. The Principles of Nuclear Magnetism. Am. J. Phys. 29, 860–861. https://doi.org/10.1119/1.1937646

Acosta-Cabronero, J., Williams, G.B., Pengas, G., Nestor, P.J., 2010. Absolute diffusivities define the landscape of white matter degeneration in Alzheimer's disease. Brain 133, 529–539. https://doi.org/10.1093/brain/awp257

Albert, M., Zhu, Y., Moghekar, A., Mori, S., Miller, M.I., Soldan, A., Pettigrew, C., Selnes, O., Li, S., Wang, M.C., 2018. Predicting progression from normal cognition to mild cognitive impairment for individuals at 5 years. Brain 141, 877–887. https://doi.org/10.1093/brain/awx365

Albert, M.S., DeKosky, S.T., Dickson, D., Dubois, B., Feldman, H.H., Fox, N.C., Gamst, A., Holtzman, D.M., Jagust, W.J., Petersen, R.C., Snyder, P.J., Carrillo, M.C., Thies, B., Phelps, C.H., 2011. The diagnosis of mild cognitive impairment due to Alzheimer's disease: Recommendations from the National Institute on Aging-Alzheimer's Association workgroups on diagnostic guidelines for Alzheimer's disease. Alzheimer's Dement. 7, 270–279. https://doi.org/10.1016/j.jalz.2011.03.008

Andersson, J.L.R., Sotiropoulos, S.N., 2016. An integrated approach to correction for off-resonance effects and subject movement in diffusion MR imaging. Neuroimage 125, 1063–1078. https://doi.org/10.1016/j.neuroimage.2015.10.019

Atkinson, A.J., Colburn, W.A., DeGruttola, V.G., DeMets, D.L., Downing, G.J., Hoth, D.F., Oates, J.A., Peck, C.C., Schooley, R.T., Spilker, B.A., Woodcock, J., Zeger, S.L., 2001. Biomarkers and surrogate endpoints: Preferred definitions and conceptual framework. Clin. Pharmacol. Ther. 69, 89–95. https://doi.org/10.1067/mcp.2001.113989

Avants, B.B., Epstein, C.L., Grossman, M., Gee, J.C., 2008. Symmetric diffeomorphic image registration with cross-correlation: Evaluating automated labeling of elderly and neurodegenerative brain. Med. Image Anal. 12, 26–41. https://doi.org/10.1016/j.media.2007.06.004

Ballinger, E.C., Ananth, M., Talmage, D.A., Role, L.W., 2016. Basal Forebrain Cholinergic Circuits and Signaling in Cognition and Cognitive Decline. Neuron 91, 1199–1218. https://doi.org/10.1016/j.neuron.2016.09.006

Bartus, R.T., Dean, R.L., Beer, B., Lippa, A.S., 1982. The cholinergic hypothesis of geriatric memory dysfunction. Science 217, 408–417. https://doi.org/10.1126/science.7046051

Behrens, T.E.J., Berg, H.J., Jbabdi, S., Rushworth, M.F.S., Woolrich, M.W., 2007. Probabilistic diffusion tractography with multiple fibre orientations: What can we gain? Neuroimage 34, 144–155. https://doi.org/10.1016/j.neuroimage.2006.09.018

Behrens, T.E.J., Woolrich, M.W., Jenkinson, M., Johansen-Berg, H., Nunes, R.G., Clare, S., Matthews, P.M., Brady, J.M., Smith, S.M., 2003. Characterization and Propagation of Uncertainty in Diffusion-Weighted MR Imaging. Magn. Reson. Med. 50, 1077–1088. https://doi.org/10.1002/mrm.10609

Benedet MJ, A.M., 1998. TAVEC: Test de Aprendizaje Verbal España-Complutense. TEA, Madrid.

Benedictus, M.R., Van Harten, A.C., Leeuwis, A.E., Koene, T., Scheltens, P., Barkhof, F., Prins, N.D., Van Der Flier, W.M., 2015. White Matter Hyperintensities Relate to Clinical Progression in Subjective Cognitive Decline. Stroke 46, 2661–2664. https://doi.org/10.1161/STROKEAHA.115.009475

Biswal, B., Zerrin Yetkin, F., Haughton, V.M., Hyde, J.S., 1995. Functional connectivity in the motor cortex of resting human brain using echo-planar mri. Magn. Reson. Med. 34, 537–541. https://doi.org/10.1002/mrm.1910340409

Blennow, K., Zetterberg, H., 2018. The Past and the Future of Alzheimer's Disease Fluid Biomarkers. J. Alzheimer's Dis. 62, 1125–1140. https://doi.org/10.3233/JAD-170773

Bohnen, N.I., Frey, K.A., 2007. Imaging of cholinergic and monoaminergic neurochemical changes in neurodegenerative disorders. Mol. imaging Biol. 9, 243–257. https://doi.org/10.1007/S11307-007-0083-6

Bohnen, N.I., Kaufer, D.I., Hendrickson, R., Ivanco, L.S., Lopresti, B., Davis, J.G., Constantine, G., Mathis,

C.A., Moore, R.Y., DeKosky, S.T., 2005. Cognitive correlates of alterations in acetylcholinesterase in Alzheimer's disease. Neurosci. Lett. 380, 127–132. https://doi.org/10.1016/j.neulet.2005.01.031

Bowen, D.M., Smith, C.B., White, P., Davison, A.N., 1976. Neurotransmitter-related enzymes and indices of hypoxia in senile dementia and other abiotrophies. Brain 99, 459–496. https://doi.org/10.1093/brain/99.3.459

Brands, A.M.A., Kessels, R.P.C., Hoogma, R.P.L.M., Henselmans, J.M.L., Van Der Beek Boter, J.W., Kappelle, L.J., De Haan, E.H.F., Biessels, G.J., 2006. Cognitive performance, psychological well-being, and brain magnetic resonance imaging in older patients with type 1 diabetes. Diabetes 55, 1800–1806. https://doi.org/10.2337/db05-1226

Breiman, L., 2001. Random forests. Mach. Learn. 45, 5–32. https://doi.org/10.1023/A:1010933404324

Buchhave, P., Minthon, L., Zetterberg, H., Wallin, Å.K., Blennow, K., Hansson, O., 2012. Cerebrospinal fluid levels of β-amyloid 1-42, but not of tau, are fully changed already 5 to 10 years before the onset of Alzheimer dementia. Arch. Gen. Psychiatry 69, 98–106. https://doi.org/10.1001/archgenpsychiatry.2011.155

Cavedo, E., Dubois, B., Colliot, O., Lista, S., Croisile, B., Tisserand, G.L., Touchon, J., Bonafe, A., Ousset, P.J., Rouaud, O., Ricolfi, F., Vighetto, A., Pasquier, F., Galluzzi, S., Delmaire, C., Ceccaldi, M., Girard, N., Lehericy, S., Duveau, F., Chupin, M., Sarazin, M., Dormont, D., Hampel, H., 2016. Reduced regional cortical thickness rate of change in donepezil-Treated subjects with suspected prodromal Alzheimer's disease. J. Clin. Psychiatry 77, e1631–e1638. https://doi.org/10.4088/JCP.15m10413

Cavedo, E., Grothe, M.J., Colliot, O., Lista, S., Chupin, M., Dormont, Di., Houot, M., Lehéricy, S., Teipel, S., Dubois, B., Hampel, H., Croisile, B., Louis Tisserand, G., Bonafe, A., Ousset, P.J., Rouaud, O., Ricolfi, F., Vighetto, A., Pasquier, F., Delmaire, C., Ceccaldi, M., Girard, N., Duveau, F., Sarazin, M., 2017. Reduced basal forebrain atrophy progression in a randomized Donepezil trial in prodromal Alzheimer's disease. Sci. Rep. 7, 1–10. https://doi.org/10.1038/s41598-017-09780-3

Cedres, N., Ferreira, D., Machado, A., Shams, S., Sacuiu, S., Waern, M., Wahlund, L.O., Zettergren, A., Kern, S., Skoog, I., Westman, E., 2020. Predicting Fazekas scores from automatic segmentations of white matter signal abnormalities. Aging (Albany. NY). 12, 894–901. https://doi.org/10.18632/aging.102662

Cedres, N., Ferreira, D., Nemy, M., Machado, A., Pereira, J.B., Shams, S., Wahlund, L.O., Zettergren, A., Stepankova, O., Vyslouzilova, L., Eriksdotter, M., Teipel, S., Grothe, M.J., Blennow, K., Zetterberg, H., Schöll, M., Kern, S., Skoog, I., Westman, E., 2022. Association of Cerebrovascular and Alzheimer Disease Biomarkers With Cholinergic White Matter Degeneration in Cognitively Unimpaired Individuals. Neurology 99, e1619–e1629. https://doi.org/10.1212/WNL.0000000000200930

Choi, S.H., Jung, T.M., Lee, J.E., Lee, S.K., Sohn, Y.H., Lee, P.H., 2012. Volumetric analysis of the substantia innominata in patients with Parkinson's disease according to cognitive status. Neurobiol. Aging 33, 1265–1272. https://doi.org/10.1016/j.neurobiolaging.2010.11.015

Coughlan, G., Laczó, J., Hort, J., Minihane, A.M., Hornberger, M., 2018. Spatial navigation deficits — Overlooked cognitive marker for preclinical Alzheimer disease? Nat. Rev. Neurol. 14, 496–506. https://doi.org/10.1038/s41582-018-0031-x

Coughlin, J.M., Rubin, L.H., Du, Y., Rowe, S.P., Crawford, J.L., Rosenthal, H.B., Frey, S.M., Marshall, E.S., Shinehouse, L.K., Chen, A., Speck, C.L., Wang, Y., Lesniak, W.G., Minn, I., Bakker, A., Kamath, V., Smith, G.S., Albert, M.S., Azad, B.B., Dannals, R.F., Horti, A., Wong, D.F., Pomper, M.G., 2020. High Availability of the a7-Nicotinic Acetylcholine Receptor in Brains of Individuals with Mild Cognitive Impairment: A Pilot Study Using 18F-ASEM PET. J. Nucl. Med. 61, 423–426. https://doi.org/10.2967/JNUMED.119.230979

Coughlin, J.M., Slania, S., Du, Y., Rosenthal, H.B., Lesniak, W.G., Minn, I., Smith, G.S., Dannals, R.F., Kuwabara, H., Wong, D.F., Wang, Y., Horti, A.G., Pomper, M.G., 2018. 18F-XTRA PET for enhanced imaging of the extrathalamic α4β2 nicotinic acetylcholine receptor. J. Nucl. Med. 59, 1603–1608. https://doi.org/10.2967/jnumed.117.205492

Dauguet, J., Peled, S., Berezovskii, V., Delzescaux, T., Warfield, S.K., Born, R., Westin, C.F., 2007. Comparison of fiber tracts derived from in-vivo DTI tractography with 3D histological neural tract tracer reconstruction on a macaque brain. Neuroimage 37, 530–538. https://doi.org/10.1016/j.neuroimage.2007.04.067

Davies, P., Maloney, A.J.F., 1976. Selective Loss of Central Cholinergic Neurons in Alzheimer'S Disease. Lancet 308, 1403. https://doi.org/10.1016/S0140-6736(76)91936-X

de Reus, M.A., van den Heuvel, M.P., 2013. Estimating false positives and negatives in brain networks. Neuroimage 70, 402–409. https://doi.org/10.1016/j.neuroimage.2012.12.066

Drachman, D.A., Leavitt, J., 1974. Human Memory and the Cholinergic System: A Relationship to Aging? Arch. Neurol. 30, 113–121. https://doi.org/10.1001/archneur.1974.00490320001001

Dubois, B., Chupin, M., Hampel, H., Lista, S., Cavedo, E., Croisile, B., Louis Tisserand, G., Touchon, J., Bonafe, A., Ousset, P.J., Ait Ameur, A., Rouaud, O., Ricolfi, F., Vighetto, A., Pasquier, F., Delmaire, C., Ceccaldi, M., Girard, N., Dufouil, C., Lehericy, S., Tonelli, I., Duveau, F., Colliot, O., Garnero, L., Sarazin, M., Dormont, D., 2015. Donepezil decreases annual rate of hippocampal atrophy in suspected prodromal Alzheimer's disease. Alzheimer's Dement. 11, 1041–1049. https://doi.org/10.1016/j.jalz.2014.10.003

Dubois, B., Feldman, H.H., Jacova, C., DeKosky, S.T., Barberger-Gateau, P., Cummings, J., Delacourte, A., Galasko, D., Gauthier, S., Jicha, G., Meguro, K., O'Brien, J., Pasquier, F., Robert, P., Rossor, M., Salloway, S., Stern, Y., Visser, P.J., Scheltens, P., 2007. Research criteria for the diagnosis of Alzheimer's disease: revising the NINCDS–ADRDA criteria. Lancet Neurol. 6, 734–746. https://doi.org/10.1016/S1474-4422(07)70178-3

Dubois, B., Feldman, H.H., Jacova, C., Hampel, H., Molinuevo, J.L., Blennow, K., Dekosky, S.T., Gauthier, S., Selkoe, D., Bateman, R., Cappa, S., Crutch, S., Engelborghs, S., Frisoni, G.B., Fox, N.C., Galasko, D., Habert, M.O., Jicha, G.A., Nordberg, A., Pasquier, F., Rabinovici, G., Robert, P., Rowe, C., Salloway, S., Sarazin, M., Epelbaum, S., de Souza, L.C., Vellas, B., Visser, P.J., Schneider, L., Stern, Y., Scheltens, P., Cummings, J.L., 2014. Advancing research diagnostic criteria for Alzheimer's disease: The IWG-2 criteria. Lancet Neurol. 13, 614–629. https://doi.org/10.1016/S1474-4422(14)70090-0

Dubois, B., Hampel, H., Feldman, H.H., Scheltens, P., Aisen, P., Andrieu, S., Bakardjian, H., Benali, H., Bertram, L., Blennow, K., Broich, K., Cavedo, E., Crutch, S., Dartigues, J.F., Duyckaerts, C., Epelbaum, S., Frisoni, G.B., Gauthier, S., Genthon, R., Gouw, A.A., Habert, M.O., Holtzman, D.M., Kivipelto, M., Lista, S., Molinuevo, J.L., O'Bryant, S.E., Rabinovici, G.D., Rowe, C., Salloway, S., Schneider, L.S., Sperling, R., Teichmann, M., Carrillo, M.C., Cummings, J., Jack, C.R., 2016. Preclinical Alzheimer's disease: Definition, natural history, and diagnostic criteria. Alzheimer's Dement. 12, 292–323. https://doi.org/10.1016/j.jalz.2016.02.002

Dumas, J.A., Newhouse, P.A., 2011. The cholinergic hypothesis of cognitive aging revisited again: Cholinergic functional compensation. Pharmacol. Biochem. Behav. 99, 254–261. https://doi.org/10.1016/j.pbb.2011.02.022

Fernández-Cabello, S., Kronbichler, M., van Dijk, K.R.A., Goodman, J.A., Nathan Spreng, R., Schmitz, T.W., 2020. Basal forebrain volume reliably predicts the cortical spread of Alzheimer's degeneration. Brain 143, 993–1009. https://doi.org/10.1093/brain/awaa012

Ferreira, D., Machado, A., Molina, Y., Nieto, A., Correia, R., Westman, E., Barroso, J., 2017. Cognitive variability during middle-age: Possible association with neurodegeneration and cognitive reserve. Front. Aging Neurosci. 9, 188. https://doi.org/10.3389/fnagi.2017.00188

Fischl, B., Salat, D.H., Busa, E., Albert, M., Dieterich, M., Haselgrove, C., Van Der Kouwe, A., Killiany, R., Kennedy, D., Klaveness, S., Montillo, A., Makris, N., Rosen, B., Dale, A.M., 2002. Whole brain segmentation: Automated labeling of neuroanatomical structures in the human brain. Neuron 33, 341–355. https://doi.org/10.1016/S0896-6273(02)00569-X

Friston, K.J., Ashburner, J., Frith, C.D., Poline, J. -B, Heather, J.D., Frackowiak, R.S.J., 1995. Spatial registration and normalization of images. Hum. Brain Mapp. 3, 165–189. https://doi.org/10.1002/hbm.460030303

Fritz, H.C.J., Ray, N., Dyrba, M., Sorg, C., Teipel, S., Grothe, M.J., 2019. The corticotopic organization of the human basal forebrain as revealed by regionally selective functional connectivity profiles. Hum. Brain Mapp. 40, 868–878. https://doi.org/10.1002/hbm.24417

Gee, J.C., 1999. On matching brain volumes. Pattern Recognit. 32, 99–111. https://doi.org/10.1016/S0031-3203(98)00093-4

George, S., Mufson, E.J., Leurgans, S., Shah, R.C., Ferrari, C., DeToledo-Morrell, L., 2011. MRI-based volumetric measurement of the substantia innominata in amnestic MCI and mild AD. Neurobiol. Aging 32, 1756–1764. https://doi.org/10.1016/j.neurobiolaging.2009.11.006

Geula, C., Nagykery, N., Nicholas, A., Wu, C.K., 2008. Cholinergic neuronal and axonal abnormalities are present early in aging and in Alzheimer disease. J. Neuropathol. Exp. Neurol. 67, 309–318. https://doi.org/10.1097/NEN.0b013e31816a1df3

Geula, C., Schatz, C.R., Mesulam, M.M., 1993. Differential localization of nadph-diaphorase and calbindin-D28k within the cholinergic neurons of the basal forebrain, striatum and brainstem in the rat, monkey, baboon and human. Neuroscience 54, 461–476. https://doi.org/10.1016/0306-4522(93)90266-I

Gray, S.L., Anderson, M.L., Dublin, S., Hanlon, J.T., Hubbard, R., Walker, R., Yu, O., Crane, P.K., Larson, E.B., 2015. Cumulative use of strong anticholinergics and incident dementia: A prospective cohort study. JAMA Intern. Med. 175, 401–407. https://doi.org/10.1001/jamainternmed.2014.7663

Grinberg, L.T., Heinsen, H., 2007. Computer-assisted 3D reconstruction of the human basal forebrain complex. Dement. Neuropsychol. 1, 140–146. https://doi.org/10.1590/s1980-57642008dn10200005

Grothe, M., Heinsen, H., Teipel, S., 2013. Longitudinal measures of cholinergic forebrain atrophy in the transition from healthy aging to Alzheimer's disease. Neurobiol. Aging 34, 1210–1220. https://doi.org/10.1016/j.neurobiolaging.2012.10.018

Grothe, M., Heinsen, H., Teipel, S.J., 2012. Atrophy of the cholinergic basal forebrain over the adult age range and in early stages of Alzheimer's disease. Biol. Psychiatry 71, 805–813. https://doi.org/10.1016/j.biopsych.2011.06.019

Grothe, M., Zaborszky, L., Atienza, M., Gil-Neciga, E., Rodriguez-Romero, R., Teipel, S.J., Amunts, K., Suarez-Gonzalez, A., Cantero, J.L., 2010. Reduction of basal forebrain cholinergic system parallels cognitive impairment in patients at high risk of developing alzheimer's disease. Cereb. Cortex 20, 1685–1695. https://doi.org/10.1093/cercor/bhp232

Grothe, M.J., Heinsen, H., Amaro, E., Grinberg, L.T., Teipel, S.J., 2016. Cognitive Correlates of Basal Forebrain Atrophy and Associated Cortical Hypometabolism in Mild Cognitive Impairment. Cereb. Cortex 26, 2411–2426. https://doi.org/10.1093/cercor/bhv062

Guerchet, M., Prince, M., Prina, M., 2020. Numbers of people with dementia worldwide: An update to the estimates in the World Alzheimer Report 2015 [WWW Document]. Int. Alzheimer's Dis. URL https://www.alzint.org/resource/numbers-of-people-with-dementia-worldwide/ (accessed 3.6.23).

Gustavsson, A.M., Stomrud, E., Abul-Kasim, K., Minthon, L., Nilsson, P.M., Hansson, O., Nägga, K., 2015. Cerebral Microbleeds and White Matter Hyperintensities in Cognitively Healthy Elderly: A Cross-Sectional Cohort Study Evaluating the Effect of Arterial Stiffness. Cerebrovasc. Dis. Extra 5, 41–51. https://doi.org/10.1159/000377710

Habes, M., Erus, G., Toledo, J.B., Zhang, T., Bryan, N., Launer, L.J., Rosseel, Y., Janowitz, D., Doshi, J., Van Der Auwera, S., Von Sarnowski, B., Hegenscheid, K., Hosten, N., Homuth, G., Völzke, H., Schminke, U., Hoffmann, W., Grabe, H.J., Davatzikos, C., 2016. White matter hyperintensities and imaging patterns of brain ageing in the general population. Brain 139, 1164–1179. https://doi.org/10.1093/brain/aww008

Hahn, E.L., 1950. Spin echoes. Phys. Rev. 80, 580–594. https://doi.org/10.1103/PhysRev.80.580

Halliday, G.M., Cullen, K., Cairns, M.J., 1993. Quantitation and three-dimensional reconstruction of Ch4 nucleus in the human basal forebrain. Synapse 15, 1–16. https://doi.org/10.1002/syn.890150102

Hasselmo, M.E., Stern, C.E., 2014. Theta rhythm and the encoding and retrieval of space and time. Neuroimage 85, 656–666. https://doi.org/10.1016/j.neuroimage.2013.06.022

Herdick, M., Dyrba, M., Fritz, H.C.J., Altenstein, S., Ballarini, T., Brosseron, F., Buerger, K., Can Cetindag, A., Dechent, P., Dobisch, L., Duezel, E., Ertl-Wagner, B., Fliessbach, K., Dawn Freiesleben, S., Frommann, I., Glanz, W., Dylan Haynes, J., Heneka, M.T., Janowitz, D., Kilimann, I., Laske, C., Metzger, C.D., Munk, M.H., Peters, O., Priller, J., Roy, N., Scheffler, K., Schneider, A., Spottke, A., Jakob Spruth, E., Tscheuschler, M., Vukovich, R., Wiltfang, J., Jessen, F., Teipel, S., Grothe, M.J., 2020. Multimodal MRI analysis of basal forebrain structure and function across the Alzheimer's disease spectrum. NeuroImage Clin. 28, 102495. https://doi.org/10.1016/j.nicl.2020.102495

Hernández, M., Guerrero, G.D., Cecilia, J.M., García, J.M., Inuggi, A., Jbabdi, S., Behrens, T.E.J., Sotiropoulos, S.N., 2013. Accelerating Fibre Orientation Estimation from Diffusion Weighted Magnetic Resonance Imaging Using GPUs. PLoS One 8. https://doi.org/10.1371/journal.pone.0061892

Hess, C.P., Mukherjee, P., Han, E.T., Xu, D., Vigneron, D.B., 2006. Q-ball reconstruction of multimodal fiber orientations using the spherical harmonic basis. Magn. Reson. Med. 56, 104–117. https://doi.org/10.1002/mrm.20931

Heywood, W.E., Hallqvist, J., Heslegrave, A.J., Zetterberg, H., Fenoglio, C., Scarpini, E., Rohrer, J.D., Galimberti, D., Mills, K., 2018. CSF pro-orexin and amyloid-β38 expression in Alzheimer's disease and frontotemporal dementia. Neurobiol. Aging 72, 171–176. https://doi.org/10.1016/j.neurobiolaging.2018.08.019

Higley, M.J., Picciotto, M.R., 2014. Neuromodulation by acetylcholine: Examples from schizophrenia and depression. Curr. Opin. Neurobiol. 29, 88–95. https://doi.org/10.1016/j.conb.2014.06.004

Hong, J.H., Jang, S.H., 2010. Neural pathway from nucleus basalis of Meynert passing through the cingulum in the human brain. Brain Res. 1346, 190–194. https://doi.org/10.1016/j.brainres.2010.05.088

Howe, W.M., Berry, A.S., Francois, J., Gilmour, G., Carp, J.M., Tricklebank, M., Lustig, C., Sarter, M., 2013. Prefrontal cholinergic mechanisms Instigating shifts from monitoring for cues to Cue-Guided performance: Converging electrochemical and fMRI evidence from rats and humans. J. Neurosci. 33, 8742–8752. https://doi.org/10.1523/JNEUROSCI.5809-12.2013

Iyo, M., Namba, H., Fukushi, K., Shinotoh, H., Nagatsuka, S., Suhara, T., Sudo, Y., Suzuki, K., Irie, T., 1997. Measurement of acetylcholinesterase by positron emission tomography in the brains of healthy controls and patients with Alzheimer's disease. Lancet 349, 1805–1809. https://doi.org/10.1016/S0140-6736(96)09124-6

Jack, C.R., Bennett, D.A., Blennow, K., Carrillo, M.C., Dunn, B., Haeberlein, S.B., Holtzman, D.M., Jagust, W., Jessen, F., Karlawish, J., Liu, E., Molinuevo, J.L., Montine, T., Phelps, C., Rankin, K.P., Rowe, C.C., Scheltens, P., Siemers, E., Snyder, H.M., Sperling, R., Elliott, C., Masliah, E., Ryan, L., Silverberg, N., 2018. NIA-AA Research Framework: Toward a biological definition of Alzheimer's disease. Alzheimer's Dement. 14, 535–562. https://doi.org/10.1016/j.jalz.2018.02.018

Jack, C.R., Holtzman, D.M., 2013. Biomarker modeling of alzheimer's disease. Neuron 80, 1347–1358. https://doi.org/10.1016/j.neuron.2013.12.003

Jack, C.R., Knopman, D.S., Jagust, W.J., Petersen, R.C., Weiner, M.W., Aisen, P.S., Shaw, L.M., Vemuri, P., Wiste, H.J., Weigand, S.D., Lesnick, T.G., Pankratz, V.S., Donohue, M.C., Trojanowski, J.Q., 2013. Tracking pathophysiological processes in Alzheimer's disease: An updated hypothetical model of dynamic biomarkers. Lancet Neurol. 12, 207–216. https://doi.org/10.1016/S1474-4422(12)70291-0

Janelidze, S., Mattsson, N., Palmqvist, S., Smith, R., Beach, T.G., Serrano, G.E., Chai, X., Proctor, N.K., Eichenlaub, U., Zetterberg, H., Blennow, K., Reiman, E.M., Stomrud, E., Dage, J.L., Hansson, O., 2020. Plasma P-tau181 in Alzheimer's disease: relationship to other biomarkers, differential diagnosis, neuropathology and longitudinal progression to Alzheimer's dementia. Nat. Med. 26, 379–386. https://doi.org/10.1038/s41591-020-0755-1

Janelidze, S., Zetterberg, H., Mattsson, N., Palmqvist, S., Vanderstichele, H., Lindberg, O., van Westen, D., Stomrud, E., Minthon, L., Blennow, K., Hansson, O., 2016. CSF Aβ42/Aβ40 and Aβ42/Aβ38 ratios: Better diagnostic markers of Alzheimer disease. Ann. Clin. Transl. Neurol. 3, 154–165. https://doi.org/10.1002/acn3.274

Jansen, W.J., Ossenkoppele, R., Knol, D.L., Tijms, B.M., Scheltens, P., Verhey, F.R.J., Visser, P.J., 2015. Prevalence of cerebral amyloid pathology in persons without dementia: A meta-analysis. JAMA - J. Am. Med. Assoc. 313, 1924–1938. https://doi.org/10.1001/jama.2015.4668

Jenkinson, M., Pechaud, M., Smith, S., 2005. BET2: MR-based estimation of brain, skull and scalp surfaces, in: Eleventh Annual Meeting of the Organization for Human Brain Mapping.

Jessen, F., Amariglio, R.E., Van Boxtel, M., Breteler, M., Ceccaldi, M., Chételat, G., Dubois, B., Dufouil, C., Ellis, K.A., Van Der Flier, W.M., Glodzik, L., Van Harten, A.C., De Leon, M.J., McHugh, P., Mielke, M.M., Molinuevo, J.L., Mosconi, L., Osorio, R.S., Perrotin, A., Petersen, R.C., Rabin, L.A., Rami, L., Reisberg, B., Rentz, D.M., Sachdev, P.S., De La Sayette, V., Saykin, A.J., Scheltens, P., Shulman, M.B.,

Slavin, M.J., Sperling, R.A., Stewart, R., Uspenskaya, O., Vellas, B., Visser, P.J., Wagner, M., 2014. A conceptual framework for research on subjective cognitive decline in preclinical Alzheimer's disease. Alzheimer's Dement. 10, 844–852. https://doi.org/10.1016/j.jalz.2014.01.001

Jessen, F., Feyen, L., Freymann, K., Tepest, R., Maier, W., Heun, R., Schild, H.H., Scheef, L., 2006. Volume reduction of the entorhinal cortex in subjective memory impairment. Neurobiol. Aging 27, 1751–1756. https://doi.org/10.1016/j.neurobiolaging.2005.10.010

Jessen, F., Spottke, A., Boecker, H., Brosseron, F., Buerger, K., Catak, C., Fliessbach, K., Franke, C., Fuentes, M., Heneka, M.T., Janowitz, D., Kilimann, I., Laske, C., Menne, F., Nestor, P., Peters, O., Priller, J., Pross, V., Ramirez, A., Schneider, A., Speck, O., Spruth, E.J., Teipel, S., Vukovich, R., Westerteicher, C., Wiltfang, J., Wolfsgruber, S., Wagner, M., Düzel, E., 2018. Design and first baseline data of the DZNE multicenter observational study on predementia Alzheimer's disease (DELCODE). Alzheimer's Res. Ther. 10, 21. https://doi.org/10.1186/s13195-017-0314-2

Kanaan, N.M., Pigino, G.F., Brady, S.T., Lazarov, O., Binder, L.I., Morfini, G.A., 2013. Axonal degeneration in Alzheimer's disease: When signaling abnormalities meet the axonal transport system. Exp. Neurol. 246, 44–53. https://doi.org/10.1016/j.expneurol.2012.06.003

Kilimann, I., Grothe, M., Heinsen, H., Alho, E.J.L., Grinberg, L., Amaro, E., Dos Santos, G.A.B., Da Silva, R.E., Mitchell, A.J., Frisoni, G.B., Bokde, A.L.W., Fellgiebel, A., Filippi, M., Hampel, H., Klöppel, S., Teipel, S.J., 2014. Subregional basal forebrain atrophy in alzheimer's disease: A multicenter study. J. Alzheimer's Dis. 40, 687–700. https://doi.org/10.3233/JAD-132345

Klaassens, B.L., van Gerven, J.M.A., van der Grond, J., de Vos, F., Möller, C., Rombouts, S.A.R.B., 2017. Diminished posterior precuneus connectivity with the default mode network differentiates normal aging from Alzheimer's Disease. Front. Aging Neurosci. 9. https://doi.org/10.3389/fnagi.2017.00097

Knox, D., Keller, S.M., 2016. Cholinergic neuronal lesions in the medial septum and vertical limb of the diagonal bands of Broca induce contextual fear memory generalization and impair acquisition of fear extinction. Hippocampus 26, 718–726. https://doi.org/10.1002/hipo.22553

Kuhl, D.E., Koeppe, R.A., Minoshima, S., Snyder, S.E., Ficaro, E.P., Foster, N.L., Frey, K.A., Kilbourn, M.R., 1999. In vivo mapping of cerebral acetylcholinesterase activity in aging and Alzheimer's disease. Neurology 52, 691–691. https://doi.org/10.1212/WNL.52.4.691

Kuhl, D.E., Minoshima, S., Frey, K.A., Foster, N.L., Kilbourn, M.R., Koeppe, R.A., 2000. Limited donepezil inhibition of acetylcholinesterase measured with positron emission tomography in living Alzheimer cerebral cortex. Ann. Neurol. 48, 391–395. https://doi.org/10.1002/1531-8249(200009)48:3<391::AID-ANA17>3.0.CO;2-H

Kuwabara, H., Horti, A., Brasic, J., Gao, Y., Guevara, M.R., Zaidi, E., Wong, D., 2011. Evaluation of [18F]AZAN for quantification of nicotinic acetylcholine receptors in human brain. J. Nucl. Med. 52.

Lammers, F., Mobascher, A., Musso, F., Shah, N.J., Warbrick, T., Zaborszky, L., Winterer, G., 2016. Effects of Ncl. Basalis Meynert volume on the Trail-Making-Test are restricted to the left hemisphere. Brain Behav. 6, 1–9. https://doi.org/10.1002/brb3.421

Lao, P.J., Betthauser, T.J., Tudorascu, D.L., Barnhart, T.E., Hillmer, A.T., Stone, C.K., Mukherjee, J., Christian, B.T., 2017. [18F]Nifene test–retest reproducibility in first-in-human imaging of α4β2* nicotinic acetylcholine receptors. Synapse 71. https://doi.org/10.1002/syn.21981

Lebedev, A. V., Westman, E., Van Westen, G.J.P., Kramberger, M.G., Lundervold, A., Aarsland, D., Soininen, H., Kłoszewska, I., Mecocci, P., Tsolaki, M., Vellas, B., Lovestone, S., Simmons, A., 2014. Random Forest ensembles for detection and prediction of Alzheimer's disease with a good between-cohort robustness. NeuroImage Clin. 6, 115–125. https://doi.org/10.1016/j.nicl.2014.08.023

Lee, P.L., Chou, K.H., Chung, C.P., Lai, T.H., Zhou, J.H., Wang, P.N., Lin, C.P., 2020. Posterior Cingulate Cortex Network Predicts Alzheimer's Disease Progression. Front. Aging Neurosci. 12, 466. https://doi.org/10.3389/fnagi.2020.608667

Li, X., Li, T.Q., Andreasen, N., Wiberg, M.K., Westman, E., Wahlund, L.O., 2014. The association between biomarkers in cerebrospinal fluid and structural changes in the brain in patients with Alzheimer's disease. J. Intern. Med. 275, 418–427. https://doi.org/10.1111/joim.12164

Li, X., Westman, E., Ståhlbom, A.K., Thordardottir, S., Almkvist, O., Blennow, K., Wahlund, L.O., Graff, C., 2015. White matter changes in familial Alzheimer's disease. J. Intern. Med. 278, 211–218. https://doi.org/10.1111/joim.12352

Lin, C.-P., Frigerio, I., Boon, B.D.C., Zhou, Z., Rozemuller, A.J.M., Bouwman, F.H., Schoonheim, M.M., van de Berg, W.D.J., Jonkman, L.E., 2022. Structural (dys)connectivity associates with cholinergic cell density in Alzheimer's disease. Brain 145, 2869–2881. https://doi.org/10.1093/brain/awac093

Liu, Q., Zhu, Z., Teipel, S.J., Yang, J., Xing, Y., Tang, Y., Jia, J., 2017. White matter damage in the cholinergic system contributes to cognitive impairment in subcortical vascular cognitive impairment, no dementia. Front. Aging Neurosci. 9, 47. https://doi.org/10.3389/fnagi.2017.00047

Marcus, C., Mena, E., Subramaniam, R.M., 2014. Brain PET in the diagnosis of Alzheimer's disease. Clin. Nucl. Med. 39, e413–e426. https://doi.org/10.1097/RLU.0000000000000547

Markello, R.D., Spreng, R.N., Luh, W.M., Anderson, A.K., De Rosa, E., 2018. Segregation of the human basal forebrain using resting state functional MRI. Neuroimage 173, 287–297. https://doi.org/10.1016/j.neuroimage.2018.02.042

McKhann, G., Drachman, D., Folstein, M., Katzman, R., Price, D., Stadlan, E.M., 1984. Clinical diagnosis of alzheimer's disease: Report of the NINCDS-ADRDA work group⋆ under the auspices of department of health and human services task force on alzheimer's disease. Neurology 34, 939–944. https://doi.org/10.1212/wnl.34.7.939

McKhann, G.M., Knopman, D.S., Chertkow, H., Hyman, B.T., Jack, C.R., Kawas, C.H., Klunk, W.E., Koroshetz, W.J., Manly, J.J., Mayeux, R., Mohs, R.C., Morris, J.C., Rossor, M.N., Scheltens, P., Carrillo, M.C., Thies, B., Weintraub, S., Phelps, C.H., 2011. The diagnosis of dementia due to Alzheimer's disease: Recommendations from the National Institute on Aging-Alzheimer's Association workgroups on diagnostic guidelines for Alzheimer's disease. Alzheimer's Dement. 7, 263–269. https://doi.org/10.1016/j.jalz.2011.03.005

Mesulam, M., Shaw, P., Mash, D., Weintraub, S., 2004. Cholinergic nucleus basalis tauopathy emerges early in the aging-MCI-AD continuum. Ann. Neurol. 55, 815–828. https://doi.org/10.1002/ana.20100

Mesulam, M.M., 2013. Cholinergic circuitry of the human nucleus basalis and its fate in Alzheimer's disease. J. Comp. Neurol. 521, 4124–4144. https://doi.org/10.1002/cne.23415

Mesulam, M.M., 1976. A horseradish peroxidase method for the identification of the efferents of acetyl cholinesterase containing neurons. J. Histochem. Cytochem. 24, 1281–1285. https://doi.org/10.1177/24.12.826585

Mesulam, M.M., Geula, C., 1988. Nucleus basalis (Ch4) and cortical cholinergic innervation in the human brain: Observations based on the distribution of acetylcholinesterase and choline acetyltransferase. J. Comp. Neurol. 275, 216–240. https://doi.org/10.1002/cne.902750205

Mesulam, M.M., Mufson, E.J., Levey, A.I., Wainer, B.H., 1983. Cholinergic innervation of cortex by the basal forebrain: Cytochemistry and cortical connections of the septal area, diagonal band nuclei, nucleus basalis (Substantia innominata), and hypothalamus in the rhesus monkey. J. Comp. Neurol. 214, 170–197. https://doi.org/10.1002/cne.902140206

Mesulam, M.M., Mufson, E.J., Wainer, B.H., 1986. Three-dimensional representation and cortical projection topography of the nucleus basalis (Ch4) in the macaque: concurrent demonstration of choline acetyltransferase and retrograde transport with a stabilized tetramethylbenzidine method for horseradish p. Brain Res. 367, 301–308. https://doi.org/10.1016/0006-8993(86)91607-0

Mesulam, M.M., Van Hoesen, G.W., 1976. Acetylcholinesterase-rich projections from the basal forebrain of the rhesus monkey to neocortex. Brain Res. 109, 152–157. https://doi.org/10.1016/0006-8993(76)90385-1

Mewaldt, S.P., Ghoneim, M.M., 1979. The effects and interactions of scopolamine, physostigmine and methamphetamine on human memory. Pharmacol. Biochem. Behav. 10, 205–210. https://doi.org/10.1016/0091-3057(79)90088-1

Mitchell, A.J., Beaumont, H., Ferguson, D., Yadegarfar, M., Stubbs, B., 2014. Risk of dementia and mild cognitive impairment in older people with subjective memory complaints: Meta-analysis. Acta Psychiatr. Scand. 130, 439–451. https://doi.org/10.1111/acps.12336

Mohs, R.C., Knopman, D., Petersen, R.C., Ferris, S.H., Ernesto, C., Grundman, M., Sano, M., Bieliauskas, L., Geldmacher, D., Clark, C., Thal, L.J., 1997. Development of cognitive instruments for use in clinical trials of antidementia drugs: Additions to the Alzheimer's disease assessment scale that broaden its scope. Alzheimer Dis. Assoc. Disord. 11. https://doi.org/10.1097/00002093-199700112-00003

Mori, S., Crain, B.J., Chacko, V.P., Van Zijl, P.C.M., 1999. Three-dimensional tracking of axonal projections in the brain by magnetic resonance imaging. Ann. Neurol. 45, 265–269. https://doi.org/10.1002/1531-8249(199902)45:2<265::AID-ANA21>3.0.CO;2-3

Mori, S., Wakana, S., Van Zijl, P.C., Nagae-Poetscher, L., 2005. MRI atlas of human white matter. Elsevier, Amsterdam.

Mosconi, L., 2013. Glucose metabolism in normal aging and Alzheimer's disease: Methodological and physiological considerations for PET studies. Clin. Transl. Imaging 1, 217–233. https://doi.org/10.1007/s40336-013-0026-y

Mulugeta, E., Londos, E., Ballard, C., Alves, G., Zetterberg, H., Blennow, K., Skogseth, R., Minthon, L., Aarsland, D., 2011. CSF amyloid β38 as a novel diagnostic marker for dementia with Lewy bodies. J. Neurol. Neurosurg. Psychiatry 82, 160–164. https://doi.org/10.1136/jnnp.2009.199398

Nelson, P.T., Head, E., Schmitt, F.A., Davis, P.R., Neltner, J.H., Jicha, G.A., Abner, E.L., Smith, C.D., Van Eldik, L.J., Kryscio, R.J., Scheff, S.W., 2011. Alzheimer's disease is not "brain aging": Neuropathological, genetic, and epidemiological human studies. Acta Neuropathol. 121, 571–587. https://doi.org/10.1007/s00401-011-0826-y

Nemy, M., Cedres, N., Grothe, M.J., Muehlboeck, J.S., Lindberg, O., Nedelska, Z., Stepankova, O., Vyslouzilova, L., Eriksdotter, M., Barroso, J., Teipel, S., Westman, E., Ferreira, D., 2020. Cholinergic white matter pathways make a stronger contribution to attention and memory in normal aging than cerebrovascular health and nucleus basalis of Meynert. Neuroimage 211, 116607. https://doi.org/10.1016/j.neuroimage.2020.116607

Nemy, M., Dyrba, M., Brosseron, F., Buerger, K., Dechent, P., Dobisch, L., Ewers, M., Fliessbach, K., Glanz, W., Goerss, D., Heneka, M.T., Hetzer, S., Incesoy, E.I., Janowitz, D., Kilimann, I., Laske, C., Maier, F., Munk, M.H., Perneczky, R., Peters, O., Preis, L., Priller, J., Rauchmann, B.-S., Röske, S., Roy, N., Scheffler, K., Schneider, A., Schott, B.H., Spottke, A., Spruth, E.J., Wagner, M., Wiltfang, J., Yakupov, R., Eriksdotter, M., Westman, E., Stepankova, O., Vyslouzilova, L., Düzel, E., Jessen, F., Teipel, S.J., Ferreira, D., 2022. Cholinergic white matter pathways along the Alzheimer's disease continuum. Brain. https://doi.org/10.1093/brain/awac385

Nishioka, C., Liang, H.F., Barsamian, B., Sun, S.W., 2019. Amyloid-beta induced retrograde axonal degeneration in a mouse tauopathy model. Neuroimage 189, 180–191. https://doi.org/10.1016/j.neuroimage.2019.01.007

Nordberg, A., Rinne, J.O., Kadir, A., Lngström, B., 2010. The use of PET in Alzheimer disease. Nat. Rev. Neurol. 6, 78–87. https://doi.org/10.1038/nrneurol.2009.217

Nusbaum, M.P., 2008. Modulatory Projection Neurons, in: Encyclopedia of Neuroscience. Springer, Berlin, Heidelberg, pp. 2385–2388. https://doi.org/10.1007/978-3-540-29678-2_3538

Palmqvist, S., Schöll, M., Strandberg, O., Mattsson, N., Stomrud, E., Zetterberg, H., Blennow, K., Landau, S., Jagust, W., Hansson, O., 2017. Earliest accumulation of β-amyloid occurs within the default-mode network and concurrently affects brain connectivity. Nat. Commun. 8, 1–13. https://doi.org/10.1038/s41467-017-01150-x

Parikh, V., Kozak, R., Martinez, V., Sarter, M., 2007. Prefrontal Acetylcholine Release Controls Cue Detection on Multiple Timescales. Neuron 56, 141–154. https://doi.org/10.1016/j.neuron.2007.08.025

Passingham, R.E., 2013. What we can and cannot tell about the wiring of the human brain. Neuroimage 80, 14–17. https://doi.org/10.1016/j.neuroimage.2013.01.010

Patenaude, B., Smith, S.M., Kennedy, D.N., Jenkinson, M., 2011. A Bayesian model of shape and appearance for subcortical brain segmentation. Neuroimage 56, 907–22. https://doi.org/10.1016/j.neuroimage.2011.02.046

Pearson, J.M., Heilbronner, S.R., Barack, D.L., Hayden, B.Y., Platt, M.L., 2011. Posterior cingulate cortex:

Adapting behavior to a changing world. Trends Cogn. Sci. 15, 143–151. https://doi.org/10.1016/j.tics.2011.02.002

Pepeu, G., Grazia Giovannini, M., 2017. The fate of the brain cholinergic neurons in neurodegenerative diseases. Brain Res. 1670, 173–184. https://doi.org/10.1016/j.brainres.2017.06.023

Perrotin, A., Mormino, E.C., Madison, C.M., Hayenga, A.O., Jagust, W.J., 2012. Subjective cognition and amyloid deposition imaging: A Pittsburgh compound B positron emission tomography study in normal elderly individuals. Arch. Neurol. 69, 223–229. https://doi.org/10.1001/archneurol.2011.666

Petersen, R.C., 2004. Mild cognitive impairment as a diagnostic entity, in: Journal of Internal Medicine. J Intern Med, pp. 183–194. https://doi.org/10.1111/j.1365-2796.2004.01388.x

Petersen, R.C., 1977. Scopolamine induced learning failures in man. Psychopharmacology (Berl). 52, 283–289. https://doi.org/10.1007/BF00426713

Petrou, M., Frey, K.A., Kilbourn, M.R., Scott, P.J.H., Raffel, D.M., Bohnen, N.I., Müller, M.L.T.M., Albin, R.L., Koeppe, R.A., 2014. In vivo imaging of human cholinergic nerve terminals with (-)-5- 18F-fluoroethoxybenzovesamicol: Biodistribution, dosimetry, and tracer kinetic analyses. J. Nucl. Med. 55, 396–404. https://doi.org/10.2967/jnumed.113.124792

Preston, A.R., Eichenbaum, H., 2013. Interplay of hippocampus and prefrontal cortex in memory. Curr. Biol. 23. https://doi.org/10.1016/j.cub.2013.05.041

Raz, N., Yang, Y., Dahle, C.L., Land, S., 2012. Volume of white matter hyperintensities in healthy adults: Contribution of age, vascular risk factors, and inflammation-related genetic variants. Biochim. Biophys. Acta - Mol. Basis Dis. 1822, 361–369. https://doi.org/10.1016/j.bbadis.2011.08.007

Reber, P.J., Wong, E.C., Buxton, R.B., Frank, L.R., 1998. Correction of off resonance-related distortion in echo-planar imaging using EPI-based field maps. Magn. Reson. Med. 39, 328–330. https://doi.org/10.1002/mrm.1910390223

Reinert, J., Martens, H., Huettenrauch, M., Kolbow, T., Lannfelt, L., Ingelsson, M., Paetau, A., Verkkoniemi-Ahola, A., Bayer, T.A., Wirths, O., 2014. Aβ38 in the brains of patients with sporadic and familial Alzheimer's disease and transgenic mouse models. J. Alzheimer's Dis. 39, 871–881. https://doi.org/10.3233/JAD-131373

Reitan, R.M., 1958. Validity of the Trail Making Test as an Indicator of Organic Brain Damage. Percept. Mot. Skills 8, 271–276. https://doi.org/10.2466/pms.1958.8.3.271

Richter, N., Beckers, N., Onur, O.A., Dietlein, M., Tittgemeyer, M., Kracht, L., Neumaier, B., Fink, G.R., Kukolja, J., 2018. Effect of cholinergic treatment depends on cholinergic integrity in early Alzheimer's disease. Brain 141, 903–915. https://doi.org/10.1093/brain/awx356

Risacher, S.L., McDonald, B.C., Tallman, E.F., West, J.D., Farlow, M.R., Unverzagt, F.W., Gao, S., Boustani, M., Crane, P.K., Petersen, R.C., Jack, C.R., Jagust, W.J., Aisen, P.S., Weiner, M.W., Saykin, A.J., 2016. Association between anticholinergic medication use and cognition, brain metabolism, and brain atrophy in cognitively normal older adults. JAMA Neurol. 73, 721–732. https://doi.org/10.1001/jamaneurol.2016.0580

Robin, X., Turck, N., Hainard, A., Tiberti, N., Lisacek, F., Sanchez, J.C., Müller, M., 2011. pROC: An open-source package for R and S+ to analyze and compare ROC curves. BMC Bioinformatics 12, 77. https://doi.org/10.1186/1471-2105-12-77

Rydberg Sterner, T., Ahlner, F., Blennow, K., Dahlin-Ivanoff, S., Falk, H., Havstam Johansson, L., Hoff, M., Holm, M., Hörder, H., Jacobsson, T., Johansson, B., Johansson, L., Kern, J., Kern, S., Machado, A., Mellqvist Fässberg, M., Nilsson, J., Ribbe, M., Rothenberg, E., Rydén, L., Sadeghi, A., Sacuiu, S., Samuelsson, J., Sigström, R., Skoog, J., Thorvaldsson, V., Waern, M., Westman, E., Wetterberg, H., Zetterberg, H., Zetterberg, M., Zettergren, A., Östling, S., Skoog, I., 2019. The Gothenburg H70 Birth cohort study 2014–16: design, methods and study population. Eur. J. Epidemiol. 34, 191–209. https://doi.org/10.1007/s10654-018-0459-8

Sabri, O., Becker, G.A., Meyer, P.M., Hesse, S., Wilke, S., Graef, S., Patt, M., Luthardt, J., Wagenknecht, G., Hoepping, A., Smits, R., Franke, A., Sattler, B., Habermann, B., Neuhaus, P., Fischer, S., Tiepolt, S., Deuther-Conrad, W., Barthel, H., Schönknecht, P., Brust, P., 2015. First-in-human PET quantification

study of cerebral α4β2* nicotinic acetylcholine receptors using the novel specific radioligand (-)-[18F]Flubatine. Neuroimage 118, 199–208. https://doi.org/10.1016/j.neuroimage.2015.05.065

Sabri, O., Meyer, P.M., Gräf, S., Hesse, S., Wilke, S., Becker, G.A., Rullmann, M., Patt, M., Luthardt, J., Wagenknecht, G., Hoepping, A., Smits, R., Franke, A., Sattler, B., Tiepolt, S., Fischer, S., Deuther-Conrad, W., Hegerl, U., Barthel, H., Schönknecht, P., Brust, P., 2018. Cognitive correlates of α4β2 nicotinic acetylcholine receptors in mild Alzheimer's dementia. Brain 141, 1840–1854. https://doi.org/10.1093/brain/awy099

Salahudeen, M.S., Duffull, S.B., Nishtala, P.S., 2015. Anticholinergic burden quantified by anticholinergic risk scales and adverse outcomes in older people: A systematic review. BMC Geriatr. 15, 1–14. https://doi.org/10.1186/s12877-015-0029-9

Sassin, I., Schultz, C., Thal, D.R., Rüb, U., Arai, K., Braak, E., Braak, H., 2000. Evolution of Alzheimer's disease-related cytoskeletal changes in the basal nucleus of Meynert. Acta Neuropathol. 100, 259–269. https://doi.org/10.1007/s004019900178

Schilling, L.P., Zimmer, E.R., Shin, M., Leuzy, A., Pascoal, T.A., Benedet, A.L., Borelli, W.V., Palmini, A., Gauthier, S., Rosa-Neto, P., 2016. Imaging Alzheimer's disease pathophysiology with PET. Dement. Neuropsychol. 10, 79–90. https://doi.org/10.1590/S1980-5764-2016DN1002003

Schmitz, T.W., Nathan Spreng, R., 2016. Basal forebrain degeneration precedes and predicts the cortical spread of Alzheimer's pathology. Nat. Commun. 7, 1–13. https://doi.org/10.1038/ncomms13249

Schuhfried, G., 1992. Vienna reaction unit (manual). Schuhfried Ges. mbH, Mödling, Austria.

Schultz, S.A., Oh, J.M., Koscik, R.L., Dowling, N.M., Gallagher, C.L., Carlsson, C.M., Bendlin, B.B., LaRue, A., Hermann, B.P., Rowley, H.A., Asthana, S., Sager, M.A., Johnson, S.C., Okonkwo, O.C., 2015. Subjective memory complaints, cortical thinning, and cognitive dysfunction in middle-age adults at risk of AD. Alzheimer's Dement. Diagnosis, Assess. Dis. Monit. 1, 33–40. https://doi.org/10.1016/j.dadm.2014.11.010

Schulz, J., Pagano, G., Fernández Bonfante, J.A., Wilson, H., Politis, M., 2018. Nucleus basalis of Meynert degeneration precedes and predicts cognitive impairment in Parkinson's disease. Brain 141, 1501–1516. https://doi.org/10.1093/brain/awy072

Schumacher, J., Ray, N.J., Hamilton, C.A., Donaghy, P.C., Firbank, M., Roberts, G., Allan, L., Durcan, R., Barnett, N., O'brien, J.T., Taylor, J.P., Thomas, A.J., 2022. Cholinergic white matter pathways in dementia with Lewy bodies and Alzheimer's disease. Brain 145, 1773–1784. https://doi.org/10.1093/brain/awab372

Selden, N.R., Gitelman, D.R., Salamon-Murayama, N., Parrish, T.B., Mesulam, M.M., 1998. Trajectories of cholinergic pathways within the cerebral hemispheres of the human brain. Brain 121, 2249–2257. https://doi.org/10.1093/brain/121.12.2249

Serrano-Pozo, A., Qian, J., Monsell, S.E., Blacker, D., Gómez-Isla, T., Betensky, R.A., Growdon, J.H., Johnson, K.A., Frosch, M.P., Sperling, R.A., Hyman, B.T., 2014. Mild to moderate Alzheimer dementia with insufficient neuropathological changes. Ann. Neurol. 75, 597–601. https://doi.org/10.1002/ana.24125

Shinotoh, H., Hirano, S., Shimada, H., 2021. PET Imaging of Acetylcholinesterase, in: PET and SPECT of Neurobiological Systems. Springer, Cham, pp. 193–220. https://doi.org/10.1007/978-3-030-53176-8_7

Sittironnarit, G., Ames, D., Bush, A.I., Faux, N., Flicker, L., Foster, J., Hilmer, S., Lautenschlager, N.T., Maruff, P., Masters, C.L., Martins, R.N., Rowe, C., Szoeke, C., Ellis, K.A., 2011. Effects of anticholinergic drugs on cognitive function in older Australians: Results from the AIBL study. Dement. Geriatr. Cogn. Disord. 31, 173–178. https://doi.org/10.1159/000325171

Slot, R.E.R., Sikkes, S.A.M., Berkhof, J., Brodaty, H., Buckley, R., Cavedo, E., Dardiotis, E., Guillo-Benarous, F., Hampel, H., Kochan, N.A., Lista, S., Luck, T., Maruff, P., Molinuevo, J.L., Kornhuber, J., Reisberg, B., Riedel-Heller, S.G., Risacher, S.L., Roehr, S., Sachdev, P.S., Scarmeas, N., Scheltens, P., Shulman, M.B., Saykin, A.J., Verfaillie, S.C.J., Visser, P.J., Vos, S.J.B., Wagner, M., Wolfsgruber, S., Jessen, F., Boada, M., de Deyn, P.P., Jones, R., Frisoni, G., Spiru, L., Nobili, F., Freund-Levi, Y., Soininen, H., Verhey, F., Wallin, Å.K., Touchon, J., Rikkert, M.O., Rigaud, A.S., Bullock, R., Tsolaki, M., Vellas, B., Wilcock, G., Froelich, L., Bakardjian, H., Benali, H., Bertin, H., Bonheur, J., Boukadida, L., Boukerrou, N., Chiesa, P., Colliot, O., Dubois, B., Dubois, M., Epelbaum, S., Gagliardi, G., Genthon, R., Habert,

M.O., Houot, M., Kas, A., Lamari, F., Levy, M., Metzinger, C., Mochel, F., Nyasse, F., Poisson, C., Potier, M.C., Revillon, M., Santos, A., Andrade, K.S., Sole, M., Surtee, M., Thiebaud de Schotten, M., Vergallo, A., Younsi, N., van der Flier, W.M., 2019. Subjective cognitive decline and rates of incident Alzheimer's disease and non–Alzheimer's disease dementia. Alzheimer's Dement. 15, 465–476. https://doi.org/10.1016/j.jalz.2018.10.003

Smith, A., 1982. Symbol digit modality test (SDMT): manual (revised). Psychol. Serv. Los Angeles.

Stejskal, E.O., Tanner, J.E., 1965. Spin diffusion measurements: Spin echoes in the presence of a time-dependent field gradient. J. Chem. Phys. 42, 288–292. https://doi.org/10.1063/1.1695690

Strobl, C., Boulesteix, A.L., Zeileis, A., Hothorn, T., 2007. Bias in random forest variable importance measures: Illustrations, sources and a solution. BMC Bioinformatics 8. https://doi.org/10.1186/1471-2105-8-25

Stroop, J.R., 1935. Studies of interference in serial verbal reactions. J. Exp. Psychol. 18, 643–662. https://doi.org/10.1037/h0054651

Summers, W.K., Majovski, L.V., Marsh, G.M., Tachiki, K., Kling, A., 1986. Oral Tetrahydroaminoacridine in Long-Term Treatment of Senile Dementia, Alzheimer Type. N. Engl. J. Med. 315, 1241–1245. https://doi.org/10.1056/nejm198611133152001

Sun, X., Salat, D., Upchurch, K., Deason, R., Kowall, N., Budson, A., 2014. Destruction of white matter integrity in patients with mild cognitive impairment and Alzheimer disease. J. Investig. Med. 62, 927–933. https://doi.org/10.1097/JIM.0000000000000102

Teipel, S., Heinsen, H., Amaro, E., Grinberg, L.T., Krause, B., Grothe, M., 2014. Cholinergic basal forebrain atrophy predicts amyloid burden in Alzheimer's disease. Neurobiol. Aging 35, 482–491. https://doi.org/10.1016/j.neurobiolaging.2013.09.029

Teipel, S.J., Flatz, W., Ackl, N., Grothe, M., Kilimann, I., Bokde, A.L.W., Grinberg, L., Amaro, E., Kljajevic, V., Alho, E., Knels, C., Ebert, A., Heinsen, H., Danek, A., 2014. Brain atrophy in primary progressive aphasia involves the cholinergic basal forebrain and Ayala's nucleus. Psychiatry Res. - Neuroimaging 221, 187–194. https://doi.org/10.1016/j.pscychresns.2013.10.003

Teipel, S.J., Flatz, W.H., Heinsen, H., Bokde, A.L.W., Schoenberg, S.O., Stöckel, S., Dietrich, O., Reiser, M.F., Möller, H.J., Hampel, H., 2005. Measurement of basal forebrain atrophy in Alzheimer's disease using MRI. Brain 128, 2626–2644. https://doi.org/10.1093/brain/awh589

Teipel, S.J., Meindl, T., Grinberg, L., Grothe, M., Cantero, J.L., Reiser, M.F., Möller, H.-J.J., Heinsen, H., Hampel, H., 2011. The cholinergic system in mild cognitive impairment and Alzheimer's disease: an in vivo MRI and DTI study. Hum. Brain Mapp. 32, 1349–62. https://doi.org/10.1002/hbm.21111

Tiepolt, S., Meyer, P.M., Patt, M., Deuther-Conrad, W., Hesse, S., Barthel, H., Sabri, O., 2022. PET Imaging of Cholinergic Neurotransmission in Neurodegenerative Disorders. J. Nucl. Med. 63, 33S-44S. https://doi.org/10.2967/jnumed.121.263198

Tournier, J.D., Calamante, F., Gadian, D.G., Connelly, A., 2004. Direct estimation of the fiber orientation density function from diffusion-weighted MRI data using spherical deconvolution. Neuroimage 23, 1176–1185. https://doi.org/10.1016/j.neuroimage.2004.07.037

Tuch, D.S., 2002. Diffusion MRI of Complex Tissue Structure. Massachusetts Institute of Technology.

Villemagne, V.L., Burnham, S., Bourgeat, P., Brown, B., Ellis, K.A., Salvado, O., Szoeke, C., Macaulay, S.L., Martins, R., Maruff, P., Ames, D., Rowe, C.C., Masters, C.L., 2013. Amyloid β deposition, neurodegeneration, and cognitive decline in sporadic Alzheimer's disease: A prospective cohort study. Lancet Neurol. 12, 357–367. https://doi.org/10.1016/S1474-4422(13)70044-9

Viola, P., Wells, W.M., 1997. Alignment by Maximization of Mutual Information. Int. J. Comput. Vis. 24, 137–154. https://doi.org/10.1023/A:1007958904918

Wallace, T.L., Ballard, T.M., Pouzet, B., Riedel, W.J., Wettstein, J.G., 2011. Drug targets for cognitive enhancement in neuropsychiatric disorders. Pharmacol. Biochem. Behav. 99, 130–145. https://doi.org/10.1016/j.pbb.2011.03.022

Wang, L., Adeli, E., Wang, Q., Shi, Y., Suk, H.-I., 2016. Machine Learning in Medical Imaging.

Wardlaw, J.M., Smith, E.E., Biessels, G.J., Cordonnier, C., Fazekas, F., Frayne, R., Lindley, R.I., O'Brien, J.T., Barkhof, F., Benavente, O.R., Black, S.E., Brayne, C., Breteler, M., Chabriat, H., DeCarli, C., de Leeuw, F.E., Doubal, F., Duering, M., Fox, N.C., Greenberg, S., Hachinski, V., Kilimann, I., Mok, V., Oostenbrugge, R. van, Pantoni, L., Speck, O., Stephan, B.C.M., Teipel, S., Viswanathan, A., Werring, D., Chen, C., Smith, C., van Buchem, M., Norrving, B., Gorelick, P.B., Dichgans, M., 2013. Neuroimaging standards for research into small vessel disease and its contribution to ageing and neurodegeneration. Lancet Neurol. 12, 822–838. https://doi.org/10.1016/S1474-4422(13)70124-8

Wedeen, V.J., Hagmann, P., Tseng, W.Y.I., Reese, T.G., Weisskoff, R.M., 2005. Mapping complex tissue architecture with diffusion spectrum magnetic resonance imaging. Magn. Reson. Med. 54, 1377–1386. https://doi.org/10.1002/mrm.20642

Whitehouse, P.J., Price, D.L., Clark, A.W., Coyle, J.T., DeLong, M.R., 1981. Alzheimer disease: Evidence for selective loss of cholinergic neurons in the nucleus basalis. Ann. Neurol. 10, 122–126. https://doi.org/10.1002/ana.410100203

Wilkins, B., Lee, N., Gajawelli, N., Law, M., Leporé, N., 2015. Fiber estimation and tractography in diffusion MRI: Development of simulated brain images and comparison of multi-fiber analysis methods at clinical b-values. Neuroimage 109, 341–356. https://doi.org/10.1016/j.neuroimage.2014.12.060

Wiltfang, J., Esselmann, H., Bibl, M., Smirnov, A., Otto, M., Paul, S., Schmidt, B., Klafki, H.W., Maler, M., Dyrks, T., Bienert, M., Beyermann, M., Rüther, E., Kornhuber, J., 2002. Highly conserved and disease-specific patterns of carboxyterminally truncated Aβ peptides 1-37/38/39 in addition to 1-40/42 in Alzheimer's disease and in patients with chronic neuroinflammation. J. Neurochem. 81, 481–496. https://doi.org/10.1046/j.1471-4159.2002.00818.x

Winkler, A.M., Ridgway, G.R., Webster, M.A., Smith, S.M., Nichols, T.E., 2014. Permutation inference for the general linear model. Neuroimage 92, 381–397. https://doi.org/10.1016/j.neuroimage.2014.01.060

Winklewski, P.J., Sabisz, A., Naumczyk, P., Jodzio, K., Szurowska, E., Szarmach, A., 2018. Understanding the physiopathology behind axial and radial diffusivity changes-what do we know? Front. Neurol. 9, 92. https://doi.org/10.3389/fneur.2018.00092

Wolf, D., Grothe, M., Fischer, F.U., Heinsen, H., Kilimann, I., Teipel, S., Fellgiebel, A., 2014. Association of basal forebrain volumes and cognition in normal aging. Neuropsychologia 53, 54–63. https://doi.org/10.1016/j.neuropsychologia.2013.11.002

Wong, D.F., Kuwabara, H., Kim, J., Brašić, J.R., Chamroonrat, W., Gao, Y., Valentine, H., Willis, W., Mathur, A., McCaul, M.E., Wand, G., Gean, E.G., Dannals, R.F., Horti, A.G., 2013. PET imaging of high-affinity a4b2 nicotinic acetylcholine receptors in humans with 18F-AZAN, a radioligand with optimal brain kinetics. J. Nucl. Med. 54, 1308–1314. https://doi.org/10.2967/jnumed.112.108001

Wong, D.F., Kuwabara, H., Pomper, M., Holt, D.P., Brasic, J.R., George, N., Frolov, B., Willis, W., Gao, Y., Valentine, H., Nandi, A., Gapasin, L., Dannals, R.F., Horti, A.G., 2014. Human Brain Imaging of α7 nAChR with [18F]ASEM: a New PET Radiotracer for Neuropsychiatry and Determination of Drug Occupancy. Mol. Imaging Biol. 16, 730–738. https://doi.org/10.1007/s11307-014-0779-3

Woolf, N.J., 1991. Cholinergic systems in mammalian brain and spinal cord. Prog. Neurobiol. 37, 475–524. https://doi.org/10.1016/0301-0082(91)90006-M

World Health Organization, 1993. The ICD-10 classification of mental and behavioural disorders: Diagnostic criteria for research.

Zaborszky, L., Csordas, A., Mosca, K., Kim, J., Gielow, M.R., Vadasz, C., Nadasdy, Z., 2015. Neurons in the basal forebrain project to the cortex in a complex topographic organization that reflects corticocortical connectivity patterns: An experimental study based on retrograde tracing and 3D reconstruction. Cereb. Cortex 25, 118–137. https://doi.org/10.1093/cercor/bht210

Zaborszky, L., Hoemke, L., Mohlberg, H., Schleicher, A., Amunts, K., Zilles, K., 2008. Stereotaxic probabilistic maps of the magnocellular cell groups in human basal forebrain. Neuroimage 42, 1127–1141. https://doi.org/10.1016/j.neuroimage.2008.05.055

Zhang, B., Xu, Y., Zhu, B., Kantarci, K., 2014. The role of diffusion tensor imaging in detecting microstructural changes in prodromal Alzheimer's disease. CNS Neurosci. Ther. 20, 3–9. https://doi.org/10.1111/cns.12166

Zhang, H.Y., Wang, S.J., Xing, J., Liu, B., Ma, Z.L., Yang, M., Zhang, Z.J., Teng, G.J., 2009. Detection of PCC functional connectivity characteristics in resting-state fMRI in mild Alzheimer's disease. Behav. Brain Res. 197, 103–108. https://doi.org/10.1016/j.bbr.2008.08.012

Zhang, Y., Brady, M., Smith, S., 2001. Segmentation of brain MR images through a hidden Markov random field model and the expectation-maximization algorithm. IEEE Trans. Med. Imaging 20, 45–57. https://doi.org/10.1109/42.906424

Zhou, Y., Dougherty, J.H., Hubner, K.F., Bai, B., Cannon, R.L., Hutson, R.K., 2008. Abnormal connectivity in the posterior cingulate and hippocampus in early Alzheimer's disease and mild cognitive impairment. Alzheimer's Dement. 4, 265–270. https://doi.org/10.1016/j.jalz.2008.04.006

I

NeuroImage 211 (2020) 116607

Contents lists available at ScienceDirect

NeuroImage

journal homepage: www.elsevier.com/locate/neuroimage

Cholinergic white matter pathways make a stronger contribution to attention and memory in normal aging than cerebrovascular health and nucleus basalis of Meynert

Milan Nemy [a], Nira Cedres [b,c], Michel J. Grothe [d], J-Sebastian Muehlboeck [b], Olof Lindberg [b], Zuzana Nedelska [e,f], Olga Stepankova [g], Lenka Vyslouzilova [g], Maria Eriksdotter [b,h], José Barroso [c], Stefan Teipel [d,i], Eric Westman [b,j], Daniel Ferreira [b,c,*]

[a] Department of Cybernetics, Faculty of Electrical Engineering, Czech Technical University, Prague, Czech Republic
[b] Division of Clinical Geriatrics, Center for Alzheimer Research, Department of Neurobiology, Care Sciences and Society, Karolinska Institutet, Stockholm, Sweden
[c] Faculty of Psychology, University of La Laguna, La Laguna, Tenerife, Spain
[d] Clinical Dementia Research Section, German Center for Neurodegenerative Diseases (DZNE), Rostock, Germany
[e] Memory Clinic, Department of Neurology, Charles University, 2nd Faculty of Medicine and Motol University Hospital, Prague, Czech Republic
[f] Department of Radiology, Mayo Clinic, Rochester, MN, USA
[g] Czech Institute of Informatics, Robotics, and Cybernetics, Czech Technical University, Prague, Czech Republic
[h] Theme Aging, Karolinska University Hospital, Stockholm, Sweden
[i] Department of Psychosomatic Medicine, University Medicine Rostock, Rostock, Germany
[j] Department of Neuroimaging, Centre for Neuroimaging Sciences, Institute of Psychiatry, Psychology, and Neuroscience, King's College London, London, UK

ARTICLE INFO

Keywords:
Cholinergic system
Basal forebrain
Normal aging
Small vessel disease
Cognition
Magnetic resonance imaging

ABSTRACT

The integrity of the cholinergic system plays a central role in cognitive decline both in normal aging and neurological disorders including Alzheimer's disease and vascular cognitive impairment. Most of the previous neuroimaging research has focused on the integrity of the cholinergic basal forebrain, or its sub-region the nucleus basalis of Meynert (NBM). Tractography using diffusion tensor imaging data may enable modelling of the NBM white matter projections. We investigated the contribution of NBM volume, NBM white matter projections, small vessel disease (SVD), and age to performance in attention and memory in 262 cognitively normal individuals (39–77 years of age, 53% female). We developed a multimodal MRI pipeline for NBM segmentation and diffusion-based tracking of NBM white matter projections, and computed white matter hypointensities (WM-hypo) as a marker of SVD. We successfully tracked pathways that closely resemble the spatial layout of the cholinergic system as seen in previous post-mortem and DTI tractography studies. We found that high WM-hypo load was associated with older age, male sex, and lower performance in attention and memory. A high WM-hypo load was also associated with lower integrity of the cholinergic system above and beyond the effect of age. In a multivariate model, age and integrity of NBM white matter projections were stronger contributors than WM-hypo load and NBM volume to performance in attention and memory. We conclude that the integrity of NBM white matter projections plays a fundamental role in cognitive aging. This and other modern neuroimaging methods offer new opportunities to re-evaluate the cholinergic hypothesis of cognitive aging.

1. Introduction

Cholinergic neurons in the central nervous system provide vital control over brain circuitry responsible for cognitive functions such as memory and attention. Since its discovery, the cholinergic circuitry of the basal forebrain (BF) has been scrutinized for its possible involvement in cognitive decline characteristic of aging and age-related disorders including Alzheimer's disease (AD) and vascular cognitive impairment (Bartus et al., 1982; Drachman and Leavitt, 1974). Most of the cholinergic neurons are located in the BF nuclei (Ch1-4), as well as in the

* Corresponding author. Division of Clinical Geriatrics, Center for Alzheimer Research, Department of Neurobiology, Care Sciences and Society, NEO floor 7th, Karolinska Institutet, 141 57, Huddinge, Stockholm, Sweden.
E-mail address: daniel.ferreira.padilla@ki.se (D. Ferreira).

https://doi.org/10.1016/j.neuroimage.2020.116607
Received 25 November 2019; Received in revised form 23 January 2020; Accepted 3 February 2020
Available online 6 February 2020

pedunculo-pontine and laterodorsal tegmental nuclei in the brainstem (Ch5-6). All these regions serve together as the major sources of cholinergic projection neurons to the entire neocortex, amygdala, thalamus, and hippocampus (Mesulam et al., 1983; Woolf, 1991). However, it is the cholinergic neurons located in the nucleus basalis of Meynert (NBM, Ch4) that provide the major cholinergic input to cortical areas, and have stronger involvement in cognition.

The identification of the cholinergic cell bodies that innervate the cerebral cortex was made possible by visualization of the hydrolytic enzyme acetylcholinesterase (AChE) (Mesulam and Van Hoesen, 1976) and by immunolabeling with the synthetic enzyme of acetylcholine, choline acetyltransferase (ChAT) (Mesulam et al., 1986). More recently, magnetic resonance imaging (MRI) has been used to investigate the characteristics of the cholinergic BF *in vivo* using automated volumetric measurements of the BF structure. *In vivo* measurement of the BF has been facilitated through the development of stereotactic mappings of the cholinergic BF nuclei in MRI standard space based on cytoarchitectonic maps derived from combined histology and *post-mortem* MRI of autopsy brains (Kilimann et al., 2014; Teipel et al., 2005; Zaborszky et al., 2008). Using these cytoarchitectonic mappings as BF region of interest (ROI), a number of volumetric *in vivo* studies have shown BF atrophy in advanced aging (Grothe et al., 2013, 2012), AD dementia (Teipel et al., 2011, 2005), and mild cognitive impairment (MCI) (Grothe et al., 2010; Teipel et al., 2014). These studies could also demonstrate robust associations of BF atrophy with cognitive deficits in neurodegenerative diseases (Grothe et al., 2010, 2016), but findings on the relationship between BF structure and cognitive performance in normal aging remain inconclusive (Butler et al., 2012; Lammers et al., 2018, 2016; Wolf et al., 2014).

The cholinergic white matter (WM) projections from the NBM to the entire brain have been less widely investigated. A seminal *post mortem* study using AChE and ChAT cholinergic markers in whole-hemisphere sections identified two major cholinergic pathways, i.e. medial and lateral, passing from the NBM to the cortex (Selden et al., 1998). The medial pathway joins the WM of the gyrus rectus, curves around the rostrum to the corpus callosum, and enters the cingulum bundle, supplying the parolfactory, cingulate, and retrosplenial cortices. The lateral pathway has a perisylvian division which supplies the frontoparietal operculum, insula, and superior temporal gyrus, and a capsular division traveling in the external capsule and uncinate fasciculus, supplying the remaining parts of the frontal, parietal, and temporal neocortex. However, the precise topography of the NBM cholinergic projections to the cerebral cortex is yet unknown. MRI techniques based on resting-state functional MRI (rs-fMRI) and diffusion tensor imaging (DTI) could provide further information on the NBM cholinergic pathways *in vivo*. The rs-fMRI technique measures the spontaneous blood oxygenation level-dependent (BOLD) signal in the absence of any explicit task. This technique was recently used to investigate coordinated signal fluctuations between the BF and the cortex, revealing distinct functional connectivity patterns of the BF (Fritz et al., 2019). DTI is commonly used to assess WM microstructural integrity. Previous voxel-based DTI studies showed an association between reduced NBM volume and reduced integrity across widespread WM areas, possibly involving NBM cholinergic tracts as well (Teipel et al., 2014, 2011). Unlike voxel-based DTI analysis, probabilistic tracking can in principle reveal WM pathways connected to specific regions such as the NBM, thus providing information on cholinergic NBM WM projections in a probabilistic manner.

So far only one study used DTI to track the NBM cholinergic pathways. This study included a cohort of 25 patients with vascular cognitive impairment and 24 healthy controls (Liu et al., 2017), and showed that vascular cognitive impairment was associated with reduced integrity of NBM pathways, but not with NBM volume per se. WM hyperintensities on T2/FLAIR sequences, which appear as WM hypointensities on T1-weighted images (Wardlaw et al., 2013), are the main MRI finding associated with vascular cognitive impairment. Interestingly, WM hyperintensities are also commonly found in cognitively normal individuals (Gunning-Dixon et al., 2009), and are related to lower cognitive performance and subjective cognitive complaints in these individuals (Cedres et al., 2019; Hawkins et al., 2017; Nunley et al., 2015). These and other findings highlight the role of cerebral small vessel disease (SVD) in cognitive aging (Yang et al., 2017). Of interest, several lines of evidence suggest a central role of cholinergic deficiency in vascular cognitive impairment (Liu et al., 2017). However, the connection between SVD and cholinergic dysfunction to explain age-related cognitive decline is still unclear. The cholinergic hypothesis of cognitive aging postulates that functional disturbances in cholinergic activity occur in the brains of healthy older adults, contributing to their characteristic memory decline and related cognitive problems (Bartus et al., 1982; Dumas and Newhouse, 2011). Hence, we aimed to investigate the contribution of SVD and the integrity of the cholinergic system towards cognitive performance in cognitively normal middle-aged and older individuals. Our first aim was to identify NBM WM projections by using DTI tractography in a large cohort of cognitively normal individuals (N = 262, 39–77 years of age). We report constrained DTI tractography models guided by the findings of the only previous study in the field (Liu et al., 2017). In addition, we report unconstrained models to examine other potential cholinergic projections in an exploratory manner. Our second aim was to investigate the association of SVD (WM hypointensities) with the integrity of the cholinergic system and cognitive functions known to be mediated by the cholinergic circuitry, specifically, attention and memory (Ballinger et al., 2016). Because the effect of aging is central in this study, we report our findings in a stepwise manner: without any correction, with a correction for the effect of sex and crystallised intelligence, and with a correction for the effect of age on top of the previous correction. This strategy enables an easy and direct understanding of the role of the age variable in all our models. In addition, we also modelled the effect of age in multivariate models.

2. Materials and methods

2.1. Participants

A total of 262 individuals (39–77 years of age) were selected from the GENIC-database (Ferreira et al., 2014; Machado et al., 2018), a community-based cohort from the Canary Islands (Spain). Inclusion criteria for the current study were: (1) Normal cognitive performance in comprehensive neuropsychological assessment using pertinent clinical normative data and excluding individuals with performance below 2 SD using own sample descriptive values (i.e., individuals did not fulfil cognitive criteria for MCI or dementia); (2) preserved activities of daily living and global cognition operationalized as a Functional Activity Questionnaire (FAQ) (Pfeffer et al., 1982) score $\leq$ 5, a Blessed Dementia Rating Scale (BDRS) (Blessed et al., 1968) score $\leq$ 4, and a Mini-Mental State Examination (MMSE) (Folstein et al., 1975) score $\geq$ 24 (the MMSE cut-point of $\geq$24 is used for screening according to the demographic characteristics of our cohort, but cognitive impairment is ruled out using comprehensive neuropsychological assessment as described in criterion #1 above); (3) Availability of MRI data; (4) No abnormal findings such as stroke, tumors, hippocampal sclerosis, etc., in MRI according to an experienced neuroradiologist; (5) no medical history of neurological or psychiatric disorders (including a diagnosis of major depression), systemic diseases or head trauma; and (6) no history of substance abuse. Subjects' recruitment in the GENIC-database was done through primary care health centers, advertisements in local schools, and relatives and acquaintances of the research staff, covering a representative sample in terms of age, sex, and education. Participation was completely voluntary and all the participants gave written informed consent approved by the local ethics committee.

2.2. Clinical and cognitive assessment

From an extensive neuropsychological protocol fully described elsewhere (Ferreira et al., 2015), the following tests of memory and attention

were selected according to the aims of the current study: TAVEC (Benedet MJ, 1998), the Spanish version of the California Verbal Learning Test (CVLT), was used to measure verbal episodic memory. We included the total learning score after 5 learning trials, delayed recall after 5 min, delayed recall after 30 min, and recognition (higher values reflect better performance). Attention was measured with the first sheet (words) of the Stroop test (Stroop, 1935), as well as the Choice Reaction Times task of the PC-Vienna System (PCV – reaction time) (Schuhfried, 1992). The Stroop test – first sheet is a verbal task with higher demands on focussed attention, whereas the Choice Reaction Times is a visual task with higher demands on vigilance. For the Stroop test, participants were given 45 s to complete the task and the score obtained was the total number of words correctly read (higher values reflect better performance). For Choice Reaction Times, participants underwent a 15-min computerised vigilance task in which a response is required when a specific stimulus is displayed. Time is recorded, with higher time values and errors denoting worse performance. Both Stroop and PCV are also common tests for processing speed. Stroop is also a traditional measure for executive functioning, and PCV includes a component of motor inhibition. Depressive symptomatology was assessed with the Beck Depression Inventory (BDI, 21-item version) (Beck et al., 1961) in individuals younger than 63 years of age, and the Geriatric Depression Scale (GDS, 15-item version) (Yesavage and Sheikh, 1986) in individuals 63 years old or older. The original scores from both scales were z-transformed and combined into a single measure (BDI-GDS composite), as in previous studies (Machado et al., 2018). The Information subtest from the Wechsler Adult Intelligence Scale – Third Revision (WAIS-III) (Wechsler, 1997) was scored and used as an indicator of crystallised intelligence. In addition, global cognition was assessed with the MMSE (Folstein et al., 1975), and activities of daily living with the FAQ and the BDRS (Blessed et al., 1968).

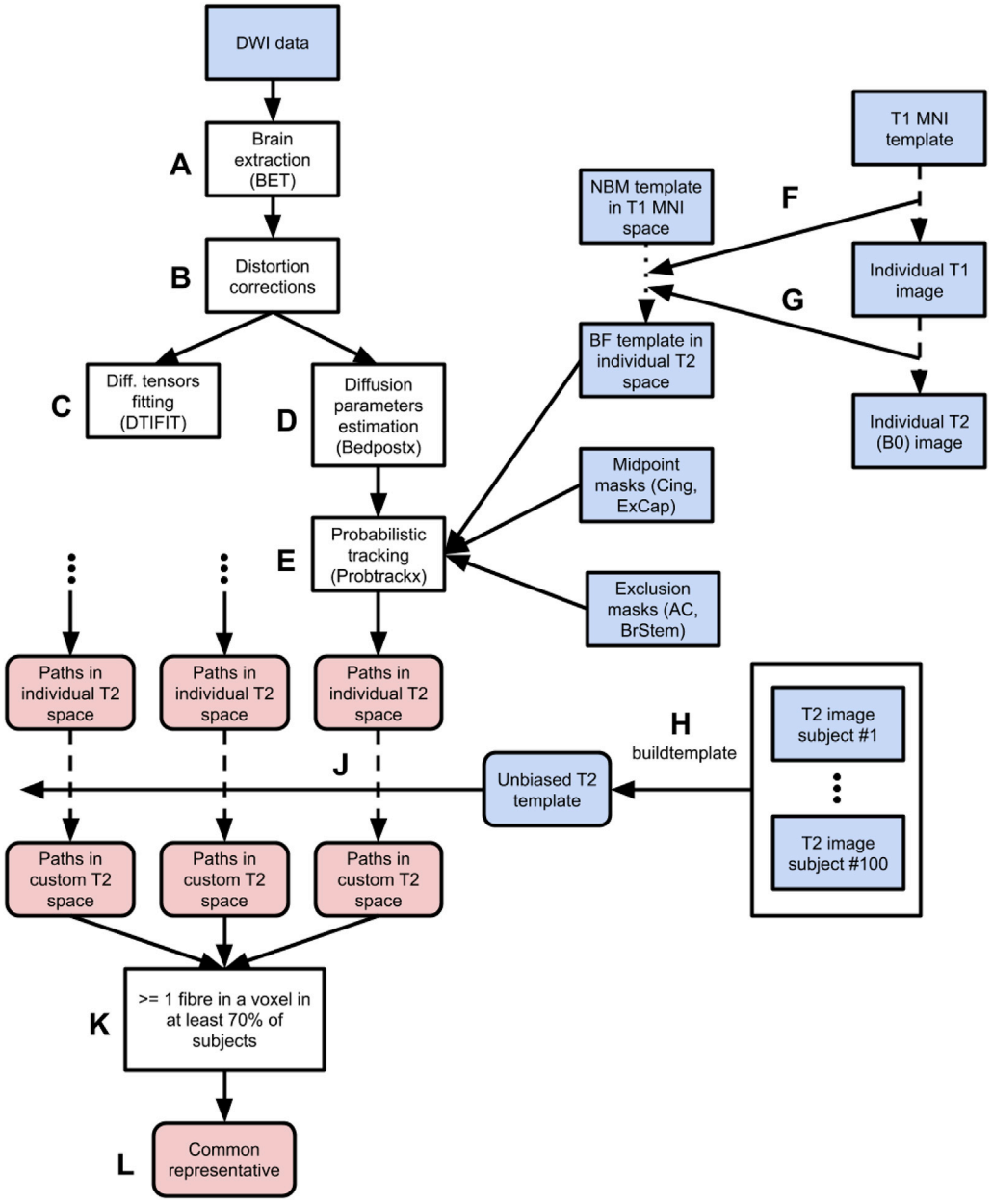

Fig. 1. Study pipeline. White boxes, programs and processes; Blue boxes, T1 and T2 images; Red boxes, tracts. DWI, diffusion-weighted imaging; NBM, nucleus basalis of Meynert; MNI, Montreal Neurological Institute; AC, anterior commissure; BrStem, brain stem. T2 images are B0 images (DWI b = 0). The I letter was intentionally omitted to improve readability.

2.3. MRI acquisition

Participants were scanned using a 3.0 T GE imaging system (General Electric, Milwaukee, WI, USA) located at the *Hospital Universitario de Canarias* in Tenerife, Spain. A three-dimensional T1-weighted fast spoiled gradient echo (FSPGR) sequence was acquired in the sagittal plane with the following parameters: repetition time/echo time = 8.73/1.74 ms, inversion time = 650 ms, field of view 250 × 250 mm, matrix 250 × 250 mm, flip angle 12°, slice thickness = 1 mm. A DTI sequence was acquired in the axial plane. The parameters were as follows: repetition time/echo time = 15000/≈72 ms, field of view 256 × 256 mm, matrix 128 × 128 mm, flip angle 90°, slice thickness = 2.4 mm, 31 isotropically distributed gradient orientations (b = 1000 s/mm^2), and 1 image without diffusion weighting (b = 0 s/mm^2, b0). Full brain and skull coverage was required for the MRI datasets and detailed quality control was carried out on all MR images according to previously published criteria (Simmons et al., 2009).

The whole processing pipeline for the MRI data is shown in Fig. 1 and is explained in detail in the next sections.

2.4. MRI data pre-processing

The DTI data were processed using the FSL toolbox (version 5.0.9, FMRIB, Oxford, UK) (Jenkinson et al., 2012). First, the non-brain tissues were removed using FSL's automated brain extraction tool (Jenkinson et al., 2005) (BET, Fig. 1A) and corrected for eddy currents and head motion (Andersson and Sotiropoulos, 2016) (Fig. 1B), followed by fitting of diffusion tensors (Fig. 1C). Next, the algorithm implemented in FSL (BedpostX) was used to calculate the diffusion parameters in a standard ball-and-sticks model (Behrens et al., 2007) for each voxel (Fig. 1D), considering 3 fibres modelled per voxel.

2.5. ROI masks and tractography

Six ROI masks were used in this study: an ROI mask of the NBM was used as the initiating seed region for probabilistic tracking; cingulum and external capsule ROI masks as midway regions for the constrained tractography model (see next paragraph); ROI masks of the anterior commissure and brainstem were used as exclusion masks in both constrained and unconstrained models (see next paragraph); and finally, an ROI of remaining WM (please see below) as a negative control mask. The NBM ROI was based on a cytoarchitectonic map of BF cholinergic nuclei in MNI space, derived from combined histology and *in cranio* MRI of a *post-mortem* brain (Kilimann et al., 2014). We obtained the NBM ROI by combining the anterior lateral, intermediate, and posterior regions of the Ch4 region of the BF mask (Kilimann et al., 2014). The cingulum and external capsule masks were based on the Johns Hopkins University (JHU) WM atlas, available as part of the FSL package (Mori et al., 2005). The cingulum and external capsule masks were also used in the previous study by Liu et al. (2017), to constrain the NBM WM tracts. The brainstem ROI mask was extracted using FSL's FIRST segmentation routine (Patenaude et al., 2011). The anterior commissure ROI mask was delineated in the MNI template by a trained expert (O.L.). The remaining WM mask was created by excluding the cholinergic tracts described below (i.e. union of external capsule and cingulum pathways) from the whole WM mask. The whole WM mask was obtained from the FSL's Automated Segmentation Tool (FAST) (Zhang et al., 2001). These six ROI masks were registered into each subject's individual space. For this purpose, the registration parameters from individual T1 space to standard T1 MNI space were inversely applied to the NBM, anterior commissure, and brainstem masks (Fig. 1F), following registration to native diffusion space (Fig. 1G). For the cingulum and external capsule ROI masks defined in a standard space DTI template, the registration parameters of an individual DTI image (B0 image) to the standard DTI template were inversely applied to register the masks from standard space to native space. All registration steps (T1 -> T1-MNI and DTI -> DTI-MNI) were carried out using the non-linear SyN registration algorithm (Avants et al., 2008) in Advanced Normalization Tools (ANTs, http://stnava.github.io/ANTs/).

Probabilistic tracking was performed by repeating 5000 random samples from each of the NBM ROI voxels and propagated through the local probability density functions of the estimated diffusion parameters (Fig. 1E). This procedure was performed in two manners: (1) a constrained manner, in which only those streamlines initiated from the NBM ROI that reach a voxel in midway cingulum or external capsule ROI masks were retained. The aim of conducting these models was to reconstruct the two major NBM cholinergic pathways projecting through the cingulum and the external capsule (Liu et al., 2017; Selden et al., 1998); (2) an unconstrained explorative manner, with streamlines initiating in the NBM and propagating across the brain with no midway constrains other than the exclusion anterior commissure and brainstem ROI masks, to avoid contamination from non-cholinergic pathways going through the anterior commissure as well as connecting to the cerebellum and medulla. The brainstem contribution to cortical cholinergic innervation is small (Mesulam, 2013). The aim of conducting this unconstrained model was to explore potential cholinergic projections not covered by the constrained model. The anterior commissure and brainstem exclusion masks were also used for the constrained models.

2.6. Common pathways

Individually tracked pathways were brought to a common space to be able to compare them across individuals. For this purpose, an unbiased template was created from 100 randomly selected pre-processed B0 images using the *buildtemplate* module in ANTs (Fig. 1H). Briefly, the initial template was obtained by taking the average of all 100 image volumes. Each image volume was then co-registered to the initial template and the average was calculated again to obtain a refined template. This process continued for 4 iterations using the non-linear registration algorithm SyN (Avants et al., 2008). The template obtained is referred to as the unbiased template. Next, warping fields co-aligning individual input B0 images to the unbiased template were used to translate the individual tracking results to the same anatomical space (Fig. 1J).

We derived a *common representative* for each tract, similar to that done in previous studies (de Reus and van den Heuvel, 2013; Liu et al., 2017). This procedure consists in thresholding all individual tracts (in the space of the unbiased template) so that only those voxels that were met by at least one tracked fibre (i.e. threshold $\geq$1) were counted (de Reus and van den Heuvel, 2013). Then, all these thresholded individual images were considered and only the voxels that were present in at least 70% of the (thresholded) cases (Fig. 1K) were retained in the final binary mask of the common representative tract (Liu et al., 2017) (Fig. 1L). The group threshold was chosen by visual inspection so that the resulting pathways were extensive, yet still specific. In contrast to (Liu et al., 2017), we did not restrict the final masks to skeletonized pathways because our aim was to identify NBM WM projections beyond and above the WM skeleton; and we used a non-linear registration tool due to the small size of the NBM. The methodological differences with de Reus and van den Heuvel (2013) are that we investigated cholinergic pathways based on probabilistic tractography, whereas de Reus and van den Heuvel (2013) used whole-brain networks based on deterministic tractography.

2.7. Extraction of diffusivity indices

To characterize the microstructure properties of the tracked cholinergic pathways, we extracted the mean diffusivity (MD) index. The MD index is sensitive to conditions that affect the barriers that restrict the movement of water, such as cell membranes (Zhang et al., 2014). We selected the MD index because it has been shown to precede changes in other DTI indexes (e.g. fractional anisotropy), as well as in the gray matter volume in pre-symptomatic individuals with familial AD (Li et al., 2015), preclinical individuals with sporadic AD (Li et al., 2014), and

individuals with AD (Acosta-Cabronero et al., 2010). Also, increased MD in the cingulum and inferior fronto-occipital fasciculus was associated with lower performance in several visual abilities of the posterior cortex in cognitively normal middle-aged individuals from the same cohort as used in the current study (Ferreira et al., 2017). Further, MD is less susceptible than fractional anisotropy to alterations due to different fibre populations in individual voxels (i.e. the crossing fibres problem). For the sake of simplicity, all representative tracts were back-transformed into individual DTI space for each subject and single number summaries were computed - an average value of MD along each representative tract. The same procedure was applied to the negative control remaining WM mask.

2.8. NBM volume

Individual NBM volumes were calculated by summing up the number of gray matter (GM) voxels within the back-transformed NBM ROI in each individual's native T1-weighted space. GM segmentation was obtained from the FSL's Automated Segmentation Tool (Zhang et al., 2001) (FAST). The total intracranial volume (TIV) was estimated based on the affine transform in the FreeSurfer 5.1.0 image analysis suite (http://surfer.nmr.mgh.harvard.edu/). NBM volumes were divided by the TIV in order to account for between-subjects variability in head size (Buckner et al., 2004).

2.9. WM hypointensities (WM-hypo)

We used WM hypointensities (WM-hypo) as a marker of SVD (Wardlaw et al., 2013). WM-hypo on T1-weighted images appear as WM hyperintensities on T2/FLAIR sequences (Wardlaw et al., 2013), and correlate with microstructural WM changes as measured on diffusion tensor imaging data (Leritz et al., 2014). Further, there is a strong correlation between WM-hypo and WM hyperintensities (Cedres et al., 2020). Segmentation of WM-hypo and corresponding volumetrics was performed on T1-weighted images using the probabilistic procedure implemented in FreeSurfer 5.1.0, subsequently extended to label WM lesions (Brands et al., 2006; Fischl et al., 2002). This procedure has demonstrated good sensitivity in measuring WM damage both in healthy individuals and in AD patients (Leritz et al., 2014; Salat et al., 2010).

2.10. Statistical analysis

Statistical analysis was carried out using the R programming language (The R Foundation for Statistical Computing; version 3.5.1). Results were deemed statistically significant at two-tailed $p < 0.05$.

Because our aim was to investigate the role of SVD, we used Gaussian mixture model estimated by expectation-maximization algorithm to identify two groups with respect to the WM-hypo load (high WM-hypo and low WM-hypo load) (Fig. 2). Demographics were compared between the high and low WM-hypo load groups using independent *t*-tests for age and Chi-square tests for sex. All cognitive measures were compared between groups in a one-way analysis of variance with covariates (ANCOVA), controlling for age, sex, and WAIS-III Information. For a better understanding of the role of these variables in our findings, in particular the role of the age variable, we report the outcome of these analyses in a stepwise manner: without any correction, with a correction for the effect of sex and WAIS-III Information as a measure of crystallised intelligence, and with a correction for the effect of age on top of the previous correction. The extracted NBM volume corrected for the TIV was also compared using ANCOVA, controlling for age, sex, and WAIS-III Information (stepwise manner). To assess whether SVD influences tract integrity, ANCOVA was applied to test for differences between high and low WM-hypo load groups in tract-specific MD measures, controlling for age, sex, and WAIS-III Information (stepwise manner). The degree of contribution of age, sex, WAIS-III Information, MD in the cingulum, external capsule tracts and in the remaining WM, NBM volume, WM-hypo, and MMSE scores to domain-specific cognitive measures was

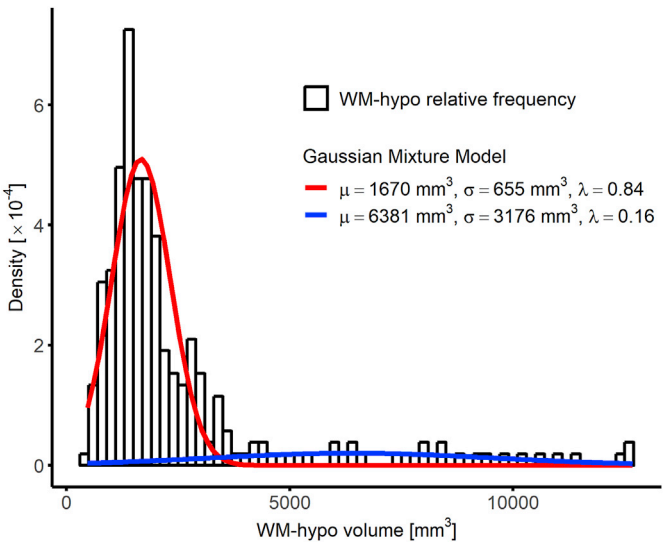

Fig. 2. Gaussian mixture model fit to separate the cohort into two groups of high and low WM-hypo load. Mixture components are characterized by Gaussian distribution with a mean value μ and a standard deviation σ; λ is a mixture weight. The intersection of the two scaled probability distribution functions (WM-hypo = 3400 mm^3) defines the threshold between the low and high WM-hypo load groups. WM-hypo, WM hypointensities on T1-weighted images appearing as WM hyperintensities on T2/FLAIR sequences (Wardlaw et al., 2013).

investigated with random forest analysis. We used random forest regression (with conditional inference tree for unbiased variable selection) instead of multiple linear regression/mediation analyses because we wanted to investigate the interactive contribution of the predictors, rather than partial effects (Machado et al., 2018). Random forest (RF) is an ensemble method in machine learning that involves growing of multiple decision trees via bootstrap aggregation (bagging). Each tree predicts a classification independently and votes for the corresponding class. The majority of the votes decides the overall prediction (Breiman, 2001, 1996). Conditional feature importance scores for random forest were computed by measuring the increase in prediction error if the values of a variable under question are permuted within a grid defined by the covariates that are associated to the variable of interest. This score is computed for each constituent tree, averaged across the entire ensemble. The conditional feature importance scores were designed to diminish an undesirable effect of preference of correlated predictor variables. The random forest was comprised of 2000 conditional inference trees. The *party* package (Strobl et al., 2007) was used in this analysis. For the sake of completeness, we also report Pearson correlation coefficients among the variables included in the random forest analysis (the point-biserial correlation coefficient was computed for the dummy variable of sex).

2.11. Data and code availability

Requests for access to the data and code used in this study should be directed to the corresponding author. Our data sharing complies with the requirements of our funders and institutes, as well as with institutional ethics approval.

3. Results

3.1. Association between WM-hypo, demographic variables and cognitive performance

Demographic data are shown in Table 1. The high WM-hypo load group was significantly older, included a higher frequency of men, had higher values in the BDRS score, and showed worse cognitive

Table 1

Demographic and clinical variables by WM-hypo load groups [mean value (SD), or count]. For age, an independent *t*-test was performed ($df = 48$; equal variances not assumed). For sex, a chi-square test was performed. For all other variables, one-way ANCOVA were performed by setting the group (low/high WM-hypo load) as the independent variable and WAIS-III Information, age, and sex as covariates ($df = 1, 260$). Since depressive symptomatology was measured with BDI or GDS, original scores were Z-transformed in order to combine both measures (BDI-GDS composite). *$p < 0.05$, **$p < 0.01$, ***$p < 0.001$ (assessed using a two-tailed alpha). M, male; F, female; WAIS-III, Wechsler Adult Intelligence Scale – Third revision; BDRS, Blessed Dementia Rating Scale; FAQ, Functional Activity Questionnaire; GDS, Geriatric Depression Scale; BDI, Beck Depression Inventory; MMSE, Mini-Mental State Examination; PCV – reaction time, PC-Vienna cognitive reactive time; TAVEC, the Spanish version of the California Verbal Learning Test (CVLT) (TAVEC: *Test de Aprendizaje Verbal España-Complutense*); NBM volume, volume of nucleus basalis of Meynert; TIV, total intracranial volume; WM-hypo, WM hypointensities on T1-weighted images appearing as WM hyperintensities on T2/FLAIR sequences (Wardlaw et al., 2013).

	Entire cohort	Low WM-hypo load group	High WM-hypo load group	$t/\chi^2/F_{1,260}$ (no correction)	$F_{1,258}$ (corrected for sex and WAIS-III Information)	$F_{1,257}$ (corrected for sex, WAIS-III Information, and age)
Count, n	262	226	36			
Age	55.6 (10.4)	53.9 (9.54)	65.2 (8.9)	−7.1***		
Sex (M/F)	122/140	97/129	25/11	8.8**		
WAIS-III Information	16.6 (5.9)	16.6 (5.9)	16.5 (5.9)	0.1		
BDRS	0.9 (1.5)	0.8 (1.3)	1.4 (2.15)	4.3*	3.6	1.6
FAQ	0.4 (0.8)	0.4 (0.8)	0.4 (0.6)	0.1	0.4	0.4
BDI-GDS composite	0 (1)	−0.04 (0.92)	0.15 (1.32)	1.2	1.6	1.3
MMSE	28.8 (1.3)	28.8 (1.2)	28.5 (1.4)	2.0	0.5	0.3
PCV – reaction time	476 (82.1)	471.0 (74.8)	511.0 (111.0)	7.9**	7.2**	0.0
STROOP – words	99.5 (18.9)	99.9 (18.6)	97.5 (21.2)	0.5	0.3	1.4
TAVEC learning	55.3 (9.1)	56.0 (9.2)	51.8 (7.4)	6.7*	2.8	0.2
TAVEC delayed recall (5 min)	11.6 (2.8)	11.8 (2.7)	10.4 (2.6)	8.8**	4.6*	0.1
TAVEC delayed recall (30 min)	13.6 (2.5)	13.8 (2.5)	12.7 (2.3)	6.8**	3.4	0.1
TAVEC recognition	15.6 (0.6)	15.7 (0.6)	15.4 (0.9)	4.5*	2.9	1.1
NBM volume (TIV corrected)	0.00025 (0.00003)	0.00025 (0.00003)	0.00023 (0.00004)	9.10**	7.87**	8.47**

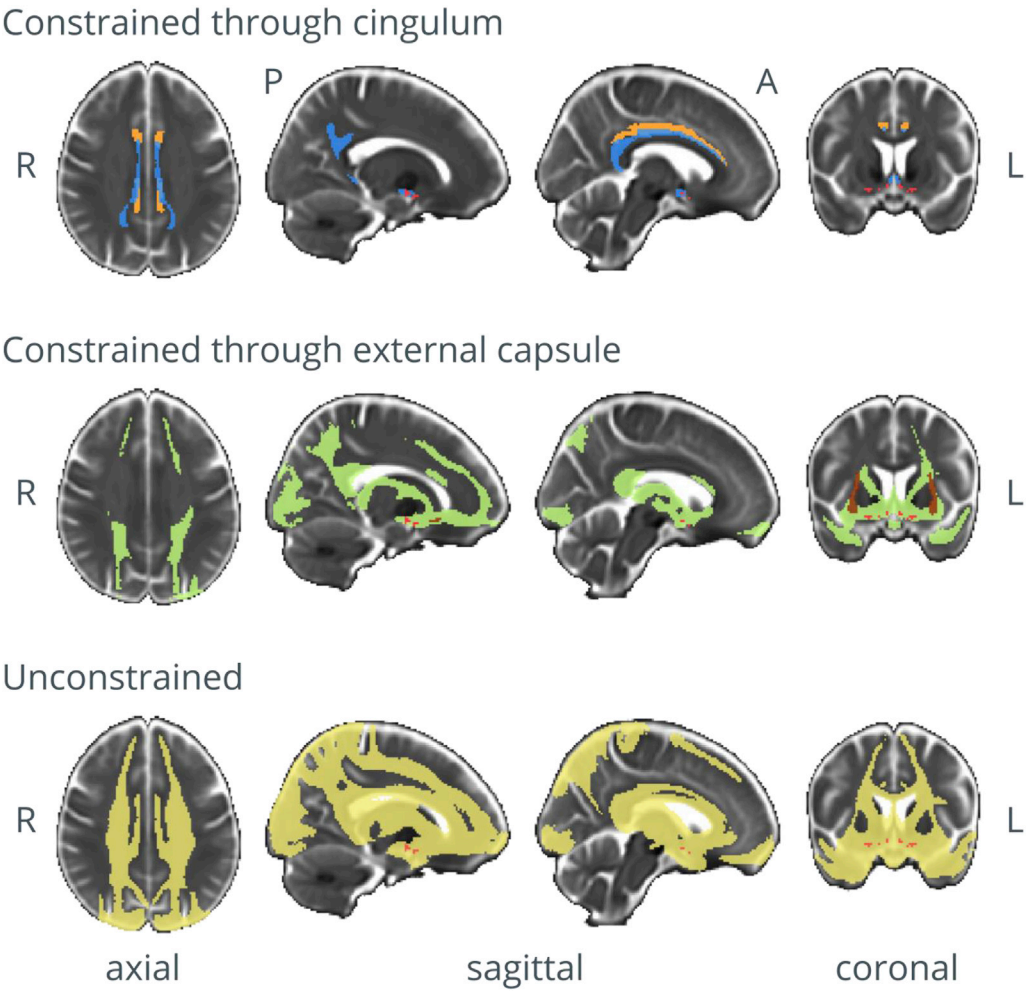

Fig. 3. Cholinergic WM pathways. Red for NBM ROI mask. (First row) Orange for the cingulum mask, blue for the pathway passing through the cingulum. (Second row) Brown for the external capsule mask, green for the pathway passing through the external capsule. (Third row) Yellow for the pathway without restrictions (no explicit midpoint masks). Tracks passing through voxels in anterior commissure and brainstem regions were excluded in the three models using the pertinent masks (please see Methods section). R, right; L, left; A, anterior; P, posterior.

performance in PCV – reaction time and all TAVEC memory measures. When controlling for sex and the WAIS-III Information subtest as a measure of crystallised intelligence, the WM-hypo groups significantly differed in PCV - reaction time and TAVEC delayed recall (5 min). These differences were no longer significant when adding age as a covariate on top of sex and WAIS-III Information (please see the stepwise analysis in Table 1).

3.2. Association between WM-hypo and NBM volume

The NBM volume (corrected for the total intracranial volume, TIV) was significantly smaller in the high WM-hypo load group (Table 1), both without and with controlling for sex, WAIS-III Information, and age.

3.3. Cholinergic pathways

Fig. 3 shows the tracked cholinergic pathways in the probabilistic analyses. The constrained models showed that the medial pathway (in blue) projects from the NBM through gyrus rectus to cingulum and continues to cingulate cortex and retrosplenial cortex. For the lateral pathway (in green), the external capsule division was successfully tracked to inferior frontal cortex (frontal pole) through the uncinate fasciculus, as well as to parietal and temporal cortex via posterior thalamic radiation and internal capsule. Even though no explicit guidance (midway mask) was used for the perisylvian division of the lateral pathway, this division was also successfully tracked throughout the insula, superior temporal gyrus, and frontoparietal operculum. The unconstrained model (in yellow) included the areas described for the medial and lateral pathways but was more widespread including other brain areas such as the posterior cingulate and superior medial areas of parietal and frontal lobes. However, the unconstrained model also included voxels from the posterior regions of the lateral ventricles.

3.4. Association between WM-hypo and integrity of the cholinergic pathways

The high WM-hypo load group showed significantly higher mean diffusivity (MD) values in the tracked cingulum and external capsule pathways as compared with the low WM-hypo load group, after controlling for sex, WAIS-III Information, and age (Table 2). In contrast, WM-hypo load did not have any significant effect on the negative control remaining WM, after controlling for sex, WAIS-III Information, and age (Table 2).

3.5. The contribution of age, WM-hypo, and integrity of the cholinergic system towards cognitive performance

The distinct contributions of MD in the cingulum and external capsule pathways, MD in remaining WM, WM-hypo (as a continuous variable), and NBM volume towards cognitive measures were examined by a random forest analysis, also including age, sex, WAIS-III Information, and the MMSE score as predictors in the models. The unconstrained model was not considered for these analyses because we were interested in specific pathway-cognition associations, and the unconstrained model is reported only for consideration of potential false negatives in the constrained models.

Overall, MD in the external capsule pathway had a stronger importance in the prediction of TAVEC delayed recall (both 5 min and 30 min; Fig. 4). MD in the cingulum pathway had a stronger importance in the prediction of PCV – reaction and TAVEC delayed recall (30 min). Performance in Stroop and TAVEC learning was mainly predicted by WAIS-III Information. MMSE, sex, and age were also important for the prediction of TAVEC learning. Although the age contributed to the prediction of performance in all our cognitive tasks, its contribution was lower than MD in the cholinergic pathways in TAVEC delayed recall (both 5 min and 30 min). WM-hypo, NBM volume, and remaining WM received low importance scores in all the random forest models. The random forest model for TAVEC recognition did not perform better than random prediction.

Fig. 5 shows the correlation matrix for all pairs of predictors of the random forest models. Age, WM-hypo, and MD in the cholinergic pathways were highly correlated with each other.

4. Discussion

In this study, we investigated the contribution of SVD and the integrity of the cholinergic system to attention and memory in normal aging. We found that high WM-hypo load, a marker of SVD, was associated with older age and male sex. High WM-hypo load was also associated with lower performance in attention and memory, but this effect was largely explained by age. In contrast, high WM-hypo load was associated with lower integrity of the cholinergic system (both NBM volume and NBM WM projections) above and beyond the effect of age. The multivariate models showed that reduced integrity of the cholinergic pathways and age, but not WM-hypo load or NBM volume, strongly contributed to performance in attention and memory in our cohort of cognitively normal middle-aged to older individuals.

We found that the WM-hypo load was higher in older individuals and in males. The same finding has repeatedly been reported in previous studies (Habes et al., 2016; Raz et al., 2012). We also found that lower performance in attention and memory in the high WM-hypo load group was accounted for by older age (and to some extent also by male sex and WAIS-III Information). This result is in line with a previous study (Gustavsson et al., 2015). Whether WM-hypo in cognitively normal older individuals indicate preclinical stages of vascular cognitive impairment or are rather a feature of normal aging when not reaching the clinical threshold is currently not known. Our data show a strong association between WM-hypo and age. However, WM-hypo do not seem to have a direct impact on attention or memory but rather an indirect effect through age and integrity of the cholinergic pathways (discussed further down).

An important finding of the current study is that, in contrast to the results on attention and memory, higher WM-hypo load was associated with lower NBM volume and reduced integrity of the cholinergic pathways above and beyond the effect of age. A previous study showed no significant association between NBM volume and vascular cognitive impairment (Liu et al., 2017). A possible explanation for the discrepancy could be the smaller sample size in the study by Liu et al. (2017). This

Table 2
Association between WM-hypo and mean diffusivity in the cholinergic NBM pathways [mean value (SD)] in high and low WM-hypo load groups. MD, mean diffusivity; WM-hypo, WM hypointensities on T1-weighted images appearing as WM hyperintensities on T2/FLAIR sequences (Wardlaw et al., 2013). *$p < 0.05$, **$p < 0.01$, ***$p < 0.001$.

	Low WM-hypo load group	High WM-hypo load group	$F_{1,260}$ (no correction)	$F_{1,258}$ (corrected for sex and WAIS-III Information	$F_{1,257}$ (corrected for sex, WAIS-III Information, and age)
MD in cingulum pathway	0.00083 (0.00003)	0.00089 (0.00006)	72.1***	62.6***	23.2***
MD in external capsule pathway	0.00090 (0.00005)	0.00102 (0.00009)	141.7***	127.3***	69.0***
MD in remaining WM	0.00079 (0.00003)	0.00080 (0.00003)	5.9*	6.6*	0.5

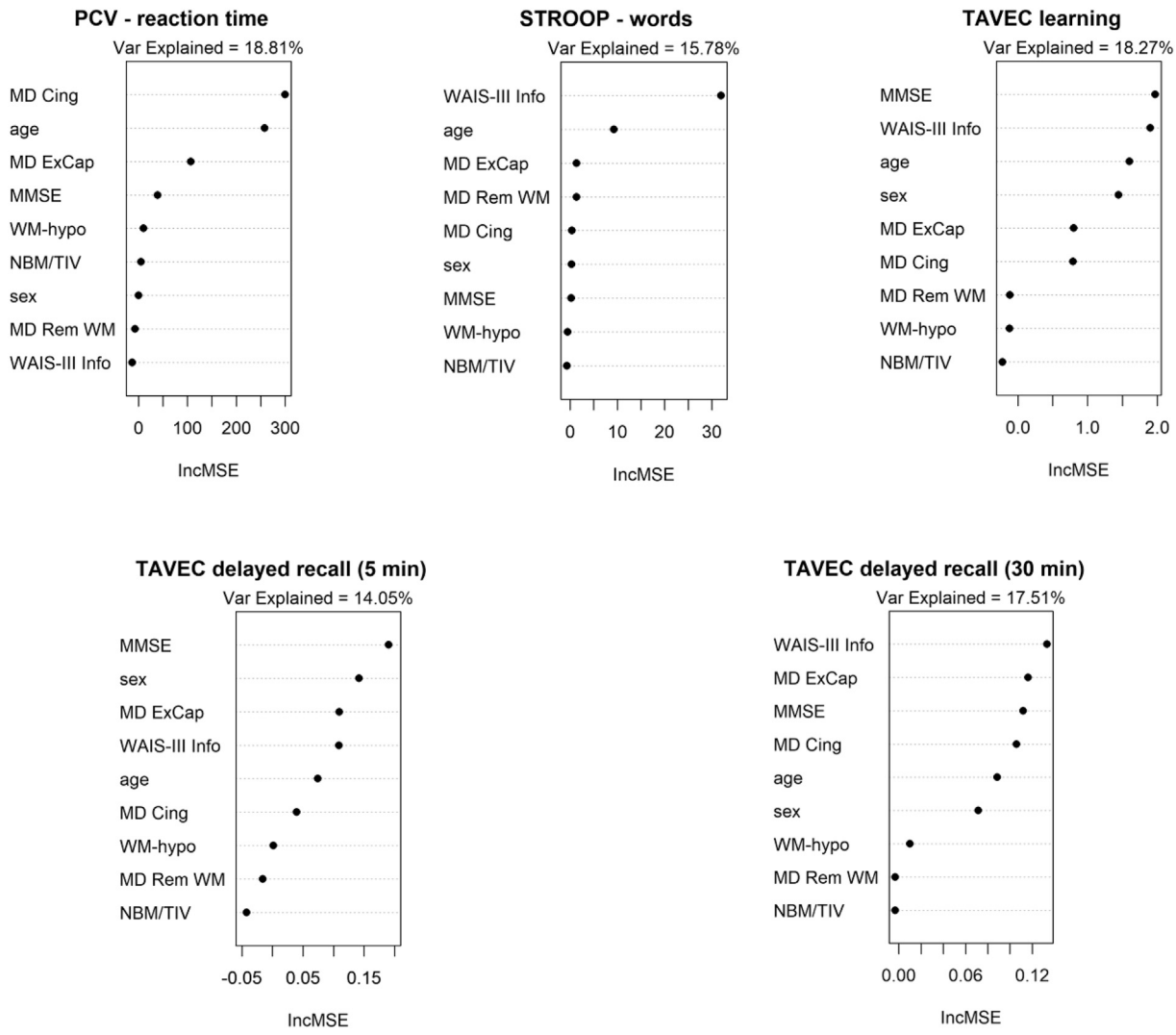

Fig. 4. Random forest models (increase in prediction error). MMSE, Mini-Mental State Examination; MD, mean diffusivity; ExCap, external capsule tract; Cing, cingulum tract; Rem WM, WM excluding cholinergic tracts; WAIS-III Info, Wechsler Adult Intelligence Scale – Third revision Information subtest; WM-hypo, WM hypointensities on T1-weighted images appearing as WM hyperintensities on T2/FLAIR sequences (Wardlaw et al., 2013); NBM/TIV, volume of nucleus basalis of Meynert scaled by total intracranial volume. IncMSE, conditional variable importance computed by increase in the mean square error of prediction as a result of a corresponding variable being permuted within a grid defined by the covariates that are associated to the variable of interest.

could potentially make it difficult to capture an association between SVD and NBM volume. Another possible explanation relates to methodological differences; SVD, one of the criteria for defining vascular cognitive impairment in Liu et al. (2017), was assessed by the Fazekas rating scale, which gives 4 rough scores from 0 to 3 based on 2D images across a limited set of brain sections. In contrast, we assessed SVD with an automated estimation of WM-hypo volume in 3D images across the entire WM. Furthermore, it is also possible that the association between NBM degeneration and SVD is stronger in normal aging, while this association may be weaker or non-existent in patients with a diagnosis of vascular cognitive impairment.

Probabilistic tractography analysis to track white matter pathways arising from the NBM was conducted in order to evaluate the integrity of these tracts *in vivo*. Our constrained models successfully revealed tracts in both medial and lateral pathways, as previously shown using AChE histochemical and ChAT and NGFr immunohistochemical analysis (Selden et al., 1998), as well as in the previous DTI tractography study (Liu et al., 2017). Our unconstrained model included the areas covered by the medial and lateral pathways and extended to other brain areas such as the posterior cingulate and superior medial areas of parietal and frontal lobes. Large portions of these areas have also been labelled as cholinergic projections in histochemical and immunohistochemical studies (Selden et al., 1998), and underlie cortical areas depicted in a recent rs-fMRI study (Fritz et al., 2019). This information may be relevant when it comes to considering potential false negatives in the cingulum and external capsule models. However, we acknowledge that the unconstrained model also included voxels from the lateral ventricles.

We found that high WM-hypo load was associated with reduced integrity in the two cholinergic pathways and the unconstrained model above and beyond the effect of age. Liu et al. (2017) also found that vascular cognitive impairment was associated with reduced integrity in medial and lateral cholinergic pathways. Thus, WM-hypo seem to have an impact on the cholinergic system both in cognitively normal individuals and in patients with vascular cognitive impairment (Liu et al., 2017). Further, the effect of WM-hypo was specific to the cholinergic pathways and did not extend to remaining WM (i.e. WM excluding the cholinergic pathways), when accounting for age.

The random forest models revealed that delayed recall in an episodic memory test (TAVEC delayed recall, both 5 min and 30 min), relies on the integrity of the external capsule pathway. This pathway contains several regions involved in memory such as the frontal cortex and hippocampal structures (Preston and Eichenbaum, 2013). In contrast,

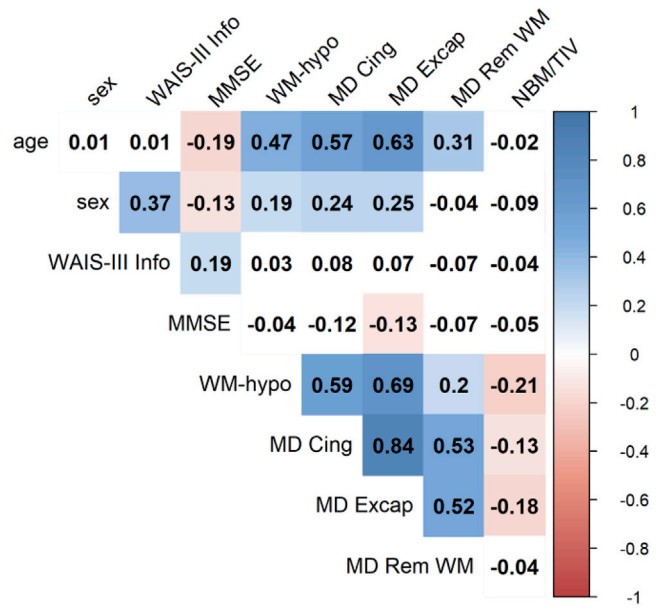

Fig. 5. Correlation matrix for the predictors of the random forest models. Background of significant correlations ($p < 0.05$) was coloured according to the value of the correlation coefficient, otherwise left white. MMSE, Mini-Mental State Examination; sex is coded as 0 for females and 1 for males; MD, mean diffusivity; ExCap, external capsule tract; Cing, cingulum tract; Rem WM, WM excluding cholinergic tracts; WAIS-III Info, Wechsler Adult Intelligence Scale – Third revision Information subtest; WM-hypo, WM hypointensities on T1-weighted images appearing as WM hyperintensities on T2/FLAIR sequences (Wardlaw et al., 2013); NBM/TIV, volume of nucleus basalis scaled by total intracranial volume.

cognitive measures with a stronger attentional component such as PCV – reaction times, as well as TAVEC delayed recall at 30 min, that also involves effortful attention, relied on the integrity of the cingulum. The cingulum involves the posterior cingulate cortex, which is related to attention and memory (Klaassens et al., 2017; Pearson et al., 2011). Of interest, the remaining WM did not contribute to performance in any of the cognitive tests. This finding demonstrates the specificity of the cholinergic pathways to performance in these tests of attention and memory. Older age had an important contribution to all our cognitive variables. However, the contribution of age was lower than that of the integrity of the cholinergic pathways in TAVEC delayed recall (both 5 min and 30 min). These findings suggest that in our cohort of cognitively normal individuals, the contribution of the cholinergic system to cognitive measures is greater and goes beyond the contribution of age in memory tasks that demand effortful attention such as delayed recall. Our findings are thus in agreement with a revisited interpretation of the cholinergic hypothesis of cognitive aging (Dumas and Newhouse, 2011), which proposes that the cholinergic system primarily contributes to effortful attention processes more than memory in cognitively normal individuals. The cholinergic system will thus be especially engaged in attention and memory tasks where the task is difficult and requires effortful attention to achieve good performance (i.e. PCV – reaction time and TAVEC delayed recall, in our study). Our result showing that none of the combinations of variables could predict the TAVEC recognition task further supports this interpretation by indicating that the cholinergic system is not involved in this easier memory task with minimal involvement of attention processes. Although NBM volume plays a key role in AD (Grothe et al., 2012, 2010) and generally in cognitive functioning (Ballinger et al., 2016), it consistently received a very low importance ranking among the other predictors in our random forest models. No association between BF or NBM volume and measures of memory and attention in cognitively normal individuals has been reported in previous studies (Grothe et al., 2016; Lammers et al., 2018, 2016; Wolf et al., 2014). In addition, WM-hypo did not play a strong role in predicting our cognitive measures either. Altogether, our findings point to the integrity of the cholinergic WM pathways as the key factor for performance in attention and memory in our cohort of normal aging. Since both NBM volume and WM-hypo yielded lower contributions in our random forest models, whereas age did yield a high contribution, it is possible that other age-related and subclinical, often mixed, brain pathologies are also contributing to reduced integrity of the cholinergic system (Rahimi and Kovacs, 2014). Using other imaging modalities and biomarkers in the future could help in testing this hypothesis.

A limitation of the current study is that WM pathways that traverse crossing fibres regions may be difficult to track accurately. Several techniques have been proposed to resolve this problem, e.g. multi-tensor fitting, Q-ball imaging, spherical deconvolution, and ball-and-sticks, among other techniques. In the current study, we used a ball-and-sticks model to predict multiple fibre directions in a voxel. While there might exist more advanced techniques, this model shows a good trade-off between model capacity and data quality (Wilkins et al., 2015). Tracking WM pathways through crossing-fibre regions can produce two common types of errors: wrongly connecting brain regions leading to false positives, and omitting existing connections between brain regions leading to false negatives (Dauguet et al., 2007; de Reus and van den Heuvel, 2013). In order to tackle this issue, we performed a combined reconstruction across the whole cohort spanning over 250 individuals that allowed us to set up a robust group threshold - a minimal number of individual cases who share a connection before it was included in the model. A high group threshold requires the connection to be present in a high number of individuals, which has previously successfully eliminated false positives (Watson et al., 2019; Wiseman et al., 2018). On the other hand, a low group threshold allows for unique tracks and ensures a low false-negative rate. In this study, we followed and adapted the methods from de Reus and van den Heuvel (2013) and Liu et al. (2017). Constraining fibre tracking by using hypothesis-driven *a priori* information also helps to reduce the amount of false-positive errors in our cingulum and external capsule models. However, this may happen at the expense of slightly increasing the amount of false-negative errors, i.e. exclusion of areas not considered in *a priori* knowledge. For this reason, we performed an unconstrained tractography model that was able to include areas of the posterior cingulate and superior medial parietal and frontal lobes with potential to be truly cholinergic (Fritz et al., 2019; Selden et al., 1998). Hence, we encourage further studies to substantiate our findings from the unconstrained model. Future advances and refinement of tractography methods are also expected to minimise the rate of false positives and false negatives. Furthermore, we favoured the MD index to other diffusion indices such as fractional anisotropy for its reduced susceptibility to the crossing-fibre problem. We investigated the NBM, which provides the major cholinergic input to cortical and subcortical areas, and has a strong involvement in cognition. However, investigating the fornix, which contains cholinergic projections from the septal nuclei to the hippocampus is warranted for future studies, due to its involvement in episodic verbal memory in cognitively healthy individuals. Investigating other cognitive functions previously linked to the cholinergic system, e.g. cognitive control, is also warranted for future studies. Random forest regression with conditional inference trees is able to handle multicollinearity to some degree, but it might lead to an underestimation of the contribution of multicollinear variables. The association among the predictors of the random forest models can be appreciated in Fig. 5. Finally, previous studies using the cholinergic pathways hyperintensities scale (CHIPS) demonstrated that WM-hypo in presumably cholinergic WM pathways have an impact on cognition in patients with AD and different clinical conditions including probable vascular dementia, vascular cognitive impairment no dementia, and subcortical ischemic vasculopathy (Jaswal et al., 2018; Kim et al., 2013; Swartz et al., 2003). Compared to the CHIPS, our current tractography method gives direct and richer information on the integrity of the cholinergic system but the WM-hypo quantification method lacks regional information. Therefore,

in the future, we will develop regional applications of our current approach.

5. Conclusions

In conclusion, using the proposed pipeline we modelled human WM tracts in a manner that closely resembles cholinergic pathways depicted in post-mortem findings (Selden et al., 1998) and a previous smaller sample DTI-tractography study (Liu et al., 2017). We show that lower integrity of these cholinergic pathways along with age are strong contributors to performance in tests of attention and memory in our cohort of cognitively normal middle-aged and older individuals. Future studies are needed to test whether the developed method could be used as an *in vivo* marker of the human cholinergic system in both cognitively normal and pathological populations. If further validated, we hope that the current method and complementary approaches such as BF functional connectivity in rs-fMRI data (Fritz et al., 2019) will provide new *in vivo* opportunities to re-evaluate the cholinergic hypothesis of cognitive aging.

Declaration of competing interest

None.

CRediT authorship contribution statement

Milan Nemy: Conceptualization, Methodology, Formal analysis, Writing - original draft, Visualization, Software. **Nira Cedres:** Conceptualization, Writing - original draft, Data curation, Investigation. **Michel J. Grothe:** Resources, Writing - review & editing. **J-Sebastian Muehlboeck:** Software, Writing - review & editing. **Olof Lindberg:** Data curation, Writing - review & editing. **Zuzana Nedelska:** Conceptualization, Writing - review & editing. **Olga Stepankova:** Resources, Writing - review & editing. **Lenka Vyslouzilova:** Resources, Writing - review & editing. **Maria Eriksdotter:** Writing - review & editing, Funding acquisition. **José Barroso:** Resources, Writing - review & editing, Funding acquisition. **Stefan Teipel:** Resources, Writing - review & editing. **Eric Westman:** Funding acquisition, Resources, Writing - review & editing. **Daniel Ferreira:** Conceptualization, Methodology, Investigation, Writing - original draft, Writing - review & editing, Supervision, Project administration, Funding acquisition.

Acknowledgements

This research was supported by the *Fundación Canaria Dr. Manuel Morales* (calls 2012, 2014 and 2017); *Fundación Cajacanarias*; the Swedish Foundation for Strategic Research (SSF), the Strategic Research Programme in Neuroscience at Karolinska Institutet (StratNeuro), the Swedish Research Council (VR), the Åke Wiberg foundation, Hjärnfonden, Alzheimerfonden, Demensfonden Stiftelsen Olle Engkvist Byggmästare, Birgitta och Sten Westerberg, Ålderssjukdomar, Gun and Bertil Stohnes, Sigurd och Elsa Goljes Minne, Gamla Tjänarinnor, Karolinska Institutet Forskningstiftelse, Demensförbundet, the Grant Agency of the Czech Technical University in Prague, grant No. SGS19/111/OHK4/2T/13, the Czech Alzheimer Foundation, and the IBRO-ISN fellowship 2018. The funders of the study had no role in the study design nor the collection, analysis, and interpretation of data, writing of the report, or decision to submit the manuscript for publication. The authors would like to thank Dr. Diaz-Flores Varela (Hospital Universitario de Canarias, Tenerife, Spain) for his collaboration in the inspection of magnetic resonance images for inclusion criteria; Dr. Antonio Rodríguez for providing access to participants and helpful assistance; and *Servicio de Resonancia Magnética para Investigaciones Biomédicas del SEGAI* (University of La Laguna, Spain). Data used in preparation of this article is part of the GENIC-database (Group of Neuropsychological Studies of the Canary Islands, University of La Laguna, Spain. Principal investigator: Professor José Barroso. Contact: Dr. Daniel Ferreira, daniel.ferreira.padilla@ki.se). The following collaborators contributed to the GENIC-database but did not participate in analysis or writing of this report (in alphabetic order by family name): Rut Correia, Patricia Diaz, Aida Figueroa, Nerea Figueroa, Eloy García, Lissett González, Teodoro González, Zaira González, Cathaysa Hernández, Edith Hernández, Nira Jiménez, Judith López, Cándida Lozano, María Antonieta Nieto, María Sabucedo, Elena Sirumal, Marta Suárez, Manuel Urbano, and Pedro Velasco.

References

Acosta-Cabronero, J., Williams, G.B., Pengas, G., Nestor, P.J., 2010. Absolute diffusivities define the landscape of white matter degeneration in Alzheimer's disease. Brain 133, 529–539. https://doi.org/10.1093/brain/awp257.

Andersson, J.L.R., Sotiropoulos, S.N., 2016. An integrated approach to correction for off-resonance effects and subject movement in diffusion MR imaging. Neuroimage 125, 1063–1078. https://doi.org/10.1016/j.neuroimage.2015.10.019.

Avants, B.B., Epstein, C.L., Grossman, M., Gee, J.C., 2008. Symmetric diffeomorphic image registration with cross-correlation: evaluating automated labeling of elderly and neurodegenerative brain. Med. Image Anal. 12, 26–41. https://doi.org/10.1016/j.media.2007.06.004.

Ballinger, E.C., Ananth, M., Talmage, D.A., Role, L.W., 2016. Basal forebrain cholinergic circuits and signaling in cognition and cognitive decline. Neuron 91, 1199–1218. https://doi.org/10.1016/j.neuron.2016.09.006.

Bartus, R.T., Dean, R.L., Beer, B., Lippa, A.S., 1982. The cholinergic hypothesis of geriatric memory dysfunction. Science 217, 408–414. https://doi.org/10.1126/SCIENCE.7046051.

Beck, A.T., Ward, C.H., Mendelson, M., Mock, J., Erbaugh, J., 1961. An inventory for measuring depression. Arch. Gen. Psychiatr. 4, 561–571.

Behrens, T.E.J., Berg, H.J., Jbabdi, S., Rushworth, M.F.S., Woolrich, M.W., 2007. Probabilistic diffusion tractography with multiple fibre orientations: what can we gain? Neuroimage. https://doi.org/10.1016/j.neuroimage.2006.09.018.

Benedet Mj, A.M., 1998. TAVEC: Test de Aprendizaje Verbal España-Complutense. TEA, Madrid.

Blessed, G., Tomlinson, B.E., Roth, M., 1968. The association between quantitative measures of dementia and of senile change in the cerebral grey matter of elderly subjects. Br. J. Psychiatry 114, 797–811. https://doi.org/10.1192/bjp.114.512.797.

Brands, A.M.A., Kessels, R.P.C., Hoogma, R.P.L.M., Henselmans, J.M.L., Van Der Beek Boter, J.W., Kappelle, L.J., De Haan, E.H.F., Biessels, G.J., 2006. Cognitive performance, psychological well-being, and brain magnetic resonance imaging in older patients with type 1 diabetes. Diabetes 55, 1800–1806. https://doi.org/10.2337/db05-1226.

Breiman, L., 2001. Random forests. Mach. Learn. 45, 5–32. https://doi.org/10.1023/A:1010933404324.

Breiman, L., 1996. Bagging predictions. Mach. Learn. 24, 123–140. https://doi.org/10.1023/A:1018054314350.

Buckner, R.L., Head, D., Parker, J., Fotenos, A.F., Marcus, D., Morris, J.C., Snyder, A.Z., 2004. A unified approach for morphometric and functional data analysis in young, old, and demented adults using automated atlas-based head size normalization: reliability and validation against manual measurement of total intracranial volume. Neuroimage 23, 724–738. https://doi.org/10.1016/J.NEUROIMAGE.2004.06.018.

Butler, T., Blackmon, K., Zaborszky, L., Wang, X., DuBois, J., Carlson, C., Barr, W.B., French, J., Devinsky, O., Kuzniecky, R., Halgren, E., Thesen, T., 2012. Volume of the human septal forebrain region is a predictor of source memory accuracy. J. Int. Neuropsychol. Soc. 18, 157–161. https://doi.org/10.1017/s1355617711001421.

Cedres, N., Ferreira, D., Machado, A., Shams, S., Sacuiu, S., Waern, M., Wahlund, L.-O., Zettergren, A., Kern, S., Skoog, I., Westman, E., 2020. Predicting Fazekas scores from automatic segmentations of white matter signal abnormalities. Aging 12, 894–901. https://doi.org/10.18632/aging.102662.

Cedres, N., Machado, A., Molina, Y., Diaz-Galvan, P., Hernández-Cabrera, J.A., Barroso, J., Westman, E., Ferreira, D., 2019. Subjective cognitive decline below and above the age of 60: a multivariate study on neuroimaging, cognitive, clinical, and demographic measures. J. Alzheim. Dis. 68, 295–309. https://doi.org/10.3233/JAD-180720.

Dauguet, J., Peled, S., Berezovskii, V., Delzescaux, T., Warfield, S.K., Born, R., Westin, C.F., 2007. Comparison of fiber tracts derived from in-vivo DTI tractography with 3D histological neural tract tracer reconstruction on a macaque brain. Neuroimage 37, 530–538. https://doi.org/10.1016/j.neuroimage.2007.04.067.

de Reus, M.A., van den Heuvel, M.P., 2013. Estimating false positives and negatives in brain networks. Neuroimage 70, 402–409. https://doi.org/10.1016/j.neuroimage.2012.12.066.

Drachman, D.A., Leavitt, J., 1974. Human memory and the cholinergic system: a relationship to aging? Arch. Neurol. 30, 113–121. https://doi.org/10.1001/archneur.1974.00490320001001.

Dumas, J.A., Newhouse, P.A., 2011. The cholinergic hypothesis of cognitive aging revisited again: cholinergic functional compensation. Pharmacol. Biochem. Behav. 99, 254–261. https://doi.org/10.1016/j.pbb.2011.02.022.

Ferreira, D., Correia, R., Nieto, A., Machado, A., Molina, Y., Barroso, J., 2015. Cognitive decline before the age of 50 can be detected with sensitive cognitive measures. Psicothema 27, 216–222. https://doi.org/10.7334/psicothema2014.192.

Ferreira, D., Machado, A., Molina, Y., Nieto, A., Correia, R., Westman, E., Barroso, J., 2017. Cognitive variability during middle-age: possible association with neurodegeneration and cognitive reserve. Front. Aging Neurosci. 9, 188. https://doi.org/10.3389/fnagi.2017.00188.

Ferreira, D., Molina, Y., Machado, A., Westman, E., Wahlund, L.O., Nieto, A., Correia, R., Junqué, C., Díaz-Flores, L., Barroso, J., 2014. Cognitive decline is mediated by gray matter changes during middle age. Neurobiol. Aging 35, 1086–1094. https://doi.org/10.1016/j.neurobiolaging.2013.10.095.

Fischl, B., Salat, D.H., Busa, E., Albert, M., Dieterich, M., Haselgrove, C., van der Kouwe, A., Killiany, R., Kennedy, D., Klaveness, S., Montillo, A., Makris, N., Rosen, B., Dale, A.M., 2002. Whole brain segmentation: automated labeling of neuroanatomical structures in the human brain. Neuron 33, 341–355. https://doi.org/10.1016/S0896-6273(02)00569-X.

Folstein, M.F., Folstein, S.E., McHugh, P.R., 1975. "Mini-mental state". A practical method for grading the cognitive state of patients for the clinician. J. Psychiatr. Res. 12, 189–198. https://doi.org/10.1016/0022-3956(75)90026-6.

Fritz, H.C.J., Ray, N., Dyrba, M., Sorg, C., Teipel, S., Grothe, M.J., 2019. The corticotopic organization of the human basal forebrain as revealed by regionally selective functional connectivity profiles. Hum. Brain Mapp. 40, 868–878. https://doi.org/10.1002/hbm.24417.

Grothe, M., Heinsen, H., Teipel, S., 2013. Longitudinal measures of cholinergic forebrain atrophy in the transition from healthy aging to Alzheimer's disease. Neurobiol. Aging 34, 1210–1220. https://doi.org/10.1016/j.neurobiolaging.2012.10.018.

Grothe, M., Heinsen, H., Teipel, S.J., 2012. Atrophy of the cholinergic basal forebrain over the adult age range and in early stages of Alzheimer's disease. Biol. Psychiatr. 71, 805–813. https://doi.org/10.1016/j.biopsych.2011.06.019.

Grothe, M., Zaborszky, L., Atienza, M., Gil-Neciga, E., Rodriguez-Romero, R., Teipel, S.J., Amunts, K., Suarez-Gonzalez, A., Cantero, J.L., 2010. Reduction of basal forebrain cholinergic system parallels cognitive impairment in patients at high risk of developing alzheimer's disease. Cerebr. Cortex 20, 1685–1695. https://doi.org/10.1093/cercor/bhp232.

Grothe, M.J., Heinsen, H., Amaro, E., Grinberg, L.T., Teipel, S.J., 2016. Cognitive correlates of basal forebrain atrophy and associated cortical hypometabolism in mild cognitive impairment. Cerebr. Cortex 26, 2411–2426. https://doi.org/10.1093/cercor/bhv062.

Gunning-Dixon, F.M., Brickman, A.M., Cheng, J.C., Alexopoulos, G.S., 2009. Aging of cerebral white matter: a review of MRI findings. Int. J. Geriatr. Psychiatr. 24, 109–117. https://doi.org/10.1002/gps.2087.

Gustavsson, A.-M., Stomrud, E., Abul-Kasim, K., Minthon, L., Nilsson, P.M., Hansson, O., Nägga, K., 2015. Cerebral microbleeds and white matter hyperintensities in cognitively healthy elderly: a cross-sectional cohort study evaluating the effect of arterial stiffness. Cerebrovasc. Dis. Extra 5, 41–51. https://doi.org/10.1159/000377710.

Habes, M., Erus, G., Toledo, J.B., Zhang, T., Bryan, N., Launer, L.J., Rosseel, Y., Janowitz, D., Doshi, J., Van der Auwera, S., von Sarnowski, B., Hegenscheid, K., Hosten, N., Homuth, G., Völzke, H., Schminke, U., Hoffmann, W., Grabe, H.J., Davatzikos, C., 2016. White matter hyperintensities and imaging patterns of brain ageing in the general population. Brain 139, 1164–1179. https://doi.org/10.1093/brain/aww008.

Hawkins, K.A., Emadi, N., Pearlson, G.D., Winkler, A.M., Taylor, B., Dulipsingh, L., King, D., Pittman, B., Blank, K., 2017. Hyperinsulinemia and elevated systolic blood pressure independently predict white matter hyperintensities with associated cognitive decrement in the middle-aged offspring of dementia patients. Metab. Brain Dis. 32, 849–857. https://doi.org/10.1007/s11011-017-9980-9.

Jaswal, G., Swardfager, W., Gao, F.-Q., Nestor, S.M., Ganda, A., Cogo-Moreira, H., Sahlas, D.J., Stuss, D.T., Moody, A., Black, S.E., 2018. Reduced substantia innominata volume mediates contributions of microvascular and macrovascular disease to cognitive deficits in Alzheimer's disease. Neurobiol. Aging 66, 23–31. https://doi.org/10.1016/j.neurobiolaging.2018.01.025.

Jenkinson, M., Beckmann, C.F., Behrens, T.E.J., Woolrich, M.W., Smith, S.M., 2012. FSL. Neuroimage 62, 782–790. https://doi.org/10.1016/j.neuroimage.2011.09.015.

Jenkinson, M., Pechaud, M., Smith, S., 2005. BET2: MR-based estimation of brain, skull and scalp surfaces. In: Eleventh Annual Meeting of the Organization for Human Brain Mapping, vol. 17, p. 167.

Kilimann, I., Grothe, M., Heinsen, H., Alho, E.J.L., Grinberg, L., Amaro, E., Dos Santos, G.A.B., Da Silva, R.E., Mitchell, A.J., Frisoni, G.B., Bokde, A.L.W., Fellgiebel, A., Filippi, M., Hampel, H., Klöppel, S., Teipel, S.J., 2014. Subregional basal forebrain atrophy in alzheimer's disease: a multicenter study. J. Alzheim. Dis. 40, 687–700. https://doi.org/10.3233/JAD-132345.

Kim, H.J., Moon, W.J., Han, S.H., 2013. Differential cholinergic pathway involvement in alzheimer's disease and subcortical ischemic vascular dementia. J. Alzheim. Dis. 35, 129–136. https://doi.org/10.3233/JAD-122320.

Klaassens, B.L., van Gerven, J.M.A., van der Grond, J., de Vos, F., Möller, C., Rombouts, S.A.R.B., 2017. Diminished posterior precuneus connectivity with the default mode network differentiates normal aging from Alzheimer's Disease. Front. Aging Neurosci. 9 https://doi.org/10.3389/fnagi.2017.00097.

Lammers, F., Borchers, F., Feinkohl, I., Hendrikse, J., Kant, I.M.J., Kozma, P., Pischon, T., Slooter, A.J.C., Spies, C., van Montfort, S.J.T., Zacharias, N., Zaborszky, L., Winterer, G., 2018. Basal forebrain cholinergic system volume is associated with general cognitive ability in the elderly. Neuropsychologia 119, 145–156. https://doi.org/10.1016/j.neuropsychologia.2018.08.005.

Lammers, F., Mobascher, A., Musso, F., Shah, N.J., Warbrick, T., Zaborszky, L., Winterer, G., 2016. Effects of Ncl. Basalis Meynert volume on the Trail-Making-Test are restricted to the left hemisphere. Brain Behav. 6, 1–9. https://doi.org/10.1002/brb3.421.

Leritz, E.C., Shepel, J., Williams, V.J., Lipsitz, L.A., Mcglinchey, R.E., Milberg, W.P., Salat, D.H., 2014. Associations between T1 white matter lesion volume and regional white matter microstructure in aging. Hum. Brain Mapp. 35, 1085–1100. https://doi.org/10.1002/hbm.22236.

Li, X., Li, T.Q., Andreasen, N., Wiberg, M.K., Westman, E., Wahlund, L.O., 2014. The association between biomarkers in cerebrospinal fluid and structural changes in the brain in patients with Alzheimer's disease. J. Intern. Med. 275, 418–427. https://doi.org/10.1111/joim.12164.

Li, X., Westman, E., Ståhlbom, A.K., Thordardottir, S., Almkvist, O., Blennow, K., Wahlund, L.O., Graff, C., 2015. White matter changes in familial Alzheimer's disease. J. Intern. Med. 278, 211–218. https://doi.org/10.1111/joim.12352.

Liu, Q., Zhu, Z., Teipel, S.J., Yang, J., Xing, Y., Tang, Y., Jia, J., 2017. White matter damage in the cholinergic system contributes to cognitive impairment in subcortical vascular cognitive impairment, no dementia. Front. Aging Neurosci. 9, 47. https://doi.org/10.3389/fnagi.2017.00047.

Machado, A., Barroso, J., Molina, Y., Nieto, A., Díaz-Flores, L., Westman, E., Ferreira, D., 2018. Proposal for a hierarchical, multidimensional, and multivariate approach to investigate cognitive aging. Neurobiol. Aging 71, 179–188. https://doi.org/10.1016/J.NEUROBIOLAGING.2018.07.017.

Mesulam, M.M., 2013. Cholinergic circuitry of the human nucleus basalis and its fate in Alzheimer's disease. J. Comp. Neurol. https://doi.org/10.1002/cne.23415.

Mesulam, M.M., Mufson, E.J., Levey, A.I., Wainer, B.H., 1983. Cholinergic innervation of cortex by the basal forebrain: cytochemistry and cortical connections of the septal area, diagonal band nuclei, nucleus basalis (Substantia innominata), and hypothalamus in the rhesus monkey. J. Comp. Neurol. 214, 170–197. https://doi.org/10.1002/cne.902140206.

Mesulam, M.M., Mufson, E.J., Wainer, B.H., 1986. Three-dimensional representation and cortical projection topography of the nucleus basalis (Ch4) in the macaque: concurrent demonstration of choline acetyltransferase and retrograde transport with a stabilized tetramethylbenzidine method for horseradish p. Brain Res. 367, 301–308. https://doi.org/10.1016/0006-8993(86)91607-0.

Mesulam, M.M., Van Hoesen, G.W., 1976. Acetylcholinesterase-rich projections from the basal forebrain of the rhesus monkey to neocortex. Brain Res. 109, 152–157. https://doi.org/10.1016/0006-8993(76)90385-1.

Mori, S., Wakana, S., Van Zijl, P.C., Nagae-Poetscher, L., 2005. MRI Atlas of Human White Matter. Elsevier, Amsterdam.

Nunley, K.A., Ryan, C.M., Orchard, T.J., Aizenstein, H.J., Jennings, J.R., Ryan, J., Zgibor, J.C., Boudreau, R.M., Costacou, T., Maynard, J.D., Miller, R.G., Rosano, C., 2015. White matter hyperintensities in middle-aged adults with childhood-onset type 1 diabetes. Neurology 84, 2062–2069. https://doi.org/10.1212/WNL.0000000000001582.

Patenaude, B., Smith, S.M., Kennedy, D.N., Jenkinson, M., 2011. A Bayesian model of shape and appearance for subcortical brain segmentation. Neuroimage 56, 907–922. https://doi.org/10.1016/j.neuroimage.2011.02.046.

Pearson, J.M., Heilbronner, S.R., Barack, D.L., Hayden, B.Y., Platt, M.L., 2011. Posterior cingulate cortex: adapting behavior to a changing world. Trends Cognit. Sci. https://doi.org/10.1016/j.tics.2011.02.002.

Pfeffer, R.I., Kurosaki, T.T., Harrah, C.H., Chance, J.M., Filos, S., 1982. Measurement of functional activities in older adults in the community. J. Gerontol. 37, 323–329.

Preston, A.R., Eichenbaum, H., 2013. Interplay of hippocampus and prefrontal cortex in memory. Curr. Biol. https://doi.org/10.1016/j.cub.2013.05.041.

Rahimi, J., Kovacs, G.G., 2014. Prevalence of mixed pathologies in the aging brain. Alzheimer's Res. Ther. 6 https://doi.org/10.1186/s13195-014-0082-1.

Raz, N., Yang, Y., Dahle, C.L., Land, S., 2012. Volume of white matter hyperintensities in healthy adults: contribution of age, vascular risk factors, and inflammation-related genetic variants. Biochim. Biophys. Acta - Mol. Basis Dis. 1822, 361–369. https://doi.org/10.1016/j.bbadis.2011.08.007.

Salat, D.H., Tuch, D.S., van der Kouwe, A.J.W., Greve, D.N., Pappu, V., Lee, S.Y., Hevelone, N.D., Zaleta, A.K., Growdon, J.H., Corkin, S., Fischl, B., Rosas, H.D., 2010. White matter pathology isolates the hippocampal formation in Alzheimer's disease. Neurobiol. Aging 31, 244–256. https://doi.org/10.1016/j.neurobiolaging.2008.03.013.

Schuhfried, G., 1992. Vienna Reaction Unit (Manual). Schuhfried Ges. mbH, Mödling, Austria.

Selden, N.R., Gitelman, D.R., Salamon-Murayama, N., Parrish, T.B., Mesulam, M.M., 1998. Trajectories of cholinergic pathways within the cerebral hemispheres of the human brain. Brain J. Neurol. 121, 2249–2257. https://doi.org/10.1093/brain/121.12.2249.

Simmons, A., Westman, E., Muehlboeck, S., Mecocci, P., Vellas, B., Tsolaki, M., Kłoszewska, I., Wahlund, L.-O., Soininen, H., Lovestone, S., Evans, A., Spenger, C., 2009. MRI measures of alzheimer's disease and the AddNeuroMed study. Ann. N. Y. Acad. Sci. 1180, 47–55. https://doi.org/10.1111/j.1749-6632.2009.05063.x.

Strobl, C., Boulesteix, A.L., Zeileis, A., Hothorn, T., 2007. Bias in random forest variable importance measures: illustrations, sources and a solution. BMC Bioinf. 8 https://doi.org/10.1186/1471-2105-8-25.

Stroop, J.R., 1935. Studies of interference in serial verbal reactions. J. Exp. Psychol. 18, 643–662. https://doi.org/10.1037/h0054651.

Swartz, R.H., Sahlas, D.J., Black, S.E., 2003. Strategic involvement of cholinergic pathways and executive dysfunction: does location of white matter signal hyperintensities matter? J. Stroke Cerebrovasc. Dis. 12, 29–36. https://doi.org/10.1053/JSCD.2003.5.

Teipel, S., Heinsen, H., Amaro, E., Grinberg, L.T., Krause, B., Grothe, M., Alzheimer's Disease Neuroimaging Initiative, M., 2014. Cholinergic basal forebrain atrophy predicts amyloid burden in Alzheimer's disease. Neurobiol. Aging 35, 482–491. https://doi.org/10.1016/j.neurobiolaging.2013.09.029.

Teipel, S.J., Flatz, W.H., Heinsen, H., Bokde, A.L.W., Schoenberg, S.O., Stöckel, S., Dietrich, O., Reiser, M.F., Möller, H.J., Hampel, H., 2005. Measurement of basal forebrain atrophy in Alzheimer's disease using MRI. Brain 128, 2626–2644. https://doi.org/10.1093/brain/awh589.

Teipel, S.J., Meindl, T., Grinberg, L., Grothe, M., Cantero, J.L., Reiser, M.F., Möller, H.-J., Heinsen, H., Hampel, H., 2011. The cholinergic system in mild cognitive impairment and Alzheimer's disease: an in vivo MRI and DTI study. Hum. Brain Mapp. 32, 1349–1362. https://doi.org/10.1002/hbm.21111.

Wardlaw, J.M., Smith, E.E., Biessels, G.J., Cordonnier, C., Fazekas, F., Frayne, R., Lindley, R.I., O'Brien, J.T., Barkhof, F., Benavente, O.R., Black, S.E., Brayne, C., Breteler, M., Chabriat, H., DeCarli, C., de Leeuw, F.E., Doubal, F., Duering, M., Fox, N.C., Greenberg, S., Hachinski, V., Kilimann, I., Mok, V., Oostenbrugge, R. van, Pantoni, L., Speck, O., Stephan, B.C.M., Teipel, S., Viswanathan, A., Werring, D., Chen, C., Smith, C., van Buchem, M., Norrving, B., Gorelick, P.B., Dichgans, M., 2013. Neuroimaging standards for research into small vessel disease and its contribution to ageing and neurodegeneration. Lancet Neurol. https://doi.org/10.1016/S1474-4422(13)70124-8.

Watson, C.G., DeMaster, D., Ewing-Cobbs, L., 2019. Graph theory analysis of DTI tractography in children with traumatic injury. NeuroImage Clin. 21, 101673. https://doi.org/10.1016/J.NICL.2019.101673.

Wechsler, D., 1997. WMS-III: Wechsler Memory Scale Administration and Scoring Manual. Psychological Corporation, San Antonio.

Wilkins, B., Lee, N., Gajawelli, N., Law, M., Leporé, N., 2015. Fiber estimation and tractography in diffusion MRI: development of simulated brain images and comparison of multi-fiber analysis methods at clinical b-values HHS Public Access. Neuroimage 109, 341–356. https://doi.org/10.1016/j.neuroimage.2014.12.060.

Wiseman, S.J., Booth, T., Ritchie, S.J., Cox, S.R., Muñoz Maniega, S., Valdés Hernández, M.D.C., Dickie, D.A., Royle, N.A., Starr, J.M., Deary, I.J., Wardlaw, J.M., Bastin, M.E., 2018. Cognitive abilities, brain white matter hyperintensity volume, and structural network connectivity in older age. Hum. Brain Mapp. 39, 622–632. https://doi.org/10.1002/hbm.23857.

Wolf, D., Grothe, M., Fischer, F.U., Heinsen, H., Kilimann, I., Teipel, S., Fellgiebel, A., 2014. Association of basal forebrain volumes and cognition in normal aging. Neuropsychologia 53, 54–63. https://doi.org/10.1016/j.neuropsychologia.2013.11.002.

Woolf, N.J., 1991. Cholinergic systems in mammalian brain and spinal cord. Prog. Neurobiol. 37, 475–524. https://doi.org/10.1016/0301-0082(91)90006-M.

Yang, T., Sun, Y., Lu, Z., Leak, R.K., Zhang, F., 2017. The impact of cerebrovascular aging on vascular cognitive impairment and dementia. Ageing Res. Rev. 34, 15. https://doi.org/10.1016/J.ARR.2016.09.007.

Yesavage, J.A., Sheikh, J.I., 1986. Geriatric depression scale (GDS). Clin. Gerontol. 5, 165–173. https://doi.org/10.1300/J018v05n01_09.

Zaborszky, L., Hoemke, L., Mohlberg, H., Schleicher, A., Amunts, K., Zilles, K., 2008. Stereotaxic probabilistic maps of the magnocellular cell groups in human basal forebrain. Neuroimage 42, 1127–1141. https://doi.org/10.1016/j.neuroimage.2008.05.055.

Zhang, B., Xu, Y., Zhu, B., Kantarci, K., 2014. The role of diffusion tensor imaging in detecting microstructural changes in prodromal Alzheimer's disease. CNS Neurosci. Ther. 20, 3–9. https://doi.org/10.1111/cns.12166.

Zhang, Y., Brady, M., Smith, S., 2001. Segmentation of brain MR images through a hidden Markov random field model and the expectation-maximization algorithm. IEEE Trans. Med. Imag. 20, 45–57. https://doi.org/10.1109/42.906424.

II

RESEARCH ARTICLE OPEN ACCESS

Association of Cerebrovascular and Alzheimer Disease Biomarkers With Cholinergic White Matter Degeneration in Cognitively Unimpaired Individuals

Nira Cedres, PhD, Daniel Ferreira, PhD, Milan Nemy, Msc, Alejandra Machado, PhD, Joana B. Pereira, PhD, Sara Shams, PhD, Lars-Olof Wahlund, PhD, Anna Zettergren, PhD, Olga Stepankova, PhD, Lenka Vyslouzilova, PhD, Maria Eriksdotter, PhD, Stefan Teipel, MD, Michel J. Grothe, PhD, Kaj Blennow, MD, PhD, Henrik Zetterberg, MD, PhD, Michael Schöll, PhD, Silke Kern, PhD, Ingmar Skoog, MD, PhD,* and Eric Westman, PhD*

Correspondence
Dr. Ferreira
daniel.ferreira.padilla@ki.se

Neurology® 2022;99:e1619-e1629. doi:10.1212/WNL.0000000000200930

Abstract

Background and Objectives

Several pathologic processes might contribute to the degeneration of the cholinergic system in aging. We aimed to determine the contribution of amyloid, tau, and cerebrovascular biomarkers toward the degeneration of cholinergic white matter (WM) projections in cognitively unimpaired individuals.

Methods

The contribution of amyloid and tau pathology was assessed through CSF levels of the $A\beta_{42/40}$ ratio and phosphorylated tau (p-tau). CSF $A\beta_{38}$ levels were also measured. Cerebrovascular pathology was assessed using automatic segmentations of WM lesions (WMLs) on MRI. Cholinergic WM projections (i.e., cingulum and external capsule pathways) were modeled using tractography based on diffusion tensor imaging data. Sex and APOE ε4 carriership were also included in the analysis as variables of interest.

Results

We included 203 cognitively unimpaired individuals from the H70 Gothenburg Birth Cohort Studies (all individuals aged 70 years, 51% female). WM lesion burden was the most important contributor to the degeneration of both cholinergic pathways (increase in mean square error [IncMSE] = 98.8% in the external capsule pathway and IncMSE = 93.3% in the cingulum pathway). Levels of $A\beta_{38}$ and p-tau also contributed to cholinergic WM degeneration, especially in the external capsule pathway (IncMSE = 28.4% and IncMSE = 23.4%, respectively). The $A\beta_{42/40}$ ratio did not contribute notably to the models (IncMSE<3.0%). APOE ε4 carriers showed poorer integrity in the cingulum pathway (IncMSE = 21.33%). Women showed poorer integrity of the external capsule pathway (IncMSE = 21.55%), which was independent of amyloid status as reflected by the nonsignificant differences in integrity when comparing amyloid-positive vs amyloid-negative women participants ($T_{201} = -1.55$; $p = 0.123$).

*These authors contributed equally to this work as co–senior authors.

From the Division of Clinical Geriatrics (N.C., D.F., A.M., J.B.P., S.S., L.-O.W., M.E., E.W.), Centre for Alzheimer Research, Department of Neurobiology, Care Sciences, and Society, and the Division of Insurance Medicine (A.M.), Department of Clinical Neuroscience, Karolinska Institutet, Stockholm; Department of Psychology (N.C.), Sensory Cognitive Interaction Laboratory (SCI-lab), Stockholm University, Sweden; Department of Radiology (D.F.), Mayo Clinic, Rochester, MN; Department of Cybernetics (M.N.), Faculty of Electrical Engineering and Czech Institute of Informatics (M.N., O.S., L.V.), Robotics, and Cybernetics, Czech Technical University, Prague, Czech Republic; Clinical Memory Research Unit (J.B.P.), Department of Clinical Sciences, Lund University, Malmö; Department of Psychiatry Cognition and Old Age Psychiatry, (A.Z., S.K., I.S.), Clinical Neurochemistry Laboratory (K.B., H.Z.), and Department of Clinical Physiology (M.S.), Sahlgrenska University Hospital, Gothenburg; Neuropsychiatric Epidemiology Unit (A.Z., K.B., H.Z., S.K., I.S.), Department of Psychiatry and Neurochemistry, Institute of Neuroscience and Physiology, the Sahlgrenska Academy, Centre for Ageing and Health (AGECAP) at the University of Gothenburg; Theme Inflammation and Aging (M.E.), Karolinska University Hospital, Huddinge, Sweden; Clinical Dementia Research Section (S.T.), Department of Psychosomatic Medicine, University Medicine Rostock; German Center for Neurodegenerative Diseases (DZNE) (S.T., M.J.G.), Rostock, Germany; Unidad de Trastornos del Movimiento (M.J.G.), Servicio de Neurología y Neurofisiología Clínica, Instituto de Biomedicina de Sevilla (IBiS), Hospital Universitario Virgen del Rocío/CSIC/Universidad de Sevilla, Spain; Department of Neurodegenerative Disease (H.Z.), UCL Institute of Neurology, London; Dementia Research Institute at UCL (H.Z.), London, UK; Hong Kong Center for Neurodegenerative Diseases (H.Z.), China; Wallenberg Centre for Molecular and Translational Medicine (M.S.) and Department of Psychiatry and Neurochemistry (M.S.), Institute of Physiology and Neuroscience, University of Gothenburg, Sweden; Dementia Research Centre (M.S.), Institute of Neurology, University College London; and Department of Neuroimaging (E.W.), Centre for Neuroimaging Sciences, Institute of Psychiatry, Psychology and Neuroscience, King's College London, UK.

Go to Neurology.org/N for full disclosures. Funding information and disclosures deemed relevant by the authors, if any, are provided at the end of the article.

The Article Processing Charge was funded by the authors.

Glossary

AD = Alzheimer disease; **CDR** = Clinical Dementia Rating; **DTI** = diffusion tensor imaging; **FA** = fractional anisotropy; **FLAIR** = Fluid-attenuated inversion recovery; **MD** = mean diffusivity; **MMSE** = Mini-Mental State Examination; **NBM** = nucleus basalis of Meynert; **RF** = random forest; **RT** = repetition time; **SWI** = susceptibility-weighted imaging; **TE** = echo time; **TIV** = total intracranial volume; **WM** = white matter; **WML** = WM lesion.

Discussion

In cognitively unimpaired older individuals, WMLs play a central role in the degeneration of cholinergic pathways. Our findings highlight the importance of WM lesion burden in the elderly population, which should be considered in the development of prevention programs for neurodegeneration and cognitive impairment.

The cholinergic neurons located in the nucleus basalis of Meynert (NBM) provide the major cholinergic input to the cerebral cortex and are essential to cognitive functioning.[1] Postmortem studies have traced 2 principal cholinergic projection pathways from the NBM to the neocortex: the medial and the lateral pathways.[1] The medial pathway advances through the white matter (WM) axons of the rectus gyrus, bends at the rostrum of the corpus callosum, and enters the cingulum bundle, projecting to the paraolfactory, cingulate, and retrosplenial cortices. The lateral pathway advances both through the claustrum and the extreme capsule (i.e., perisylvian division), projecting to the frontoparietal operculum, insula, and superior temporal gyrus, and through the external capsule and uncinate fasciculus (i.e., capsular division), projecting to the remaining parts of the frontal, parietal, and temporal neocortex. Recent diffusion tensor imaging (DTI)-based tractography studies have examined these pathways,[2–5] providing the opportunity to study the integrity of the cholinergic system and its potential association with cognitive performance and pathophysiologic processes in vivo.

The strategic location of the NBM and its connective circuitry to the cortex results in increased vulnerability to brain pathology. For example, cholinergic neurons are affected in early stages of Alzheimer disease (AD)-related tauopathy due to their proximity to heavily affected basotemporal regions, which likely also alters their connective circuitry to the cortex.[1] Furthermore, other age-related pathologies can also affect the integrity of the cholinergic system. WM lesions (WMLs), which are thought to be a marker of cerebrovascular disease, are commonly found on MRI in the elderly.[6] A recent study showed that WMLs are associated with worse integrity of the cholinergic projections in cognitively unimpaired older individuals,[4] and cholinergic projections influenced cognitive performance.[4] Of interest, despite the association of WMLs with the integrity of the cholinergic projection system, neither WML burden itself nor NBM volume contributed to cognitive performance.[4] These findings raised the question of whether other age-associated pathologies apart from WMLs might be affecting the integrity of the cholinergic projections in cognitively unimpaired individuals.

In this study, we investigated the contribution of amyloid and tau pathology in combination with cerebrovascular disease toward the degeneration of cholinergic WM projections in cognitively unimpaired individuals. It is important to address these research questions to assess whether and how other pathologies apart from cerebrovascular disease may affect the integrity of cholinergic projections in cognitively unimpaired individuals.

Methods

Participants

The study sample belongs to the Gothenburg H70 Birth Cohort Studies.[7] Every 70-year-old listed in the Swedish Population Registry as a resident in Gothenburg (Sweden) was invited to a comprehensive examination on aging and age-related factors.[7] A total of 1,203 individuals born in 1944 (response rate 72.2%; mean age 70.5 years) agreed to participate, of whom 430 consented to a lumbar puncture (response rate 35.8%). Lumbar puncture was considered as contraindicated in participants under anticoagulant therapy, immune-modulated therapy, and cancer therapy. After excluding participants not suitable for a lumbar puncture, the CSF extraction was conducted in 322 (26.8%) individuals. Every participant was also invited to take part in a brain MRI examination, of which 792 individuals (response rate 65.8%) underwent MRI conducted at Aleris in Gothenburg. The MRI examination was conducted within 3 months from the initial study visit. The lumbar puncture was conducted within 2 months from the MRI examination. The general examinations and other procedures have previously been described in detail.[7] General cognitive status was measured using the Mini-Mental State Examination (MMSE) and the Clinical Dementia Rating (CDR) scale. For the current study, inclusion criteria were (1) a CDR score of 0; (2) MMSE >24; (3) availability of CSF biomarkers; and (4) availability of MRI data, yielding a final sample of 203 individuals (51% female).

MRI Data Acquisition, Image Processing, and Assessment of WMLs

MRI data were acquired in a 3.0 T Philips Achieva system (Philips Medical Systems), using a 3D T1-weighted turbo field echo sequence (repetition time [RT] = 7.2 ms, echo time

Table 1 Study Sample Demographic and Clinical Data

	Mean (SD)
n	203
Sex (% female)	51
APOE status (% ε4 carriers)	35
MMSE	29.23 (0.98)
Education (y)	13.22 (3.95)
WML volume (mL)	3.01 (2.30)
$A\beta_{38}$ (pg/mL)	2498 (679.15)
$A\beta_{42/40}$ ratio	—
p-tau (pg/mL)	49.45 (17.56)
NBM volume (TIV corrected)	0.20 (0.03)
MD in the cingulum pathway	0.00097 (0.00006)
MD in the external capsule pathway	0.00107 (0.00008)
Hypertension (%)	73.8
Diabetes (%)	11.3
Smoking (%)	61.7
Ischemia (%)	6.04
Cerebral microbleeds (%)	16.7
Lacunes (%)	8.4
Superficial siderosis (%)	1.5

Abbreviations: Aβ = β-amyloid; MD = mean diffusivity; MMSE = Mini-Mental State Examination; NBM = nucleus basalis of Meynert; p-tau = phosphorylated tau 181; WML = white matter lesion.
Values represent mean (SD) unless another parameter is specified. % represents the percentage of individuals with the presence of vascular risk factors of the presence of cerebral microbleeds, lacunes, or superficial siderosis.

[TE] = 3.2 ms, flip angle = 9°, matrix size = 250 × 250 mm, field of view = 256 × 256, and slice thickness = 1.0 mm); a 3D Fluid-attenuated inversion recovery (FLAIR) sequence (RT = 48,000 ms, TE = 280 ms, TI = 1,650 ms, flip angle = 90°, number of slices = 140, matrix size = 250 × 237 mm, and slice thickness = 2.0 mm); a susceptibility-weighted imaging (SWI) sequence (RT = 14.59–17.60 ms, TE = 20.59–24.99 ms, flip angle = 10°, matrix size = 229 × 222 mm, and slice thickness = 1.0 mm); and a DTI sequence encoded with 1 b-value shell: 800 ks/mm^2, along with 32 directions and 1 b = 0 image (RT = 7,340 ms, TE = 83 ms, flip angle = 90°, matrix size = 112 × 112 mm, field of view = 224 × 224, and slice thickness = 3.0 mm).[7]

WMLs were measured as WM hypointensities and WM hyperintensities in T1-weighted and FLAIR sequences, respectively. WML and total intracranial volume (TIV) were automatically segmented using FreeSurfer 6.0.0. FreeSurfer detects hypointense WM signal abnormalities and automatically labels WML volumes for each participant using a probabilistic procedure.[8] Hyperintense WMLs were automatically segmented using the open source segmentation toolbox LST 2.0.15.[9] It has previously been shown that hypointense and hyperintense WMLs are strongly correlated.[6] Previous findings revealed that hypointense WMLs might represent necrotic damage closer to accumulated cerebrovascular pathology,[10] whereas hyperintense WMLs might also represent acute damage including perinflammatory processes.[11] Due to the aim of the current study, we focused on hypointense WMLs, but all the analyses were replicated using hyperintense WMLs and are reported in eFigure 1, links.lww.com/WNL/C220. MRI data management and processing was performed using theHiveDB[12] database system. WML volumes in milliliters (mL) were adjusted by TIV to account for variability in head size.[13]

Previously established ROI masks for the cholinergic WM pathways (i.e., cingulum and external capsule pathways) were used.[4] Briefly, the masks were created using probabilistic diffusion-based fiber tracking of the NBM WM projections. These ROI masks of the cholinergic WM pathways were transferred from MNI standard space to each individual DTI image (b0) in native space using the nonlinear SyN registration algorithm[14] from advanced normalization tools.[15] Native space mean diffusivity (MD) maps were calculated for each subject using the FMRIB Diffusion Toolbox from FSL.[16] Microstructural properties of each participant's cholinergic WM tracts were then calculated by averaging the MD values within the back-transformed ROI masks in native space. The MD index was preferred over the fractional anisotropy (FA) index because MD is more robust in the influence of crossing fibers.[17]

Complementary MRI Markers of Cerebrovascular Disease and Vascular Risk Factors

In addition to the automated measure of WMLs,[18] we assessed cerebral microbleeds, lacunes, and superficial siderosis for completeness of information. The presence/absence of cerebral microbleeds was visually assessed on SWI, lacunes (3–15 mm) were assessed on FLAIR images, and superficial siderosis was assessed on SWI. All visual assessments were performed by an experience neuroradiologist blinded to clinical data,[19] according to the Standards for Reporting Vascular Changes on Neuroimaging and standard scales and standardized scales.[20] We also recorded and described the frequency of vascular risk factors, including hypertension, diabetes, smoking, and ischemia as assessed through a semistructured interview and clinical examination by research nurses or medical doctors.[7]

CSF Sampling and Biomarker Analysis

Lumbar puncture for CSF sampling and determination of *APOE* e4 carriership were conducted following standard procedures.[7] CSF biomarker levels were determined by a commercially available assay.[7] CSF tau phosphorylated at threonine 181 (p-tau) was determined by immunoassay ELISA (INNOTEST PHOSPHO_TAU [181P]). The $A\beta_{42/40}$ ratio and CSF $A\beta_{38}$ were determined by the V-PLEX Aβ Peptide Panel 1 (6E10) Kit (Meso Scale Discovery, Rockville, MD). We used p-tau to assess tau neurofibrillary tangle pathology. The CSF $A\beta_{42/40}$ ratio was used as a marker of amyloidosis.[21]

Figure 1 Contribution of Amyloid, Tau, and Cerebrovascular Biomarkers Toward the Integrity of Cholinergic WM Pathways

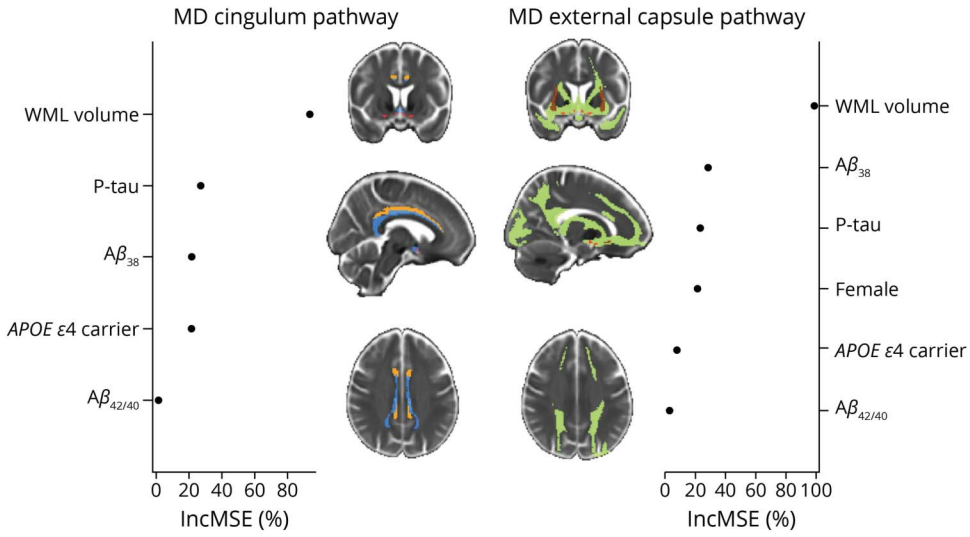

The plot represents the percentage of increase in the prediction error (% IncMSE) when removing each variable from the random forest model. NBM ROI is represented in red. The cingulum pathway is represented in blue (orange for the cingulum mask). The external capsule pathway is represented in green (brown for the external capsule mask). $A\beta_{38}$ = amyloid β_{38}; $A\beta_{42/40}$ = amyloid $\beta_{42/40}$ ratio; P-tau = phosphorylated tau; WML volume = white matter lesions based on hypointense signal abnormalities of T1-weighted 3D images.

For descriptive purposes, each individual was classified as positive (+; i.e., abnormal) or negative (−; i.e., normal) according to CSF biomarkers for Aβ (CSF $A\beta_{42}$) and p-tau (CSF p-tau) following cohort-specific cutoff values: ≤530 pg/mL for $A\beta_{42}$ and p-tau >80.[22] $A\beta_{38}$, a shorter isoform of Aβ that can also be found in the CSF, is still poorly understood. A previous study suggested that $A\beta_{38}$ could be a marker of AD.[23] Another study reported a predominant localization of $A\beta_{38}$ within the vascular vessels in patients with AD.[24] In addition, there is also evidence showing the presence of $A\beta_{38}$ in other non-AD dementias[25–27] and patients with chronic neuroinflammation.[23] These diverse findings reflect the view that the role of $A\beta_{38}$ still needs to be elucidated. Hence, we included CSF $A\beta_{38}$ in this study to determine its association with AD biomarkers and cerebrovascular disease in the general population.

Statistical Analysis

Statistical analyses were conducted using R statistical software.[28] A p value <0.05 (2 tailed) was deemed significant in all the analyses.

We used random forest (RF) regression models to assess the differential contributions of the different pathology-specific biomarkers toward the integrity of NBM projections. Two separate RF regression models, treated as the outcome variables, were fitted for the prediction of MD in the cingulum and the external capsule pathway, respectively. MD values were multiplied by a constant (c = 10,000) to facilitate the visualization of the data. WML, CSF $A\beta_{42/40}$ ratio, $A\beta_{38}$, and p-tau were included as predictors in all RF models, along with sex (i.e., male/female) and *APOE* status (i.e., at least 1 ε4 allele to be treated as carrier, otherwise noncarrier). RF is a machine learning method that estimates multiple decision trees via bootstrap aggregation (bagging). Each tree predicts a classification independently and votes for the corresponding class. The majority of the votes decide the overall prediction.[29,30] A conditional importance score is computed for each tree in RF analysis. This is performed by measuring the change in the prediction error when the values of a certain variable are permuted within a grid defined by the included covariates. Then, this conditional score is averaged across the entire ensemble. These conditional importance scores are designed to reduce the undesirable effects of collinearity among predictor variables. The final importance of each predictor denotes its contribution to the model. Importance values below or equal to zero denote no contribution. A conditional regression tree is produced as a graphical representation of the model. The RF comprised 5,000 conditional inference trees. R2 was computed to assess the quality of the RF models. Although aging is associated with WM neurodegeneration and greater WML volumes,[4,31] age was not included as a covariate in the models because it was controlled from the design (i.e., all participants were aged 70 years). For completeness of information, we also report Pearson correlation coefficients among the predictor variables included in the RF models and independent sample t tests for categorical variables that resulted important in the RF analysis. The randomForest[32] and party packages[33] were used for these analyses.

Standard Protocol Approvals, Registrations, and Patient Consents

The H70 study was approved by the Regional Ethical Review Board in Gothenburg (Approval Numbers: 869-13, T076-14, T166-14, 976-13, 127-14, T936-15, 006-14, T703-14, 006-14, T201-17, T915-14, 959-15, and T139-15) and by the Radiation Protection Committee (Approval Number: 13-64) in concordance with the 1964 Helsinki Declaration and its later amendment.

Data Availability

The authors state that anonymized data on which the article is based will be shared by request from any qualified investigator.

Figure 2 Random Forest Regression Tree for the MD in the Cingulum Pathway

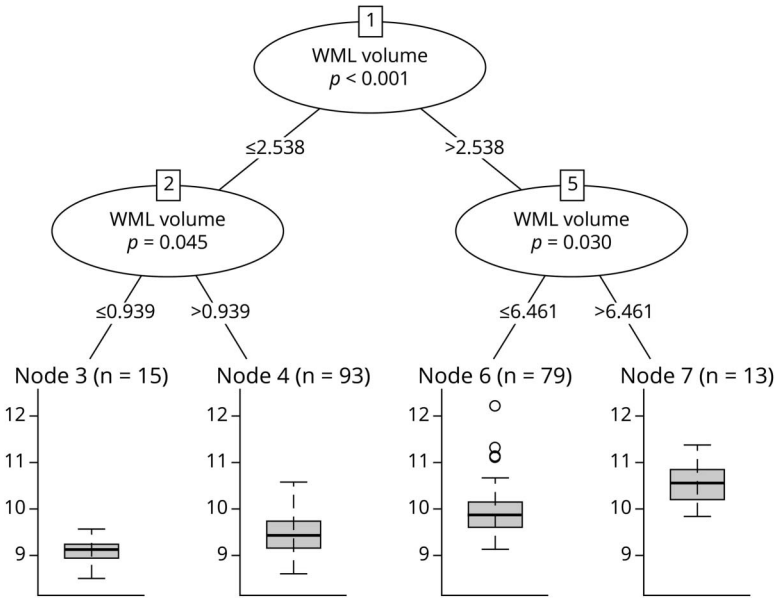

The figure represents the recursive partitioning for the MD index in the cingulum pathway and the contribution of WML volume to the portioning. Corresponding *p* values are given for each inner node. Boxplot for MD distribution is shown for each final group. MD = mean diffusivity; WML volume = white matter lesions based on hypointense signal abnormalities of T1-weighted 3D images.

Results

Demographic, clinical data, vascular risk factors, and MRI markers of cerebrovascular disease are shown in Table 1. In our sample of 203 cognitively unimpaired individuals (all aged 70 years, 51% female), 2% had an AD biomarker profile (i.e., A+ T+), 43% had abnormal CSF levels of β-amyloid only (i.e., A+ T−), and 4.4% had abnormal CSF levels of p-tau only (i.e., A− T+). Results are shown for hypointense WML volume from T1-weighted 3D images. Virtually, the same results were obtained when including hyperintense WMLs instead of hypointense WMLs in the models (eFigure 1, links.lww.com/WNL/C220).

The RF models showed that WML volume was the most important predictor for the average MD of the cingulum pathway (Figure 1). P-tau, $A\beta_{38}$, and *APOE* ε4 carriership were also important predictors in the model. The $A\beta_{42/40}$ ratio received a low importance score. Sex did not contribute to the MD in the cingulum pathway. The RF tree revealed that WML volume was the best predictor splitting individuals according to their MD in the cingulum pathway. Four groups were distinguished (Figure 2). P-tau, $A\beta_{38}$, $A\beta_{42/40}$ ratio, sex, and *APOE* ε4 carriership did not separate any of the groups based on their association with MD in the cingulum pathway.

Regarding the prediction of the MD in the external capsule pathway, WML volume was again the most important predictor (Figure 1). $A\beta_{38}$, p-tau, and sex were also important in the model. Women showed poorer integrity in the external capsule pathway. This finding was independent of amyloid status, as reflected by the nonsignificant differences in integrity when comparing amyloid-positive vs amyloid-negative women participants ($T_{201} = -1.55$; $p = 0.123$). *APOE* ε4 carriership received a low importance score, and the $A\beta_{42/40}$ ratio did not contribute to the MD in the external capsule pathway. The RF tree revealed that WML volume, $A\beta_{38}$, and p-tau were important predictors to split individuals according to their MD in the external capsule. Five groups were distinguished at the end of the tree (Figure 3).

Figure 4 shows the correlation matrix for all pairs of continuous predictors in the RF models. Greater WML volumes were associated with lower $A\beta_{38}$ levels. Higher p-tau levels were associated with lower $A\beta_{42/40}$ ratio and higher $A\beta_{38}$ levels.

Discussion

In our study, we investigated the contribution of cerebrovascular disease compared with amyloid pathology and tau pathology toward the degeneration of cholinergic WM pathways in cognitively unimpaired individuals. We demonstrated the role of WML burden as a central contributor to the degeneration of the cholinergic projections.

The NBM is well known for its key role in cognitive functioning and its deterioration is linked to cognitive impairment in AD.[1] It is important to determine the pathologic processes contributing toward degeneration of the cholinergic system as it has previously been demonstrated to be associated with cognitive impairment in advanced aging.[4] In this sample of cognitively unimpaired aged individuals, we demonstrated that WMLs were the most important contributor toward the degeneration of the studied cholinergic pathways, followed by

Figure 3 Random Forest Regression Tree for the MD in the External Capsule Pathway

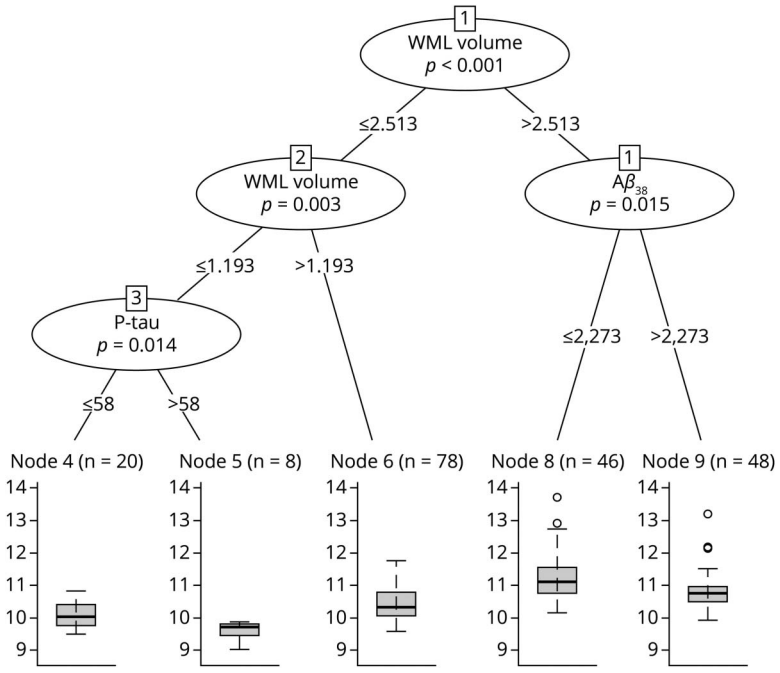

The figure represents the recursive partitioning for the MD index in the external capsule pathway and the contribution of WML volume, p-tau, and $A\beta_{38}$ to the portioning. Corresponding *p* values are given for each inner node. Boxplot for MD distribution is shown for each final group. $A\beta_{38}$ = amyloid β_{38}; MD = mean diffusivity; P-tau = phosphorylated tau; WML volume = white matter lesions based on hypointense signal abnormalities of T1-weighted 3D images.

CSF $A\beta_{38}$ and p-tau levels. Conversely, the $A\beta_{42/40}$ ratio did not show a substantial contribution.

The integrity of the cholinergic system is crucial for proper cognitive functioning.[1] The cholinergic hypothesis of cognitive aging postulates that age-related memory decline and other cognitive problems may arise due to declining cholinergic activity.[34,35] In a previous study, we demonstrated that the WM integrity of cholinergic projections was closely associated with attention and memory performance in an independent aging cohort of cognitively unimpaired individuals.[4] The influence of WML burden on cortical disconnection of the cholinergic system might be associated with subclinical cognitive impairments in the elderly. Longitudinal studies have shown that a high WML burden increases the risk of future cognitive impairment.[36] Future studies should determine the disruptive role of WMLs in the association between cholinergic projections and cognitive performance in normal aging and the continuum of AD.

Although WML burden was the most important predictor in our RF models, we found that $A\beta_{38}$ also contributed to the integrity of the cholinergic system. In contrast, the $A\beta_{42/40}$ ratio was not an important predictor of neurodegeneration of cholinergic WM projections. The role of CSF $A\beta_{38}$ and its association with neurodegeneration is still under debate.[37,38] CSF $A\beta_{38}$ levels are lower in frontotemporal dementia[25] and dementia with Lewy bodies[26,27] than in patients with AD. Furthermore, $A\beta_{38}$ has previously been linked to increased counts of lacunes and cerebral microbleeds, 2 markers of cerebrovascular disease.[39] Deposits of $A\beta_{38}$ in vascular vessels have also been found in postmortem AD studies.[24] Therefore, several studies suggest a potential association of $A\beta_{38}$ with cerebrovascular pathology. In line with this, we showed that lower CSF $A\beta_{38}$ levels were associated with a higher WML burden. In our study, both WML burden and CSF $A\beta_{38}$ were the most important predictors of WM neurodegeneration of the cholinergic system compared with AD biomarkers (CSF $A\beta_{42/40}$ and p-tau). These findings suggest an association between $A\beta_{38}$ and cerebrovascular disease in normal aging and their predilection for the cholinergic WM. Recent reports have demonstrated that higher levels of Aβ38 in the CSF may have a protective effect against future cognitive decline and AD dementia in individuals with a positive AD biomarker profile at baseline.[40] In support of this, decreased CSF $A\beta_{38}$ levels have previously been linked to reduced cingulate and insula cortex volumes in our cohort.[37] The cingulate cortex receives important cholinergic input from the medial cholinergic pathway and the insula from the lateral cholinergic pathway.[1] These areas are well known for their role in emotion regulation, behavior, and executive functioning.[41] Future studies should test whether $A\beta_{38}$, neurodegeneration of the cholinergic system and reduced cingulate and insula gray matter volumes are associated with subclinical changes in emotion regulation and executive functioning in the elderly.

The cholinergic circuitry is highly vulnerable to brain pathology. In our study, we found pathway-dependent associations of WML, $A\beta_{38}$, and tau (p-tau) pathologic markers with cholinergic WM projections. Our results show that individuals

Figure 4 Correlation Matrix for the Predictors Included in the Random Forest Models

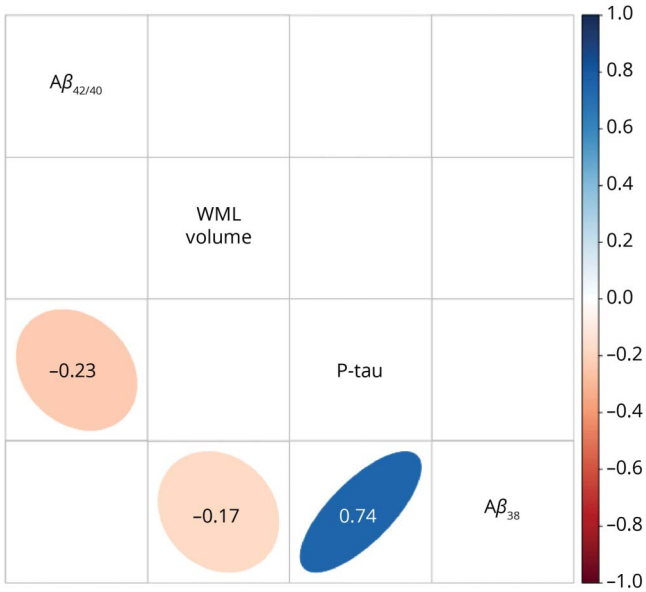

Background of significant correlations ($p < 0.05$) was colored according to the value of the correlation coefficient and shaped accordingly to the association distribution, otherwise left empty.

with decreased $A\beta_{38}$ and high WML burden had the poorest integrity of the external capsule pathway. Of interest, women also showed poorer integrity in the external capsule pathway, independently of amyloid status. In contrast, WML burden was the only predictor of the integrity in the cingulum pathway. These pathway-dependent findings point to a greater vulnerability of the cingulum pathway to vascular pathology, in comparison to amyloid/tau pathologies. Regionally, the cingulum pathway is located in periventricular regions, where the presence of WMLs increases with aging.[42] Periventricular WMLs have previously been associated with lower cortical cholinergic activity in normal aging.[43] Conversely, the external capsule pathway might be more vulnerable to cerebrovascular disease and pathologies associated with $A\beta_{38}$.

Regarding tau pathology, our results showed a negative association between p-tau and degeneration of cholinergic WM projections (i.e., a poorer integrity of WM projections was associated with lower levels of CSF p-tau). This counterintuitive finding might be the result of a selection bias in our sample. All our participants were cognitively unimpaired 70-year-olds, and only 6.4% had abnormal CSF p-tau levels. It is important to take into consideration that the combination of abnormal levels of p-tau with other brain pathologies such as WMLs will most probably result in cognitive impairment, and therefore, those individuals may have been excluded from our study. Whether increased CSF p-tau levels are associated with degeneration of cholinergic WM projections needs to be further tested in more diverse populations of older individuals, including patients with cognitive impairment.

The data provided by this study describe the contribution of the CSF $A\beta_{42/40}$ ratio, $A\beta_{38}$, and p-tau levels in combination with WML burden toward the degeneration of the cholinergic system in cognitively unimpaired elderly from a population-based cohort.[7] However, all individuals included were aged 70 years; therefore, results can only be partially generalized to other age groups. A limitation of the current study, intrinsic to the tractography approach used to generate the cholinergic WM projection masks, is the existence of transverse crossing WM fibers that can lead to distorted information about the WM integrity. We aimed to partly overcome this limitation by using the MD index instead of FA because MD is less affected by crossing fibers.[17] The associations between amyloid/tau biomarkers and WMLs might lead to collinearity problems. Using RF regression with conditional inference trees, we were able to handle multicollinearity to some degree. Alternative information about the spatial location of WMLs and cholinergic functional activity profiles based on fMRI could complement the findings of our current study.[2] We demonstrated an association between Aβ38 and the degeneration of the cholinergic system. Nevertheless, the literature about the role of Aβ38 in neurodegenerative processes is still limited, and further research is needed. There is currently a discussion ongoing as to whether the validated biomarker cutoffs for dementia diagnosis are clinically relevant for preclinical stages of the disease.[44] Subthreshold pathology in individuals exhibiting normal biomarker profiles might already be affecting the brain integrity leading to WM degeneration. Thus, in our study, we used continuous values as the input for the analysis. The integrity of the cholinergic projections across abnormal amyloid/tau profiles in clinical stages of AD needs to be further elucidated. Finally, a previous study demonstrated that WMLs can also be related to AD pathology.[45] However, in our study, WMLs were not associated with CSF levels of $A\beta_{42/40}$ and p-tau, which suggests that our WML measure likely does not reflect AD pathology.[20]

This study highlights the importance of cerebrovascular pathology relative to amyloid and tau pathology in their contribution to cholinergic neurodegeneration in cognitively unimpaired individuals. WMLs within cholinergic pathways correlate with cognitive impairment[46] and executive dysfunction[47] in patients with dementia. Given the central role of the cholinergic system in cognition, our study suggests that management of cholinergic WMLs and vascular risk factors should be considered in the development of prevention programs for neurodegeneration and cognitive impairment. As these data are replicated in independent cohorts, it may help in clinical considerations with regard to cerebrovascular and AD biomarkers, cholinergic dysfunction, and cognitive impairment. This knowledge could eventually support therapeutic decisions in the context of acetylcholinesterase inhibitors.

Study Funding

This research was supported by the Swedish Research Council (2012-5041, 2013-8717, 2015-02830, 2016-02282, 2016-02282, 2020-02014, and 2021-01861), the Swedish

Research Council for Health, Working Life and Welfare (2013-1202, AGECAP 2013-2300, 2013-2496, and 2013-0475), the Swedish Foundation for Strategic Research (SSF, RB13-0192), the Strategic Research Programme in Neuroscience at Karolinska Institutet (StratNeuro), the Swedish State under the agreement between the Swedish government and the county councils, the ALF agreement (FoUI-954893 and FoUI-962240), the Center for Medical Innovation (CIMED, FoUI-954459 and FoUUI-20200505), the Swedish Alzheimer Foundation (AF-967495, AF-939687, and AF-968032), the Swedish Brain Foundation (FO2020-0150, FO2021-0119, and FO2022-0175), Stonhes Stiftelse, Stiftelsen för Gamla Tjänarinnor, Demensförbundet, Neurofonden, Lindhés Advokatbyrå AB, Eivind och Elsa K: son Sylvans Stiftelse, Stiftelsen Demensfonden, Stiftelsen Hjalmar Svenssons Forskningsfond, Stiftelsen Wilhelm och Martina Lundgrens Vetenskapsfond, Funding for Geriatric diseases at Karolinska Institutet, Research funding at Karolinska Institutet, Fundacion Canaria Dr. Manuel Morales, and the Czech Alzheimer Foundation. MJG is supported by the "Miguel Servet" program [CP19/00031] and a research grant [PI20/00613] of the Instituto de Salud Carlos III-Fondo Europeo de Desarrollo Regional (ISCIII-FEDER). J.B. Pereira is supported by grants from the Swedish Research Council (2018-02201), the Strategic Research Programme in Neuroscience at Karolinska Institutet (StratNeuro Startup Grant), The Center for Medical Innovation (20200695), Gamla Tjänarinnor (2019-00803), Demensforbundet, Stonhes, and a Senior Researcher faculty position from Karolinska Institutet. H. Zetterberg is a Wallenberg Scholar supported by grants from the Swedish Research Council (#2018–02532), the European Research Council (#681712), Swedish State Support for Clinical Research (ALFGBG-720931), the Alzheimer Drug Discovery Foundation (ADDF), USA (201809-2016862), the AD Strategic Fund and the Alzheimer's Association (ADSF-21-831376-C, ADSF-21-831381-C, and ADSF-21-831377-C), the Olav Thon Foundation, the Erling-Persson Family Foundation, Stiftelsen för Gamla Tjänarinnor, Hjärnfonden, Sweden (#FO2019-0228), the European Union's Horizon 2020 research and innovation program under the Marie Skłodowska-Curie grant agreement No 860197 (MIRIADE), and the UK Dementia Research Institute at UCL. S. Kern was financed by grants from the Swedish state under the agreement between the Swedish government and the county councils, the ALF agreement (ALF GBG-81392 and ALF GBG-771071), the Alzheimerfonden (AF-842471, AF-737641, and AF-939825), and the Swedish Research Council (2019-02075) Stiftelsen Demensfonden, Stiftelsen Hjalmar Svenssons Forskningsfond, Stiftelsen Wilhelm och Martina Lundgrens Vetenskapsfond.

Disclosure

M. Eriksdotter has served as a consultant for Biogen unrelated to the present study. H. Zetterberg has served on scientific advisory boards and/or as a consultant for Alector, Eisai, Denali, Roche Diagnostics, Wave, Samumed, Siemens Healthineers, Pinteon Therapeutics, Nervgen, AZTherapies, CogRx, and Red Abbey Labs; has given lectures in symposia sponsored by Cellectricon, Fujirebio, Alzecure, and Biogen; and is a cofounder of Brain Biomarker Solutions in Gothenburg AB (BBS), which is a part of the GU Ventures Incubator Program (outside submitted work). S. Kern has served on a scientific advisory board and/or as a consultant for Geras Solutions and Biogen, unrelated to the present study. The other authors report no relevant disclosures. Go to Neurology.org/N for full disclosures.

Publication History

Received by *Neurology* October 28, 2021. Accepted in final form May 19, 2022. Submitted and externally peer reviewed. The handling editor was Rawan Tarawneh, MD.

Appendix Authors

Name	Location	Contribution
Nira Cedres, PhD	Division of Clinical Geriatrics, Centre for Alzheimer Research, Department of Neurobiology, Care Sciences, and Society, Karolinska Institutet, Stockholm, Sweden; Department of Psychology, Sensory Cognitive Interaction Laboratory (SCI-lab), Stockholm University, Stockholm, Sweden	Drafting/revision of the manuscript for content, including medical writing for content; study concept or design; and analysis or interpretation of data
Daniel Ferreira, PhD	Division of Clinical Geriatrics, Centre for Alzheimer Research, Department of Neurobiology, Care Sciences, and Society, Karolinska Institutet, Stockholm, Sweden; Department of Radiology, Mayo Clinic, Rochester, MN	Drafting/revision of the manuscript for content, including medical writing for content; study concept or design; and analysis or interpretation of data
Milan Nemy, MSc	Department of Cybernetics, Faculty of Electrical Engineering, Czech Technical University, Prague, Czech Republic; Czech Institute of Informatics, Robotics, and Cybernetics, Czech Technical University, Prague, Czech Republic	Drafting/revision of the manuscript for content, including medical writing for content; study concept or design; and analysis or interpretation of data
Alejandra Machado, PhD	Division of Clinical Geriatrics, Centre for Alzheimer Research, Department of Neurobiology, Care Sciences, and Society, Karolinska Institutet, Stockholm, Sweden; Division of Insurance Medicine, Department of Clinical Neuroscience, Karolinska Institutet, Stockholm, Sweden	Drafting/revision of the manuscript for content, including medical writing for content, and analysis or interpretation of data
Joana B. Pereira, PhD	Division of Clinical Geriatrics, Centre for Alzheimer Research, Department of Neurobiology, Care Sciences, and Society, Karolinska Institutet, Stockholm, Sweden; Clinical Memory Research Unit, Department of Clinical Sciences, Lund University, Malmö, Sweden	Drafting/revision of the manuscript for content, including medical writing for content, and analysis or interpretation of data

Appendix *(continued)*

Name	Location	Contribution
Sara Shams, PhD	Division of Clinical Geriatrics, Centre for Alzheimer Research, Department of Neurobiology, Care Sciences, and Society, Karolinska Institutet, Stockholm, Sweden	Analysis or interpretation of data
Lars-Olof Wahlund, PhD	Division of Clinical Geriatrics, Centre for Alzheimer Research, Department of Neurobiology, Care Sciences, and Society, Karolinska Institutet, Stockholm, Sweden	Drafting/revision of the manuscript for content, including medical writing for content, and study concept or design
Anna Zettergren, PhD	Region Västra Götaland, Sahlgrenska University Hospital, Department of Psychiatry Cognition and Old Age Psychiatry, Gothenburg, Sweden; Neuropsychiatric Epidemiology Unit, Department of Psychiatry and Neurochemistry, Institute of Neuroscience and Physiology, the Sahlgrenska Academy, Centre for Ageing and Health (AGECAP) at the University of Gothenburg, Gothenburg, Sweden	Drafting/revision of the manuscript for content, including medical writing for content, and major role in the acquisition of data
Olga Stepankova, PhD	Czech Institute of Informatics, Robotics, and Cybernetics, Czech Technical University, Prague, Czech Republic	Drafting/revision of the manuscript for content, including medical writing for content, and study concept or design
Lenka Vyslouzilova, PhD	Czech Institute of Informatics, Robotics, and Cybernetics, Czech Technical University, Prague, Czech Republic	Drafting/revision of the manuscript for content, including medical writing for content, and study concept or design
Maria Eriksdotter, PhD	Division of Clinical Geriatrics, Centre for Alzheimer Research, Department of Neurobiology, Care Sciences, and Society, Karolinska Institutet, Stockholm, Sweden; Theme Inflammation and aging, Karolinska University Hospital, Huddinge, Sweden	Drafting/revision of the manuscript for content, including medical writing for content, and study concept or design
Stefan Teipel, MD	Clinical Dementia Research Section, Department of Psychosomatic Medicine, University Medicine Rostock, Rostock, Germany; German Center for Neurodegenerative Diseases (DZNE), Rostock, Germany	Drafting/revision of the manuscript for content, including medical writing for content, and study concept or design
Michel J. Grothe, PhD	German Center for Neurodegenerative Diseases (DZNE), Rostock, Germany; Unidad de Trastornos del Movimiento, Servicio de Neurología y Neurofisiología Clínica, Instituto de Biomedicina de Sevilla (IBiS), Hospital Universitario Virgen del Rocío/CSIC/Universidad de Sevilla, Seville, Spain	Drafting/revision of the manuscript for content, including medical writing for content, and study concept or design

Appendix *(continued)*

Name	Location	Contribution
Kaj Blennow, MD, PhD	Neuropsychiatric Epidemiology Unit, Department of Psychiatry and Neurochemistry, Institute of Neuroscience and Physiology, the Sahlgrenska Academy, Centre for Ageing and Health (AGECAP) at the University of Gothenburg, Gothenburg, Sweden; Clinical Neurochemistry Laboratory, Sahlgrenska University Hospital, Sweden	Drafting/revision of the manuscript for content, including medical writing for content, and major role in the acquisition of data
Henrik Zetterberg, MD, PhD	Neuropsychiatric Epidemiology Unit, Department of Psychiatry and Neurochemistry, Institute of Neuroscience and Physiology, the Sahlgrenska Academy, Centre for Ageing and Health (AGECAP) at the University of Gothenburg, Gothenburg, Sweden; Clinical Neurochemistry Laboratory, Sahlgrenska University Hospital, Sweden; Department of Neurodegenerative Disease, UCL Institute of Neurology, London, United Kingdom; UK Dementia Research Institute at UCL, London, United Kingdom; Hong Kong Center for Neurodegenerative Diseases, Hong Kong, China	Drafting/revision of the manuscript for content, including medical writing for content, and major role in the acquisition of data
Michael Schöll, PhD	Wallenberg Centre for Molecular and Translational Medicine, University of Gothenburg, Gothenburg, Sweden; Department of Psychiatry and Neurochemistry, Institute of Physiology and Neuroscience, University of Gothenburg, Gothenburg, Sweden; Dementia Research Centre, Institute of Neurology, University College London, London, UK; Department of Clinical Physiology, Sahlgrenska University Hospital, Gothenburg, Sweden	Drafting/revision of the manuscript for content, including medical writing for content, and major role in the acquisition of data
Silke Kern, PhD	Region Västra Götaland, Sahlgrenska University Hospital, Department of Psychiatry Cognition and Old Age Psychiatry, Gothenburg, Sweden; Neuropsychiatric Epidemiology Unit, Department of Psychiatry and Neurochemistry, Institute of Neuroscience and Physiology, the Sahlgrenska Academy, Centre for Ageing and Health (AGECAP) at the University of Gothenburg, Gothenburg, Sweden	Drafting/revision of the manuscript for content, including medical writing for content, and major role in the acquisition of data

Continued

Appendix *(continued)*

Name	Location	Contribution
Ingmar Skoog, MD, PhD	Region Västra Götaland, Sahlgrenska University Hospital, Department of Psychiatry Cognition and Old Age Psychiatry, Gothenburg, Sweden; Neuropsychiatric Epidemiology Unit, Department of Psychiatry and Neurochemistry, Institute of Neuroscience and Physiology, the Sahlgrenska Academy, Centre for Ageing and Health (AGECAP) at the University of Gothenburg, Gothenburg, Sweden	Drafting/revision of the manuscript for content, including medical writing for content, and major role in the acquisition of data
Eric Westman, PhD	Division of Clinical Geriatrics, Centre for Alzheimer Research, Department of Neurobiology, Care Sciences, and Society, Karolinska Institutet, Stockholm, Sweden; Department of Neuroimaging, Centre for Neuroimaging Sciences, Institute of Psychiatry, Psychology and Neuroscience, King's College London, London, UK	Drafting/revision of the manuscript for content, including medical writing for content; study concept or design; and analysis or interpretation of data

References

1. Mesulam M-M. Cholinergic circuitry of the human nucleus basalis and its fate in Alzheimer's disease. *J Comp Neurol.* 2013;521(18):4124-4144. doi.wiley.com/10.1002/cne.23415.
2. Herdick M, Dyrba M, Fritz H-CJ, et al. Multimodal MRI analysis of basal forebrain structure and function across the Alzheimer's disease spectrum. *Neuroimage Clin.* 2020;28:102495. doi.org/10.1016/j.nicl.2020.102495.
3. Fritz HCJ, Ray N, Dyrba M, Sorg C, Teipel S, Grothe MJ. The corticotopic organization of the human basal forebrain as revealed by regionally selective functional connectivity profiles. *Hum Brain Mapp.* 2019;40(3):868-878.
4. Nemy M, Cedres N, Grothe MJ, et al. Cholinergic white matter pathways make a stronger contribution to attention and memory in normal aging than cerebrovascular health and nucleus basalis of Meynert. *Neuroimage.* 2020;211:116607.
5. Teipel SJ, Meindl T, Grinberg L, et al. The cholinergic system in mild cognitive impairment and Alzheimer's disease: an in vivo MRI and DTI study. *Hum Brain Mapp.* 2011;32(9):1349-1362.
6. Cedres N, Ferreira D, Machado A, et al. Predicting Fazekas scores from automatic segmentations of white matter signal abnormalities. *Aging (Albany NY).* 2020;12(1):894-901. aging-us.com/article/102662/text.
7. Rydberg Sterner T, Ahlner F, Blennow K, et al. The Gothenburg H70 Birth cohort study 2014-16: design, methods and study population. *Eur J Epidemiol.* 2019;34(2):191-209. link.springer.com/10.1007/s10654-018-0459-8.
8. Fischl B, Salat DH, Busa E, et al. Whole brain segmentation: automated labeling of neuroanatomical structures in the human brain. *Neuron.* 2002;33(3):341-355.
9. Schmidt P, Gaser C, Arsic M, et al. An automated tool for detection of FLAIR-hyperintense white-matter lesions in Multiple Sclerosis. *Neuroimage.* 2012;59(4):3774-3783. dx.doi.org/10.1016/j.neuroimage.2011.11.032.
10. Riphagen JM, Gronenschild EHBM, Salat DH, et al. Shades of white: diffusion properties of T1- and FLAIR-defined white matter signal abnormalities differ in stages from cognitively normal to dementia. *Neurobiol Aging.* 2018;68:48-58. linkinghub.elsevier.com/retrieve/pii/S0197458018301180.
11. Olsson E, Klasson N, Berge J, et al. White matter lesion assessment in patients with cognitive impairment and healthy controls: reliability comparisons between visual rating, a manual, and an automatic volumetrical MRI method–the gothenburg MCI study. *J Aging Res.* 2013;2013:198471.
12. Muehlboeck J-S, Westman E, Simmons A. TheHiveDB image data management and analysis framework. *Front Neuroinform.* 2014;7:49-13. journal.frontiersin.org/article/10.3389/fninf.2013.00049/abstract.
13. Voevodskaya O. The effects of intracranial volume adjustment approaches on multiple regional MRI volumes in healthy aging and Alzheimer's disease. *Front Aging Neurosci.* 2014;6:1-14.
14. Avants BB, Epstein CL, Grossman M, Gee JC. Symmetric diffeomorphic image registration with cross-correlation: evaluating automated labeling of elderly and neurodegenerative brain. *Med Image Anal.* 2008;12(1):26-41. ncbi.nlm.nih.gov/pmc/articles/PMC3624763/pdf/nihms412728.pdf.
15. Avants BB, Yushkevich P, Pluta J, Minkoff D, Korczykowski M, Detre J, Gee JC. The optimal template effect in hippocampus studies of diseased populations. *Neuroimage.* 2010;49(3):2457-66. doi: 10.1016/j.neuroimage.2009.09.062.
16. Smith S.M, Jenkinson M, Woolrich M.W, Beckmann CF, Behrens T.E.J, Johansen-Berg H, et al. Advances in functional and structural MR image analysis and implementation as FSL. *Neuroimage.* 2004;23(S1):208-19.
17. Dauguet J, Peled S, Berezovskii V, et al. Comparison of fiber tracts derived from in-vivo DTI tractography with 3D histological neural tract tracer reconstruction on a macaque brain. *Neuroimage.* 2007;37(2):530-538. sciencedirect.com/science/article/pii/S105381190700328X.
18. Badji A, Pereira JB, Shams S, et al. Cerebrospinal fluid biomarkers, brain structural and cognitive performances between normotensive and hypertensive controlled, uncontrolled and untreated 70-year-old adults. *Front Aging Neurosci.* 2021;13:777475.
19. Rydén L, Sacuiu S, Wetterberg H, et al. Atrial fibrillation, stroke, and silent cerebrovascular disease: a population-based MRI study. *Neurology.* 2021;97(16):E1608-E1619.
20. Wardlaw JM, Smith EE, Biessels GJ, et al, Standards for ReportIng Vascular Changes on Neuroimaging STRIVE v1. Neuroimaging standards for research into small vessel disease and its contribution to ageing and neurodegeneration. *Lancet Neurol.* 2013;12(8):822-838. ncbi.nlm.nih.gov/pubmed/23867200.
21. Hansson O, Lehmann S, Otto M, Zetterberg H, Lewczuk P. Advantages and disadvantages of the use of the CSF Amyloid β (Aβ) 42/40 ratio in the diagnosis of Alzheimer's Disease. *Alzheimers Res Ther.* 2019;11:1-15.
22. Kern S, Zetterberg H, Zettergren A, et al. The prevalence of preclinical Alzheimer's disease in a population study of 70-year-olds. *Alzheimers Dement.* 2017;13:P848. linkinghub.elsevier.com/retrieve/pii/S1552526017314279.
23. Wiltfang J, Esselmann H, Bibl M, et al. Highly conserved and disease-specific patterns of carboxyterminally truncated Abeta peptides 1-37/38/39 in addition to 1-40/42 in Alzheimer's disease and in patients with chronic neuroinflammation. *J Neurochem.* 2002;81(3):481-496.
24. Reinert J, Martens H, Huettenrauch M, et al. Aβ38 in the brains of patients with sporadic and familial Alzheimer's disease and transgenic mouse models. *J Alzheimers Dis.* 2014;39(4):871-881.
25. Heywood WE, Hallqvist J, Heslegrave AJ, et al. CSF pro-orexin and amyloid-β38 expression in Alzheimer's disease and frontotemporal dementia. *Neurobiol Aging.* 2018;72:171-176. doi.org/10.1016/j.neurobiolaging.2018.08.019.
26. Mulugeta E, Londos E, Ballard C, et al. CSF amyloid β38 as a novel diagnostic marker for dementia with Lewy bodies. *J Neurol Neurosurg Psychiatry.* 2011;82(2):160-164.
27. Van Steenoven I, Van Der Flier WM, Scheltens P, Teunissen CE, Lemstra AW. Amyloid-β peptides in cerebrospinal fluid of patients with dementia with Lewy bodies. *Alzheimers Res Ther.* 2019;11:8-10.
28. R Core Team. *R: A language and environment for statistical computing.* R Foundation for Statistical Computing, Vienna, Austria. 2022. https://www.R-project.org/.
29. Breiman L. Bagging predictions. *Mach Learn.* 1996;24:123-140.
30. Breiman L Random forests. *Mach Learn.*2001;45(1):5-32.
31. Cedres N, Diaz-Galvan P, Diaz-Flores L, et al. The interplay between gray matter and white matter neurodegeneration in subjective cognitive decline. *Aging (Albany NY).* 2021;13(16):19963-19977.
32. Liaw AL, Wiener M. Classification and regression by randomForest. *R News 2.* 2003;3:18-22.
33. Hothorn T, Hornik K, Strobl C, Zeileis A. *party: A Laboratory for Recursive Partytioning. R Package Version 09-0.* 2015:37. http//CRAN R-project orgparty.r-forge.r-project.org/.
34. Dumas JA, Kutz AM, Mcdonald BC, et al. Aged women with cognitive complaints. *Neurobiol Aging.* 2014;34:1145-1147.
35. Contestabile A. The history of the cholinergic hypothesis. *Behav Brain Res.* 2011;221(2):334-340. dx.doi.org/10.1016/j.bbr.2009.12.044.
36. Benedictus MR, Van Harten AC, Leeuwis AE, et al. White matter hyperintensities relate to clinical progression in subjective cognitive decline. *Stroke.* 2015;46(9):2661-2664.
37. Lindberg O, Kern S, Skoog J, et al. Effects of amyloid pathology and the APOE ε4 allele on the association between cerebrospinal fluid Aβ38 and Aβ40 and brain morphology in cognitively normal 70-years-old. *Neurobiol Aging.* 2021;101:1-12.
38. Bibl M, Mollenhauer B, Lewczuk P, et al. Cerebrospinal fluid tau, p-tau 181 and amyloid-$\beta_{38/40/42}$ in frontotemporal dementias and primary progressive aphasias, *Dement Geriatr Cogn Disord.* 2011;31:37-44. karger.com/DOI/10.1159/000322370.
39. Hilal S, Akoudad S, Van Duijn CM, et al. Plasma amyloid-β levels, cerebral small vessel disease, and cognition: The Rotterdam study. *J Alzheimers Dis.* 2017;60(3):977-987.
40. Cullen N, Janelidze S, Palmqvist S, Stomrud E, Mattsson-Carlgren N, Hansson O, Alzheimer's Disease Neuroimaging Initiative. Association of CSF Aβ38 levels with risk of Alzheimer disease–related decline. *Neurology.* 2022;98(9):e958-e967. doi: 10.1212/WNL.0000000000013228.
41. Hadland KA, Rushworth MFS, Gaffan D, Passingham RE. The effect of cingulate lesions on social behaviour and emotion. *Neuropsychologia.* 2003;41(8):919-931.
42. de Leeuw FE, de Groot JC, Achten E, et al. Prevalence of cerebral white matter lesions in elderly people: a population based magnetic resonance imaging study. The Rotterdam Scan Study. *J Neurol Neurosurg Psychiatry.* 2001;70(1):9-14. ncbi.nlm.nih.gov/pubmed/11118237.
43. Bohnen NI, Müller MLTM, Kuwabara H, Constantine GM, Studenski SA. Age-associated leukoaraiosis and cortical cholinergic deafferentation. *Neurology.* 2009;72(16):1411-1416.

44. Miller A-M, Balasa M, Blennow K, et al. Current approaches and clinician attitudes to the use of cerebrospinal fluid biomarkers in diagnostic evaluation of dementia in europe. *J Alzheimers Dis.* 2017;60(1):201-210.
45. McAleese KE, Firbank M, Dey M, et al. Cortical tau load is associated with white matter hyperintensities. *Acta Neuropathologica Commun.* 2015;3:60. dx.doi.org/10.1186/s40478-015-0240-0.
46. Kim SH, Kang HS, Kim HJ, et al. The effect of ischemic cholinergic damage on cognition in patients with subcortical vascular cognitive impairment. *J Geriatr Psychiatry Neurol.* 2012;25(2):122-127. doi.org/10.1177/0891988712445089.
47. Behl P, Bocti C, Swartz RH, et al. Strategic subcortical hyperintensities in cholinergic pathways and executive function decline in treated Alzheimer patients. *Arch Neurol.* 2007;64(2):266-272.

Association of Cerebrovascular and Alzheimer Disease Biomarkers With Cholinergic White Matter Degeneration in Cognitively Unimpaired Individuals

Nira Cedres, Daniel Ferreira, Milan Nemy, et al.

Neurology 2022;99;e1619-e1629 Published Online before print August 2, 2022
DOI 10.1212/WNL.0000000000200930

III

https://doi.org/10.1093/brain/awac385 BRAIN 2023: 0; 1–14 | 1

BRAIN
ORIGINAL ARTICLE

Cholinergic white matter pathways along the Alzheimer's disease continuum

Milan Nemy,[1,2,3] Martin Dyrba,[4] Frederic Brosseron,[5] Katharina Buerger,[6,7] Peter Dechent,[8] Laura Dobisch,[9] Michael Ewers,[6,7] Klaus Fliessbach,[5,10] Wenzel Glanz,[9] Doreen Goerss,[4,11] Michael T. Heneka,[5,10] Stefan Hetzer,[12] Enise I. Incesoy,[9,13] Daniel Janowitz,[7] Ingo Kilimann,[4,11] Christoph Laske,[14,15] Franziska Maier,[16] Matthias H. Munk,[14,15] Robert Perneczky,[6,17,18,19,20] Oliver Peters,[21,22] Lukas Preis,[22] Josef Priller,[21,23,24,25] Boris-Stephan Rauchmann,[17] Sandra Röske,[5] Nina Roy,[5] Klaus Scheffler,[26] Anja Schneider,[5,10] Björn H. Schott,[27,28,29] Annika Spottke,[5,30] Eike J. Spruth,[21,23] Michael Wagner,[5,10] Jens Wiltfang,[27,28,31] Renat Yakupov,[9] Maria Eriksdotter,[3,32] Eric Westman,[3,33] Olga Stepankova,[2] Lenka Vyslouzilova,[2] Emrah Düzel,[9,13] Frank Jessen,[5,16,34] Stefan J. Teipel[4,11,†] and Daniel Ferreira[3,†]

[†]These authors contributed equally to this work.

Previous studies have shown that the cholinergic nucleus basalis of Meynert and its white matter projections are affected in Alzheimer's disease dementia and mild cognitive impairment. However, it is still unknown whether these alterations can be found in individuals with subjective cognitive decline, and whether they are more pronounced than changes found in conventional brain volumetric measurements. To address these questions, we investigated microstructural alterations of two major cholinergic pathways in individuals along the Alzheimer's disease continuum using an *in vivo* model of the human cholinergic system based on neuroimaging.

We included 402 participants (52 Alzheimer's disease, 66 mild cognitive impairment, 172 subjective cognitive decline and 112 healthy controls) from the Deutsches Zentrum für Neurodegenerative Erkrankungen Longitudinal Cognitive Impairment and Dementia Study. We modelled the cholinergic white matter pathways with an enhanced diffusion neuroimaging pipeline that included probabilistic fibre-tracking methods and prior anatomical knowledge. The integrity of the cholinergic white matter pathways was compared between stages of the Alzheimer's disease continuum, in the whole cohort and in a CSF amyloid-beta stratified subsample. The discriminative power of the integrity of the pathways was compared to the conventional volumetric measures of hippocampus and nucleus basalis of Meynert, using a receiver operating characteristics analysis. A multivariate model was used to investigate the role of these pathways in relation to cognitive performance.

We found that the integrity of the cholinergic white matter pathways was significantly reduced in all stages of the Alzheimer's disease continuum, including individuals with subjective cognitive decline. The differences involved posterior cholinergic white matter in the subjective cognitive decline stage and extended to anterior frontal white matter in mild cognitive impairment and Alzheimer's disease dementia stages. Both cholinergic pathways and conventional volumetric measures showed higher predictive power in the more advanced stages of the disease, i.e. mild cognitive impairment and Alzheimer's disease dementia. In contrast, the integrity of cholinergic pathways was more informative in distinguishing subjective cognitive decline from healthy controls, as compared with the volumetric measures. The multivariate model revealed a moderate contribution of the cholinergic white matter pathways but

Received June 12, 2022. Revised September 12, 2022. Accepted September 19, 2022. Advance access publication October 26, 2022

not of volumetric measures towards memory tests in the subjective cognitive decline and mild cognitive impairment stages.
In conclusion, we demonstrated that cholinergic white matter pathways are altered already in subjective cognitive decline individuals, preceding the more widespread alterations found in mild cognitive impairment and Alzheimer's disease. The integrity of the cholinergic pathways identified the early stages of Alzheimer's disease better than conventional volumetric measures such as hippocampal volume or volume of cholinergic nucleus basalis of Meynert.

1 Department of Cybernetics, Faculty of Electrical Engineering, Czech Technical University in Prague, Prague, Czech Republic
2 Department of Biomedical Engineering and Assistive Technology, Czech Institute of Informatics, Robotics and Cybernetics, Czech Technical University in Prague, Prague, Czech Republic
3 Division of Clinical Geriatrics, Center for Alzheimer Research, Department of Neurobiology, Care Sciences and Society, Karolinska Institute, Stockholm, Sweden
4 German Center for Neurodegenerative Diseases (DZNE), Rostock, Germany
5 German Center for Neurodegenerative Diseases (DZNE), Bonn, Germany
6 German Center for Neurodegenerative Diseases (DZNE), Munich, Germany
7 Institute for Stroke and Dementia Research (ISD), University Hospital, LMU Munich, Munich, Germany
8 MR-Research in Neurosciences, Department of Cognitive Neurology, Georg-August-University Goettingen, Goettingen, Germany
9 German Center for Neurodegenerative Diseases (DZNE), Magdeburg, Germany
10 Department for Neurodegenerative Diseases and Geriatric Psychiatry, University Hospital Bonn, Bonn, Germany
11 Department of Psychosomatic Medicine, Rostock University Medical Center, Rostock, Germany
12 Berlin Center for Advanced Neuroimaging, Charité—Universitätsmedizin Berlin, Berlin, Germany
13 Institute of Cognitive Neurology and Dementia Research, Otto-von-Guericke University, Magdeburg, Germany
14 German Center for Neurodegenerative Diseases (DZNE), Tübingen, Germany
15 Section for Dementia Research, Hertie Institute for Clinical Brain Research and Department of Psychiatry and Psychotherapy, University of Tübingen, Tübingen, Germany
16 Department of Psychiatry, Medical Faculty, University of Cologne, Cologne, Germany
17 Department of Psychiatry and Psychotherapy, University Hospital, LMU Munich, Munich, Germany
18 Munich Cluster for Systems Neurology (SyNergy), Munich, Germany
19 Ageing Epidemiology Research Unit (AGE), School of Public Health, Imperial College London, London, UK
20 Sheffield Institute for Translational Neurosciences (SITraN), University of Sheffield, Sheffield, UK
21 German Center for Neurodegenerative Diseases (DZNE), Berlin, Germany
22 Department of Psychiatry, Charité-Universitätsmedizin Berlin, Campus Benjamin Franklin, Berlin, Germany
23 Department of Psychiatry and Psychotherapy, Charité, Berlin, Germany
24 Department of Psychiatry and Psychotherapy, School of Medicine, Technical University of Munich, Munich, Germany
25 Centre for Clinical Brain Sciences, University of Edinburgh and UK DRI, Edinburgh, UK
26 Department for Biomedical Magnetic Resonance, University of Tübingen, Tübingen, Germany
27 German Center for Neurodegenerative Diseases (DZNE), Goettingen, Germany
28 Department of Psychiatry and Psychotherapy, University Medical Center Goettingen, University of Goettingen, Goettingen, Germany
29 Leibniz Institute for Neurobiology, Magdeburg, Germany
30 Department of Neurology, University of Bonn, Bonn, Germany
31 Neurosciences and Signaling Group, Institute of Biomedicine (iBiMED), Department of Medical Sciences, University of Aveiro, Aveiro, Portugal
32 Theme Inflammation and Aging, Karolinska University Hospital, Stockholm, Sweden
33 Department of Neuroimaging, Centre for Neuroimaging Science, Institute of Psychiatry, Psychology, and Neuroscience, King's College London, London, UK
34 Excellence Cluster on Cellular Stress Responses in Aging-Associated Diseases (CECAD), University of Cologne, Cologne, Germany

Correspondence to: Daniel Ferreira
Division of Clinical Geriatrics, Center for Alzheimer Research
Department of Neurobiology, Care Sciences and Society
NEO floor 7th, Karolinska Institutet, 141 57
Huddinge, Stockholm, Sweden
E-mail: daniel.ferreira.padilla@ki.se

Keywords: cholinergic system; nucleus basalis of Meynert; Alzheimer's disease; CSF markers; MRI

Introduction

Current research in the field of Alzheimer's disease[1–3] suggests that pathological changes in the human brain can be observed decades before the onset of clinically detectable dementia.[4] Therefore, a disease continuum has been described, ranging from subjective cognitive decline (SCD) or preclinical Alzheimer's disease to mild cognitive impairment (MCI) and fully developed dementia.[5] In the later stages of the continuum, major pathological and clinical changes are present, e.g. extracellular amyloid-beta (Aβ) plaques and intracellular neurofibrillary tangle pathology, memory loss and other cognitive alterations.[6] However, the brain changes taking place in the very early stages are less known. Capturing the earliest neurodegenerative changes is challenging because conventional quantitative biomarkers might not be sensitive enough.

Neurons in the hippocampus, basal forebrain (BF) and its subregion including the nucleus basalis of Meynert (NBM), are selectively vulnerable to Alzheimer's disease pathology.[7] Both hippocampus and NBM are among the first brain structures to show signs of deterioration. They can be assessed through *in vivo* volumetric measurements based on MRI.[8] Recent studies have shown that NBM volume is an earlier biomarker of Alzheimer's disease-like neurodegeneration, as compared with the more conventional hippocampal volumetric measures.[9] This finding suggests that the loss of NBM neurons might be one of the earliest events of neurodegeneration in Alzheimer's disease. The NBM and its cholinergic circuitry are heavily involved in cognitive decline characteristic of aging and age-related disorders, including Alzheimer's disease.[10] Furthermore, neurons with long axonal connections are particularly susceptible to Alzheimer's disease-related pathology.[11] These vulnerable groups of neurons seem to follow a dying-back pattern of degeneration, in which defects in myelinization and synaptic dysfunction forego somatic cell death.[11] There is also evidence that the early white matter (WM) changes can be observed *in vivo* using diffusion MRI.[12,13] A recent study demonstrated alterations in mean diffusivity of NBM WM projections in patients with Alzheimer's disease and patients with MCI, using diffusion MRI.[14] What remains unknown is how cholinergic projections change in the preclinical stage of Alzheimer's disease and how these changes relate to other common biomarkers.

The overall goal of the current study was to investigate neurodegeneration of the human cholinergic system using diffusion-weighted MRI across the stages of the Alzheimer's disease continuum. We hypothesized that microstructural biomarkers (diffusion-based imaging indices) would detect signs of neurodegeneration earlier in the Alzheimer's disease continuum than conventional volumetric measures (hippocampal and NBM volumes). Our first aim was to investigate differences in cholinergic WM pathways between stages of the Alzheimer's disease continuum and a control group (healthy controls, HC), and to compare their predictive power to the volumetric measures. The second aim was to demonstrate the association of WM pathways and NBM volumetric changes with cognitive performance across stages of the Alzheimer's disease continuum. As cognitive measures, we focused on attention and memory as they are known to be mediated by the cholinergic circuitry.[15] Our diagnostic groups of SCD, MCI and Alzheimer's disease dementia are clinically in the Alzheimer's disease continuum, but, since they rely on a clinical diagnosis, it is possible that some individuals do not have an Alzheimer's pathologic change as defined currently by a positive Aβ biomarker.[6] For this reason, to confirm our results in a biomarker-supported Alzheimer's disease continuum subsample, we repeated all our analyses in a subsample of amyloid-positive SCD, MCI and Alzheimer's disease dementia groups, as well as amyloid-negative HC.

Materials and methods

Participants

We used data from the interim baseline data set of the multicentre DZNE-longitudinal Cognitive Impairment and Dementia Study (DELCODE), conducted by the German Center for Neurodegenerative Diseases (DZNE).[16] After excluding all cases with insufficient image quality, diffusion MRI data from 402 participants from 10 centres were included (52 AD, 66 MCI, 172 SCD and 112 HC). The participants underwent a clinical assessment of their cognitive status, including the Mini Mental State Examination (MMSE)[17] and an extensive neuropsychological testing battery as described previously.[16] Depressive symptoms were assessed with the Geriatric Depression Scale.[18] The DELCODE exclusion criteria are current major depressive episode, past or present major psychiatric disorders, neurological diseases other than Alzheimer's disease or MCI, or unstable medical conditions.[16]

Subjective cognitive decline was defined as a persistent self-perceived cognitive impairment in the absence of objective cognitive impairment, lasting at least for 6 months and being unrelated to an acute event.[19] The MCI patients met the core clinical criteria for MCI according to National Institute on Aging-Alzheimer's Association (NIA-AA) workgroup guidelines.[20] The Alzheimer's disease patients had a clinical diagnosis of probable Alzheimer's disease dementia according to the NIA-AA workgroup guidelines.[21] Additionally, for a subsample, we requested amyloid positivity for the SCD, MCI and Alzheimer's disease dementia groups.

The HC participants had no objective cognitive impairment in cognitive tests, no history of neurological or psychiatric disease, and did not report a self-perceived cognitive decline. For a subsample, we requested amyloid negativity for the HC group.

All participants or their legal representatives provided written informed consent. The study protocol was approved by the local institutional review boards and ethics committees of the participating centres. DELCODE was conducted in accord with the Helsinki Declaration of 1975.

Cognitive assessment

DELCODE uses an extensive neuropsychological test battery covering specific domains of memory, executive functions, language, visuospatial abilities, as well as attention and working memory.[16] The following tests of memory and attention were selected according to the aims of the current study: selected tasks of the Alzheimer's Disease Assessment Scale–Cognitive 13-item subscale (ADAS-Cog 13),[22] including ADAS word list learning (immediate recall), ADAS word list recall (delayed recall) and ADAS figure learning, to assess verbal and spatial episodic memory. Attention was measured with the oral form of the Symbol Digit Modalities Test[23] and the Trail Making Test A and B[24] forms.

CSF biomarkers

Procedures for CSF acquisition, processing and analysis in DELCODE have been previously described.[16] In the current study, we used the CSF Aβ42/Aβ40 ratio as a biomarker for amyloid-β pathology, CSF–phosphorylated tau181 levels as a biomarker for tau neurofibrillary tangles and total CSF tau levels as a biomarker for

unspecific neurodegeneration, according to the most recent NIA-AA guidelines AT(N) system.[6] The cut-off value for the Aβ42/Aβ40 ratio was <0.09, based on a previous study[25]: cases below the cut-off of 0.09 were designated amyloid positive and cases above the cut-off as amyloid negative. CSF biomarkers were determined using commercially available kits according to vendor specifications: V-PLEX Aβ Peptide Panel 1 (6E10) Kit (K15200E) and V-PLEX Human Total Tau Kit (K151LAE) (Mesoscale Diagnostics LLC), and Innotest Phospho-Tau(181P) (81 581; Fujirebio Germany GmbH).

CSF was sampled in those participants who consented to a lumbar punction (overall CSF sampling rate in DELCODE is around 50%). In the current study, we report the data for all participants with available CSF samples ($n = 185$; Supplementary Table 1). Participants with CSF samples did not differ from participants without CSF samples ($n = 217$) in key demographic variables and MMSE scores (Supplementary Table 2).

APOE genotyping

Genotypes for rs7412 and rs429358, the single nucleotide polymorphisms (SNPs) defining the ε-2, ε-3 and ε-4 alleles of *APOE*, were genotyped using the commercially available TaqMan® SNP Genotyping Assay (ThermoFisher Scientific). Both SNP assays were amplified on genomic DNA using a StepOnePlus Real-Time Polymerase Chain Reaction System (ThermoFisher Scientific). Visual inspection of cluster formation was performed for each SNP before genotype data were used to define ε-2, ε-3 and ε-4 alleles in each sample. Participants were classified as *APOE*4 carriers if they were ε3/ε4 or ε4/ε4 carriers.

MRI acquisition

The data were acquired from ten Siemens 3.0 T MRI scanners using identical acquisition parameters and harmonized procedures. To ensure high image quality throughout the acquisition phase, all scans had to pass a semiautomated quality check during the study conduction so that protocol deviations could be reported to the study sites, and the acquisition at the respective site could be adjusted.

High-resolution T_1-weighted anatomical images were obtained using a sagittal magnetization-prepared rapid gradient echo sequence (field of view 256 × 256 mm, matrix size 256 × 256, isotropic voxel size 1 mm, echo time 4.37 ms, flip angle 7°, repetition time 2500 ms, number of slices 192, parallel imaging acceleration factor 2).

An axial diffusion sequence was measured on the basis of a single-shot echo-planar imaging (EPI) multi-shell sequence (field of view 240 × 240 mm, matrix size 120 × 120, isotropic voxel size 2 mm, repetition time 12 100 ms, echo time 88 ms, flip angle 90°, number of slices 72, parallel imaging acceleration factor 2) with two diffusion-weighted shells at $b = 700$ s/mm^2 (30 volumes) and $b = 1000$ s/mm^2 (30 volumes). The sequence included 10 non-diffusion-weighted scans ($b = 0$ s/mm^2) evenly interspersed throughout the diffusion-weighted volumes.

A B0 field map was collected with matching geometry for use in unwarping EPI distortions due to magnetic field inhomogeneity.[26] The field map acquisition was performed with a 3D dual-echo spoiled gradient echo pulse sequence (field of view 240 × 240 mm, matrix size 80 × 80, isotropic voxel size 3 mm, number of slices 48, repetition time 675 ms, echo time 1 = 4.92 ms, echo time 2 = 7.38 ms, flip angle 60°).

Diffusion MRI-based modelling of the human cholinergic system

To characterize the microstructural properties of the human cholinergic system, a diffusion MRI-based *in vivo* model was derived. We followed the procedure described in a previous study.[27] Briefly, the diffusion-weighted imaging data were preprocessed using FSL (FMRIB Software Library).[28] The non-brain tissue was removed,[29] EPI distortion was corrected using EPI-based field mapping[30] and eddy currents and head motion were corrected.[31]

The estimation of the diffusion parameters in a standard ball-and-sticks model[32] for each voxel was performed with the graphics processing units accelerated version of the bedpostX toolbox,[33] considering three fibres modelled per voxel.

Next, two WM pathways originating from the NBM were captured, one traversing through the cingulum and one through the external capsule.[34] The NBM region of interest (ROI) was based on a cytoarchitectonic map of BF cholinergic nuclei in MNI space, derived from combined histology and *in cranio* MRI of a post-mortem brain.[35] The cingulum and external capsule masks were based on the Johns Hopkins University (JHU) WM atlas, available as part of the FSL package.[36]

Probabilistic tracking was performed by repeating 5000 random samples from each of the NBM ROI voxels and propagated through the local probability density functions of the estimated diffusion parameters.[37] Only the tracts traversing through the cingulum or external capsule ROI were kept.

Next, an unbiased template was created based on B0 preprocessed images from all HC cases using the Advanced Normalization Tools (http://stnava.github.io/ANTs/). After that, both pathways (through cingulum and external capsule) of all HC cases were non-linearly warped into the space of this unbiased template. Finally, pathway-specific binary masks were created by considering all the individual warped tracts and retaining only the voxels that were present (i.e. met by at least one fibre) in at least 60% of the cases. The 60% group threshold was chosen by visual inspection so that the resulting pathways were extensive yet still specific.

Extraction of diffusion indices

To characterize the microstructure properties of the tracked cholinergic pathways, we extracted the widely used indices of mean diffusivity (MD) and fractional anisotropy (FA) from the diffusion tensor model.

We calculated an average value of MD and FA indices for each participant and pathway, i.e. an average value of the diffusion index map within the cingulum and external capsule binary masks.

As a control, the remaining WM mask was created by excluding the two cholinergic WM pathways described before (i.e. a union of external capsule and cingulum pathways) from the whole WM mask. Then, we extracted the average values of MD and FA indices within the remaining WM mask using the same procedure.

We favoured the MD index to the FA index for its reduced susceptibility to the crossing-fibre problem. Nonetheless, we report FA results in the global analysis for reference.

NBM and hippocampal volumes

To evaluate the cell body damage of the cholinergic neurons, the NBM volume was estimated from the T_1-weighted MR images. First, all the images were skull-stripped[29] and corrected for bias field.[38] Then, a non-linear spatial transformation to the MNI space

where the NBM ROI resides was derived using Advanced Normalization Tools. Finally, an individual NBM volume was calculated as the number of grey matter (GM) voxels with the back-transformed NBM ROI in native T1-weighted space. The GM segmentation was obtained from the FSL's Automated Segmentation Tool.[38] The final NBM volume was adjusted by partial volume information provided by FSL's Automated Segmentation Tool. The total intracranial volume (TIV) was estimated based on the affine transformation in the FreeSurfer v.6.0 image analysis suite (http://surfer.nmr.mgh.harvard.edu/). FreeSurfer was also used to segment the hippocampus (bilateral). Both the NBM and hippocampal volumes were normalized by the TIV to account for between-subject variability in head size.[39]

WM hypointensities

Previous studies have shown that the amount of small vessel disease influences the integrity of the cholinergic WM pathways.[27,40] Hence, we included information about small vessel disease status by means of WM hypointensities. WM hypointensities on T_1-weighted images strongly correlate with WM hyperintensities as seen on T_2/FLAIR images,[41] and with microstructural WM changes as measured on diffusion tensor imaging (DTI) data.[42] Segmentation of WM hypointensities and corresponding volumetrics was performed on T_1-weighted images using the probabilistic procedure implemented in FreeSurfer v.6.0.[43]

Statistical analysis

Statistical analysis was carried out using the R programming language (The R Foundation for Statistical Computing, v.4.0.3). Results were deemed statistically significant at two-tailed $P < 0.05$.

Demographics

Demographics were group-wise compared between HC and all other diagnostic groups using independent *t*-tests for age and years of education, and chi-square tests for sex and *APOE* genotype. Differences in cognitive measures and CSF biomarkers between diagnostic groups were compared using a one-way analysis of variance with covariates (ANCOVA) with age and sex as covariates. ANCOVA was followed by paired *post hoc t*-tests adjusting for multiple comparisons with the Tukey method. Our comparisons of interest were SCD versus HC, MCI versus HC and Alzheimer's disease dementia versus HC. The extracted NBM and hippocampus volumes corrected for the TIV, and WM hypointensities load were also compared using ANCOVA, controlling for age and sex.

Pathway integrity comparison (global and voxel-wise)

To assess the differences in the integrity of the tracked pathways between groups, we ran analysis both in aggregated (average, as a global measure) and voxel-wise manner. First, we analysed group-wise differences of the FA and MD averages in the cingulum, external capsule and remaining WM control mask using analyses of covariance (ANCOVA) with age and sex as covariates. ANCOVA was followed by paired *post hoc t*-tests adjusting for multiple comparisons with the Tukey method. Our comparisons of interest were SCD versus HC, MCI versus HC and Alzheimer's disease dementia versus HC. However, we also report the results for the remaining pairs for the sake of completeness (SCD versus MCI, SCD versus Alzheimer's disease dementia and MCI versus Alzheimer's disease dementia). Next, to assess the more detailed spatial differences in the integrity of the pathways, we applied a voxel-wise generalized linear model using permutation-based non-parametric testing ('randomise')[44] and correcting for multiple comparisons across space (threshold-free cluster enhancement, TFCE), with age and sex as covariates. For this, we previously warped all individual MD maps into a common space of the unbiased template using non-linear warp field originated from registering respective individual B0 images to the unbiased template. Significance maps were corrected for multiple comparisons using a familywise error rate of $P < 0.05$. To assess the association between CSF biomarkers of Alzheimer's disease-related pathology and integrity in cholinergic WM pathways, we performed Pearson correlations.

Importance analysis using random forest

To assess the association of MRI markers of the cholinergic system with cognitive performance, we conducted several random forest (RF) analyses with cognitive performance as outcome variables and MD in the cingulum WM pathway, MD in the external capsule WM pathway and NBM volume as predictors. We also included MD in the remaining WM as a negative control for the cholinergic WM. Further, we included WM hypointensities as an extra predictor because our clinical groups differed in WM-hypointensity load, and we had previously demonstrated that WM hypointensities make a major contribution to integrity in cholinergic WM pathways.[27,45] Finally, we also included age, sex and years of education to consider the contribution of these variables, as they usually influence cognitive performance. To compare the role of the integrity of the cholinergic pathways and the NBM volume along the Alzheimer's disease continuum, we created two separate RF models: one for HC and SCD combined, and one for MCI and Alzheimer's disease combined. We combined the groups to gain sufficient statistical power, keeping separated RF models for groups with normal cognition (HC and SCD) and groups with impaired cognition (MCI and Alzheimer's disease dementia).

We used RF regression with a conditional inference tree for unbiased variable selection. RF is an ensemble method in machine learning that involves growing multiple decision trees via bootstrap aggregation (bagging). Each tree predicts a classification independently and votes for the corresponding class. The majority of the votes decides the overall prediction.[46,47] RF has important advantages over other regression techniques in terms of ability to handle highly non-linear biological data, robustness to noise and tuning simplicity.[48]

Conditional feature importance scores for RF were computed by measuring the increase in prediction error if the values of a variable under question were permuted within a grid defined by the covariates that were associated with the variable of interest. This score was computed for each constituent tree and averaged across the entire ensemble. The conditional feature importance scores were designed to diminish an undesirable effect of preference of correlated predictor variables. Variables receiving higher importance scores are more likely to be closely linked to the output variable (cognitive scores). The RF was composed of 2000 conditional inference trees. The party package[49] was used for this analysis.

Biomarker discriminative power (receiver operating characteristic analysis)

To investigate the capacity of the suggested biomarkers (integrity of all considered pathways and BF and hippocampus volumes) to discriminate the different clinical groups from the HC group, the receiver operating characteristic (ROC) curve analysis was carried out. The analysis was performed each time between the HC group and one of the clinical groups, resulting in three different performance

models (one for SCD, one for MCI and one for Alzheimer's disease dementia subjects). Next, we computed the area under the ROC curve (AUC) for each curve as a cumulative statistic of the overall discriminative power of the biomarker in question. AUCs were then pair-wise compared using the bootstrap method (2000 replications) from the 'pROC' package.[50]

Data availability

Requests for access to the data and code used in this study should be directed to the corresponding author. Our data sharing complies with the requirements of our funders and institutes, as well as with institutional ethics approval. The data, which support this study, are not publically available, but may be provided upon reasonable request via https://www.dzne.de/en/research/studies/clinical-studies/delcode.

Results

Demographic characteristics, cognitive performance and MRI and CSF biomarkers across study groups

Demographic data are shown in Table 1. All clinical groups (SCD, MCI, Alzheimer's disease dementia) were significantly older than the HC group ($P_{SCD} = 0.005$, $P_{MCI} < 0.001$, $P_{AD} < 0.001$). The SCD and MCI groups had a higher frequency of men than the HC group ($P_{SCD} = 0.033$, $P_{MCI} = 0.004$). The Alzheimer's disease dementia group had significantly fewer years of education ($P_{AD} < 0.001$) and together with the MCI group showed worse performance in the MMSE than the HC group ($P_{MCI} < 0.001$, $P_{AD} < 0.001$). MCI and Alzheimer's disease dementia groups (but not SCD) performed worse than the HC group in ADAS word list learning (immediate recall) ($P_{MCI} < 0.001$, $P_{AD} < 0.001$), ADAS figure learning (recall) ($P_{MCI} < 0.001$, $P_{AD} < 0.001$), Trail making test A ($P_{MCI} = 0.043$, $P_{AD} < 0.001$), Trail making test B ($P_{MCI} < 0.001$, $P_{AD} < 0.001$) and symbol digit modalities ($P_{MCI} < 0.001$, $P_{AD} < 0.001$). There were differences in ADAS word list learning (delayed recall) in all diagnostic groups when compared with the HC group ($P_{SCD} = 0.043$, $P_{MCI} < 0.001$, $P_{AD} < 0.001$).

NBM and hippocampal volumes were significantly lower in all clinical groups as compared with the HC group (NBM volume: $P_{SCD} = 0.049$, $P_{MCI} < 0.001$, $P_{AD} < 0.001$, hippocampal volume: $P_{SCD} = 0.018$, $P_{MCI} < 0.001$, $P_{AD} < 0.001$), with age and sex adjusted in the model. WM-hypointensity volume was significantly higher only in MCI and Alzheimer's disease dementia groups as compared with the HC group ($P_{MCI} = 0.031$, $P_{AD} < 0.001$), with age and sex adjusted in the model. The frequency of *APOE4* carriers was significantly higher only in the MCI and AD groups in comparison to the HC group ($P_{MCI} < 0.001$, $P_{AD} < 0.001$). Qualitative inspection shows that 31% of the SCD individuals were APOE4 carriers, while only 22% of the HC individuals were APOE4 carriers.

The subset with available CSF biomarkers ($n = 185$, 46% of the total sample) showed no significant differences between SCD and HC groups in any of the CSF biomarkers. On the other hand, MCI and Alzheimer's disease dementia groups showed a significant decrease in the $A\beta_{42}/A\beta_{40}$ ratio, and a significant increase in total tau and p-tau181 levels ($A\beta_{42}/A\beta_{40}$ ratio: $P_{MCI} < 0.001$, $P_{AD} < 0.001$, total tau: $P_{MCI} = 0.035$, $P_{AD} < 0.001$, p-tau181: $P_{MCI} = 0.044$, $P_{AD} < 0.001$), as compared with the HC group. Moreover, MCI and Alzheimer's disease dementia groups also showed a significant decrease in the $A\beta_{42}/A\beta_{40}$ ratio, and a significant increase in total tau and p-tau181 levels ($P < 0.001$ in all comparisons), as compared with the SCD group. All CSF biomarker analyses included age and sex as covariates.

Integrity of cholinergic pathways along the AD continuum: global analysis

Figure 1 and Supplementary Table 6 show the average FA and MD values of the tracked pathways along the Alzheimer's disease continuum, with all analyses controlled for age and sex. We observed a significant average decrease of FA and an average increase of MD in SCD individuals as compared with the HC group ($P < 0.001$ in all comparisons, for both pathways), demonstrating early alterations of cholinergic pathways in the Alzheimer's disease continuum.

The same differences in FA and MD average measures were observed in the MCI and Alzheimer's disease dementia groups compared to the HC group ($P < 0.001$ in all comparisons, for both pathways). In the remaining WM, only the average FA values in MCI and Alzheimer's disease, and the average MD values in SCD and Alzheimer's disease showed significant differences when compared to the HC group (average FA: $P_{MCI} = 0.002$, $P_{AD} < 0.001$, average MD: $P_{SCD} = 0.020$, $P_{AD} < 0.001$).

In the amyloid stratified subsample, we observed a similar pattern of findings in both cholinergic pathways (Supplementary Fig. 1). In contrast with the whole sample, the group differences in the remaining WM in SCD and MCI groups when compared to the HC group were non-significant.

All pair-wise *post hoc* statistics are summarized in Supplementary Tables 3 and 4.

Last, we observed a statistically significant correlation between integrity of cholinergic WM pathways with CSF biomarkers of Alzheimer's disease pathology: MD in cingulum pathway and $A\beta_{42/40}$: $r_{(183)} = -0.221$, $P < 0.01$; MD in external capsule pathway and $A\beta_{42/40}$: $r_{(183)} = -0.248$, $P < 0.001$; MD in cingulum pathway and p-tau: $r_{(183)} = 0.169$, $P < 0.05$; MD in external capsule pathway and p-tau: $r_{(183)} = 0.199$, $P < 0.01$; MD in cingulum pathway and total tau: $r_{(183)} = 0.198$, $P < 0.01$; and MD in external capsule pathway and total tau: $r_{(183)} = 0.247$, $P < 0.001$.

Integrity of cholinergic pathways along the Alzheimer's disease continuum: regional (voxel-wise) analysis

Figures 2 and 3 show statistical maps of voxel-wise differences in MD between groups, in cingulum and external capsule pathways. All analyses were controlled for age and sex.

The cingulum pathway (Fig. 2) showed significantly higher MD values in the retrosplenial and posterior cingulate already in the SCD group when compared with the HC, suggesting an early regional vulnerability of posterior cholinergic WM in the Alzheimer's disease continuum.

In the MCI group, these differences were spatially more pronounced and complemented by significant differences in a small area in the rostral anterior cingulate. In the Alzheimer's disease dementia group, all the differences visible in the MCI group were present, but further spatially extended and were statistically more pronounced with additional significant differences in the dorsal anterior cingulate. Differences in MD values in the WM underneath NBM emerged only in the MCI and Alzheimer's disease dementia groups, but not in the SCD group, when compared with the HC group. This could suggest that it is distal cholinergic WM what shows the earliest alterations in the Alzheimer's disease continuum.

The external capsule pathway (Fig. 3) showed a resembling pattern of differences in MD values in the SCD and MCI groups: in the external capsule, retrosplenial and posterior cingulate, and parts of

Table 1 Demographic and clinical variables by group

	Whole sample	HC	SCD	MCI	AD dementia	F-value/χ^2-value
n	402	112	172	66	52	
Age	71.5 (6.5) [59–89]	69.1 (5.6) [60–81]	71.6 (6.3)** [59–87]	72.6 (6.4)** [61–86]	75.2 (6.8)*** [60–89]	12.6, $P < 0.001$
Sex (M/F)	210/192	48/64	96/76*	43/23**	23/29^{ns}	10.6, $P < 0.05$
Years of education	14.3 (3.0)	14.8 (2.7)	14.5 (3.0)^{ns}	14.1 (3.1)^{ns}	12.6 (3.0)***	6.9, $P < 0.001$
MMSE total score	28.1 (2.9)	29.4 (0.9)	29.2 (0.9)^{ns}	27.8 (1.8)***	21.9 (3.1)***	324, $P < 0.001$
ADAS word list learning (immediate recall)	19.8 (5.5)	23.2 (3.5)	21.6 (3.7)^{ns}	16.4 (3.9)***	10.7 (4.0)***	151, $P < 0.001$
ADAS word list recall (delayed recall)	6.20 (2.95)	8.09 (1.62)	7.23 (1.78)*	4.03 (2.44)***	1.24 (1.61)***	191, $P < 0.001$
ADAS figure learning (recall)	8.35 (3.40)	9.99 (1.60)	9.78 (1.79)^{ns}	6.64 (3.22)***	1.98 (2.18)***	201, $P < 0.001$
Trail making test A	51.0 (30.3)	43.9 (17.3)	41.0 (14.7)^{ns}	57.0 (27.1)*	94.2 (52.2)***	52.0, $P < 0.001$
Trail making test B	116.6 (62.8)	90.5 (25.8)	101.0 (38.4)^{ns}	133.0 (60.7)***	244.0 (84.0)***	100, $P < 0.001$
Symbol digit modalities test	42.4 (13.3)	49.6 (9.2)	45.7 (9.8)^{ns}	37.3 (9.8)***	21.2 (12.0)***	90.0, $P < 0.001$
NBM volume (μl) (TIV corrected)	236 (68)	272 (50)	246 (61)*	208 (62)***	160 (58)***	39.1, $P < 0.001$
hippocampal volume (μl) (TIV corrected)	6000 (1100)	6680 (870)	6200 (1100)*	5430 (950)***	4790 (870)***	43.9, $P < 0.001$
WMH load (μl)	3954 (4826)	2421 (3311)	3516 (3870)^{ns}	5071 (5654)*	7285 (7039)***	9.7, $P < 0.001$
APOE genotype, *n*	388	109	166	63	50	
APOE4 genotype, *n* (%)	132 (34.0)	24 (22.0)	51 (30.7)^{ns}	30 (47.6)***	27 (54.0)***	21.9, $P < 0.001$
CSF biomarkers, *n*	185	40	73	47	25	
$A\beta_{42}/A\beta_{40}$	0.079 (0.029)	0.097 (0.023)	0.088 (0.027)^{ns}	0.066 (0.028)***	0.052 (0.017)***	17.3, $P < 0.001$
total tau (pg/ml)	486 (299)	368 (143)	378 (188)^{ns}	544 (257)*	883 (438)***	23.1, $P < 0.001$
p-tau181 (pg/ml)	64.1 (36.7)	51.3 (17.3)	52.5 (24.7)^{ns}	70.1 (31.8)*	107.0 (58.4)***	16.8, $P < 0.001$

Variables in the SCD, MCI and AD dementia groups were all statistically compared to the corresponding variable in the HC group. For age and years of education an independent *t*-test was performed. For sex and APOE4 genotype, a chi-square test was performed. For all other variables, one-way ANCOVA were performed by setting a diagnostic group as the independent variable and age and sex as covariates. *P*-values result from *post hoc* tests between a diagnostic group and HC with Tukey correction for multiple comparisons. ns, not statistically significant ($P > 0.05$), *$P < 0.05$, **$P < 0.01$, ***$P < 0.001$ (assessed using a two-tailed alpha). Values reflect mean value (SD) [range] or count. AD = Alzheimer's disease; M = male; F = female; WMH = WM hypointensities.

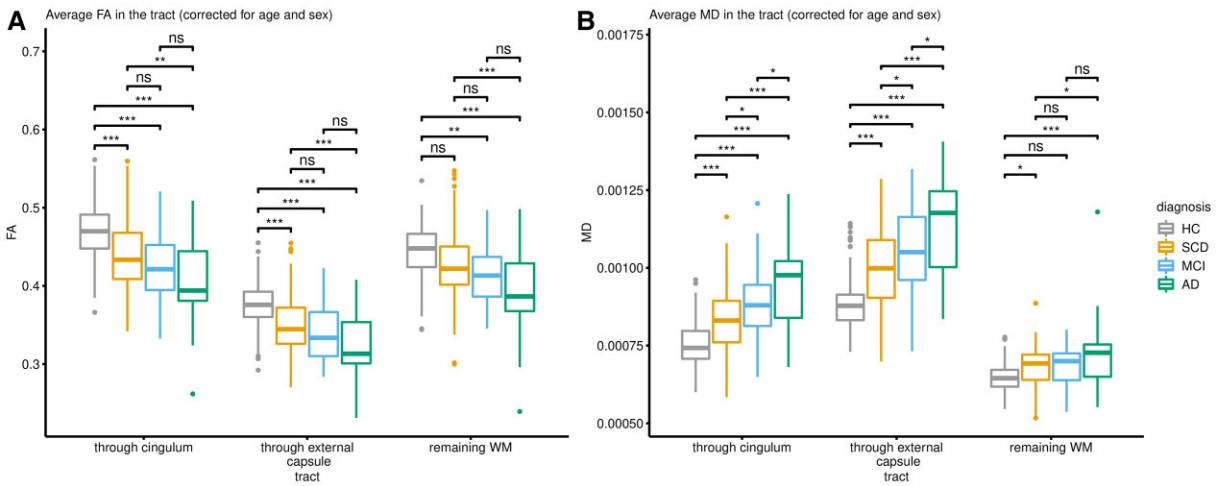

Figure 1 Parameters of diffusivity in cholinergic pathways and remaining WM. All clinical groups differed in FA and MD compared to the HC groups in all observed pathways. (**A**) Average FA. (**B**) Average MD. ns = not statistically significant ($P > 0.05$), *$P < 0.05$, **$P < 0.01$, ***$P < 0.001$ (assessed using a two-tailed alpha). AD = Alzheimer's disease dementia.

the uncinate fasciculus. In the Alzheimer's disease dementia group, there were noticeable additional differences in temporal and prefrontal WM areas when compared with the HC group. Hence, again, these findings suggest an early regional vulnerability of posterior cholinergic WM in the Alzheimer's disease continuum.

The same overall pattern of results could be observed when we repeated the voxel-wise analysis in the amyloid stratified subsample (Supplementary Figs 2 and 3). Despite the reduced statistical power, we again observed significant differences already in the SCD group, both in cingulum and external capsule pathways, which became more prominent in the MCI and Alzheimer's disease groups.

Contribution of the integrity of cholinergic pathways to cognitive performance

Figure 4 shows the degree of contribution of MD in cingulum and external capsule pathways, MD in remaining WM, WM hypointensities and NBM volume towards cognitive measures of memory and attention, as examined by RF analysis. Additional independent

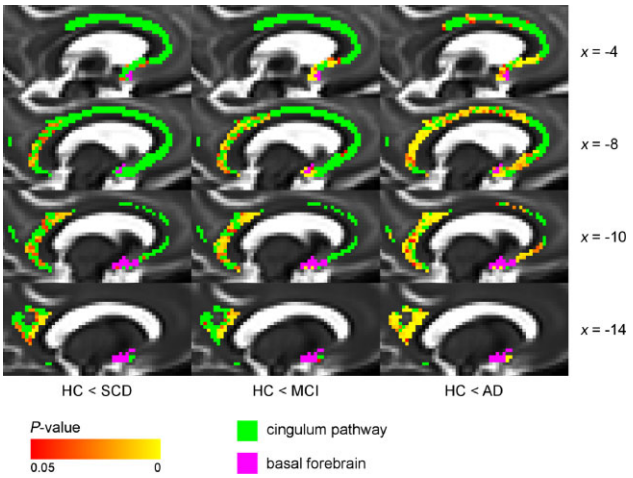

Figure 2 Voxel-wise differences in MD between diagnostic groups and controls (cingulum pathway), controlling for age and sex. The cingulum pathway showed significantly higher MD values in the posterior/retrosplenial cingulate already in the SCD group compared with the HC group. Additional differences were present in the rostral and dorsal anterior cingulate in MCI and Alzheimer's disease dementia groups. Voxel-wise analyses of the diffusion data (MD values) were performed using non-parametric permutation testing. Identification of significant clusters in the data was performed using TFCE. Significance maps were corrected for multiple comparisons using a familywise error rate of $P < 0.05$ (non-significant voxels are shown in green). BF mask (in purple) was inflated for illustrative purposes. AD = Alzheimer's disease dementia.

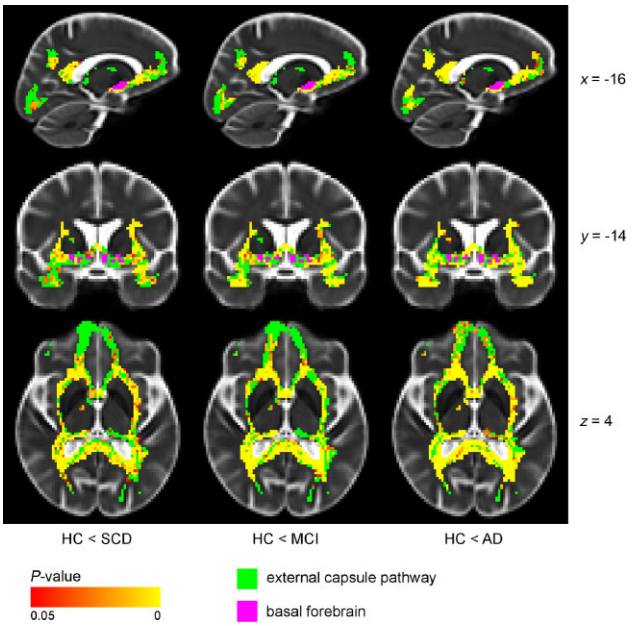

Figure 3 Voxel-wise difference in MD between diagnostic groups and controls (external capsule pathway), controlling for age and sex. The external capsule pathway showed differences in the external capsule, posterior/retrosplenial cingulate and parts of the uncinate fasciculus in SCD and MCI compared with HC. Additional differences were present in temporal and prefrontal areas in the Alzheimer's disease dementia group. Voxel-wise analyses of the diffusion data (MD values) were performed using non-parametric permutation testing. Identification of significant clusters in the data was performed using TFCE. Significance maps were corrected for multiple comparisons using a familywise error rate of $P < 0.05$ (statistically non-significant voxels are shown in green). BF mask (in purple) was inflated for illustrative purposes. AD = Alzheimer's disease dementia.

variables were age, sex and years of education. These analyses were conducted separately for the groups with normal cognition (HC and SCD) and the groups with impaired cognition (MCI and Alzheimer's disease dementia). Independent variables in each plot in Fig. 4 are presented in descending order of their importance score.

In the normal cognition groups (HC and SCD), sex, age and years of education were among the most important variables in the prediction of ADAS memory tests. MD in the external capsule pathway had a stronger importance in attention tests (Symbol digit modalities test, and Trail making test B). NBM volume and WM hypointensities received low importance scores in all the RF models. Scores from the Trail making test A failed to be predicted by the respective RF model.

In the impaired cognition groups (MCI and Alzheimer's disease dementia), NBM volume was among the most important predictors for ADAS word list learning and recall, Symbol digit modalities test and Trail making test B. MD in the external capsule pathway was important towards all ADAS memory tests and Trail making test A. MD in the cingulum pathway was a noticeable contributor only in the prediction of Trail making test A. WM hypointensities and MD in the remaining WM received low importance scores in all the RF models.

In summary, particularly the integrity of the external capsule pathway contributed to predict performance in attention tests in HC and SCD individuals. The contribution of cholinergic pathways (and NBM volume) to cognitive performance became stronger in the MCI and Alzheimer's disease dementia groups, both for memory and attention tests and also including the cingulum pathway.

Integrity of cholinergic pathways discriminate the SCD group better than conventional volumetric measures (ROC analysis)

The ROC curves and their corresponding AUCs indicated how well each of the considered biomarkers can be used to distinguish between a clinical group and the HC group. Please see Fig. 5 for *P*-values and Supplementary Table 5 for AUC values.

MD in the external capsule (ExCap) ($AUC_{ExCap} = 0.736$) performed significantly better than all the other biomarkers in distinguishing SCD from HC. The second-best performing biomarker was MD in the cingulum (Cing) ($AUC_{Cing} = 0.713$). AUCs of MD in the remaining WM (rem), NBM volume and hippocampus volume had the lowest discriminative performance and were not significantly different from each other: $AUC_{MD\_rem} = 0.663$, $AUC_{NBM\_vol} = 0.625$ and $AUC_{hipp\_vol} = 0.660$.

In the case of MCI, all biomarkers except for MD (rem. WM) reached statistically comparable high AUC values: $AUC_{NBM\_vol} = 0.792$, $AUC_{hipp\_vol} = 0.845$, $AUC_{MD\_Cing} = 0.813$ and $AUC_{MD\_ExCap} = 0.833$. In contrast, MD (rem. WM) performed significantly poorer than all the other biomarkers ($AUC_{MD\_rem} = 0.676$).

For the AD dementia group, hippocampus volume, NBM volume, and MD (ExCap) performed equally high: $AUC_{hipp\_vol} = 0.936$, $AUC_{NBM\_vol} = 0.936$ and $AUC_{MD\_ExCap} = 0.901$. *P*-values showed that MD (Cing) ($AUC_{Cing} = 0.869$) showed slightly worse performance than hippocampus volume and MD (ExCap), and MD (rem. WM) had the worst value ($AUC_{MD\_rem} = 0.745$).

In summary, the results of the ROC analysis were stage specific. Cholinergic WM pathways outperformed other biomarkers in the SCD group. Generally, all the considered biomarkers performed better with a more advanced clinical stage of the disease in the Alzheimer's disease continuum.

The findings were very similar in the amyloid stratified subsample (Supplementary Fig. 4 and Supplementary Table 4). In the

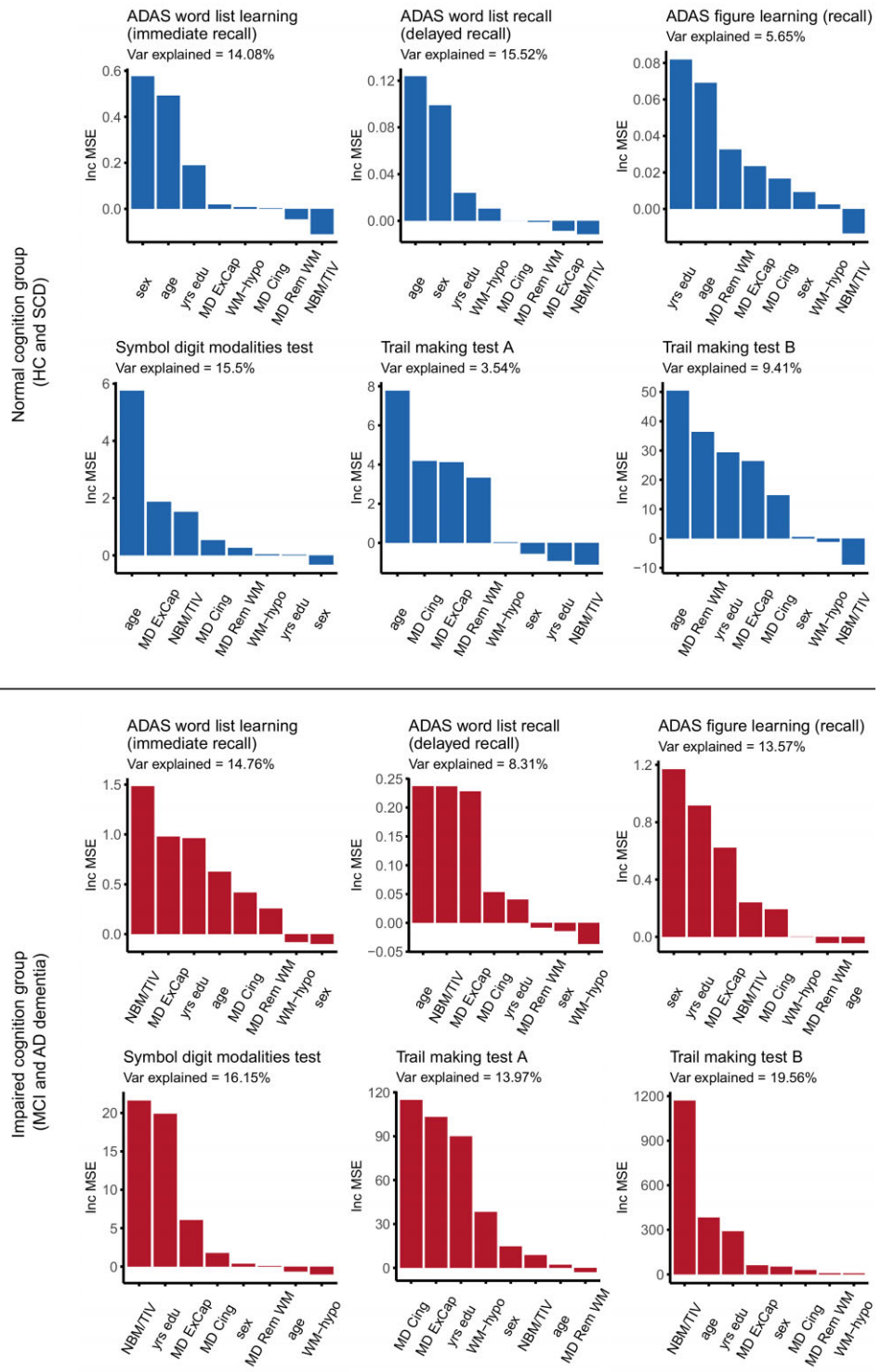

Figure 4 RF models (increase in prediction error). In the normal cognition groups (HC and SCD), MD in the external capsule pathway was important in predicting scores in attention tests, while NBM volume and WM hypointensities received low importance scores in all models. In the impaired cognition groups (MCI and Alzheimer's disease dementia), NBM volume and MD in external capsule and cingulum pathways were important in predicting scores in most memory and attention tests. ExCap = external capsule pathway; Cing = cingulum pathway; Rem WM = WM excluding cholinergic pathways; NBM/TIV = volume of NBM scaled by TIV; Var = variance; yrs = years. IncMSE = conditional variable importance computed by increase in the mean square error of prediction. This IncMSE is the result of a corresponding variable being permuted within a grid defined by the covariates that are associated to the variable of interest.

amyloid-positive SCD cases, the NBM volume performed worse than all the other biomarkers. In the amyloid-positive MCI cases, MD (Cing), MD (ExCap) and hippocampus volume were better than NBM volume and MD (rem. WM). In the amyloid-positive AD dementia cases, all biomarkers performed better than MD (rem. WM).

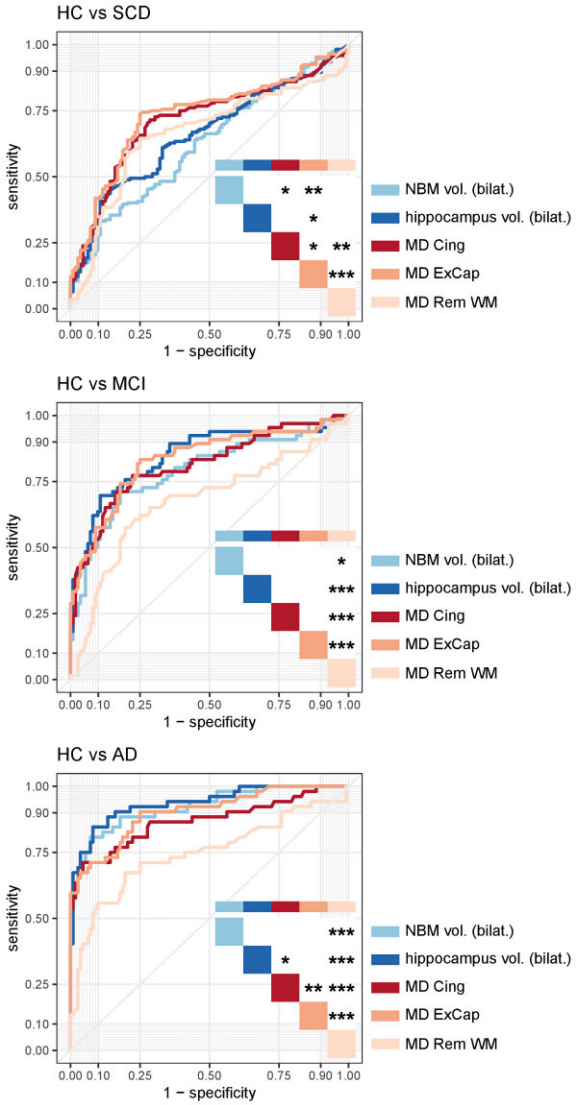

Figure 5 ROC curves for diffusion and conventional MRI biomarkers. The figures show that cholinergic WM pathways outperformed other MRI biomarkers in the SCD group, and that all considered biomarkers performed better with a more advanced clinical stage of the disease in the Alzheimer's disease continuum, in distinguishing between a clinical group and HC. *P < 0.05, **P < 0.01, ***P < 0.001 (assessed using a two-tailed alpha). AD = Alzheimer's disease dementia; ExCap = external capsule pathway; Cing = cingulum pathway; Rem WM = WM excluding cholinergic pathways; NBM vol. = volume of NBM scaled by TIV; hippocampus vol. = volume of hippocampus scaled by TIV.

Discussion

We investigated DTI-based integrity of the human cholinergic system along the Alzheimer's disease continuum, including SCD individuals as a group reflecting the preclinical stage of Alzheimer's disease (particularly amyloid-positive SCD individuals). The study focused on the integrity of the cholinergic WM pathways, including differences between clinical stages, their predictive power compared to conventional volumetric MRI biomarkers, and their association to cognitive performance. We found reduced integrity of the cholinergic pathways in all the stages of the Alzheimer's disease continuum (SCD, MCI and Alzheimer's disease dementia). The spatial distribution of these differences followed a posterior–anterior pattern. Differences in the SCD stage involved posterior cholinergic WM and, at more advanced stages, we also found differences in anterior frontal WM. All considered biomarkers (conventional volumetric and novel measures of WM integrity) showed higher predictive power at more advanced stages within the Alzheimer's disease continuum. However, measures of the integrity of the cholinergic pathways were more informative in distinguishing SCD from HC than all other biomarkers. The multivariate models showed that the integrity of the cholinergic pathways and NBM volume, but not the integrity of the rest of WM, strongly contributed to performance in attention and memory in cognitively impaired individuals (MCI and Alzheimer's disease dementia).

In the whole sample, we found that the integrity of the cholinergic WM pathways was reduced in all stages of the Alzheimer's disease continuum. The findings for the MCI and Alzheimer's disease dementia groups thus agree with a recent study that showed that NBM degeneration is accompanied by alterations of cholinergic WM pathways in MCI and Alzheimer's disease dementia.[14] Additionally, a recent post-mortem study based on post-mortem MRI and histopathology reported no significant differences between Alzheimer's disease and HC in cholinergic WM pathways, but demonstrated that decreased cholinergic cell density in NBM was associated with reduced integrity of cholinergic WM pathways towards the temporal lobe.[51] Our current study extends these previous studies by showing that the integrity of cholinergic pathways is already altered at the stage of SCD.

We did not observe any statistically significant differences in CSF biomarkers between the SCD and HC groups. These results are in line with previous studies that showed no significant differences in CSF biomarkers in SCD compared to HC.[52–55] There are, however, some reports about significant differences in CSF biomarkers between SCD and HC groups.[56] These differences have also been observed in CSF and PET AD biomarkers in SCD individuals who progressed to MCI or dementia.[57,58] The observed lack of statistical differences in our study and by others could mean that degeneration of the cholinergic system may precede measurable changes in conventional biomarkers for Alzheimer's disease pathology (Aβ and tau biomarkers). A similar conclusion has been made by a study of BF volume.[9] Alternatively, perhaps more sensitive CSF biomarkers such as N-224 could detect Alzheimer's disease pathology in the absence of statistical differences for $A\beta_{42}/A\beta_{40}$ ratio and p-tau181 CSF biomarkers.[56,59]

The reduced integrity of the cholinergic pathways in all stages of the Alzheimer's disease continuum was replicated in the amyloid stratified subsample, thus supporting our findings both in clinically and biologically defined study groups. In addition, the integrity of the remaining WM was reduced in all stages of the continuum, in the whole sample. This global WM degeneration has also been reported by others.[60] However, this reduction of integrity of remaining WM could not be clearly observed in the amyloid stratified subsample. Although this could be explained by the small sample size, the integrity of both cholinergic pathways remained significantly different between clinical groups and HC in the amyloid stratified subsample, hence, with the same sample size. This could possibly mean that while the remaining WM deteriorates and its changes in integrity provide information about the global degeneration, the considered cholinergic pathways and their integrity are particularly sensitive to an Alzheimer's pathologic change (Aβ positivity). This hypothesis could be further supported by our statistically significant correlation between CSF Aβ levels and integrity of cingulum and external capsule pathways. In addition, we also showed a statistically significant correlation between CSF tau

biomarkers and integrity of cingulum and external capsule pathways, supporting the association between cholinergic WM and Alzheimer's disease-related pathology. Although there are no studies investigating *in vivo* cholinergic projections in Alzheimer's disease other than the recent study by Schumacher *et al.*,[14] studies focusing on NBM volume similarly reported that NBM volume is more closely associated with Alzheimer's disease-related pathology than other GM areas.[9,61] This finding is also supported by our ROC analysis, in which the integrity of remaining WM performed consistently poorer in all cases.

Another finding this study provides is the spatial distribution of differences in WM integrity of the cholinergic pathways, along the Alzheimer's disease continuum. We demonstrated that the SCD group already showed a clear pattern of reduced integrity in the retrosplenial and posterior cingulate cortex, as well as in the external capsule. These regions were previously identified as the ones with the earliest neuronal and metabolic changes and reduced connectivity, emerging as a vulnerable Alzheimer's disease-associated epicentre.[62] Also, these regions have been associated with early accumulation of amyloid in PET studies.[63] Differences in the MCI group included the same areas as in the SCD group and, additionally, involved the rostral anterior cingulate. In Alzheimer's disease dementia, WM integrity alterations extended to the dorsal anterior cingulate and temporal and prefrontal areas. These areas are usually associated with increased neuronal loss in MCI and Alzheimer's disease dementia,[64] but here we show involvement of the cholinergic WM. Despite the cross-sectional nature of our analyses, the replication of regional damage as the disease progresses, as well as the stepwise addition of cholinergic WM areas following a posterior–anterior pattern of degeneration is a robust finding. If replicated in longitudinal designs, these findings could help understanding the progression of cholinergic system changes *in vivo*, along the development of Alzheimer's disease.

Finally, RF analysis showed a substantially different set of important predictors of cognitive scores in cognitively unimpaired and impaired groups. In the analysis of HC and SCD groups combined, it was mainly age, sex and years of education that counted towards the cognitive performance. On top of that, the integrity of the external capsule pathway played a moderately important role in tests of attention. The external capsule pathway projects to cortices involved in attention such as regions located in frontal lobe and posterior cortex. On the other hand, in the analysis involving cognitively impaired groups (MCI and Alzheimer's disease dementia), integrity in the external capsule and cingulum pathways was important towards most of the tests of memory and attention. In addition to frontal and posterior cortical areas, the external capsule pathway also projects to cortices related to memory such as medial temporal structures. The cingulum pathway also projects to cortices related to memory such as hippocampal structures and posterior cingulate cortex. These findings reflect the role of cholinergic system in cognitive process of effortful attention and memory. Integrity in the remaining WM was not important. Similar results have recently been reported in studies conducted in healthy ageing[27] and in Alzheimer's disease and dementia with Lewy bodies.[14,51] In our cognitively unimpaired groups (HC and SCD), we could practically replicate the results in Nemy *et al.*[27] that were based on independent data. First, we observed that age and sex were important variables towards the prediction of most of the cognitive tests. Second, the integrity of cholinergic pathways received considerably high importance score only towards tests involving effortful attention. The difference in average age of 15 years between our current cohort and the participants in Nemy *et al.*[27] suggests that these findings may be generalizable across age groups. In addition, in the current study we observed that NBM volume was important towards performance in memory and attention tests in the MCI and Alzheimer's disease dementia groups. This is in line with other studies investigating Alzheimer's disease[65] and Parkinson's disease,[66] which found that NBM volume is an important predictor of disease progression. Altogether, these findings suggest that the cholinergic system may deteriorate earlier in the WM, and NBM volume would follow in more advanced stages of the disease. In keeping with the posterior–anterior pattern of WM cholinergic disruption, this observation might suggest that NBM starts deteriorating when enough cholinergic WM damage has occurred. This dying-back pattern of degeneration known as 'Wallerian-like degeneration' has been demonstrated in Alzheimer's disease in several experimental and pathological studies.[11,67] All in all, these results illustrate the early involvement of cholinergic pathways in the Alzheimer's disease continuum and add additional evidence that the used methodology using DTI tracking is a promising and emerging potential biomarker of microstructural changes within earliest stages of Alzheimer's disease.

All the findings discussed here are further underlined by the results of our ROC analysis. First, all considered biomarkers, both conventional volumetric and novel measures of WM integrity, showed higher predictive importance with the progression of the disease. This finding validates the conventional volumetric biomarkers but also suggests that the proposed measures of WM integrity are sensitive to neurodegeneration changes along the Alzheimer's disease continuum. Consistent low predictive power of remaining WM integrity in ROC analysis points out that the measures of the cholinergic system pathways are not only sensitive but also specific. Second, the ROC data showed significantly better predictive power of integrity of cholinergic WM pathways than the conventional volumetric measures in the SCD group. This might suggest that the proposed cholinergic biomarkers are more suitable for detecting very early changes in the disease. Third, whereas in the whole sample the predictive power of the NBM volume appeared approximately on the same level as the integrity of at least one of the cholinergic WM pathways, in the amyloid-positive subsample the NBM volume performed significantly worse than both cholinergic WM pathways in distinguishing SCD and MCI from HC. This further supports the hypothesis that alterations of cholinergic WM projections occur earlier than neurodegeneration in NBM, in the context of an Alzheimer's pathologic change (Aβ positivity).

This study has some limitations. We primarily aimed to investigate cross-sectional differences along the Alzheimer's disease continuum and interpretations about cholinergic WM pathways and clinical progression were based on different groups. Whereas this approach serves as a preliminary demonstration of early differences in cholinergic WM pathways in the SCD group, that extends to other WM areas in the MCI and Alzheimer's disease dementia groups, it will be important to expand our current approach to include longitudinal analyses in the future. Longitudinal analyses will be needed to confirm our preliminary interpretation of cholinergic alterations preceding Alzheimer's disease pathology (positivity both in Aβ and tau biomarkers). Next, CSF biomarkers were not available for all subjects in the cohort. Although the CSF biomarker subsample was large enough to allow for replication of the main results, the analysis would benefit from having an even larger CSF sample. Our comparison of participants with and without CSF data available did not show any difference in terms of key demographic variables and MMSE scores, suggesting a low risk for selection bias with regards the subsample with CSF data available.

Furthermore, even with standardized MRI acquisition protocols and careful image quality control, we cannot completely exclude that inter-scanner variance may have influenced some of our results.[68] However, since the focus of this study mostly involved comparison of within-subject measures (i.e. conventional volumetric versus cholinergic WM integrity biomarkers), our main conclusions should not be affected by inter-scanner variance. We also provide the breakdown of study participants by scanner in Supplementary Table 7, for the reader's interest. Last, voxel-wise analysis showed significant differences in MD in posterior parts of the cholinergic pathways between SCD and HC. However, when using an average measure of MD in the entire cholinergic pathways, we did not observe a pronounced contribution of the cholinergic pathways to cognition in the RF models. Future studies could explore the contribution of more regional measures of MD to cognitive performance in SCD individuals.

In conclusion, we modelled *in vivo* cholinergic WM pathways and investigated their integrity along the stages of the Alzheimer's disease continuum, and in relation to cognitive performance. We showed that the integrity of the cholinergic WM pathways is associated to Alzheimer's disease-related pathology, and it reveals alterations as early as the stage of SCD. The cholinergic WM pathways differentiated between SCD and HC groups better than the integrity of non-cholinergic WM and conventional measures of hippocampal and NBM volumes. These findings suggest that the integrity of WM cholinergic pathways is a sensitive and specific biomarker of early neurodegeneration in individuals with an Alzheimer's pathologic change (Aβ positivity).

Funding

This study was supported by the Swedish Research Council (2020-02014); the regional agreement on medical training and clinical research (ALF) between Stockholm County Council and Karolinska Institutet; Center for Innovative Medicine (CIMED); the Swedish Alzheimer Foundation; the Swedish Brain Foundation; Neuro Fonden, the Czech Alzheimer Foundation; and Demensfonden. Research by M.N., O.S. and L.V. was partially supported by institutional resources of Czech Technical University in Prague. The work was further supported by a grant to S.J.T. within the CureDem funding of the Bundesministerium für Bildung und Forschung (BMBF), grant number 01KX2130. The funding sources did not have any involvement in the study design; collection, analysis and interpretation of data; writing of the report and the decision to submit the article for publication.

Competing interests

S.J.T. participated in scientific advisory boards of Roche Pharma AG, Biogen, GRIFOLS, EISAI and MSD and received lecture fees from Roche and MSD. The other authors report no competing interests.

Supplementary material

Supplementary material is available at *Brain* online.

References

1. Buchhave P, Minthon L, Zetterberg H, Wallin ÅK, Blennow K, Hansson O. Cerebrospinal fluid levels of β-amyloid 1–42, but not of tau, are fully changed already 5 to 10 years before the onset of Alzheimer dementia. *Arch Gen Psychiatry*. 2012;69:98-106.
2. Villemagne VL, Burnham S, Bourgeat P, *et al*. Amyloid β deposition, neurodegeneration, and cognitive decline in sporadic Alzheimer's disease: A prospective cohort study. *Lancet Neurol*. 2013;12:357-367.
3. Albert M, Zhu Y, Moghekar A, *et al*. Predicting progression from normal cognition to mild cognitive impairment for individuals at 5 years. *Brain*. 2018;141:877-887.
4. Sperling RA, Aisen PS, Beckett LA, *et al*. Toward defining the preclinical stages of Alzheimer's disease: Recommendations from the National Institute on Aging-Alzheimer's Association workgroups on diagnostic guidelines for Alzheimer's disease. *Alzheimer's Dement*. 2011;7:280-292.
5. Dubois B, Hampel H, Feldman HH, *et al*. Preclinical Alzheimer's disease: Definition, natural history, and diagnostic criteria. *Alzheimer's Dement*. 2016;12:292-323.
6. Jack CR, Bennett DA, Blennow K, *et al*. NIA-AA research framework: Toward a biological definition of Alzheimer's disease. *Alzheimer's Dement*. 2018;14:535-562.
7. Fu H, Hardy J, Duff KE. Selective vulnerability in neurodegenerative diseases. *Nat Neurosci*. 2018;21:1350-1358.
8. Brueggen K, Dyrba M, Barkhof F, *et al*. Basal forebrain and hippocampus as predictors of conversion to Alzheimer's disease in patients with mild cognitive impairment–A multicenter DTI and volumetry study. *J Alzheimer's Dis*. 2015;48:197-204.
9. Schmitz TW, Nathan Spreng R, Alzheimer's Disease Neuroimaging Initiative. Basal forebrain degeneration precedes and predicts the cortical spread of Alzheimer's pathology. *Nat Commun*. 2016;7:13249.
10. Bartus RT, Dean RL, Beer B, Lippa AS. The cholinergic hypothesis of geriatric memory dysfunction. *Science*. 1982;217:408-414.
11. Kanaan NM, Pigino GF, Brady ST, Lazarov O, Binder LI, Morfini GA. Axonal degeneration in Alzheimer's disease: When signaling abnormalities meet the axonal transport system. *Exp Neurol*. 2013;246:44-53.
12. Li X, Li TQ, Andreasen N, Wiberg MK, Westman E, Wahlund LO. The association between biomarkers in cerebrospinal fluid and structural changes in the brain in patients with Alzheimer's disease. *J Intern Med*. 2014;275:418-427.
13. Li X, Westman E, Ståhlbom AK, *et al*. White matter changes in familial Alzheimer's disease. *J Intern Med*. 2015;278:211-218.
14. Schumacher J, Ray NJ, Hamilton CA, *et al*. Cholinergic white matter pathways in dementia with Lewy bodies and Alzheimer's disease. *Brain*. 2022;145(5):1773-1784.
15. Ballinger EC, Ananth M, Talmage DA, Role LW. Basal forebrain cholinergic circuits and signaling in cognition and cognitive decline. *Neuron*. 2016;91:1199-1218.
16. Jessen F, Spottke A, Boecker H, *et al*. Design and first baseline data of the DZNE multicenter observational study on predementia Alzheimer's disease (DELCODE). *Alzheimer's Res Ther*. 2018;10:21.
17. Folstein MF, Folstein SE, McHugh PR. Mini-mental state". A practical method for grading the cognitive state of patients for the clinician. *J Psychiatr Res*. 1975;12:189-198.
18. Yesavage JA, Sheikh JI. Geriatric Depression Scale (GDS). *Clin Gerontol*. 1986;5:165-173.
19. Jessen F, Amariglio RE, Van Boxtel M, *et al*. A conceptual framework for research on subjective cognitive decline in preclinical Alzheimer's disease. *Alzheimer's Dement*. 2014;10:844-852.
20. Albert MS, DeKosky ST, Dickson D, *et al*. The diagnosis of mild cognitive impairment due to Alzheimer's disease: Recommendations from the National Institute on Aging-Alzheimer's

Association workgroups on diagnostic guidelines for Alzheimer's disease. *Alzheimer's Dement*. 2011;7:270-279.
21. McKhann GM, Knopman DS, Chertkow H, *et al*. The diagnosis of dementia due to Alzheimer's disease: Recommendations from the National Institute on Aging-Alzheimer's Association workgroups on diagnostic guidelines for Alzheimer's disease. *Alzheimer's Dement*. 2011;7:263-269.
22. Mohs RC, Knopman D, Petersen RC, *et al*. Development of cognitive instruments for use in clinical trials of antidementia drugs: Additions to the Alzheimer's disease assessment scale that broaden its scope. *Alzheimer Dis Assoc Disord*. 1997;11:13-21.
23. Smith A. *Symbol digit modality test (SDMT): Manual (revised)*. Western Psychological Services; 1982.
24. Reitan RM. Validity of the trail making test as an indicator of organic brain damage. *Percept Mot Skills*. 1958;8:271-276.
25. Janelidze S, Zetterberg H, Mattsson N, *et al*. CSF Aβ42/Aβ40 and Aβ42/Aβ38 ratios: Better diagnostic markers of Alzheimer disease. *Ann Clin Transl Neurol*. 2016;3:154-165.
26. Jezzard P, Balaban RS. Correction for geometric distortion in echo planar images from B0 field variations. *Magn Reson Med*. 1995;34:65-73.
27. Nemy M, Cedres N, Grothe MJ, *et al*. Cholinergic white matter pathways make a stronger contribution to attention and memory in normal aging than cerebrovascular health and nucleus basalis of Meynert. *Neuroimage*. 2020;211:116607.
28. Jenkinson M, Beckmann CF, Behrens TEJ, Woolrich MW, Smith SM. FSL. *Neuroimage*. 2012;62:782-790.
29. Smith SM. Fast robust automated brain extraction. *Hum Brain Mapp*. 2002;17:143-155.
30. Reber PJ, Wong EC, Buxton RB, Frank LR. Correction of off resonance-related distortion in echo-planar imaging using EPI-based field maps. *Magn Reson Med*. 1998;39:328-330.
31. Andersson JLR, Sotiropoulos SN. An integrated approach to correction for off-resonance effects and subject movement in diffusion MR imaging. *Neuroimage*. 2016;125:1063-1078.
32. Behrens TEJ, Berg HJ, Jbabdi S, Rushworth MFS, Woolrich MW. Probabilistic diffusion tractography with multiple fibre orientations: What can we gain? *Neuroimage*. 2007;34:144-155.
33. Hernández M, Guerrero GD, Cecilia JM, *et al*. Accelerating fibre orientation estimation from diffusion weighted magnetic resonance imaging using GPUs. *PLoS ONE*. 2013;8:e61892.
34. Selden NR, Gitelman DR, Salamon-Murayama N, Parrish TB, Mesulam MM. Trajectories of cholinergic pathways within the cerebral hemispheres of the human brain. *Brain*. 1998;121:2249-2257.
35. Kilimann I, Grothe M, Heinsen H, *et al*. Subregional basal forebrain atrophy in Alzheimer's disease: A multicenter study. *J Alzheimer's Dis*. 2014;40:687-700.
36. Mori S, Wakana S, Van Zijl PC, Nagae-Poetscher L. *MRI atlas of human white matter*. Elsevier; 2005.
37. Behrens TEJ, Woolrich MW, Jenkinson M, *et al*. Characterization and propagation of uncertainty in diffusion-weighted MR imaging. *Magn Reson Med*. 2003;50:1077-1088.
38. Zhang Y, Brady M, Smith S. Segmentation of brain MR images through a hidden Markov random field model and the expectation-maximization algorithm. *IEEE Trans Med Imaging*. 2001;20:45-57.
39. Buckner RL, Head D, Parker J, *et al*. A unified approach for morphometric and functional data analysis in young, old, and demented adults using automated atlas-based head size normalization: Reliability and validation against manual measurement of total intracranial volume. *Neuroimage*. 2004;23:724-738.
40. Kim HJ, Moon WJ, Han SH. Differential cholinergic pathway involvement in Alzheimer's disease and subcortical ischemic vascular dementia. *J Alzheimer's Dis*. 2013;35:129-136.
41. Cedres N, Ferreira D, Machado A, *et al*. Predicting Fazekas scores from automatic segmentations of white matter signal abnormalities. *Aging (Albany NY)*. 2020;12:894-901.
42. Leritz EC, Shepel J, Williams VJ, *et al*. Associations between T1 white matter lesion volume and regional white matter microstructure in aging. *Hum Brain Mapp*. 2014;35:1085-1100.
43. Fischl B, Salat DH, Busa E, *et al*. Whole brain segmentation: Automated labeling of neuroanatomical structures in the human brain. *Neuron*. 2002;33:341-355.
44. Winkler AM, Ridgway GR, Webster MA, Smith SM, Nichols TE. Permutation inference for the general linear model. *Neuroimage*. 2014;92:381-397.
45. Cedres N, Ferreira D, Nemy M, *et al*. Association of cerebrovascular and Alzheimer disease biomarkers with cholinergic white matter degeneration in cognitively unimpaired individuals. *Neurology*. 2022;99(15):e1619-e1629.
46. Breiman L. Random forests. *Mach Learn*. 2001;45:5-32.
47. Breiman L. Bagging predictions. *Mach Learn*. 1996;24:123-140.
48. Lebedev AV, Westman E, Van Westen GJP, *et al*. Random forest ensembles for detection and prediction of Alzheimer's disease with a good between-cohort robustness. *Neuroimage Clin*. 2014;6:115-125.
49. Strobl C, Boulesteix AL, Zeileis A, Hothorn T. Bias in random forest variable importance measures: Illustrations, sources and a solution. *BMC Bioinf*. 2007;8:25.
50. Robin X, Turck N, Hainard A, *et al*. pROC: An open-source package for R and S+ to analyze and compare ROC curves. *BMC Bioinf*. 2011;12:77.
51. Lin C-P, Frigerio I, Boon BDC, *et al*. Structural (dys)connectivity associates with cholinergic cell density in Alzheimer's disease. *Brain*. 2022;145:2869-2881.
52. Wolfsgruber S, Kleineidam L, Guski J, *et al*. Minor neuropsychological deficits in patients with subjective cognitive decline. *Neurology*. 2020;95:e1134-e1143.
53. Rami L, Fortea J, Bosch B, *et al*. Cerebrospinal fluid biomarkers and memory present distinct associations along the continuum from healthy subjects to AD patients. *J Alzheimer's Dis*. 2011;23:319-326.
54. Visser PJ, Verhey F, Knol DL, *et al*. Prevalence and prognostic value of CSF markers of Alzheimer's disease pathology in patients with subjective cognitive impairment or mild cognitive impairment in the DESCRIPA study: A prospective cohort study. *Lancet Neurol*. 2009;8:619-627.
55. Antonell A, Fortea J, Rami L, *et al*. Different profiles of Alzheimer's disease cerebrospinal fluid biomarkers in controls and subjects with subjective memory complaints. *J Neural Transm*. 2011;118:259-262.
56. Sánchez-Benavides G, Suárez-Calvet M, Milà-Alomà M, *et al*. Amyloid-β positive individuals with subjective cognitive decline present increased CSF neurofilament light levels that relate to lower hippocampal volume. *Neurobiol Aging*. 2021;104:24-31.
57. Ferreira D, Falahati F, Linden C, *et al*. A "disease severity index" to identify individuals with subjective memory decline who will progress to mild cognitive impairment or dementia. *Sci Rep*. 2017;7:44368.
58. Ebenau JL, Pelkmans W, Verberk IMW, *et al*. Association of CSF, plasma, and imaging markers of neurodegeneration with clinical progression in people with subjective cognitive decline. *Neurology*. 2022;98:E1315-E1326.
59. Cicognola C, Hansson O, Scheltens P, *et al*. Cerebrospinal fluid N-224 tau helps discriminate Alzheimer's disease from subjective cognitive decline and other dementias. *Alzheimer's Res Ther*. 2021;13:38.

60. Sun X, Salat D, Upchurch K, Deason R, Kowall N, Budson A. Destruction of white matter integrity in patients with mild cognitive impairment and Alzheimer disease. *J Investig Med*. 2014; 62:927-933.
61. Teipel S, Heinsen H, Amaro E, *et al*. Cholinergic basal forebrain atrophy predicts amyloid burden in Alzheimer's disease. *Neurobiol Aging*. 2014;35:482-491.
62. Lee PL, Chou KH, Chung CP, *et al*. Posterior cingulate cortex network predicts Alzheimer's disease progression. *Front Aging Neurosci*. 2020;12:466.
63. Palmqvist S, Schöll M, Strandberg O, *et al*. Earliest accumulation of β-amyloid occurs within the default-mode network and concurrently affects brain connectivity. *Nat Commun*. 2017;8:1-13.
64. Coughlan G, Laczó J, Hort J, Minihane AM, Hornberger M. Spatial navigation deficits–overlooked cognitive marker for preclinical Alzheimer disease? *Nat Rev Neurol*. 2018;14:496-506.
65. Fernández-Cabello S, Kronbichler M, van Dijk KRA, Goodman JA, Nathan Spreng R, Schmitz TW. Basal forebrain volume reliably predicts the cortical spread of Alzheimer's degeneration. *Brain*. 2020;143:993-1009.
66. Schulz J, Pagano G, Fernández Bonfante JA, Wilson H, Politis M. Nucleus basalis of Meynert degeneration precedes and predicts cognitive impairment in Parkinson's disease. *Brain*. 2018;141: 1501-1516.
67. Nishioka C, Liang HF, Barsamian B, Sun SW. Amyloid-beta induced retrograde axonal degeneration in a mouse tauopathy model. *Neuroimage*. 2019;189:180-191.
68. Teipel SJ, Kuper-Smith JO, Bartels C, *et al*. Multicenter tract-based analysis of microstructural lesions within the Alzheimer's disease Spectrum: Association with amyloid pathology and diagnostic usefulness. *J Alzheimers Dis*. 2019;72: 455-465.